(12) INTERNATIONAL APPLICATION PUBLISHED UNDER THE PATENT COOPERATION TREATY (PCT)

(19) World Intellectual Property Organization
International Bureau

(43) International Publication Date
14 February 2002 (14.02.2002)

PCT

(10) International Publication Number
WO 02/12544 A2

(51) International Patent Classification[7]: C12Q 1/00

(21) International Application Number: PCT/EP01/09140

(22) International Filing Date: 7 August 2001 (07.08.2001)

(25) Filing Language: English

(26) Publication Language: English

(30) Priority Data:
60/223,436 7 August 2000 (07.08.2000) US

(71) Applicant *(for all designated States except US)*: **BIONETWORKS GMBH** [DE/DE]; Jakob-Klar-Strasse 7, 80796 München (DE).

(72) Inventor; and

(75) Inventor/Applicant *(for US only)*: **WILCKENS, Thomas** [DE/DE]; Jakob-Klar-Strasse 7, 80796 München (DE).

(74) Agent: **WEICKMANN & WEICKMANN**; Postfach 860 820, 81635 München (DE).

(81) Designated States *(national)*: AE, AG, AL, AM, AT, AU, AZ, BA, BB, BG, BR, BY, BZ, CA, CH, CN, CO, CR, CU, CZ, DE, DK, DM, DZ, EC, EE, ES, FI, GB, GD, GE, GH, GM, HR, HU, ID, IL, IN, IS, JP, KE, KG, KP, KR, KZ, LC, LK, LR, LS, LT, LU, LV, MA, MD, MG, MK, MN, MW, MX, MZ, NO, NZ, PL, PT, RO, RU, SD, SE, SG, SI, SK, SL, TJ, TM, TR, TT, TZ, UA, UG, US, UZ, VN, YU, ZA, ZW.

(84) Designated States *(regional)*: ARIPO patent (GH, GM, KE, LS, MW, MZ, SD, SL, SZ, TZ, UG, ZW), Eurasian patent (AM, AZ, BY, KG, KZ, MD, RU, TJ, TM), European patent (AT, BE, CH, CY, DE, DK, ES, FI, FR, GB, GR, IE, IT, LU, MC, NL, PT, SE, TR), OAPI patent (BF, BJ, CF, CG, CI, CM, GA, GN, GQ, GW, ML, MR, NE, SN, TD, TG).

Published:
— *without international search report and to be republished upon receipt of that report*

For two-letter codes and other abbreviations, refer to the "Guidance Notes on Codes and Abbreviations" appearing at the beginning of each regular issue of the PCT Gazette.

WO 02/12544 A2

(54) Title: SHORT CHAIN DEHYDROGENASES/REDUCTASES (SDR)

(57) Abstract: The present invention relates to a method for identifying or verifying members of the short chain dehydrogenase (SDR) family, to a method for providing modulators for members of the SDR family and to the preparation of pharmaceutical agents using these modulators.

Short chain dehydrogenases/reductases (SDR)

Description

The present invention relates to a method for identifying or verifying members of the short chain dehydrogenase (SDR) family, to identified SDRs, to a method for providing modulators for members of the SDR family and to the preparation of pharmaceutical agents using these modulators.

Technical Background

The short chain dehydrogenase/reductase (SDR) protein family (H. Jörnvall et al., Biochemistry 34 (1995), 6003-6013) is an old conserved protein family, the members of which show a residue identity level of only 20-30%. However, it has been found that the three-dimensional structure of members of the SDR family are highly similar, determining their functions and affiliation to the SDR family (U. Oppermann et al., Enzymology and Molecular Biology of Carbonyl Metabolism 6, Weiner et al. eds., Plenum Press, New York (1996), p. 403-415).

While initially only two structures of SDR enzymes restricted to bacterial and insect enzymes have been discovered, rapid progress on the knowledge of short chain dehydrogenases/reductases resulted in an increasing number of structures, which could be assigned to the SDR family. Currently, about 1.600 putative members are known, from which up to 100 may be derived from human, such as hydroxysteroid dehydrogenases (HSD).

An approach to identify SDR proteins is described in W.N. Grundy et al., Biochemical and Biophysical Research Communications 231 (1997) 760-766 and in T.L. Bailey et al., J. Steroid Biochem. Molec. Biol. 62 (1) (1997)

29-44. Therein homologies are searched for via a hidden Markov model, i.e. a self-training model, and thus classified to a certain protein family. A classification based on the function is not made in these models.

Since the SDR enzymes are involved in various metabolitic pathways and show different activities, such as oxidoreductases, lyases, or epimerases and, as discussed above, show only a low identity of 20-30%, it has been difficult, to assign new members unambiguously to the SDR family and to find modulators therefor.

However, since HSD and other SDR play a critical role in higher vertebrates, it is desirable to discover further members of the SDR family and establish modulators for known and new SDR enzymes.

It was therefore an object of the present invention to provide an algorithm which allows for the identification or verification of SDR family members with high confidence levels.

It was a further object of the invention to provide an algorithm which provides a search hierarchy with various levels.

It was another object of the present invention to provide modulators for SDR family members.

Still another object of the invention was to provide pharmaceutical agents based on members of the SDR family.

Summary of the invention

The present invention relates to a method for identifying or verifying members of the short chain dehydrogenase (SDR) family based on an algorithm using core SDR motifs for searching members of the SDR family.

Further, the present invention relates to a method for providing modulators for such members of the short chain dehydrogenase (SDR) family, which enhance or inhibit the activity therefrom as well as a method for providing a pharmaceutical agent using modulators for members of the SDR family.

In particular the present invention provides a combination of the steps (i) screening databases to search and find SDR sequences, (ii) store the data on an appropriate medium, rank and validate the hits and (iii) using the SDR sequences found to develop new drugs.

Detailed description of the invention

Members of the SDR protein family have a common core sequence, which is about 250-350, preferably about 260-290 and in particular about 270 amino acids in length. SDR proteins can have extensions at the N-terminus and/or at the C-terminus. Typically, these extensions have a length of 20 to several hundred, in particular up to 500 amino acids. These extensions can be membrane anchors or other signals or they can constitute completely distinct protein domains. Therefore, according to the invention it is primarily searched for SDR core domains, the rest of the protein being analysed only later on.

In a first embodiment the invention provides a method for identifying or verifying members of the short chain dehydrogenase (SDR) family comprising the steps

(a) providing a target sequence of molecules to be classified,

(b) comparing said target sequence with core SDR motifs selected from

(i) MV1 being derived from the motif MT1:TGxxxGxG by replacement of 0 to 2 amino acids,

(ii) MT2:NN(0-2:x)AG,

(iii) MT3:N, located at a position 90-110 relative to MT1,

(iv) MV4 being derived from the motif MT4:S(11-52:x)YxxxK by replacement of 0-2 amino acids and

(v) MT5:PG,

(c) determining positive SDR candidates containing

(i) at least the core SDR motifs MV1 and MV4 and

(ii) at least 7 of the 14 amino acids contained in the motifs MT1, MT2, MT3, MT4 and MT5 and

(d) classifiying positive SDR candidates as belonging to the SDR family.

It has been found in many SDR proteins that several motifs of the SDR core domain often occur in combination. However, it is not obligatory that all SDR core motifs are present for a protein to be an SDR enzyme. Since SDR proteins may lack one or several of the core SDR motifs, they may not be found by simple comparison of the complete SDR core domains.

Within the SDR core the following functional motifs frequently are found. The motifs are given in order from N-terminus to C-terminus assigning a position number 0 to the start of the first motif MT1, which of course need not be the start of the complete SDR protein.

MT1:TGxxxGxG (circa position 0-7);
MT2:NNAG (circa position 75-78);
MT3:N (circa position 100);
MT4:S-Y-K (circa positions 128/142/146) and
MT5:PG (circa position 170/171).

Using these motifs, the algorithm according to the invention has been developed, which allows for an assignment of target sequences to be an SDR sequence with a confidence level of more than 95%, in particular more than 98%. By relying on motifs of the core SDR region positive hits

due to indentity in non significant regions can be excluded. It is essential for the present invention that the core SDR motifs were selected because of their functional meaning and not only because of homology comparisions. The SDR motifs used form essential parts of nucleotide co-factor binding region (Rossman-fold) and the active site of members of the SDR family. The motifs MT1 and MT2 represent components of the co-factor binding site. A particular co-factor of SDR enzymes is NAD(P)(H). The motif MT3 represents a contact to the active site and the motif MT4 a part of the active site. The motif MT5 is of functional importance due to its proximity to the co-factor. Thus core SDR motifs are motifs which are essential for the functionality of the SDRs.

For detecting members of the short chain dehydrogenase (SDR) family in the method according to the invention it is therefore essential that functional aspects are considered, wherein enzymatically active SDRs are detected and not only sequences which exhibit a certain homology to other SDRs at functionally irrelevant positions.

Contrary to prior art algorithms, according to the invention those amino acids are taken into account which are essential for the function. A minimum amount of the amino acids selected thus enables a maximum amount of targets due to the divergence of the SDR family, wherein the detection of erroneously positive targets is basically excluded because of the connection between function and structure. This way the target specificity can be considerably improved over algorithms, such as neuronal networks, which are based on homology comparisons (cf. J.A Gerlt et al., Genome Biology, 1 (5) (2000), Reviews 0005.1-0005.10). In addition, further functional information can be easily included in order to screen for functional deficits, such as screening for an associated disease mutations or individualized drug metabolism.

While the individual proteins assigned to the SDR family using the algorithm of the invention may have identities of only 30% or less, they show a very similar three-dimensional structure. It is important for the correct formation of the desired three-dimensional SDR structure that motifs 1 to 5 are present in the above listed succession.

For the description of the motifs the single letter amino acid code is used. x denotes a variable amino acid, selected preferably from the 20 naturally occuring amino acids. NN(0-2:x)AG means that 0, 1 or 2 amino acids can be positioned between amino acids N and A. S(11-52:x)YxxxK means that from 11 to 52 amino acids are positioned between S and Y and 3 amino acids are positioned between Y and K.

A replacement of 0-2 amino acids refers to a replacement of any of the amino acids given (including x), whereby preferably the explicitly named amino acids are replaced. A replacement includes deletion of the amino acid or a substitution of the amino acid by another amino acid selected preferably from the 20 naturally occuring amino acids. The replacement of 1 or 2 amino acids results in a fuzzy logic including also sequences, in which the motifs are not 100% conserved. A strategy combining sequence and structure information is also disclosed by L. Yu et al., Protein Science 7 (1998), 2499-2510.

In a preferred embodiment of the invention MT2 is defined to be NNAG (i.e. without any amino acids x between NN and AG), but with possible replacement of 1-3 amino acids.

The motif MT3:N is located at position 90-110, preferably at position 95-105 and in particular at position 100 relative to the start of the motif MT1.

In a particularly preferred embodiment of the invention the second part of motif MT4 is defined to be the pattern YxASK with possible replacement of

up to 3 of these residues. In this preferred embodiment the range of possible scores is extended from 0-14 up to 0-16. In this embodiment positive candidates have a score of at least 7, preferably at least 9, more preferably at least 11 and most preferably at least 13.

Preferably the SDR motifs are located in the order given from the N-terminus to the C-terminus for a sequence to be classified as SDR sequence. The positions given in brackets above may be shifted by amino acid insertions or deletions within the sequence analyzed. Preferably the motifs are found within ± 50, more preferably ± 20 positions, in particular ± 10 positions and most preferably ± 5 positions, from the values given.

A target sequence is classified as belonging to the SDR family according to the invention, if it contains at least the core SDR motifs MV1 and MV4 and at least 7 of the 14 explicitly named amino acids contained in the motifs MT1, MT2, MT3, MT4 and MT5. The confidence level can be controlled by varying the amount of matching amino acids, which have to be present in the target sequence. Therefore, if a high confidence level, e.g. > 98%, more preferably > 99% is desired, it may be preferable to classify target sequences as positive SDR candidates, only if they contain at least 9 of the 14 amino acids, or even at least 11 or at least 12 of the 14 amino acids contained in the motifs MT1-MT5. Setting the score at a value of at least 13 results in the detection of exclusively sequences, which are an SDR with a confidence level of almost 100%, e.g. >99.8%.

In a preferred implementation of the method of the invention a file is provided containing a set of protein amino acid sequences, the input set. One sequence is taken from the input set, the query sequence. The implementation then passes the query sequence to the algorithm, which examines it for occurences of some or all of MT1-5 in the arrangements allowed. The algorithm returns a list of the best possible combinations of

occurences. If the matches contain more than a specified number of amino acids from MT1-5, they are assigned as hits.

In a particularly preferred embodiment the method of the invention is as follows:

The algorithm first searches the whole sequence for instances of the first motif MT1, allowing for up to two replacements as described. Each possible MT1 match is then taken as the origin for searches for the motifs MT2 to MT5 whose positions are defined relative to the position of MT1. A data structure based on each position of MT1 is created, which will be used to store the positions of other motifs relative to this MT1.

For a given MT1 match at position P, the preferred position of the motif MT2 is P+75. According to the rules MT2 is preferably at position (P+75)+/-50, more preferably (P+75)+/-20. This defines a window on the sequence within which instances of the motif MT2 are searched for, including any variants of MT2 with up to three replacements. Since the size of the window affects the time taken to search and the quality of the matches found, the preferred implementation allows the window sizes to be specified for each search. Any possible matches within the window are added to the result data structure as children of the current MT1.

The procedure is then repeated for instances of MT3, where the window is (P+100)+/-50, more preferably (P+100)+/-20, or any other specified window size. Again, any results found within the allowed window are added to the result data structure as children of the current MT1.

The same procedure is then followed for MT4, with a window (P+128)+/-50, more preferably (P+128)+/-20, or any other specified window size. In this case the window only specifies the position of the Serine residue of MT4, and once a candidate Serine has been found at position P_S (and

added to the result structure as a child of the current MT1), it defines a window $P_S+(11\text{-}52)$, within which instances of the second part of MT4 are searched for, allowing for replacements. Any candidates are added to the result structure as children of the current Serine match.

Since MT4 allows replacements, and those replacements could include replacements of the Serine, the implementation additonally searches for the second part for MT4 in cases where the Serine is not found. In this case, a virtual window composed of all of the possible positions of the (missing) Serine, offset by the $P_S+(11\text{-}52)$, is constructed [$P_S+(11\text{-}52)+/-20$, i.e. the range $P+128+(11\text{-}20)$ to $P+128+(52+20)$], or likewise for any specified window size. If any instances of the second part are found they are added to the result data structure as children of the current MT1.

The procedure is then repeated for instances of MT5, where the window is $(P+170)+/-50$, more preferably $(P+170)+/-20$, or any other specified window size. Again, any results found within the allowed window are added to the result data structure as children of the current MT1.

At this stage the implementation holds in memory a tree-structured data structure where the possible matches with the specified pattern correspond to depth-first traversals of the tree. The implementation enumerates the possible combinations of the full or partial motifs, adds up a score calculated from the number of residues in the motifs which were actually matched, and discards the instances where the overlapping windows have given rise to motifs where the ordering is not MT1-MT2-MT3-MT4-MT5. Any combination with a score equal to the maximum score found is kept and added to a list, and it is this list with its score, the motifs found, and the position in the sequence of each amino acid matched which is returned as the result at this stage of the implementation.

The preferred implementation includes significant enhancements, in particular:

- MT2 is defined to be NNAG without the presence of 1 or 2 amino acid insertions between the NN and AG parts. The implemenation allows for replacement of 1-3 of the residues, and will continue to search for other motifs even if no instance of MT2 is found.
- The second part of MT4 is defined to be the pattern Y*ASK instead of Y**K, but again the implementation allows replacement of up to 3 of these residues. This makes the range of possible scores 0-16 instead of 0-14.
- The absence of motif MT4 is not used to discard SDR candidates, but the effect on the overall score of its absence (5 out of a possible 16 matches) is significant in excluding matches which do not contain it and additionally the presence of the active site MT4 tyrosine is indicated for each result, as a significant indicator of possible SDR catalytic activity.

In a further preferred embodiment an enlargement or optimization, of the algorithm is performed also on human extended SDRs. Thus it is taken into account that compared to the other SDRs often only a motif MT_x1 (TGxxGxxG) as well as a motif MT_x4 (YxxxK) is present, wherein MT_x1 is a variant of TGxxxGxG. For determining human extended SDRs with this enlarged algorithm motifs 2, 3 and 5 can even be missing.

In a particularly preferred embodiment the algorithm according to the invention comprises the import of a data set, e.g. from data bases, organizing the data set by using the method according to the invention, ranking the SDR hits and further analyzing and managing the data of the detected hits, such as a cross-linking to data bases, to BLAST or to other tools.

Subject matter of the invention is also a data carrier, particularly a diskette containing the method according to the invention and particularly the above described algorithm.

Whereas the method according to the invention itself already has a very high specificity and reliability in the selection of SDR candidates, the SDR candidates detected can be subjected to further evaluation criteria. These criteria are e.g. comparing the 3D-structure of the candidates detected with the 3D-structure of known SDR proteins or a standardized 3D-structure, which is derived from SDR candidates identified by the method according to the invention. Thus, in a further preferred embodiment of the invention the polypeptides classified as positive SDR candidates in the method according to the invention are subjected to another evaluation step in view of their three-dimensional structure in order to further improve the selectivity and specificity of the method. Thus it is possible to use known three-dimensional structures of SDR family members (cf. e.g. H. Jörnvall, Biochemistry 34 (1995), 6003-6013; U. Oppermann et al., Adv. Exp. Meth. Biol. 414 (1997), 403-415 or J. Benach et al., J. Mol. Biol. 282 (1998), 383-399). However, it is also possible to determine the three-dimensional structures of the SDR candidates detected with the method according to the invention and to prepare a common comparative three-dimensional structure therefrom. This way it can be examined, e.g. whether the positive SDR candidates exhibit the co-factor binding site typical of SDRs. A further criteria may be the presence of amino acid Y at position 152 ± 20, particularly ± 10. Further, it is possible to compare the amino acids sequences detected with known SDR sequences, e.g. via an alignment.

After the sequences have been classified as SDRs it is also possible to search for further domains, e.g. membrane domains in order to thus classify them to a certain type of tissue.

An important subgroup of SDRs are FabGs, which are derived from pathogens and which can be identified via the method according to the invention. Since FabGs are often strongly degenerated and thus exhibit a relatively low score (e.g. 9 or more) in the method according to the invention, it can be advantageous to examine possible FabG-SDR candidates in a second step in view of the presence of the following motif variations: MT_y2:VxVNNAG, wherein V can be replaced particularly by I, as well as MT_y5:PGFI, wherein F and/or I can be missing.

A list of FabG proteins which were identified by the method according to the invention is shown in Table 4. FabGs are involved in the lipid metabolism of bacteria and are particularly suitable for the development of antibiotics.

A further group of SDRs which can be identified by the method according to the invention are bacterial SDRs. Bacterial SDRs detected with the algorithm according to the invention are shown in Table 3.

Further, it is possible to detect production enzymes as well as thermostable enzymes with the method according to the invention.

In a most preferred embodiment, the so-called SDR_Finder, the method according to the invention is based on the implementation of functional data both on the three-dimensional structure and on the biological function (NADP(H)-dependend enzymes). The implementation is hierarchically structured according to the smallest common denominator having a functional meaning. Contrary to known tools not motifs, but SDR candidates are searched for and thus also for those having a very low homology or hardly conserved core motifs, respectively. The search for SDR candidates according to the invention enables a considerably higher specificity. The SDR candidates detected are of biologically functional

relevance. At the same time a greater number of hits is found due to the use of the smallest common denominator.

Further, it is possible to establish a ranking with the algorithm according to the invention, to export the data in different formats and to selectively search for species. Thus, the SDR_Finder represents an "all-in-one" analysis solution including various obtainable possibilites, particularly the woldwide web. The implementation of hyperlinks to NCBI, EMBL and their tools (e.g. Blast, ClustalW, PfaM, PDB, Medline, OMIN) represents an "in silico" analysis/drug development software of modular structure which is particularly developed for SDR. Further modules which can be connected thereto are the examination of three-dimensional structures, the determination of active centres and the substrate docking simulation. The latter can also be implemented directly into the SDR_Finder and allow direct access, e.g. to 3D-databases and chemical libraries via the worldwide web.

In a preferred embodiment the SDR_Finder is equipped with fuzzy logic.

In addition, experimental data can be used, e.g. to evaluate the exchange of one amino acid in a motif regarding the functional consequences. This is of importance both for the individual adjustment of therapies and the evaluation of pathological problems or for the development of diagnostica, respectively.

Moreover, it is possible to enlarge the algorithm subgroup-specifically, as is shown herein for the FabG_SDRs.

The method according to the invention can be used to verify sequences, which are already classified as (putative) SDR sequences, e.g. by automatic alignment (BLAST), to belong to the SDR family or not. Further, it can be used to search for and find new members of the SDR family or to

search for and find new isoforms of SDR proteins. Therefore, the method of the invention provides additional information with regard to known sequences as well as to novel sequences. From the knowledge that a target sequence belongs to the SDR family as well as from the information obtained from the ranking findings about substrates and functions can be obtained. An important selection criteria thereby is the drugability of the SDR candidates detected.

The method according according to the invention can be used to detect e.g. human SDRs (human extended SDRs), animal SDRs, particularly mammalian SDRs, but also bacterial SDRs, FabG_SDRs, fungi SDRs, SDRs of pathogens, SDRs of parasites, e.g. plant parasites.

The SDR proteins classified with the algorithm according to the invention thus can serve as platform for novel drug development. Human SDR proteins can particularly serve as starting point for the treatment of diseases or malfunctions of the body, whereas bacterial SDRs particularly provide a starting point for the development of novel antibiotics. Further, respecticve SDRs can serve for the development of antimicotica, pesticides, herbicides etc...

While the algorithm of the present invention preferably is used to search for protein sequences, it is also possible the convert the motifs given into nucleic acid sequences and screen nucleic acid databases. A method to convert amino acid sequences into nucleic acid sequences while considering the degeneration of the genetic code is e.g. given from H. Jörnvall, FEBS Letters 456 (1999), 85-88. A search on the nucleic acid level can preferably be used to preselect sequences, which are then confirmed by an alignment in the protein level.

For the search on nucleic acid level these protein sequences are preferably converted to DNA sequences in particular cDNA sequences and used for

the detection of further SDR candidates via a fuzzy logic or a hidden Markov model or via neuronal networks.

The method of the invention therefore also provides a tool for preselection of SDR candidates on the genomic level.

Preferably a ranking of the positive SDR candidate is performed e.g. according to the number of amino acids matching with motifs MT1-MT5. This way a hierarchy and/or an evolutionary relationship of the obtained SDR candidates can be obtained.

In a particularly preferred embodiment the target sequences classified as positive SDR candidates contain at least the core SDR motifs MT1 and MT4.

By hierarchically classifying the verification of the individual core SDR motifs several levels to detect SDR proteins can be obtained.

By using the algorithm according to the invention the search for SDR candidates and consequently the development of pharmaceuticals can be decisively enhanced. So far for the production of pharmaceuticals in vitro tissue cultures were admixed with different substrates. From cultures, wherein a certain substrate was converted, the target protein was isolated. According to the invention, this step and thus the knowledge of a substrate for the development of inhibitors or for the development of pharmaceuticals is not necessary. Moreover, starting from the sequence found a modulator, in particular an inhibitor or activator can be derived. This modulator can e.g. be derived from known modulators of other, in particular of related SDR proteins, suitable substrates, related functions and tissue distribution for 17ß HSD isoforms are described e.g. by H. Peltoketo et al., J. Molecular Endocrinology 23 (1999), 1-11. Further, it is possible to derive a modulator from the 3D-structure of the SDR sequence.

Such a 3D-structure can be obtained experimentally, e.g. by X-ray chrystallography or by computer based calculations, e.g. ab initio, force field, or rule based methods. Further, by inhibiting the active site of the SDR protein the function thereof can be determined.

The searching for SDR family members and ranking is also applicable to evaluate lead-candidates for possible inhibitors or modifiers of a specific enzyme. Leads may be derived from metabolites of evolutionary closely related or very distant enzymes from other species, if the same metabolite may not be found in the respective target organism. The evolutionary relationship of SDRs and their distinction from MDRs (medium chain dehydrogenase) is e.g. described by H. Jörnvall et al., FEBS Letters 445 (1999), 261-264 and AKRs (T.M. Penning, Endocrine Rev. 18(3) (1997) 281-305).

SDR enzymes are often involved in intermediary metabolisms, as well as in hormone and mediator metabolisms.

Substrates of known SDR proteins include e.g. steroids, such as estrone/estradiol, cortisone/cortisol and testosterone/3α-androstenediol. Thus, after classifying a sequence as SDR sequence functional tests for steroid substrates result in higher hit rates.

Further substrates of SDR proteins are UDP-glucose, UDP-N-actetylglucosamine, sepiapterin, dihydropteridine, R-3-OH-butyrate, dienoyl CoA, trans-Enoyl CoA, fatty acids, L-3-OH-acyl CoA. These substrates are particularly converted of SDR enzymes, which are involved in the intermediary metabolism. Further substrates of SDR proteins, particularly of SDR enyzmes, which are involved in hormone, mediator and xenobiotic metabolisms, are several hydroxy steroids, e.g. 3-beta-hydroxysteroids, 11-beta-hydroxy steroids or 17-beta-hydroxy steroids as well as prostaglandines and retinoides.

Further, searching SDRs, ranking and comparing evolutionary patterns can also be used to detect clinically relevant polymorphisms and/or single nucleotide polymorphisms (SNPs). This approach can be used to characterize diseased mechanisms as well as metabolism of xenobiotics, e.g. drug metabolism.

The identification of SDR members, ranking and comparing evolutionary patterns also allows for the identification of structure-function relationships. These structure-function relationsships are a key for identification of substrates of ORFs with unknown functions.

Within a lead oriented characterization first binding of a positive SDR candidate is evaluated. Starting from the binding a modulator, e.g. an inhibitor or activator, can be developed. Useful information for developing an inhibitor can be obtained from protein sequence alignment of full-length sequences, e.g. by comparison with known SDRs. Further, valuable information can be obtained from expressed sequence tags (EST) and gene sequence comparison. The procedure using the algorithm according to the invention allows for a great reduction of possible modulator candidates to be analysed and practically excludes target sequences, which are not SDR sequences. Therefore, an analysis of the functions in vitro or in vivo can be performed with much less effort than in the state of the art due to the reduced number of compounds to be tested. While in the methods according of the state of the art often the substrate must be known, this knowledge is not essential for developing modulators or/and drugs according to the invention. It is even possible to derive possible substrates in a subsequent step from the functions of the SDR enzymes found according to the invention. Ligands can be derived according to the procedure described by G.R. Lenz et al., DDT, 5(4) (2000), 145-156.

The validation of the potential SDRs found according to the algorithm of the invention, which can be used as new targets for drug development,

can then be performed by experimental biochemical methods, such as high-throughput function screening for function identification, ultra high-throughput screening for lead compounds, transfection assays, knock out experiments, microarrays, tissue expression, cDNA arrays or analysis of disease in animal or in vitro model systems. However, it is also possible to use virtual methods using e.g. computers for validation of the new targets, e.g. by molecular homology modelling or substrate docking simulations.

Suitable strategies include e.g. gene expression of an identified SDR protein to obtain the protein molecule and subsequently performing biological functional assays and observe the behaviour of the cell.

Alternatively, the 3D-structure may be derived from the SDR sequence and an inhibitor for the active site provided. Using the inhibitor the function of the SDR within an organism can be evaluated.

Small weight inhibitors for SDR enzymes, which can be used as starting point for developing new or modified inhibitors, in particular inhibitors for newly identified SDR enzymes include:

1) Steroidal-based inhibitors like steroid carboxylates, acrylates, enolates 3,4-and 16,17-fused ring pyrazoles, 3 alpha, 17-beta or 20-beta-spiro-oxiranes as well as steroidal spirolactones, progestins, ursodexycholate, synthetic analogs of estrone sulfate and estrone-3-amino derivatives.

2) Inhibitors based on flavonoides and dihydropterin derivatives.

3) Inhibitors based on polyphenols and derivatives of 2,3-dihydroxy-1-naphthoic acids like gossypol (1,1',6,6',7,7'-hexahydroxy-5-5'-diisopropyl-3,3'-dimethyl-2,2'-binaphthalene-8,8'-dicarbaldehyde).

4) Inhibitors based on glycyrrhizin (3beta,20beta)-29-hydroxy-11,29-dioxoolean-12-en-3-yl 2-O-beta-D glucopyranuronosyl-alpha-D-glucopyranosiduronic acid) and components of enzymatically hydrolysed licorice extract like 3-O-beta-D-glucoronopyranosyl-24-hydroxy-18beta-glycyrrhetinic acid, 3-O-beta-D-glucur-onopyranosyl-18beta-glycyrrhetinic acid and 3-O-beta-D-glucuronopyranosyl-18beta-liquiritic acid, monoglycosylated derivatives of glycyrrhizin as well as carbenoxolone.

5) Pharmaceutically acceptable salts of the above mentioned molecules such as alkali metal (e.g. sodium), alkaline earth metal (e.g. magnesium) or ammonium as well as salts of organic carboxylic acids, such as acetic, citric, oxalic, lactic, tartaric, malic, isothionic, lactobionic, ascorbic and succinic acids; organic sulfonic acids, such as methanesulfonic, ethanesulfonic, benzenesulfonic and p-tolysulfonic acids; and inorganic acids, such as hydrochloric, sulfuric, phosphoric, and sulfamic acids.

Further candidates for inhibitors are chalcones (cf. Life Sci 68 (7) (2001) 751-761) as well as phytoestrogens (cf. Life Sci 66 (14) (2000) 1281-1291) and frenolicin and its derivatives.

Further, inhibitors can be derived from 3D-structures of the SDRs found, confirmed, identified or verified with the method of this invention, as is described e.g. by Liao et al., Structure, Vol. 9 (2001) 19-27.

Since SDR enzymes, in particular human SDR enzymes have been found to be involved in many pathways of the body, they are outstanding targets for developing new drugs. In particular human SDR enzymes have been found to be involved in intermediary metabolism, lipid mediator/hormone metabolism or xenobiotic phase I metabolism. On the other hand, SDR enzymes often constitute pathogenic factors causing diseases. Thus, e.g. the AME syndrome is associated with 11ß HSD-2, bile acid metabolism is associated with 3ß HSD, polycystic kidney disease is associated with

Ke6(17ß HSD-8) and Alzheimer's disease is associated with ERAB(17-ß HSD-10).

Further diseases which can be effected by influencing, modulating or inhibiting SDRs comprise e.g. DHPR deficiency, phenylketonuria, dienoyl CoA reductase deficiency, galactosemia III, tetrahydrobiopterine deficiency, adrenal hyperplasia, adrenogenital syndrome, 11-oxoreductase deficiency, apparent mineralocorticoid excess syndrome, ovarian/breast cancer, male pyseudohermophroditism, Zellweger syndrome, pregnancy/ovarian cancer, polycystic kidney disease, Alzheimer's disease, retinits punctata albescens, retinitis pigmentosa, Down's syndrome, arterial hypertension, oncogenes, follicuolar lymphoma, hepatocarcinogenesis, aging related hormone deficiencies and immunity in general.

Since many of the SDR enzyme are bidirectional (reversible oxidoreaction) depending on the environment, it is also possible to provide a means for selectively enhance one of the enzymatic reaction, i.e. oxidation or reduction or to reverse the action observed.

Thus, providing new SDR sequences and modulators therefor, as described above, allows for the preparation of drugs or pharmaceutical agents, which can be used to control many different diseases. In particular drugs for treatment of cancer, e.g. breast cancer or prostate cancer, obesity, diabetes, fertility, osteoporosis, glucose metabolism, or conditions related to aging can be prepared. Further applications include steroid resistance, in particular ostrogen resistance and glucocorticoid resistance.

Further, SDR proteins and in particular hydroxy steroid dehydrogenases (HSDs) are outstanding targets for tissue-specific modulation of hormone-dependent or sensitive diseases, e.g. cancer, in particular prostate or breast cancer.

The present invention is in particular useful for providing a pharmaceutical agent for affecting immune regulation is provided by developing a modulator for 17ß HSD type 3, 17ß HSD type 7, 17ß HSD type 8, 17ß HSD type 10, 11ß HSD-1, CR1, UDP glucose epimerase, SDR_SRL, AF067174, AF151840, AF151844, AF0078850, Fvt-1, HEP-27, DKFZ_ORF, WWOX_ORF, or CR3, a pharmaceutical agent for affecting autoimmunity is provided by developing a modulator for 17ß HSD-3, 17ß HSD-8, 11ß HSD-1, AF057034, U89717, CR1, AF0078850, HEP-27, or CR-3, a pharmaceutical agent for wound healing or partial recovery is provided by developing a modulator for 17ß HSD-3, 17ß HSD-8, 11ß HSD-1, U89717, CR1, AF0078850, HEP-27, or CR-3, a pharmaceutical agent for treatment of leukemia is provided by developing modulators for 17-ß HSD-10 or Fvt-1 or a pharmaceutical agent for apoptosis regulation is provided by developing a modulator for 17ß HSD-10, U89717, SDR_SRL; or for providing a pharmaceutical agent for affecting immune response by providing a modulator for AF016509, or providing a pharmaceutical agent for the treatement of cancer by providing modulators for AF016509, or providing a pharmaceutial agent for affecting cell growth by providing a modulator for U89717, or providing a pharmaceutical agent for the treatment of lung carcinoma by providing a modulator for SDR_SRL, or providing a pharmaceutical agent for the regulation of inflammation or vasculitis by providing a modulator for DKFZ_ORF.

The SDR candidates detected according to the invention can be used particularly for the production of inhibitors, such as antibodies on protein level or antisense on nucleic acid level. Moreover, it is possible to provide diagnostica by using the SDR candidates detected according to the invention, e.g. in order to show a malfunction.

An important aspect of the present invention in view of the development of new drugs for the diagnosis and/or treatment of a disease is that the inventive approach aims on a target family, i.e. SDRs and not on a specific

disease. This allows for the development of a number of drugs, which all influence the same target family. By this approach the amount of experiments, effort and money necessary to develop a new drug can be significantly reduced, since many results can be used parallel for further members of the same target family leading to further new drugs for different medical applications. Further this approach allows for affecting a target which is known or suspected to be highly relevant for a person's health. In contrast to the classical approach wherein starting from a disease a suitable target must identified, this time and effort consuming procedure is not necessary with the inventive approach.

The invention is further elucidated by the following figures wherein

Fig. 1 represents the search engine for SDR candiates; The target sequence is compared to the specified core SDR motif, preferably in order from the N-terminus to the C-terminus.

Fig. 2 shows flow charts for the preferred implementation of the algorithm. Fig. 2a shows a flow chart for data processing, while Fig. 2b shows a flow chart for the algorithm.

Fig. 3 depicts the development of pharmaceuticals on the basis of the SDR search according to the invention; The combination of virtual screening and classifying sequences to belong to the SDR family with the development of new drugs, as provided herein, is an efficient novel drug development strategy. By using the search results of the virtual SDR search new targets are obtained, from which drugs can be derived by various procedures.

Fig. 4 shows an alignment of human SDRs. 39 human SDR proteins were found in a database using the algorithm according to the invention. Throughout the various SDR proteins highly conserved amino acids

are underlaid in grey. As can be seen from this figure the motifs selected for the algorithm of the invention are present in most of the human SDRs.

Tab. 1 Table 1 shows human and/or vertebrate SDRs detection with the algorithm according to the invention. The detected SDRs are also subject matter of this invention. Further, Table 1 includes an EST search for each SDR detected, with which the corresponding function and localization in tissue can be found or localized.

Tab.2 Table 2 shows mouse SDRs detected with the method according to the invention and the results of EST searches by using these mouse SDRs in human tissue. Thus using SDRs of various species, e.g. mammals, allows for localization and identification of new SDRs, in particular human SDRs on a genomic level. A preselection and/or identification of the SDR employed can be performed with the method according to the invention.

Tab. 3 Table 3 shows in bacterial SDRs which were detected with the method according to the invention. Such bacterial SDRs are particularly suitable for the development of novel antibiotics.

Tab. 4 Table 4 shows FabG_ proteins, i.e. an SDR subgroup. It is possible with the method according to the invention specifically identify desired subgroups by selection of further criteria in a second search step.

Tab. 5 Table 5 shows SDRs from different fungi.

Table 1: Human and/or vertebrates SDRs in non_redundant NCBI Database

Proteins or putative proteins not annotated SDRs

>gi¦14035824¦emb¦CAC38508.1¦ unnamed protein product [Homo sapiens]

EST search:

Sequences producing significant alignments: (bits) Value

gi¦12777652¦emb¦AL514158.1¦AL514158 AL514158 LTI_NFL006_PL2... 1865 0.0
gi¦12791977¦emb¦AL528484.1¦AL528484 AL528484 LTI_NFL003_NBC... 1590 0.0
gi¦10355379¦gb¦BE893726.1¦BE893726 601436638F1 NIH_MGC_72 H... 1178 0.0
gi¦11984517¦gb¦BF699109.1¦BF699109 602126730F1 NIH_MGC_56 H... 1144 0.0
gi¦10352047¦gb¦BE892079.1¦BE892079 601434975F1 NIH_MGC_72 H... 1126 0.0
gi¦13577989¦gb¦BG570336.1¦BG570336 602590763F1 NIH_MGC_77 H... 1122 0.0
gi¦13570346¦gb¦BG562694.1¦BG562694 602581487F1 NIH_MGC_76 H... 1104 0.0
gi¦8156043¦gb¦AW966207.1¦AW966207 EST378280 MAGE resequence... 993 0.0
gi¦13295675¦gb¦BG402227.1¦BG402227 602465788F1 NIH_MGC_75 H... 987 0.0
gi¦6199963¦gb¦AW152065.1¦AW152065 xf74a01.x1 NCI_CGAP_Gas4 ... 918 0.0
gi¦1967863¦gb¦AA315514.1¦AA315514 EST187305 Colon carcinoma... 831 0.0
gi¦1957444¦gb¦AA305116.1¦AA305116 EST176117 Colon carcinoma... 831 0.0
gi¦13332753¦gb¦BG426247.1¦BG426247 602492423F1 NIH_MGC_75 H... 797 0.0
gi¦12346843¦gb¦BF979524.1¦BF979524 602288151F1 NIH_MGC_97 H... 789 0.0
gi¦13573087¦gb¦BG565434.1¦BG565434 602583580F1 NIH_MGC_76 H... 743 0.0
gi¦13339499¦gb¦BG432993.1¦BG432993 602495921F1 NIH_MGC_75 H... 733 0.0
gi¦13966961¦gb¦BG699051.1¦BG699051 602678687F1 NIH_MGC_95 H... 720 0.0
gi¦13336564¦gb¦BG430058.1¦BG430058 602499427F1 NIH_MGC_75 H... 712 0.0

>gi¦14035828¦emb¦CAC38510.1¦ unnamed protein product [Homo sapiens]

EST Search:

Sequences producing significant alignments: (bits) Value

gi¦12777652¦emb¦AL514158.1¦AL514158 AL514158 LTI_NFL006_PL2... 1865 0.0
gi¦12791977¦emb¦AL528484.1¦AL528484 AL528484 LTI_NFL003_NBC... 1590 0.0
gi¦13577989¦gb¦BG570336.1¦BG570336 602590763F1 NIH_MGC_77 H... 1197 0.0
gi¦10355379¦gb¦BE893726.1¦BE893726 601436638F1 NIH_MGC_72 H... 1178 0.0
gi¦10352047¦gb¦BE892079.1¦BE892079 601434975F1 NIH_MGC_72 H... 1156 0.0
gi¦11984517¦gb¦BF699109.1¦BF699109 602126730F1 NIH_MGC_56 H... 1144 0.0
gi¦6199963¦gb¦AW152065.1¦AW152065 xf74a01.x1 NCI_CGAP_Gas4 ... 1134 0.0
gi¦13570346¦gb¦BG562694.1¦BG562694 602581487F1 NIH_MGC_76 H... 1104 0.0
gi¦8156043¦gb¦AW966207.1¦AW966207 EST378280 MAGE resequence... 993 0.0
gi¦13295675¦gb¦BG402227.1¦BG402227 602465788F1 NIH_MGC_75 H... 987 0.0
gi¦13573087¦gb¦BG565434.1¦BG565434 602583580F1 NIH_MGC_76 H... 959 0.0
gi¦13336564¦gb¦BG430058.1¦BG430058 602499427F1 NIH_MGC_75 H... 928 0.0
gi¦10908030¦dbj¦AV750182.1¦AV750182 AV750182 NPC Homo sapie... 856 0.0
gi¦1967863¦gb¦AA315514.1¦AA315514 EST187305 Colon carcinoma... 831 0.0
gi¦1957444¦gb¦AA305116.1¦AA305116 EST176117 Colon carcinoma... 831 0.0
gi¦13332753¦gb¦BG426247.1¦BG426247 602492423F1 NIH_MGC_75 H... 797 0.0
gi¦12346843¦gb¦BF979524.1¦BF979524 602288151F1 NIH_MGC_97 H... 789 0.0
gi¦13339499¦gb¦BG432993.1¦BG432993 602495921F1 NIH_MGC_75 H... 733 0.0
gi¦13966961¦gb¦BG699051.1¦BG699051 602678687F1 NIH_MGC_95 H... 720 0.0

>gi|14035944|emb|CAC38568.1| unnamed protein product [Homo sapiens]

EST search

Sequences producing significant alignments: (bits) Value

gi|14077603|gb|BG766950.1|BG766950 602740653F1 NIH_MGC_49 H... 1340 0.0
gi|8156902|gb|AW967066.1|AW967066 EST379140 MAGE resequence... 995 0.0
gi|10964840|gb|BF125800.1|BF125800 601763002F1 NIH_MGC_20 H... 866 0.0
gi|10718270|dbj|AV701940.1|AV701940 AV701940 ADB Homo sapie... 835 0.0
gi|13987850|gb|BG709476.1|BG709476 602674749F1 NIH_MGC_96 H... 765 0.0
gi|10370049|gb|BE856729.1|BE856729 7f66h09.x1 Soares_NSF_F8... 724 0.0
gi|1523078|gb|AA044874.1|AA044874 zk72b09.r1 Soares_pregnan... 720 0.0
gi|12102027|gb|BF796973.1|BF796973 602258193F1 NIH_MGC_85 H... 712 0.0
gi|3180757|gb|AA994212.1|AA994212 ou49b10.s1 NCI_CGAP_Br2 H... 680 0.0
gi|12672383|gb|BG165680.1|BG165680 602345187F1 NIH_MGC_89 H... 670 0.0
gi|5394770|gb|AI808204.1|AI808204 wf93f01.x1 Soares_NSF_F8_... 640 0.0
gi|4334141|gb|AI472051.1|AI472051 tj85e10.x1 Soares_NSF_F8_... 626 e-177

>gi|14272510|emb|CAC39693.1| unnamed protein product [Homo sapiens]

EST search

Sequences producing significant alignments: (bits) Value

gi|12901640|emb|AL557739.1|AL557739 AL557739 LTI_FL012_TC1 ... 1608 0.0
gi|12878927|emb|AL546120.1|AL546120 AL546120 LTI_NFL006_PL2... 1558 0.0
gi|13523805|gb|BG532267.1|BG532267 602561357F1 NIH_MGC_61 H... 1441 0.0
gi|13672847|gb|BG621476.1|BG621476 602617846F1 NIH_MGC_79 H... 1425 0.0
gi|14046767|gb|BG776463.1|BG776463 602663549F1 NIH_MGC_59 H... 1421 0.0
gi|13664977|gb|BG613606.1|BG613606 602641959F1 NIH_MGC_61 H... 1421 0.0
gi|13584148|gb|BG576495.1|BG576495 602598552F1 NIH_MGC_87 H... 1405 0.0
gi|13668653|gb|BG617282.1|BG617282 602615306F1 NIH_MGC_76 H... 1370 0.0
gi|12892303|emb|AL552940.1|AL552940 AL552940 LTI_NFL006_PL2... 1342 0.0
gi|13281485|gb|BG388039.1|BG388039 602412885F1 NIH_MGC_92 H... 1334 0.0
gi|13574212|gb|BG566559.1|BG566559 602585587F1 NIH_MGC_76 H... 1322 0.0
gi|13047273|gb|BG290431.1|BG290431 602388279F1 NIH_MGC_93 H... 1316 0.0
gi|13672765|gb|BG621394.1|BG621394 602617948F1 NIH_MGC_79 H... 1310 0.0
gi|13457137|gb|BG495622.1|BG495622 602539957F1 NIH_MGC_59 H... 1279 0.0
gi|12945031|emb|AL579716.1|AL579716 AL579716 LTI_FL012_TC1 ... 1215 0.0
gi|13458168|gb|BG496651.1|BG496651 602537992F1 NIH_MGC_59 H... 1209 0.0
gi|12878925|emb|AL546119.1|AL546119 AL546119 LTI_NFL006_PL2... 1187 0.0
gi|11111112|gb|BF217526.1|BF217526 601885224F1 NIH_MGC_57 H... 1162 0.0
gi|13574437|gb|BG566784.1|BG566784 602585667F1 NIH_MGC_76 H... 1138 0.0
gi|10359779|gb|BE895909.1|BE895909 601432850F1 NIH_MGC_72 H... 1136 0.0
gi|11943020|gb|BF669125.1|BF669125 602119975F1 NIH_MGC_56 H... 1114 0.0
gi|12417036|gb|BG027942.1|BG027942 602294540F1 NIH_MGC_86 H... 1102 0.0
gi|8013169|gb|AW875350.1|AW875350 RC1-PT0009-130400-014-b10... 1100 0.0
gi|9777316|gb|BE548671.1|BE548671 601074578F1 NIH_MGC_12 Ho... 1096 0.0
gi|11154063|gb|BF240140.1|BF240140 601905643F1 NIH_MGC_54 H... 1092 0.0
gi|10889708|gb|BF107182.1|BF107182 601824254F1 NIH_MGC_79 H... 1080 0.0
gi|10330550|gb|BE881774.1|BE881774 601484764F1 NIH_MGC_69 H... 1055 0.0
gi|8146025|gb|AW956342.1|AW956342 EST368412 MAGE resequence... 1047 0.0
gi|13524925|gb|BG533385.1|BG533385 601860775F2 NIH_MGC_76 H... 1043 0.0
gi|10738331|gb|BF030619.1|BF030619 601559988F1 NIH_MGC_58 H... 1037 0.0
gi|11163033|gb|BF247518.1|BF247518 601858547F1 NIH_MGC_58 H... 1019 0.0
gi|11982430|gb|BF697022.1|BF697022 602129407F1 NIH_MGC_56 H... 1011 0.0
gi|12937892|emb|AL576092.1|AL576092 AL576092 LTI_NFL006_PL2... 1009 0.0
gi|1158188|gb|N37046.1|N37046 yy40g06.s1 Soares melanocyte ... 1009 0.0
gi|13527789|gb|BG536244.1|BG536244 602565467F1 NIH_MGC_77 H... 1007 0.0
gi|12335519|gb|BF968304.1|BF968304 602269321F1 NIH_MGC_84 H... 1003 0.0
gi|10201134|gb|BE779936.1|BE779936 601467963F1 NIH_MGC_67 H... 993 0.0
gi|7948662|gb|AW853145.1|AW853145 RC1-CT0249-200400-027-b02... 979 0.0
gi|7456666|gb|AW664126.1|AW664126 hi04f06.x1 NCI_CGAP_GU1 H... 975 0.0
gi|12603373|gb|BG109867.1|BG109867 602279533F1 NIH_MGC_86 H... 967 0.0

gi|1404392|gb|W88681.1|W88681 zh71d08.r1 Soares_fetal_liver... 967 0.0
gi|10889990|gb|BF107464.1|BF107464 601824089F1 NIH_MGC_79 H... 965 0.0
gi|11941446|gb|BF667451.1|BF667451 602121811F1 NIH_MGC_56 H... 959 0.0
gi|12673375|gb|BG166672.1|BG166672 602339069F1 NIH_MGC_89 H... 955 0.0
gi|7949266|gb|AW853521.1|AW853521 RC1-CT0252-140300-026-g05... 940 0.0
gi|10584751|gb|BE971415.1|BE971415 601651403F1 NIH_MGC_81 H... 930 0.0
gi|2903664|gb|AA830565.1|AA830565 oc55a03.s1 NCI_CGAP_GCB1 ... 902 0.0
gi|6921588|gb|AW402833.1|AW402833 UI-HF-BK0-aaq-e-07-0-UI.r... 900 0.0

>gi|14110766|gb|AAE57306.1| Sequence 2 from patent US 6171837

EST Search:

Sequences producing significant alignments: (bits) Value

gi|12381756|gb|BF964481.1|BF964481 RC1-NN0233-311200-016-f0... 86 2e-14
gi|11593828|gb|BF510530.1|BF510530 UI-H-BI4-apa-e-11-0-UI.s... 86 2e-14
gi|11081688|gb|BF195132.1|BF195132 7n15f01.x1 NCI_CGAP_Brn2... 86 2e-14
gi|8908990|gb|BE221672.1|BE221672 hu27e10.x1 NCI_CGAP_Mel15... 86 2e-14
gi|7703339|gb|AW771285.1|AW771285 hn62d04.x1 NCI_CGAP_Kid11... 86 2e-14
gi|6661708|gb|AW274678.1|AW274678 xv32d08.x1 Soares_NFL_T_G... 86 2e-14
gi|5854635|gb|AW005857.1|AW005857 wz80d08.x1 NCI_CGAP_Gas4 ... 86 2e-14
gi|5527702|gb|AI863595.1|AI863595 wj18h11.x1 NCI_CGAP_Kid12... 86 2e-14
gi|5396293|gb|AI809727.1|AI809727 wh77a07.x1 NCI_CGAP_CLL1 ... 86 2e-14
gi|4900121|gb|AI688827.1|AI688827 wd41d07.x1 Soares_NFL_T_G... 86 2e-14
gi|4618930|gb|AI609763.1|AI609763 tf83a04.x1 NCI_CGAP_Brn23... 86 2e-14
gi|4264406|gb|AI418475.1|AI418475 tf74h03.x1 NCI_CGAP_Brn23... 86 2e-14
gi|4114767|gb|AI363146.1|AI363146 qy55a02.x1 NCI_CGAP_Brn23... 86 2e-14
gi|3279324|gb|AI040130.1|AI040130 ox08h01.x1 Soares_fetal_l... 86 2e-14
gi|2656640|gb|AA680173.1|AA680173 zi11b06.s1 Soares_fetal_l... 86 2e-14
gi|2525787|gb|AA621911.1|AA621911 nq30b08.s1 NCI_CGAP_Co10 ... 86 2e-14
gi|1728087|gb|AA156462.1|AA156462 zl51h03.s1 Soares_pregnan... 86 2e-14
gi|1716962|gb|AA147453.1|AA147453 zl51h03.r1 Soares_pregnan... 86 2e-14
gi|1524638|gb|AA046712.1|AA046712 zk62h02.s1 Soares_pregnan... 86 2e-14
gi|1524527|gb|AA046629.1|AA046629 zk62h02.r1 Soares_pregnan... 86 2e-14
gi|1477375|gb|AA016309.1|AA016309 ze38g07.s1 Soares retina ... 86 2e-14
gi|1448465|gb|AA004598.1|AA004598 zh87b01.s1 Soares_fetal_l... 86 2e-14
gi|1190064|gb|N48898.1|N48898 yy77e08.s1 Soares_multiple_sc... 86 2e-14
gi|1188267|gb|N47101.1|N47101 yy85f02.s1 Soares_multiple_sc... 86 2e-14
gi|1059355|gb|H81266.1|H81266 yu74b01.s1 Soares fetal liver... 86 2e-14
gi|1018746|gb|H63945.1|H63945 yr55b01.s1 Soares fetal liver... 86 2e-14
gi|916188|gb|H40136.1|H40136 yp59c04.s1 Soares fetal liver ... 86 2e-14
gi|14292293|gb|BG911817.1|BG911817 602810064F1 NCI_CGAP_Brn... 84 7e-14
gi|2557096|gb|AA633882.1|AA633882 ac32g07.s1 Stratagene hNT... 84 7e-14
gi|2505366|gb|AA618161.1|AA618161 nq14d10.s1 NCI_CGAP_Thy1 ... 84 7e-14
gi|1448549|gb|AA004494.1|AA004494 zh87b01.r1 Soares_fetal_l... 84 7e-14
gi|812358|gb|R50456.1|R50456 yj56e10.r1 Soares breast 2NbHB... 84 7e-14
gi|5592866|gb|AI887702.1|AI887702 wm17d06.x1 NCI_CGAP_Ut4 H... 82 3e-13
gi|1891000|gb|AA256871.1|AA256871 zr81f03.r1 Soares_NhHMPu_... 82 3e-13
gi|14001745|gb|BG722558.1|BG722558 602694526F1 NIH_MGC_97 H... 80 1e-12

>gi|14110767|gb|AAE57307.1| Sequence 3 from patent US 6171837

no DNA sequence available with acc # provided

>gi¦14110768¦gb¦AAE57308.1¦ Sequence 4 from patent US 6171837

no DNA sequence available with acc # provided

>gi¦14110769¦gb¦AAE57309.1¦ Sequence 5 from patent US 6171837

no DNA sequence available with acc # provided

>gi¦3994625¦gb¦AAC88053.1¦AR010436 Sequence 1 from patent US 5756299

EST Search:

Sequences producing significant alignments: (bits) Value

gi¦13413874¦gb¦BG481595.1¦BG481595 602528316F1 NIH_MGC_21 H... 1483 0.0
gi¦14178945¦gb¦BG831358.1¦BG831358 602766220F1 NIH_MGC_42 H... 1463 0.0
gi¦14177680¦gb¦BG830093.1¦BG830093 602764845F1 NIH_MGC_42 H... 1463 0.0
gi¦13404430¦gb¦BG472244.1¦BG472244 602513756F1 NIH_MGC_16 H... 1415 0.0
gi¦14568476¦gb¦BI117575.1¦BI117575 602866754F1 NIH_MGC_7 Ho... 1392 0.0
gi¦13982131¦gb¦BG706614.1¦BG706614 602674104F1 NIH_MGC_96 H... 1354 0.0
gi¦13976241¦gb¦BG703674.1¦BG703674 602686647F1 NIH_MGC_95 H... 1342 0.0
gi¦10390490¦gb¦BE901372.1¦BE901372 601674675F1 NIH_MGC_21 H... 1326 0.0
gi¦12343809¦gb¦BF976594.1¦BF976594 602244271F1 NIH_MGC_48 H... 1300 0.0
gi¦11641972¦gb¦BF568592.1¦BF568592 602184218F1 NIH_MGC_42 H... 1298 0.0
gi¦11970704¦gb¦BF685296.1¦BF685296 602141648F1 NIH_MGC_46 H... 1279 0.0
gi¦11252161¦gb¦BF305282.1¦BF305282 601892747F1 NIH_MGC_17 H... 1279 0.0
gi¦11098442¦gb¦BF204856.1¦BF204856 601867158F1 NIH_MGC_17 H... 1275 0.0
gi¦9137251¦gb¦BE263706.1¦BE263706 601192146F1 NIH_MGC_7 Hom... 1251 0.0
gi¦10404479¦gb¦BE909167.1¦BE909167 601501782F1 NIH_MGC_70 H... 1249 0.0
gi¦11151599¦gb¦BF237681.1¦BF237681 601841865F1 NIH_MGC_46 H... 1247 0.0
gi¦9156256¦gb¦BE281240.1¦BE281240 601155341F1 NIH_MGC_21 Ho... 1247 0.0
gi¦12342418¦gb¦BF975203.1¦BF975203 602244705F1 NIH_MGC_48 H... 1243 0.0
gi¦14058856¦gb¦BG748203.1¦BG748203 602705827F1 NIH_MGC_43 H... 1235 0.0
gi¦11263622¦gb¦BF315274.1¦BF315274 601902672F1 NIH_MGC_19 H... 1211 0.0
gi¦11098117¦gb¦BF204531.1¦BF204531 601868138F1 NIH_MGC_17 H... 1211 0.0
gi¦9133208¦gb¦BE313377.1¦BE313377 601147921F1 NIH_MGC_19 Ho... 1209 0.0
gi¦12683322¦gb¦BG176619.1¦BG176619 602313206F1 NIH_MGC_85 H... 1207 0.0
gi¦9882826¦dbj¦AV661812.1¦AV661812 AV661812 GLC Homo sapien... 1205 0.0
gi¦12615652¦gb¦BG122143.1¦BG122143 602349585F1 NIH_MGC_90 H... 1199 0.0
gi¦11251336¦gb¦BF304588.1¦BF304588 601887980F1 NIH_MGC_17 H... 1174 0.0
gi¦4536632¦gb¦AI573258.1¦AI573258 tn03e05.x1 NCI_CGAP_Brn25... 1170 0.0
gi¦13032709¦gb¦BG283133.1¦BG283133 602406785F1 NIH_MGC_91 H... 1168 0.0
gi¦10346623¦gb¦BE889373.1¦BE889373 601513264F1 NIH_MGC_71 H... 1162 0.0
gi¦13137904¦gb¦BG331552.1¦BG331552 602433326F1 NIH_MGC_18 H... 1160 0.0
gi¦8167102¦gb¦AW975880.1¦AW975880 EST387989 MAGE resequence... 1158 0.0
gi¦9155643¦gb¦BE280635.1¦BE280635 601155778F1 NIH_MGC_21 Ho... 1156 0.0
gi¦11258150¦gb¦BF310575.1¦BF310575 601895295F2 NIH_MGC_19 H... 1146 0.0
gi¦8147508¦gb¦AW957825.1¦AW957825 EST369895 MAGE resequence... 1130 0.0
gi¦13340715¦gb¦BG434209.1¦BG434209 602506154F1 NIH_MGC_79 H... 1114 0.0
gi¦10216172¦gb¦BE794974.1¦BE794974 601589746F1 NIH_MGC_7 Ho... 1102 0.0
gi¦11949082¦gb¦BF675187.1¦BF675187 602138110F1 NIH_MGC_83 H... 1088 0.0
gi¦4194952¦gb¦AI382182.1¦AI382182 te70b01.x1 Soares_NFL_T_G... 1086 0.0
gi¦8147585¦gb¦AW957902.1¦AW957902 EST369972 MAGE resequence... 1084 0.0
gi¦14620169¦gb¦BI160168.1¦BI160168 602864026F1 NIH_MGC_42 H... 1076 0.0
gi¦6588561¦gb¦AW245568.1¦AW245568 2822726.5prime NIH_MGC_7 ... 1076 0.0
gi¦9137978¦gb¦BE264422.1¦BE264422 601191730F1 NIH_MGC_7 Hom... 1065 0.0
gi¦6588571¦gb¦AW245578.1¦AW245578 2822726.3prime NIH_MGC_7 ... 1061 0.0

gi|11617689|gb|BF530338.1|BF530338 602071618F1 NCI_CGAP_Brn... 1055 0.0
gi|14320386|gb|BG925863.1|BG925863 HNC21-1-B11.R HNC (Human... 1053 0.0
gi|2726589|gb|AA714315.1|AA714315 nw06c05.s1 NCI_CGAP_SS1 H... 1015 0.0
gi|2537901|gb|AA625514.1|AA625514 af72e06.r1 Soares_NhHMPu_... 1007 0.0
gi|2155441|gb|AA442766.1|AA442766 zv60c08.s1 Soares_testis_... 1007 0.0
gi|2464707|gb|AA613669.1|AA613669 no39h10.s1 NCI_CGAP_Pr23 ... 997 0.0
gi|13137575|gb|BG331137.1|BG331137 602431839F1 NIH_MGC_18 H... 993 0.0
gi|1211129|gb|N63300.1|N63300 yy71a11.s1 Soares_multiple_sc... 993 0.0
gi|1148734|gb|N30214.1|N30214 yw83h09.s1 Soares_placenta_8t... 989 0.0
gi|9866354|dbj|AV645340.1|AV645340 AV645340 GLA Homo sapien... 983 0.0
gi|12412330|gb|BG025585.1|BG025585 602274505F1 NIH_MGC_85 H... 981 0.0
gi|3230271|gb|AI015935.1|AI015935 ov26c11.x1 Soares_testis_... 977 0.0
gi|9882981|dbj|AV661967.1|AV661967 AV661967 GLC Homo sapien... 975 0.0
gi|6399823|gb|AW168298.1|AW168298 xg62g11.x1 NCI_CGAP_Ut4 H... 969 0.0
gi|3840076|gb|AI244679.1|AI244679 qj97c09.x1 NCI_CGAP_Kid3 ... 969 0.0
gi|2243999|gb|AA507560.1|AA507560 ng88h09.s1 NCI_CGAP_Pr6 H... 965 0.0
gi|14058983|gb|BG748330.1|BG748330 602706579F1 NIH_MGC_43 H... 963 0.0
gi|5838015|gb|AI991112.1|AI991112 wu38c07.x1 Soares_Dieckgr... 954 0.0
gi|10216094|gb|BE794896.1|BE794896 601589638F1 NIH_MGC_7 Ho... 948 0.0
gi|9140017|gb|BE266440.1|BE266440 601193195F1 NIH_MGC_7 Hom... 938 0.0
gi|1210879|gb|N63050.1|N63050 yy70g11.s1 Soares_multiple_sc... 926 0.0
gi|8750451|gb|BE207053.1|BE207053 ba09d08.y1 NIH_MGC_7 Homo... 920 0.0
gi|5395010|gb|AI808444.1|AI808444 wf94h12.x1 Soares_NSF_F8_... 918 0.0
gi|10813709|dbj|AV716557.1|AV716557 AV716557 DCB Homo sapie... 914 0.0
gi|2883312|gb|AA813327.1|AA813327 ai81a07.s1 Soares_testis_... 908 0.0
gi|10144813|gb|BE730821.1|BE730821 601570791F1 NIH_MGC_21 H... 906 0.0
gi|1193558|gb|N52392.1|N52392 yv49g09.s1 Soares fetal liver... 898 0.0
gi|2138860|gb|AA433946.1|AA433946 zw52g09.s1 Soares_total_f... 888 0.0
gi|4489892|gb|AI557529.1|AI557529 pt2.1-06.D05.r tumor2 Hom... 884 0.0
gi|12431844|gb|BG036553.1|BG036553 602326326F1 NIH_MGC_91 H... 880 0.0
gi|2221812|gb|AA492250.1|AA492250 ng79d12.s1 NCI_CGAP_Pr6 H... 876 0.0
gi|3803259|gb|AI221056.1|AI221056 qg09c12.x1 Soares_placent... 874 0.0
gi|3422302|gb|AI083879.1|AI083879 qf22c05.x1 NCI_CGAP_Brn25... 874 0.0
gi|11955171|gb|BF681276.1|BF681276 602155553F1 NIH_MGC_83 H... 872 0.0
gi|5591001|gb|AI885837.1|AI885837 wl62c01.x1 NCI_CGAP_Brn25... 866 0.0
gi|2159247|gb|AA446582.1|AA446582 zw84d08.s1 Soares_total_f... 862 0.0
gi|2341742|gb|AA568688.1|AA568688 nm06f08.s1 NCI_CGAP_Co10 ... 856 0.0
gi|4833888|gb|AI669114.1|AI669114 wb80e10.x1 NCI_CGAP_Pr28 ... 854 0.0
gi|10293455|dbj|AV691592.1|AV691592 AV691592 GKC Homo sapie... 839 0.0
gi|3988221|gb|AI304532.1|AI304532 qo55a06.x1 NCI_CGAP_Co8 H... 833 0.0
gi|2731990|gb|AA720021.1|AA720021 zh22e05.s1 Soares_pineal_... 831 0.0
gi|1965893|gb|AA313563.1|AA313563 EST185441 Colon carcinoma... 831 0.0
gi|7316134|gb|AW615416.1|AW615416 ba09d08.x1 NIH_MGC_7 Homo... 821 0.0
gi|9875231|dbj|AV654217.1|AV654217 AV654217 GLC Homo sapien... 815 0.0
gi|4489893|gb|AI557530.1|AI557530 pt2.1-06.D05b.r tumor2 Ho... 811 0.0
gi|4598919|gb|AI589871.1|AI589871 tm81d01.x1 NCI_CGAP_Brn25... 803 0.0

>gi¦3994626¦gb¦AAC88054.1¦AR010437 Sequence 3 from patent US 5756299

no DNA sequence available with acc # provided

>gi¦3994627¦gb¦AAC88055.1¦AR010438 Sequence 4 from patent US 5756299

no DNA sequence available with acc # provided

>gi¦3994628¦gb¦AAC88056.1¦AR010439 Sequence 5 from patent US 5756299

no DNA sequence available with acc # provided

>gi¦10049861¦gb¦AAE26768.1¦ Sequence 1 from patent US 5952209

EST Search:

Sequences producing significant alignments: (bits) Value

gi¦10850515¦dbj¦AV732970.1¦AV732970 AV732970 cdA Homo sapie... 80 2e-12
gi¦14051966¦gb¦BG741313.1¦BG741313 602634450F1 NCI_CGAP_Skn... 78 8e-12
gi¦14051796¦gb¦BG741143.1¦BG741143 602631813F1 NCI_CGAP_Skn... 78 8e-12
gi¦8158534¦gb¦AW968693.1¦AW968693 EST380769 MAGE resequence... 78 8e-12
gi¦7846487¦gb¦AW794617.1¦AW794617 RC6-UM0014-290300-013-A08... 78 8e-12
gi¦6924798¦gb¦AW405741.1¦AW405741 UI-HF-BL0-abv-g-11-0-UI.r... 78 8e-12
gi¦6463032¦gb¦AW188672.1¦AW188672 xk02a07.x1 NCI_CGAP_Co18 ... 78 8e-12
gi¦2458420¦gb¦AA609992.1¦AA609992 af18a10.s1 Soares_testis_... 78 8e-12
gi¦2210648¦gb¦AA481096.1¦AA481096 aa29b12.r1 NCI_CGAP_GCB1 ... 78 8e-12
gi¦1957157¦gb¦AA304808.1¦AA304808 EST175827 Monocytes, stim... 78 8e-12
gi¦1291544¦gb¦W17165.1¦W17165 zb12g01.r1 Soares_fetal_lung_... 78 8e-12
gi¦11594354¦gb¦BF511056.1¦BF511056 UI-H-BI4-apl-h-02-0-UI.s... 76 3e-11
gi¦7280943¦gb¦AW593685.1¦AW593685 xl97h06.x1 NCI_CGAP_Ut1 H... 76 3e-11
gi¦7246189¦gb¦AW574650.1¦AW574650 UI-HF-BL0-abv-g-11-0-UI.s... 76 3e-11
gi¦6652091¦gb¦AW059769.1¦AW059769 LE4e05.yg DNC15 Homo sapi... 76 3e-11
gi¦5809845¦gb¦AI982593.1¦AI982593 wt53b01.x1 NCI_CGAP_Pan1 ... 76 3e-11
gi¦5803948¦gb¦AI978918.1¦AI978918 wr61h01.x1 NCI_CGAP_Ut1 H... 76 3e-11
gi¦4457857¦gb¦AI540484.1¦AI540484 tq24e12.x1 NCI_CGAP_Ut1 H... 76 3e-11
gi¦4110322¦gb¦AI358701.1¦AI358701 qx14a10.x1 NCI_CGAP_Lym12... 76 3e-11
gi¦2563996¦gb¦AA640217.1¦AA640217 03 subtracted 3' EST libr... 76 3e-11
gi¦2457366¦gb¦AA608938.1¦AA608938 af03f01.s1 Soares_testis_... 76 3e-11
gi¦2210593¦gb¦AA481041.1¦AA481041 aa29b12.s1 NCI_CGAP_GCB1 ... 76 3e-11
gi¦1934027¦gb¦AA287021.1¦AA287021 zs57c03.s1 NCI_CGAP_GCB1 ... 76 3e-11

>gi¦10049862¦gb¦AAE26769.1¦ Sequence 3 from patent US 5952209

no DNA sequence available with acc # provided

>gi¦5942061¦gb¦AAE01593.1¦ Sequence 1 from patent US 5858750

no DNA sequence available with acc # provided

>gi|5942061|gb|AAE01593.1| Sequence 1 from patent US 5858750

no DNA sequence available with acc # provided

>gi|5942062|gb|AAE01594.1| Sequence 3 from patent US 5858750

no DNA sequence available with acc # provided

>gi|14272566|emb|CAC39721.1| unnamed protein product [Homo sapiens]

EST Search
Sequences producing significant alignments: (bits) Value

gi|14169716|gb|BG822129.1|BG822129 602726271F1 NIH_MGC_15 H... 1518 0.0
gi|14568272|gb|BI117371.1|BI117371 602867919F1 NIH_MGC_7 Ho... 1451 0.0
gi|9803527|gb|BE559808.1|BE559808 601346972F1 NIH_MGC_8 Hom... 1404 0.0
gi|10150139|gb|BE736147.1|BE736147 601307226F1 NIH_MGC_39 H... 1380 0.0
gi|12041329|gb|BF725418.1|BF725418 bx15f11.y1 Human Iris cD... 1300 0.0
gi|5545428|gb|AI871379.1|AI871379 wl81d08.x1 NCI_CGAP_Brn25... 1298 0.0
gi|10162791|gb|BE748799.1|BE748799 601572007T1 NIH_MGC_55 H... 1296 0.0
gi|10162316|gb|BE748324.1|BE748324 601572007F1 NIH_MGC_55 H... 1255 0.0
gi|12758392|gb|BG248576.1|BG248576 602400744F1 NIH_MGC_15 H... 1201 0.0
gi|11251209|gb|BF304472.1|BF304472 601887831F1 NIH_MGC_17 H... 1197 0.0
gi|9803869|gb|BE560051.1|BE560051 601347483F1 NIH_MGC_8 Hom... 1197 0.0
gi|12670294|gb|BG163591.1|BG163591 602338741F1 NIH_MGC_89 H... 1191 0.0
gi|5178261|gb|AI762594.1|AI762594 wi56b09.x1 NCI_CGAP_Co16 ... 1185 0.0
gi|9122527|gb|BE252388.1|BE252388 601117771F1 NIH_MGC_16 Ho... 1170 0.0
gi|14620762|gb|BI160761.1|BI160761 602864839F1 NIH_MGC_42 H... 1148 0.0
gi|6709871|gb|AW300271.1|AW300271 xs58h07.x1 NCI_CGAP_Kid11... 1144 0.0
gi|14057456|gb|BG746803.1|BG746803 602704139F1 NIH_MGC_15 H... 1132 0.0
gi|5108921|gb|AI740633.1|AI740633 wg23g01.x1 Soares_NSF_F8_... 1090 0.0
gi|13343784|gb|BG437278.1|BG437278 602490558F1 NIH_MGC_18 H... 1068 0.0
gi|6570140|gb|AW237763.1|AW237763 xm81b04.x1 NCI_CGAP_Kid11... 1059 0.0
gi|4372796|gb|AI479628.1|AI479628 tm32d07.x1 NCI_CGAP_CLL1 ... 1051 0.0
gi|5540213|gb|AI867197.1|AI867197 wa01c10.x1 NCI_CGAP_Kid11... 1045 0.0
gi|13792425|gb|BG655016.1|BG655016 ib44h01.y1 HR85 islet Ho... 1041 0.0
gi|11448154|gb|BF435839.1|BF435839 nab42e01.x1 Soares_NSF_F... 1035 0.0
gi|10938383|gb|BF108693.1|BF108693 7l44e02.x1 Soares_NSF_F8... 1033 0.0
gi|8169897|gb|AW978626.1|AW978626 EST390735 MAGE resequence... 1031 0.0
gi|10036058|gb|BE675517.1|BE675517 7f10f02.x1 NCI_CGAP_CLL1... 1013 0.0
gi|5933828|gb|AW058189.1|AW058189 wv83h01.x1 Soares_thymus_... 1011 0.0
gi|4190356|gb|AI380503.1|AI380503 tf95d02.x1 NCI_CGAP_CLL1 ... 1007 0.0
gi|5113008|gb|AI744631.1|AI744631 wg04g09.x1 Soares_NSF_F8_... 1005 0.0
gi|5450901|gb|AI830241.1|AI830241 wj78h11.x1 NCI_CGAP_Lu19 ... 1003 0.0
gi|4598007|gb|AI588959.1|AI588959 tk15d10.x1 Soares_NhHMPu_... 999 0.0
gi|9970354|gb|BE646054.1|BE646054 7e92d04.x1 NCI_CGAP_CLL1 ... 995 0.0
gi|5232040|gb|AI765531.1|AI765531 wi81b11.x1 NCI_CGAP_Kid12... 973 0.0
gi|4113265|gb|AI361644.1|AI361644 qy86d07.x1 NCI_CGAP_Brn25... 971 0.0
gi|11082796|gb|BF195666.1|BF195666 7n86g02.x1 NCI_CGAP_Ov18... 961 0.0
gi|11682572|gb|BF590248.1|BF590248 nab22a02.x1 Soares_NSF_F... 957 0.0
gi|4311958|gb|AI457940.1|AI457940 tj55h09.x1 Soares_NSF_F8_... 957 0.0
gi|6710832|gb|AW301155.1|AW301155 xs57a11.x1 NCI_CGAP_Kid11... 950 0.0
gi|5663387|gb|AI927423.1|AI927423 wo75e11.x1 NCI_CGAP_Pr22 ... 950 0.0
gi|5766733|gb|AI969915.1|AI969915 wq77e03.x1 NCI_CGAP_Pr28 ... 948 0.0
gi|2463985|gb|AA612947.1|AA612947 nq38e11.s1 NCI_CGAP_Co10 ... 948 0.0
gi|5664220|gb|AI928256.1|AI928256 wo67a08.x1 NCI_CGAP_Pr22 ... 946 0.0
gi|6746198|gb|AW316942.1|AW316942 xw13a08.x1 NCI_CGAP_Brn53... 934 0.0
gi|1377082|gb|W68057.1|W68057 zd42h12.r1 Soares_fetal_heart... 930 0.0
gi|1959057|gb|AA306658.1|AA306658 EST177664 Jurkat T-cells ... 918 0.0
gi|5660470|gb|AI924506.1|AI924506 wn61a01.x1 NCI_CGAP_Lu19 ... 912 0.0
gi|3095277|gb|AA937166.1|AA937166 ok13a08.s1 Soares_NSF_F8_... 908 0.0
gi|2986172|gb|AA877095.1|AA877095 ob09d05.s1 NCI_CGAP_Kid3 ... 900 0.0

>gi|5942062|gb|AAE01594.1| Sequence 3 from patent US 5858750

No cDNA sequence available with accession # provided

>gi|12821846|gb|AAE48287.1| Sequence 2 from patent US 6106829

No cDNA sequence available with accession # provided

>gi|11340737|emb|CAC17063.1| unnamed protein product [Homo sapiens]

EST search

Sequences producing significant alignments: (bits) Value

gi|13401922|gb|BG469647.1|BG469647 602534103F1 NIH_MGC_15 H... 1550 0.0
gi|13746560|gb|BG220539.1|BG220539 RST40325 Athersys RAGE L... 1483 0.0
gi|13963233|gb|BG697241.1|BG697241 602660481F1 NCI_CGAP_Skn... 1463 0.0
gi|14053553|gb|BG742900.1|BG742900 602632481F1 NCI_CGAP_Skn... 1457 0.0
gi|13967002|gb|BG699072.1|BG699072 602678713F1 NIH_MGC_95 H... 1439 0.0
gi|14053781|gb|BG743128.1|BG743128 602634270F1 NCI_CGAP_Skn... 1427 0.0
gi|13410718|gb|BG478523.1|BG478523 602524002F1 NIH_MGC_20 H... 1419 0.0
gi|14064290|gb|BG753637.1|BG753637 602732827F1 NIH_MGC_43 H... 1409 0.0
gi|9146489|gb|BE272160.1|BE272160 601141656F1 NIH_MGC_9 Hom... 1409 0.0
gi|14047524|gb|BG777207.1|BG777207 602664432F1 NIH_MGC_59 H... 1402 0.0
gi|14651659|gb|BI196639.1|BI196639 602755427F1 NIH_MGC_19 H... 1388 0.0
gi|14059064|gb|BG748411.1|BG748411 602705974F1 NIH_MGC_43 H... 1380 0.0
gi|13336094|gb|BG429588.1|BG429588 602501268F1 NIH_MGC_75 H... 1368 0.0
gi|9124275|gb|BE253854.1|BE253854 601112818F1 NIH_MGC_16 Ho... 1364 0.0
gi|12604238|gb|BG110732.1|BG110732 602279029F1 NIH_MGC_86 H... 1358 0.0
gi|12607924|gb|BG114418.1|BG114418 602285710F1 NIH_MGC_86 H... 1348 0.0
gi|13527202|gb|BG535657.1|BG535657 602563366F1 NIH_MGC_77 H... 1344 0.0
gi|13289966|gb|BG396518.1|BG396518 602459353F1 NIH_MGC_16 H... 1342 0.0
gi|10399800|gb|BE906369.1|BE906369 601498517F1 NIH_MGC_70 H... 1340 0.0
gi|10156435|gb|BE742443.1|BE742443 601575210F1 NIH_MGC_9 Ho... 1330 0.0
gi|6361758|gb|AI305108.1|AI305108 HA2404 Human fetal liver ... 1316 0.0
gi|13570738|gb|BG563086.1|BG563086 602581878F1 NIH_MGC_76 H... 1314 0.0
gi|14565107|gb|BI114206.1|BI114206 602862564F1 NIH_MGC_17 H... 1302 0.0
gi|14566335|gb|BI115434.1|BI115434 602863311F1 NIH_MGC_17 H... 1296 0.0
gi|6359266|gb|AI064994.1|AI064994 HA0821 Human fetal liver ... 1296 0.0
gi|9186637|gb|BE302889.1|BE302889 ba70g10.y1 NIH_MGC_20 Hom... 1289 0.0
gi|14566302|gb|BI115401.1|BI115401 602863260F1 NIH_MGC_17 H... 1279 0.0
gi|4763039|gb|AI659469.1|AI659469 tu30g07.x1 NCI_CGAP_Pr28 ... 1271 0.0
gi|9328145|gb|BE382780.1|BE382780 601298459F1 NIH_MGC_19 Ho... 1259 0.0
gi|10160188|gb|BE746196.1|BE746196 601578644F1 NIH_MGC_9 Ho... 1253 0.0
gi|13459320|gb|BG497803.1|BG497803 602543080F1 NIH_MGC_60 H... 1251 0.0
gi|12761697|gb|BG251881.1|BG251881 602364502F1 NIH_MGC_90 H... 1251 0.0
gi|13999085|gb|BG719898.1|BG719898 602691430F1 NIH_MGC_97 H... 1247 0.0
gi|13969001|gb|BG700048.1|BG700048 602681055F1 NIH_MGC_95 H... 1241 0.0
gi|12678524|gb|BG171821.1|BG171821 602322603F1 NIH_MGC_89 H... 1237 0.0
gi|9179232|gb|BE295680.1|BE295680 601175688F1 NIH_MGC_17 Ho... 1235 0.0
gi|13523981|gb|BG532442.1|BG532442 602561968F1 NIH_MGC_61 H... 1227 0.0
gi|13406852|gb|BG474575.1|BG474575 602517363F1 NIH_MGC_16 H... 1227 0.0

gi|9346825|gb|BE410375.1|BE410375 601302363F1 NIH_MGC_21 Ho... 1219 0.0
gi|12609069|gb|BG115563.1|BG115563 602317253F1 NIH_MGC_88 H... 1213 0.0
gi|2398040|gb|AA587226.1|AA587226 nn82b08.s1 NCI_CGAP_Co9 H... 1213 0.0
gi|13534026|gb|BG541793.1|BG541793 602569677F1 NIH_MGC_77 H... 1211 0.0
gi|12770117|gb|BG260301.1|BG260301 602371417F1 NIH_MGC_93 H... 1203 0.0
gi|10741086|gb|BF033374.1|BF033374 601458081F1 NIH_MGC_66 H... 1199 0.0
gi|9323581|gb|BE378216.1|BE378216 601237991F1 NIH_MGC_44 Ho... 1199 0.0
gi|14471561|gb|BI064034.1|BI064034 IL3-UT0119-120401-430-G0... 1197 0.0
gi|9722042|gb|BE514828.1|BE514828 601316764F1 NIH_MGC_9 Hom... 1191 0.0
gi|9339021|gb|BE393656.1|BE393656 601310379F1 NIH_MGC_44 Ho... 1187 0.0
gi|11952823|gb|BF678928.1|BF678928 602153555F1 NIH_MGC_83 H... 1183 0.0
gi|6568025|gb|AW235636.1|AW235636 xn20g09.x1 NCI_CGAP_Kid11... 1168 0.0
gi|13972135|gb|BG701616.1|BG701616 602682503F1 NIH_MGC_95 H... 1158 0.0
gi|8144363|gb|AW954680.1|AW954680 EST366750 MAGE resequence... 1150 0.0
gi|9331236|gb|BE385871.1|BE385871 601275933F1 NIH_MGC_20 Ho... 1144 0.0
gi|12687397|gb|BG180694.1|BG180694 602329481F1 NIH_MGC_91 H... 1142 0.0
gi|11953928|gb|BF680033.1|BF680033 602154752F1 NIH_MGC_83 H... 1132 0.0
gi|13458797|gb|BG497280.1|BG497280 602537844F1 NIH_MGC_59 H... 1128 0.0
gi|9179583|gb|BE296026.1|BE296026 601175058F1 NIH_MGC_17 Ho... 1128 0.0
gi|9770617|gb|BE541972.1|BE541972 601064273F1 NIH_MGC_10 Ho... 1126 0.0
gi|12612166|gb|BG118660.1|BG118660 602348226F1 NIH_MGC_90 H... 1124 0.0
gi|1544739|gb|AA053804.1|AA053804 ze25e09.s1 Soares_fetal_h... 1120 0.0
gi|6361052|gb|AI174674.1|AI174674 HA2365 Human fetal liver ... 1118 0.0
gi|13282164|gb|BG388718.1|BG388718 602414406F1 NIH_MGC_92 H... 1116 0.0
gi|5080879|gb|AF063505.1|AF063505 AF063505 Homo sapiens lib... 1106 0.0
gi|6359496|gb|AI110631.1|AI110631 HA0057 Human fetal liver ... 1106 0.0
gi|11952959|gb|BF679064.1|BF679064 602153322F1 NIH_MGC_83 H... 1094 0.0
gi|11954261|gb|BF680366.1|BF680366 602154150F1 NIH_MGC_83 H... 1092 0.0
gi|2167857|gb|AA454188.1|AA454188 zx48a12.s1 Soares_testis_... 1088 0.0
gi|13336068|gb|BG429562.1|BG429562 602501238F1 NIH_MGC_75 H... 1076 0.0
gi|11613456|gb|BF526180.1|BF526180 602071089F1 NCI_CGAP_Brn... 1076 0.0
gi|11954238|gb|BF680343.1|BF680343 602154124F1 NIH_MGC_83 H... 1070 0.0
gi|12062595|gb|BF735895.1|BF735895 QV1-KT0023-131100-480-b0... 1068 0.0
gi|2154395|gb|AA442517.1|AA442517 zv68a01.r1 Soares_total_f... 1068 0.0
gi|13727617|gb|BG205930.1|BG205930 RST25365 Athersys RAGE L... 1067 0.0
gi|12062768|gb|BF736094.1|BF736094 QV1-KT0023-131100-475-h0... 1067 0.0
gi|5839186|gb|AI992281.1|AI992281 ws41g11.x1 NCI_CGAP_Brn25... 1065 0.0
gi|14471624|gb|BI064110.1|BI064110 IL3-UT0119-170401-458-F0... 1063 0.0
gi|12158715|gb|BF820301.1|BF820301 CM0-RT0018-181100-706-e0... 1063 0.0
gi|11947983|gb|BF674088.1|BF674088 602137489F1 NIH_MGC_83 H... 1059 0.0
gi|5864305|gb|AW015548.1|AW015548 UI-H-BI0p-aau-e-01-0-UI.s... 1059 0.0
gi|14178068|gb|BG830481.1|BG830481 602767043F1 NIH_MGC_42 H... 1057 0.0
gi|5767638|gb|AI970812.1|AI970812 wr20b02.x1 NCI_CGAP_Pr28 ... 1057 0.0
gi|11954070|gb|BF680175.1|BF680175 602154923F1 NIH_MGC_83 H... 1055 0.0
gi|11947422|gb|BF673610.1|BF673610 602136021F1 NIH_MGC_83 H... 1055 0.0
gi|9135943|gb|BE262703.1|BE262703 601146057F1 NIH_MGC_19 Ho... 1055 0.0
gi|5663000|gb|AI927036.1|AI927036 wo87b07.x1 NCI_CGAP_Kid11... 1055 0.0
gi|12523600|gb|BG057848.1|BG057848 naf13d09.x1 Soares_NPBMC... 1051 0.0
gi|11107340|gb|BF213754.1|BF213754 601847654F1 NIH_MGC_55 H... 1051 0.0
gi|12062604|gb|BF735904.1|BF735904 QV1-KT0023-131100-480-h0... 1047 0.0
gi|11947265|gb|BF673370.1|BF673370 602135837F1 NIH_MGC_83 H... 1047 0.0
gi|4897519|gb|AI686225.1|AI686225 tu40f05.x1 NCI_CGAP_Pr28 ... 1045 0.0
gi|2703194|gb|AA700231.1|AA700231 zj52f03.s1 Soares_fetal_l... 1045 0.0
gi|13714218|gb|BG192531.1|BG192531 RST11646 Athersys RAGE L... 1043 0.0
gi|9189288|gb|BE336903.1|BE336903 bb68f05.y1 NIH_MGC_9 Homo... 1043 0.0
gi|5364540|gb|AI799068.1|AI799068 we98b05.x1 Soares_NFL_T_G... 1041 0.0
gi|10348906|gb|BE890514.1|BE890514 601431585F1 NIH_MGC_72 H... 1037 0.0

gi|5768230|gb|AI971404.1|AI971404 wr04e08.x1 NCI_CGAP_GC6 H... 1033 0.0
gi|14471659|gb|BI064132.1|BI064132 IL3-UT0119-170401-459-H0... 1025 0.0
gi|7280592|gb|AW593334.1|AW593334 hg13d03.x1 Soares_NFL_T_G... 1023 0.0
gi|10587293|gb|BE973957.1|BE973957 601680275F1 NIH_MGC_83 H... 1021 0.0
gi|14565160|gb|BI114259.1|BI114259 602862449F1 NIH_MGC_17 H... 1017 0.0Formularende

>gi|10045089|emb|CAC07797.1| unnamed protein product [unidentified]

EST search:

Sequences producing significant alignments: (bits) Value

gi|12797915|emb|AL534422.1|AL534422 AL534422 LTI_FL013_FBm... 1756 0.0
gi|12929551|emb|AL571847.1|AL571847 AL571847 LTI_NFL006_PL2... 1731 0.0
gi|12795330|emb|AL531837.1|AL531837 AL531837 LTI_NFL001_NBC... 1659 0.0
gi|13908294|gb|BG676897.1|BG676897 602623506F1 NCI_CGAP_Skn... 1624 0.0
gi|12914346|emb|AL564189.1|AL564189 AL564189 LTI_NFL001_NBC... 1602 0.0
gi|12879740|emb|AL546532.1|AL546532 AL546532 LTI_NFL006_PL2... 1540 0.0
gi|10948684|dbj|AU123968.1|AU123968 AU123968 NT2RM2 Homo sa... 1479 0.0
gi|10949847|dbj|AU125131.1|AU125131 AU125131 NT2RM4 Homo sa... 1471 0.0
gi|10992681|dbj|AU132327.1|AU132327 AU132327 NT2RP3 Homo sa... 1453 0.0
gi|3214525|gb|AI005015.1|AI005015 ou91a01.x1 NCI_CGAP_Kid3 ... 1451 0.0
gi|3674126|gb|AI146444.1|AI146444 qb93a03.x1 Soares_fetal_h... 1425 0.0
gi|3412550|gb|AI078142.1|AI078142 oz30b04.x1 Soares_total_f... 1417 0.0
gi|13721603|gb|BG199916.1|BG199916 RST19212 Athersys RAGE L... 1413 0.0
gi|5409861|emb|AL040917.1|AL040917 DKFZp434J2215_s1 434 (sy... 1396 0.0
gi|13911524|gb|BG680127.1|BG680127 602628285F1 NCI_CGAP_Skn... 1394 0.0
gi|10991451|dbj|AU131097.1|AU131097 AU131097 NT2RP3 Homo sa... 1390 0.0
gi|10991758|dbj|AU131404.1|AU131404 AU131404 NT2RP3 Homo sa... 1362 0.0
gi|10795143|dbj|AV713626.1|AV713626 AV713626 DCB Homo sapie... 1348 0.0
gi|11004302|dbj|AU142781.1|AU142781 AU142781 Y79AA1 Homo sa... 1344 0.0
gi|10932266|dbj|AU117308.1|AU117308 AU117308 HEMBA1 Homo sa... 1338 0.0
gi|10996985|dbj|AU136446.1|AU136446 AU136446 PLACE1 Homo sa... 1336 0.0
gi|9769065|gb|BE540420.1|BE540420 601065826F1 NIH_MGC_10 Ho... 1332 0.0
gi|10144826|gb|BE730834.1|BE730834 601569914F1 NIH_MGC_21 H... 1322 0.0
gi|12429277|gb|BG035291.1|BG035291 602324913F1 NIH_MGC_90 H... 1320 0.0
gi|3002065|gb|AA886957.1|AA886957 oi14e10.s1 NCI_CGAP_GC4 H... 1314 0.0
gi|8169585|gb|AW978321.1|AW978321 EST390430 MAGE resequence... 1306 0.0
gi|10365912|gb|BE898933.1|BE898933 601682360F1 NIH_MGC_9 Ho... 1302 0.0
gi|10992834|dbj|AU132480.1|AU132480 AU132480 NT2RP3 Homo sa... 1292 0.0
gi|14512082|gb|BI093752.1|BI093752 602860460F1 NIH_MGC_10 H... 1283 0.0
gi|10579372|gb|BE968667.1|BE968667 601650086F1 NIH_MGC_74 H... 1271 0.0
gi|6439061|gb|AW173113.1|AW173113 xj83d12.x1 Soares_NFL_T_G... 1271 0.0
gi|10352702|gb|BE892403.1|BE892403 601433879F1 NIH_MGC_72 H... 1259 0.0
gi|11264224|gb|BF315938.1|BF315938 601895882F1 NIH_MGC_19 H... 1247 0.0
gi|10355660|gb|BE893865.1|BE893865 601436228F1 NIH_MGC_72 H... 1221 0.0
gi|10321137|gb|BE872361.1|BE872361 601448614F1 NIH_MGC_65 H... 1215 0.0
gi|10038238|gb|BE677697.1|BE677697 7d90e10.x1 Lupski_dorsal... 1211 0.0
gi|10098245|gb|BE710071.1|BE710071 IL3-HT0618-030800-233-G0... 1209 0.0
gi|10725045|dbj|AV707780.1|AV707780 AV707780 ADB Homo sapie... 1201 0.0
gi|13704200|gb|BG182513.1|BG182513 RST1389 Athersys RAGE Li... 1191 0.0
gi|11283822|gb|BF337571.1|BF337571 602035323F1 NCI_CGAP_Brn... 1191 0.0
gi|5393242|gb|AI806676.1|AI806676 wf35d04.x1 Soares_NFL_T_G... 1191 0.0
gi|12416699|gb|BG027664.1|BG027664 602294679F1 NIH_MGC_86 H... 1183 0.0
gi|4875177|gb|AI674697.1|AI674697 wd19d06.x1 Soares_NFL_T_G... 1183 0.0
gi|10098237|gb|BE710063.1|BE710063 IL3-HT0618-030800-233-C0... 1172 0.0

gi|6661159|gb|AW274129.1|AW274129 xv27b02.x1 Soares_NFL_T_G... 1172 0.0
gi|1799096|gb|AA203386.1|AA203386 zx57f11.r1 Soares_fetal_l... 1170 0.0
gi|5393220|gb|AI806654.1|AI806654 wf35b04.x1 Soares_NFL_T_G... 1168 0.0
gi|12101942|gb|BF796888.1|BF796888 602258274F1 NIH_MGC_85 H... 1166 0.0
gi|10965228|gb|BF126270.1|BF126270 601650451F1 NIH_MGC_76 H... 1154 0.0
gi|11968943|gb|BF683535.1|BF683535 602139737F1 NIH_MGC_46 H... 1144 0.0
gi|2992678|gb|AA883079.1|AA883079 am24a03.s1 Soares_NFL_T_G... 1138 0.0
gi|10823746|dbj|AV721848.1|AV721848 AV721848 HTB Homo sapie... 1136 0.0
gi|4893253|gb|AI683071.1|AI683071 tx01b04.x1 NCI_CGAP_Ut4 H... 1134 0.0
gi|10951089|dbj|AU126373.1|AU126373 AU126373 NT2RP1 Homo sa... 1132 0.0
gi|10995386|dbj|AU134847.1|AU134847 AU134847 PLACE1 Homo sa... 1130 0.0
gi|13050584|gb|BG292110.1|BG292110 602386409F1 NIH_MGC_93 H... 1126 0.0
gi|11978501|gb|BF693093.1|BF693093 602080115F1 NIH_MGC_81 H... 1126 0.0
gi|4610274|gb|AI601245.1|AI601245 ar88b08.x1 Barstead colon... 1122 0.0
gi|12614085|gb|BG120576.1|BG120576 602346709F1 NIH_MGC_90 H... 1118 0.0
gi|6451107|gb|AW182647.1|AW182647 xj45a04.x1 Soares_NFL_T_G... 1112 0.0
gi|9132373|gb|BE312992.1|BE312992 601150276F1 NIH_MGC_19 Ho... 1110 0.0
gi|10299269|dbj|AV697406.1|AV697406 AV697406 GKC Homo sapie... 1104 0.0
gi|12040732|gb|BF724821.1|BF724821 bx09b01.y1 Human Iris cD... 1098 0.0
gi|10825009|dbj|AV722480.1|AV722480 AV722480 HTB Homo sapie... 1088 0.0
gi|13980573|gb|BG705833.1|BG705833 602669317F1 NIH_MGC_96 H... 1082 0.0
gi|12674928|gb|BG168225.1|BG168225 602339543F1 NIH_MGC_89 H... 1082 0.0
gi|2185694|gb|AA460574.1|AA460574 zx60a12.r1 Soares_testis_... 1080 0.0
gi|8149925|gb|AW960241.1|AW960241 EST372312 MAGE resequence... 1076 0.0
gi|2261844|gb|AA521301.1|AA521301 aa79f07.s1 NCI_CGAP_GCB1 ... 1076 0.0
gi|3922551|gb|AI284318.1|AI284318 qj65c07.x1 NCI_CGAP_Kid3 ... 1070 0.0
gi|4833752|gb|AI668978.1|AI668978 wb82g01.x1 NCI_CGAP_Pr28 ... 1057 0.0
gi|12768489|gb|BG258673.1|BG258673 602379803F1 NIH_MGC_92 H... 1051 0.0
gi|10990261|dbj|AU129907.1|AU129907 AU129907 NT2RP2 Homo sa... 1047 0.0
gi|6881860|gb|AW377197.1|AW377197 IL3-CT0220-111199-028-D09... 1041 0.0
gi|12916948|emb|AL565505.1|AL565505 AL565505 LTI_FL013_FBrn... 1031 0.0
gi|1350109|gb|W52530.1|W52530 zc54d04.r1 Soares_senescent_f... 1025 0.0
gi|5036667|gb|AI719411.1|AI719411 as64c11.x1 Barstead colon... 1017 0.0
gi|10203989|gb|BE782791.1|BE782791 601471972F1 NIH_MGC_67 H... 1015 0.0
gi|9871380|dbj|AV650366.1|AV650366 AV650366 GLC Homo sapien... 1011 0.0
gi|1961448|gb|AA309123.1|AA309123 EST179897 Colon carcinoma... 1011 0.0
gi|2335271|gb|AA563632.1|AA563632 ng47f08.s1 NCI_CGAP_Co3 H... 1007 0.0
gi|2933392|gb|AA845633.1|AA845633 ai90c08.s1 Soares_parathy... 993 0.0
gi|14403997|gb|BG999925.1|BG999925 MR1-HN0069-040101-015-g1... 991 0.0
gi|10299583|dbj|AV697720.1|AV697720 AV697720 GKC Homo sapie... 991 0.0
gi|11263172|gb|BF314998.1|BF314998 601899017F1 NIH_MGC_19 H... 985 0.0
gi|6038150|gb|AW082998.1|AW082998 xb72d12.x1 Soares_NFL_T_G... 983 0.0
gi|3844111|gb|AI248714.1|AI248714 qh72c04.x1 Soares_fetal_l... 983 0.0
gi|11012858|dbj|AU151337.1|AU151337 AU151337 NT2RP2 Homo sa... 981 0.0
gi|5449606|gb|AI828935.1|AI828935 wj37h08.x1 NCI_CGAP_Lu19 ... 975 0.0
gi|14172393|gb|BG824806.1|BG824806 602725101F1 NIH_MGC_15 H... 971 0.0
gi|11015393|dbj|AU153872.1|AU153872 AU153872 NT2RP3 Homo sa... 971 0.0
gi|2838179|gb|AA778848.1|AA778848 zj42a03.s1 Soares_fetal_l... 969 0.0
gi|3742671|gb|AI191462.1|AI191462 qe32f11.s1 Soares_fetal_l... 963 0.0
gi|3596240|gb|AI127726.1|AI127726 qc26h03.x1 Soares_pregnan... 963 0.0
gi|4270907|gb|AI424976.1|AI424976 tg38g11.x1 Soares_NFL_T_G... 959 0.0
gi|9877013|dbj|AV655999.1|AV655999 AV655999 GLC Homo sapien... 957 0.0
gi|2704986|gb|AA701873.1|AA701873 zi56b08.s1 Soares_fetal_l... 955 0.0
gi|4073260|gb|AI336333.1|AI336333 qt43f09.x1 Soares_fetal_l... 948 0.0
gi|10200888|gb|BE779690.1|BE779690 601465210F1 NIH_MGC_67 H... 942 0.0
gi|4073310|gb|AI336383.1|AI336383 qt51c08.x1 Soares_fetal_l... 940 0.0

>gi|14598964|emb|CAC43882.1| 21676 ADH [Homo sapiens]

EST Search:

Organ: skin

Organ: kidney
Tissue type: renal cell adenocarcinoma

Organ: lung
Tissue type: small cell carcinoma

Organ: testis

Organ: skin
Tissue type: melanotic melanoma

Sequences producing significant alignments: (bits) Value

gi|14052242|gb|BG741589.1|BG741589 602635416F1 NCI_CGAP_Skn... 1559 0.0
gi|13130914|gb|BG324477.1|BG324477 602422421F1 NIH_MGC_14 H... 1509 0.0
gi|10217667|gb|BE796469.1|BE796469 601589817F1 NIH_MGC_7 Ho... 1366 0.0
gi|12347068|gb|BF979853.1|BF979853 602288368T1 NIH_MGC_97 H... 1285 0.0
gi|13031288|gb|BG282361.1|BG282361 602402863F1 NIH_MGC_20 H... 1283 0.0
gi|12419347|gb|BG030249.1|BG030249 602297547F1 NIH_MGC_87 H... 1235 0.0
gi|9888236|gb|BE617298.1|BE617298 601441804F1 NIH_MGC_65 Ho... 1213 0.0
gi|12335074|gb|BF967768.1|BF967768 602287657T1 NIH_MGC_96 H... 1203 0.0
gi|10358131|gb|BE895089.1|BE895089 601436007F1 NIH_MGC_72 H... 1183 0.0
gi|12922282|emb|AL568188.1|AL568188 AL568188 LTI_FL013_FBm... 1163 0.0
gi|10318693|gb|BE869917.1|BE869917 601446563F1 NIH_MGC_65 H... 1155 0.0
gi|9875587|db|AV654573.1|AV654573 AV654573 GLC Homo sapien... 1155 0.0
gi|9331605|gb|BE386240.1|BE386240 601273447F1 NIH_MGC_20 Ho... 1145 0.0
gi|12904138|emb|AL559036.1|AL559036 AL559036 LTI_NFL008_TC2... 1124 0.0
gi|12432922|gb|BG037061.1|BG037061 602288368F1 NIH_MGC_97 H... 1122 0.0
gi|12727118|gb|BG231973.1|BG231973 naf34g12.x1 Soares_NPBMC... 1058 0.0
gi|5848488|gb|AW001572.1|AW001572 wu34f05.x1 Soares_Dieckgr... 1012 0.0
gi|11764835|gb|BE962188.2|BE962188 601655404R1 NIH_MGC_65 H... 1000 0.0
gi|14818515|gb|BI260323.1|BI260323 602969342F1 NIH_MGC_12 H... 994 0.0
gi|9186562|gb|BE302814.1|BE302814 ba69c04.y1 NIH_MGC_20 Hom... 988 0.0
gi|1365172|gb|W58459.1|W58459 zd25h06.s1 Soares_fetal_heart... 972 0.0
gi|12904136|emb|AL559035.1|AL559035 AL559035 LTI_NFL008_TC2... 962 0.0
gi|1365130|gb|W58347.1|W58347 zd25b06.s1 Soares_fetal_heart... 958 0.0
gi|10457801|gb|BE931725.1|BE931725 QV4-HT0539-240800-380-d1... 956 0.0
gi|3593739|gb|AI125225.1|AI125225 qd87f01.x1 Soares_testis_... 939 0.0
gi|9340527|gb|BE395162.1|BE395162 601309505F1 NIH_MGC_44 Ho... 931 0.0
gi|1365185|gb|W58472.1|W58472 zd25b06.r1 Soares_fetal_heart... 931 0.0
gi|8165401|gb|AW974208.1|AW974208 EST386311 MAGE resequence... 923 0.0
gi|5369162|gb|AI803690.1|AI803690 tc19e02.x1 Soares_NhHMPu_... 923 0.0
gi|5912884|gb|AW050614.1|AW050614 wz19c10.x1 Soares_Dieckgr... 911 0.0
gi|4853165|gb|AI673434.1|AI673434 wf19a10.x1 Soares_Dieckgr... 911 0.0
gi|9340769|gb|BE395404.1|BE395404 601309913F1 NIH_MGC_44 Ho... 905 0.0
gi|6133237|gb|AW131630.1|AW131630 xf32d02.x1 NCI_CGAP_Brn50... 903 0.0
gi|5912902|gb|AW050632.1|AW050632 wz19e08.x1 Soares_Dieckgr... 885 0.0
gi|4187886|gb|AI378033.1|AI378033 te67g09.x1 Soares_NFL_T_G... 877 0.0
gi|1365227|gb|W58514.1|W58514 zd25h06.r1 Soares_fetal_heart... 871 0.0
gi|3048078|gb|AA908673.1|AA908673 ol04d06.s1 NCI_CGAP_Lu5 H... 857 0.0
gi|13520318|gb|BG528781.1|BG528781 602580128F1 NIH_MGC_60 H... 853 0.0
gi|3598437|gb|AI129923.1|AI129923 qc41d08.x1 Soares_pregnan... 847 0.0
gi|3778197|gb|AI214596.1|AI214596 qm28h07.x1 NCI_CGAP_Lu5 H... 837 0.0
gi|2161847|gb|AA448177.1|AA448177 zw83b12.s1 Soares_testis_... 833 0.0
gi|6992857|gb|AW452081.1|AW452081 UI-H-BI3-aln-c-06-0-UI.s1... 825 0.0
gi|13996787|gb|BG717600.1|BG717600 602698216F1 NIH_MGC_97 H... 787 0.0
gi|3752620|gb|AI200014.1|AI200014 qf90d03.x1 Soares_placent... 762 0.0
gi|2350443|gb|AA575928.1|AA575928 nm56b12.s1 NCI_CGAP_Br3 H... 760 0.0
gi|4629290|gb|AI620164.1|AI620164 tu46c12.x1 NCI_CGAP_Pr28 ... 756 0.0
gi|14385896|gb|BG983161.1|BG983161 IL5-CN0068-060301-381-h0... 754 0.0

gi|2879112|gb|AA809706.1|AA809706 nk96f06.s1 NCI_CGAP_Co3 H... 738 0.0
gi|3803861|gb|AI221658.1|AI221658 qg93d04.x1 Soares_NFL_T_G... 712 0.0

>gi|14598968|emb|CAC43884.1| 21615 ADH [Homo sapiens]

EST Search:

Organ: brain
Tissue type: neuroblastoma cells

Tissue type: placenta

Tissue type: placenta

Sex: male
Organ: brain
Tissue type: neuroblastoma cells

Sequences producing significant alignments: (bits) Value

gi|12786589|emb|AL523096.1|AL523096 AL523096 LTI_NFL003_NBC... 1707 0.0
gi|12889983|emb|AL551741.1|AL551741 AL551741 LTI_NFL006_PL2... 1653 0.0
gi|12936195|emb|AL575230.1|AL575230 AL575230 LTI_NFL006_PL2... 1487 0.0
gi|12793625|emb|AL530132.1|AL530132 AL530132 LTI_NFL001_NBC... 1457 0.0
gi|13294054|gb|BG400606.1|BG400606 602464263F1 NIH_MGC_75 H... 1443 0.0
gi|13452667|gb|BG491155.1|BG491155 602518792F1 NIH_MGC_18 H... 1401 0.0
gi|13982652|gb|BG706873.1|BG706873 602672037F1 NIH_MGC_96 H... 1387 0.0
gi|3281013|gb|AI041819.1|AI041819 oy34a10.x1 Soares_parathy... 1352 0.0
gi|12793624|emb|AL530131.1|AL530131 AL530131 LTI_NFL001_NBC... 1346 0.0
gi|13545674|gb|BG547009.1|BG547009 602573805F1 NIH_MGC_77 H... 1340 0.0
gi|13976480|gb|BG703780.1|BG703780 602686804F1 NIH_MGC_95 H... 1338 0.0
gi|14051133|gb|BG740480.1|BG740480 602633875F1 NCI_CGAP_Skn... 1330 0.0
gi|13039621|gb|BG286600.1|BG286600 602381608F1 NIH_MGC_93 H... 1314 0.0
gi|11257955|gb|BF310393.1|BF310393 601895043F1 NIH_MGC_19 H... 1304 0.0
gi|2839375|gb|AA780044.1|AA780044 zj24e12.s1 Soares_fetal_l... 1302 0.0
gi|11265005|gb|BF316648.1|BF316648 601903206F1 NIH_MGC_19 H... 1272 0.0
gi|8154981|gb|AW965145.1|AW965145 EST377218 MAGE resequence... 1272 0.0
gi|3238050|gb|AI022809.1|AI022809 ow55f02.x1 Soares_parathy... 1256 0.0
gi|13544541|gb|BG545876.1|BG545876 602573161F1 NIH_MGC_77 H... 1238 0.0
gi|12598260|gb|BG104418.1|BG104418 602311036F1 NIH_MGC_20 H... 1225 0.0
gi|12598014|gb|BG104172.1|BG104172 602310736F1 NIH_MGC_20 H... 1221 0.0
gi|12606210|gb|BG112704.1|BG112704 602282264F1 NIH_MGC_86 H... 1219 0.0
gi|2877836|gb|AA808430.1|AA808430 oe53b08.s1 NCI_CGAP_Lu5 H... 1207 0.0
gi|4073201|gb|AI336274.1|AI336274 qt45e02.x1 Soares_fetal_l... 1201 0.0
gi|6471396|gb|AW192697.1|AW192697 xl48h04.x1 NCI_CGAP_Pan1 ... 1183 0.0
gi|9323894|gb|BE378429.1|BE378429 601236767F1 NIH_MGC_44 Ho... 1151 0.0
gi|12910323|emb|AL562168.1|AL562168 AL562168 LTI_NFL003_NBC... 1149 0.0
gi|9186202|gb|BE302454.1|BE302454 ba65f04.y1 NIH_MGC_20 Hom... 1107 0.0
gi|9186195|gb|BE302447.1|BE302447 ba65e04.y1 NIH_MGC_20 Hom... 1101 0.0
gi|5813571|gb|AI986294.1|AI986294 wz64c08.x1 NCI_CGAP_Mel15... 1078 0.0
gi|4435368|gb|AI521233.1|AI521233 to66f02.x1 NCI_CGAP_Gas4 ... 1076 0.0
gi|12875811|emb|AL543333.1|AL543333 AL543333 LTI_NFL006_PL2... 1070 0.0
gi|5109073|gb|AI740785.1|AI740785 wg24b10.x1 Soares_NSF_F8_... 1056 0.0
gi|2993433|gb|AA883903.1|AA883903 aj13a01.s1 Soares_parathy... 1056 0.0
gi|3400111|gb|AI073467.1|AI073467 ov45a08.x1 Soares_testis_... 1048 0.0
gi|10350081|gb|BE891095.1|BE891095 601432208F1 NIH_MGC_72 H... 1046 0.0
gi|6228615|gb|AW157214.1|AW157214 au92h07.x1 Schneider feta... 1038 0.0
gi|5858190|gb|AW009412.1|AW009412 ws82c11.x1 NCI_CGAP_Co3 H... 1030 0.0
gi|2324986|gb|AA554447.1|AA554447 nl14h10.s1 NCI_CGAP_Br2 H... 1028 0.0
gi|5546002|gb|AI871953.1|AI871953 wm53h05.x1 NCI_CGAP_Ut2 H... 1024 0.0
gi|2955773|gb|AA863294.1|AA863294 og93b12.s1 NCI_CGAP_Kid5 ... 1014 0.0
gi|2690528|gb|AA689601.1|AA689601 nv66b12.s1 NCI_CGAP_GCB1 ... 1008 0.0
gi|13294752|gb|BG401304.1|BG401304 602465415F1 NIH_MGC_75 H... 1006 0.0

gi|4598887|gb|AI589839.1|AI589839 tm81a02.x1 NCI_CGAP_Brn25... 1006 0.0
gi|4834180|gb|AI669406.1|AI669406 ty32b07.x1 NCI_CGAP_Ut2 H... 1002 0.0

>gi|14598962|emb|CAC43881.1| 33756 ADH [Homo sapiens]

EST Search:

Organ: brain
Tissue type: anaplastic oligodendroglioma

Organ: colon
Tissue type: colon tumor, RER+

Organ: kidney

Organ: colon
Tissue type: adenocarcinoma cell line

Sequences producing significant alignments: (bits) Value

gi|5545428|gb|AI871379.1|AI871379 wl81d08.x1 NCI_CGAP_Brn25... 1291 0.0
gi|5178261|gb|AI762594.1|AI762594 wi56b09.x1 NCI_CGAP_Co16 ... 1193 0.0
gi|6709871|gb|AW300271.1|AW300271 xs58h07.x1 NCI_CGAP_Kid11... 1136 0.0
gi|5108921|gb|AI740633.1|AI740633 wg23g01.x1 Soares_NSF_F8_... 1067 0.0
gi|14169716|gb|BG822129.1|BG822129 602726271F1 NIH_MGC_15 H... 1061 0.0
gi|6570140|gb|AW237763.1|AW237763 xm81b04.x1 NCI_CGAP_Kid11... 1051 0.0
gi|10938383|gb|BF108693.1|BF108693 7l44e02.x1 Soares_NSF_F8... 1025 0.0
gi|5540213|gb|AI867197.1|AI867197 wa01c10.x1 NCI_CGAP_Kid11... 1021 0.0
gi|11448154|gb|BF435839.1|BF435839 nab42e01.x1 Soares_NSF_F... 1011 0.0
gi|5933828|gb|AW058189.1|AW058189 wv83h01.x1 Soares_thymus_... 1003 0.0
gi|4190356|gb|AI380503.1|AI380503 tf95d02.x1 NCI_CGAP_CLL1 ... 999 0.0
gi|5450901|gb|AI830241.1|AI830241 wj78h11.x1 NCI_CGAP_Lu19 ... 995 0.0
gi|5113008|gb|AI744631.1|AI744631 wg04g09.x1 Soares_NSF_F8_... 981 0.0
gi|4598007|gb|AI588959.1|AI588959 tk15d10.x1 Soares_NhHMPu_... 975 0.0
gi|11682572|gb|BF590248.1|BF590248 nab22a02.x1 Soares_NSF_F... 950 0.0
gi|5232040|gb|AI765531.1|AI765531 wi81b11.x1 NCI_CGAP_Kid12... 950 0.0
gi|4311958|gb|AI457940.1|AI457940 tj55h09.x1 Soares_NSF_F8_... 950 0.0
gi|6710832|gb|AW301155.1|AW301155 xs57a11.x1 NCI_CGAP_Kid11... 942 0.0
gi|5664220|gb|AI928256.1|AI928256 wo67a08.x1 NCI_CGAP_Pr22 ... 938 0.0
gi|6746198|gb|AW316942.1|AW316942 xw13a08.x1 NCI_CGAP_Brn53... 926 0.0
gi|5663387|gb|AI927423.1|AI927423 wo75e11.x1 NCI_CGAP_Pr22 ... 926 0.0
gi|5766733|gb|AI969915.1|AI969915 wq77e03.x1 NCI_CGAP_Pr28 ... 924 0.0
gi|9803527|gb|BE559808.1|BE559808 601346972F1 NIH_MGC_8 Hom... 918 0.0
gi|10819930|gb|BF061020.1|BF061020 7j62f12.x1 Soares_NSF_F8... 890 0.0
gi|3095277|gb|AA937166.1|AA937166 ok13a08.s1 Soares_NSF_F8_... 888 0.0
gi|10941529|gb|BF111839.1|BF111839 7l36c03.x1 Soares_NSF_F8... 886 0.0
gi|5837771|gb|AI990886.1|AI990886 ws24b02.x1 NCI_CGAP_GC6 H... 880 0.0
gi|3960152|gb|AI300806.1|AI300806 qn47b02.x1 NCI_CGAP_Kid5 ... 880 0.0
gi|12041329|gb|BF725418.1|BF725418 bx15f11.y1 Human Iris cD... 878 0.0
gi|10809455|gb|BF055559.1|BF055559 7j81h04.x1 Soares_NSF_F8... 872 0.0
gi|5366102|gb|AI800708.1|AI800708 tc13c01.x1 Soares_NhHMPu_... 872 0.0
gi|10150139|gb|BE736147.1|BE736147 601307226F1 NIH_MGC_39 H... 864 0.0
gi|14568272|gb|BI117371.1|BI117371 602867919F1 NIH_MGC_7 Ho... 860 0.0
gi|2279509|gb|AA535256.1|AA535256 nf93b07.s1 NCI_CGAP_Co3 H... 860 0.0

gi|8908766|gb|BE221448.1|BE221448 hu25b07.x1 NCI_CGAP_Mel15... 858 0.0
gi|10938643|gb|BF108953.1|BF108953 7l55a06.x1 Soares_NSF_F8... 856 0.0
gi|6026228|gb|AW071230.1|AW071230 wz23e02.x1 Soares_Dieckgr... 841 0.0
gi|11251209|gb|BF304472.1|BF304472 601887831F1 NIH_MGC_17 H... 811 0.0

>gi|14602730|gb|AAH09881.1|AAH09881 Unknown (protein for MGC:16483) [Homo sapiens]

EST Search:
Organ: placenta
Tissue type: choriocarcinoma

Organ: lung
Tissue type: small cell carcinoma

Organ: bone marrow
Tissue type: from acute myelogenous leukemia

Organ: brain
Tissue type: anaplastic oligodendroglioma

Sequences producing significant alignments:	Score (bits)	E Value
gi|13412286|gb|BG480007.1|BG480007 602527580F1 NIH_MGC_21 H...	1469	0.0
gi|14568272|gb|BI117371.1|BI117371 602867919F1 NIH_MGC_7 Ho...	1467	0.0
gi|10388276|gb|BE900363.1|BE900363 601673230F1 NIH_MGC_21 H...	1409	0.0
gi|10394942|gb|BE903479.1|BE903479 601676737F1 NIH_MGC_21 H...	1364	0.0
gi|10162791|gb|BE748799.1|BE748799 601572007T1 NIH_MGC_55 H...	1312	0.0
gi|5545428|gb|AI871379.1|AI871379 wl81d08.x1 NCI_CGAP_Brn25...	1298	0.0
gi|14169716|gb|BG822129.1|BG822129 602726271F1 NIH_MGC_15 H...	1291	0.0
gi|12670294|gb|BG163591.1|BG163591 602338741F1 NIH_MGC_89 H...	1207	0.0
gi|5178261|gb|AI762594.1|AI762594 wi56b09.x1 NCI_CGAP_Co16 ...	1185	0.0
gi|9140120|gb|BE266541.1|BE266541 601193528F1 NIH_MGC_7 Hom...	1168	0.0
gi|6709871|gb|AW300271.1|AW300271 xs58h07.x1 NCI_CGAP_Kid11...	1144	0.0
gi|9803527|gb|BE559808.1|BE559808 601346972F1 NIH_MGC_8 Hom...	1132	0.0
gi|10150139|gb|BE736147.1|BE736147 601307226F1 NIH_MGC_39 H...	1094	0.0
gi|12041329|gb|BF725418.1|BF725418 bx15f11.y1 Human Iris cD...	1092	0.0
gi|5108921|gb|AI740633.1|AI740633 wg23g01.x1 Soares_NSF_F8_...	1090	0.0
gi|4372796|gb|AI479628.1|AI479628 tm32d07.x1 NCI_CGAP_CLL1 ...	1067	0.0
gi|6570140|gb|AW237763.1|AW237763 xm81b04.x1 NCI_CGAP_Kid11...	1059	0.0
gi|8169897|gb|AW978626.1|AW978626 EST390735 MAGE resequence...	1047	0.0
gi|5540213|gb|AI867197.1|AI867197 wa01c10.x1 NCI_CGAP_Kid11...	1045	0.0
gi|11448154|gb|BF435839.1|BF435839 nab42e01.x1 Soares_NSF_F...	1035	0.0
gi|10938383|gb|BF108693.1|BF108693 7l44e02.x1 Soares_NSF_F8...	1033	0.0
gi|10036058|gb|BE675517.1|BE675517 7f10f02.x1 NCI_CGAP_CLL1...	1029	0.0
gi|9970354|gb|BE646054.1|BE646054 7e92d04.x1 NCI_CGAP_CLL1 ...	1011	0.0
gi|5933828|gb|AW058189.1|AW058189 wv83h01.x1 Soares_thymus_...	1011	0.0
gi|11251209|gb|BF304472.1|BF304472 601887831F1 NIH_MGC_17 H...	1009	0.0
gi|4190356|gb|AI380503.1|AI380503 tf95d02.x1 NCI_CGAP_CLL1 ...	1007	0.0
gi|5113008|gb|AI744631.1|AI744631 wg04g09.x1 Soares_NSF_F8_...	1005	0.0
gi|5450901|gb|AI830241.1|AI830241 wj78h11.x1 NCI_CGAP_Lu19 ...	1003	0.0
gi|4598007|gb|AI588959.1|AI588959 tk15d10.x1 Soares_NhHMPu_...	999	0.0
gi|4113265|gb|AI361644.1|AI361644 qy86d07.x1 NCI_CGAP_Brn25...	987	0.0
gi|11082796|gb|BF195666.1|BF195666 7n86g02.x1 NCI_CGAP_Ov18...	977	0.0

gi|5232040|gb|AI765531.1|AI765531 wi81b11.x1 NCI_CGAP_Kid12... 973 0.0
gi|2463985|gb|AA612947.1|AA612947 nq38e11.s1 NCI_CGAP_Co10 ... 963 0.0
gi|12758392|gb|BG248576.1|BG248576 602400744F1 NIH_MGC_15 H... 957 0.0
gi|11682572|gb|BF590248.1|BF590248 nab22a02.x1 Soares_NSF_F... 957 0.0
gi|4311958|gb|AI457940.1|AI457940 tj55h09.x1 Soares_NSF_F8_... 957 0.0
gi|9122527|gb|BE252388.1|BE252388 601117771F1 NIH_MGC_16 Ho... 954 0.0
gi|6710832|gb|AW301155.1|AW301155 xs57a11.x1 NCI_CGAP_Kid11... 950 0.0
gi|5663387|gb|AI927423.1|AI927423 wo75e11.x1 NCI_CGAP_Pr22 ... 950 0.0
gi|5766733|gb|AI969915.1|AI969915 wq77e03.x1 NCI_CGAP_Pr28 ... 948 0.0
gi|5664220|gb|AI928256.1|AI928256 wo67a08.x1 NCI_CGAP_Pr22 ... 946 0.0
gi|1377082|gb|W68057.1|W68057 zd42h12.r1 Soares_fetal_heart... 938 0.0
gi|6746198|gb|AW316942.1|AW316942 xw13a08.x1 NCI_CGAP_Brn53... 934 0.0
gi|1959057|gb|AA306658.1|AA306658 EST177664 Jurkat T-cells ... 934 0.0
gi|9139865|gb|BE266290.1|BE266290 601191911F1 NIH_MGC_7 Hom... 932 0.0
gi|5660470|gb|AI924506.1|AI924506 wn61a01.x1 NCI_CGAP_Lu19 ... 928 0.0
gi|9803869|gb|BE560051.1|BE560051 601347483F1 NIH_MGC_8 Hom... 924 0.0
gi|2986172|gb|AA877095.1|AA877095 ob09d05.s1 NCI_CGAP_Kid3 ... 916 0.0
gi|10162316|gb|BE748324.1|BE748324 601572007F1 NIH_MGC_55 H... 914 0.0
gi|12358324|gb|BF941004.1|BF941004 hu63a05.x1 NCI_CGAP_Brn4... 908 0.0
gi|3095277|gb|AA937166.1|AA937166 ok13a08.s1 Soares_NSF_F8_... 908 0.0
gi|14057456|gb|BG746803.1|BG746803 602704139F1 NIH_MGC_15 H... 904 0.0
gi|10819930|gb|BF061020.1|BF061020 7j62f12.x1 Soares_NSF_F8... 898 0.0
gi|5837771|gb|AI990886.1|AI990886 ws24b02.x1 NCI_CGAP_GC6 H... 896 0.0
gi|10941529|gb|BF111839.1|BF111839 7l36c03.x1 Soares_NSF_F8... 894 0.0
gi|10809455|gb|BF055559.1|BF055559 7j81h04.x1 Soares_NSF_F8... 888 0.0
gi|5366102|gb|AI800708.1|AI800708 tc13c01.x1 Soares_NhHMPu_... 888 0.0
gi|6836760|gb|AW340134.1|AW340134 hc93g05.x1 Soares_NFL_T_G... 882 0.0
gi|3960152|gb|AI300806.1|AI300806 qn47b02.x1 NCI_CGAP_Kid5 ... 880 0.0
gi|4114754|gb|AI363133.1|AI363133 qy68c10.x1 NCI_CGAP_Brn25... 878 0.0
gi|8908766|gb|BE221448.1|BE221448 hu25b07.x1 NCI_CGAP_Mel15... 874 0.0
gi|10938643|gb|BF108953.1|BF108953 7l55a06.x1 Soares_NSF_F8... 872 0.0
gi|2740699|gb|AA722992.1|AA722992 zg89c05.s1 Soares_fetal_h... 872 0.0
gi|2279509|gb|AA535256.1|AA535256 nf93b07.s1 NCI_CGAP_Co3 H... 868 0.0
gi|2675026|gb|AA688120.1|AA688120 nv15h04.s1 NCI_CGAP_Pr22 ... 864 0.0
gi|13792425|gb|BG655016.1|BG655016 ib44h01.y1 HR85 islet Ho... 858 0.0
gi|10037307|gb|BE676766.1|BE676766 7f35c08.x1 NCI_CGAP_CLL1... 854 0.0
gi|6026228|gb|AW071230.1|AW071230 wz23e02.x1 Soares_Dieckgr... 854 0.0
gi|2161622|gb|AA447952.1|AA447952 zx11f06.r1 Soares_total_f... 850 0.0
gi|1670790|gb|AA115759.1|AA115759 zk96g06.s1 Soares_pregnan... 842 0.0
gi|14620762|gb|BI160761.1|BI160761 602864839F1 NIH_MGC_42 H... 831 0.0
gi|6452291|gb|AW183777.1|AW183777 xj87g06.x1 Soares_NFL_T_G... 817 0.0
gi|13343784|gb|BG437278.1|BG437278 602490558F1 NIH_MGC_18 H... 815 0.0
gi|3751123|gb|AI198517.1|AI198517 qf94h01.x1 Soares_placent... 815 0.0
gi|3739896|gb|AI188687.1|AI188687 qd10g06.x1 Soares_placent... 795 0.0
gi|11683021|gb|BF590610.1|BF590610 7h40f10.x1 NCI_CGAP_Co16... 791 0.0
gi|5449740|gb|AI829069.1|AI829069 wj38c05.x1 NCI_CGAP_Lu19 ... 791 0.0
gi|2336957|gb|AA565318.1|AA565318 nj37c11.s1 NCI_CGAP_AA1 H... 791 0.0
gi|1690504|gb|AA133534.1|AA133534 zk96g06.r1 Soares_pregnan... 787 0.0
gi|3232294|gb|AI017958.1|AI017958 ou30b01.x1 Soares_NFL_T_G... 777 0.0
gi|4223386|gb|AI393839.1|AI393839 tg59d07.x1 Soares_NSF_F8_... 763 0.0
gi|5176495|gb|AI760828.1|AI760828 wh96e10.x1 NCI_CGAP_CLL1 ... 755 0.0
gi|4113115|gb|AI361494.1|AI361494 qy48c02.x1 NCI_CGAP_Brn23... 739 0.0
gi|3117502|gb|AA953355.1|AA953355 oo88c12.s1 NCI_CGAP_Kid5 ... 739 0.0
gi|1544002|gb|AA053347.1|AA053347 zl70h05.s1 Stratagene col... 737 0.0
gi|2241423|gb|AA505286.1|AA505286 nh95c04.s1 NCI_CGAP_Br2 H... 728 0.0
gi|2218486|gb|AA488884.1|AA488884 aa55f09.s1 NCI_CGAP_GCB1 ... 728 0.0
gi|880732|gb|H15912.1|H15912 yl27c07.s1 Soares breast 3NbHB... 726 0.0

gi|2445628|gb|AA604764.1|AA604764 no84f06.s1 NCI_CGAP_AA1 H... 724 0.0
gi|3741170|gb|AI189961.1|AI189961 qd19f09.x1 Soares_placent... 722 0.0
gi|8143250|gb|AW953567.1|AW953567 EST365637 MAGE resequence... 720 0.0
gi|6142870|gb|AW138552.1|AW138552 UI-H-BI1-abx-f-03-0-UI.s1... 712 0.0
gi|2901576|gb|AA828477.1|AA828477 oc42g04.s1 NCI_CGAP_GCB1 ... 694 0.0
gi|651330|gb|T49470.1|T49470 ya75g04.s1 Stratagene placenta... 692 0.0
gi|5544123|gb|AI870155.1|AI870155 wk99b03.x1 NCI_CGAP_Lu19 ... 688 0.0
gi|843074|gb|R69557.1|R69557 yj82h11.r1 Soares breast 2NbHB... 684 0.0
gi|12397550|gb|BF991225.1|BF991225 CM0-GN0162-271000-627-h0... 676 0.0
gi|856105|gb|R79824.1|R79824 yi89a05.s1 Soares placenta Nb2... 676 0.0
gi|7039183|gb|AW469077.1|AW469077 hc76d11.x1 NCI_CGAP_Gas4 ... 664 0.0
gi|12356691|gb|BF939371.1|BF939371 nad94e01.x1 NCI_CGAP_Ov1... 658 0.0

>gi|14602625|gb|AAH09830.1|AAH09830 PAN2 protein [Homo sapiens]

EST Search:

Tissue type: placenta

Tissue type: T cells from T cell leukemia

Tissue type: Adult brain

Organ: brain
Tissue type: hippocampus

Tissue type: primary B-cells from tonsils (cell line)

Organ: colon
Tissue type: adenocarcinoma

Sequences producing significant alignments: (bits) Value

gi|12875608|emb|AL543130.1|AL543130 AL543130 LTI_NFL006_PL2... 1832 0.0
gi|12943976|emb|AL579184.1|AL579184 AL579184 LTI_FL012_TC1 ... 1727 0.0
gi|12915979|emb|AL565020.1|AL565020 AL565020 LTI_FL015_Brn1... 1505 0.0
gi|12887406|emb|AL550433.1|AL550433 AL550433 LTI_NFL006_PL2... 1455 0.0
gi|13974137|gb|BG702619.1|BG702619 602684333F1 NIH_MGC_95 H... 1429 0.0
gi|14069852|gb|BG759199.1|BG759199 602710860F1 NIH_MGC_48 H... 1423 0.0
gi|10319309|gb|BE870533.1|BE870533 601448228F1 NIH_MGC_65 H... 1283 0.0
gi|10746413|gb|BF037954.1|BF037954 601461651F1 NIH_MGC_66 H... 1275 0.0
gi|12943974|emb|AL579183.1|AL579183 AL579183 LTI_FL012_TC1 ... 1263 0.0
gi|10290446|dbj|AV688583.1|AV688583 AV688583 GKC Homo sapie... 1245 0.0
gi|10967752|gb|BF128712.1|BF128712 601810983F1 NIH_MGC_48 H... 1235 0.0
gi|10203453|gb|BE782255.1|BE782255 601466690F1 NIH_MGC_67 H... 1231 0.0
gi|14050138|gb|BG779821.1|BG779821 602667289F1 NIH_MGC_60 H... 1205 0.0
gi|10919908|dbj|AV762060.1|AV762060 AV762060 MDS Homo sapie... 1183 0.0
gi|12934358|emb|AL574292.1|AL574292 AL574292 LTI_NFL006_PL2... 1104 0.0
gi|10289308|dbj|AV687445.1|AV687445 AV687445 GKC Homo sapie... 1100 0.0
gi|12875574|emb|AL543096.1|AL543096 AL543096 LTI_NFL006_PL2... 1080 0.0
gi|13339671|gb|BG433165.1|BG433165 602496421F1 NIH_MGC_75 H... 1076 0.0
gi|10967874|gb|BF128834.1|BF128834 601811019F1 NIH_MGC_48 H... 1059 0.0
gi|10294954|dbj|AV693091.1|AV693091 AV693091 GKC Homo sapie... 1039 0.0
gi|10969105|gb|BF130065.1|BF130065 601817940F1 NIH_MGC_58 H... 1007 0.0
gi|10736896|gb|BF029184.1|BF029184 601764696F1 NIH_MGC_53 H... 922 0.0

gi|12615542|gb|BG122033.1|BG122033 602349409F1 NIH_MGC_90 H... 852 0.0
gi|4004205|gb|AI309334.1|AI309334 qo80d08.x1 NCI_CGAP_Kid5 ... 821 0.0
gi|1281106|gb|W07093.1|W07093 za93c06.r1 Soares_fetal_lung_... 811 0.0
gi|10300054|dbj|AV698167.1|AV698167 AV698167 GKC Homo sapie... 793 0.0
gi|1376483|gb|W67612.1|W67612 zd41c08.r1 Soares_fetal_heart... 787 0.0
gi|6876390|gb|AW371736.1|AW371736 CM0-BT0304-111199-093-d11... 785 0.0
gi|13576852|gb|BG569199.1|BG569199 602588473F1 NIH_MGC_76 H... 769 0.0
gi|1898399|gb|AA262838.1|AA262838 zs24c11.r1 NCI_CGAP_GCB1 ... 763 0.0
gi|8155033|gb|AW965197.1|AW965197 EST377270 MAGE resequence... 753 0.0
gi|8155021|gb|AW965185.1|AW965185 EST377258 MAGE resequence... 753 0.0
gi|10295847|dbj|AV693984.1|AV693984 AV693984 GKC Homo sapie... 720 0.0
gi|10208100|gb|BE786902.1|BE786902 601477765F1 NIH_MGC_68 H... 720 0.0
gi|10294947|dbj|AV693084.1|AV693084 AV693084 GKC Homo sapie... 708 0.0
gi|13791909|gb|BG654500.1|BG654500 ib41c07.y1 HR85 islet Ho... 680 0.0
gi|12915977|emb|AL565019.1|AL565019 AL565019 LTI_FL015_Brn1... 678 0.0
gi|10297856|dbj|AV695993.1|AV695993 AV695993 GKC Homo sapie... 652 0.0
gi|1997881|gb|AA345644.1|AA345644 EST51687 Gall bladder II ... 589 e-166
gi|4439638|gb|AI525503.1|AI525503 PT1.1_4_B01.r tumor1 Homo... 567 e-159
gi|13703589|gb|BG181902.1|BG181902 RST760 Athersys RAGE Lib... 541 e-151
gi|8907221|gb|BE219903.1|BE219903 hv64c09.x1 NCI_CGAP_Lu24 ... 531 e-148
gi|841904|gb|R68387.1|R68387 yh99g01.r1 Soares placenta Nb2... 529 e-148
gi|13545980|gb|BG547315.1|BG547315 602574734F1 NIH_MGC_77 H... 359 1e-96
gi|1239209|gb|N76631.1|N76631 yz79h10.r1 Soares_multiple_sc... 323 7e-86
gi|13319146|gb|BG413593.1|BG413593 7j63f11.x1 Soares_NSF_F8... 313 7e-83
gi|5811063|gb|AI983844.1|AI983844 wt51d12.x1 NCI_CGAP_Pan1 ... 305 2e-80
gi|5850543|gb|AW003627.1|AW003627 wx34e03.x1 NCI_CGAP_Pit1 ... 303 7e-80
gi|13791976|gb|BG654567.1|BG654567 ib41c07.x1 HR85 islet Ho... 291 3e-76
gi|1844851|gb|AA224309.1|AA224309 zr15f05.r1 Stratagene NT2... 274 6e-71
gi|5635411|gb|AI915556.1|AI915556 wg30e08.x1 Soares_NSF_F8_... 260 9e-67
gi|2366350|dbj|C75288.1|C75288 C75288 Human pancreatic isle... 258 4e-66
gi|4534171|gb|AI570797.1|AI570797 tr67c10.x1 NCI_CGAP_Pan1 ... 250 9e-64
gi|12242488|gb|BF854705.1|BF854705 RC6-FN0202-271000-011-C0... 238 3e-60
gi|2437676|gb|AA603815.1|AA603815 nn87e11.s1 NCI_CGAP_Br2 H... 216 1e-53
gi|4989930|gb|AI702030.1|AI702030 tq20e05.x1 NCI_CGAP_Ut1 H... 196 1e-47
gi|11159725|gb|BF245883.1|BF245883 601864059F1 NIH_MGC_57 H... 180 7e-43
gi|12245429|gb|BF857685.1|BF857685 RC5-FT0194-061100-031-A0... 170 7e-40
gi|12243397|gb|BF855653.1|BF855653 RC6-FN0202-171100-012-D0... 170 7e-40
gi|11019045|dbj|AU157524.1|AU157524 AU157524 PLACE1 Homo sa... 168 3e-39
gi|3424383|gb|AI085960.1|AI085960 oz86g08.x1 Soares_senesce... 167 1e-38
gi|12242489|gb|BF854706.1|BF854706 RC6-FN0202-271000-011-C0... 163 2e-37
gi|5177517|gb|AI761761.1|AI761761 wg68a02.x1 Soares_NSF_F8_... 157 1e-35
gi|3075842|gb|AA926945.1|AA926945 om68g02.s1 NCI_CGAP_GC4 H... 139 2e-30
gi|1225675|gb|N69514.1|N69514 yz79h10.s1 Soares_multiple_sc... 119 2e-24
gi|6464995|gb|AW190515.1|AW190515 xl63b10.x1 NCI_CGAP_Pan1 ... 113 1e-22
gi|3736368|gb|AI185730.1|AI185730 qe33b10.s1 Soares_fetal_l... 111 5e-22
gi|6199686|gb|AW151788.1|AW151788 xf69c11.x1 NCI_CGAP_Gas4 ... 109 2e-21
gi|4533666|gb|AI570292.1|AI570292 to77d10.x1 NCI_CGAP_Gas4 ... 109 2e-21
gi|4648078|gb|AI623153.1|AI623153 tu89d03.x1 NCI_CGAP_Gas4 ... 105 3e-20
gi|5744801|gb|AI952491.1|AI952491 wx74e04.x1 NCI_CGAP_Ov38 ... 92 5e-16
gi|3870043|gb|AI261840.1|AI261840 qk11a10.x1 NCI_CGAP_Kid3 ... 90 2e-15
gi|6834091|gb|AW337465.1|AW337465 xx57d09.x1 NCI_CGAP_Lym12... 82 5e-13
gi|1432534|dbj|C00304.1|C00304 HUMGS0006005 Human adult (K.... 72 4e-10
gi|12767084|gb|BG257268.1|BG257268 602377984F1 NIH_MGC_92 H... 44 0.10
gi|1367064|gb|W60305.1|W60305 zd29e01.s1 Soares_fetal_heart... 44 0.10
gi|14065766|gb|BG755113.1|BG755113 602711428F1 NIH_MGC_48 H... 40 1.6
gi|8472627|gb|BE082325.1|BE082325 QV2-BT0636-070500-194-h05... 40 1.6
gi|14502208|gb|BI083878.1|BI083878 602869109F1 NIH_MGC_102 ... 38 6.2

gi|14391900|gb|BG987830.1|BG987830 CM3-HT1150-110101-623-h0... 38 6.2
gi|14072079|gb|BG761426.1|BG761426 602718627F1 NIH_MGC_49 H... 38 6.2
gi|13411218|gb|BG478939.1|BG478939 602525701F1 NIH_MGC_21 H... 38 6.2
gi|12916582|emb|AL565322.1|AL565322 AL565322 LTI_FL013_FBrn... 38 6.2
gi|12288761|gb|BF897302.1|BF897302 IL2-MT0179-281100-255-C0... 38 6.2
gi|12057953|gb|BF732878.1|BF732878 nae16g05.x1 NCI_CGAP_Ov1... 38 6.2
gi|11297817|gb|BF327069.1|BF327069 RC1-BN0056-230200-012-e0... 38 6.2
gi|11766564|gb|BE963146.2|BE963146 601656952R1 NIH_MGC_67 H... 38 6.2
gi|11102818|gb|BF209128.1|BF209128 601872828F1 NIH_MGC_54 H... 38 6.2
gi|10357166|gb|BE894606.1|BE894606 601433223F1 NIH_MGC_72 H... 38 6.2
gi|10314262|gb|BE865486.1|BE865486 601677815F1 NIH_MGC_53 H... 38 6.2
gi|10201679|gb|BE780481.1|BE780481 601468751F1 NIH_MGC_67 H... 38 6.2
gi|10162316|gb|BE748324.1|BE748324 601572007F1 NIH_MGC_55 H... 38 6.2
gi|8485301|gb|BE094848.1|BE094848 CM2-BT0790-180400-164-a12... 38 6.2
gi|7280198|gb|AW593003.1|AW593003 hg07b03.x1 Soares_NFL_T_G... 38 6.2
gi|6705383|gb|AW298747.1|AW298747 UI-H-BW0-ajq-b-01-0-UI.s1... 38 6.2
gi|6462898|gb|AW188462.1|AW188462 xj99b07.x1 NCI_CGAP_Co18 ... 38 6.2
gi|6037073|gb|AW081921.1|AW081921 xb57d02.x1 NCI_CGAP_Eso2 ... 38 6.2
gi|5664247|gb|AI928283.1|AI928283 wo67d07.x1 NCI_CGAP_Pr22 ... 38 6.2
gi|3890823|gb|AI271656.1|AI271656 qi30h05.x1 Soares_NhHMPu_... 38 6.2
gi|750752|gb|R01016.1|R01016 ye87a12.r1 Soares fetal liver ... 38 6.2

>gi|14724826|ref|XP_043555.1| hypothetical protein FLJ14431 [Homo sapiens]

EST Search:

Tissue type: Adrenal gland

Organ: Liver and Spleen
Develop. stage: 20 week-post conception fetus

Organ: liver
Tissue type: adenocarcinoma, cell line

rgan: lung
Tissue type: carcinoid

Sequences producing significant alignments: (bits) Value

gi|8165991|gb|AW974788.1|AW974788 EST386893 MAGE resequence... 1057 0.0
gi|10721718|dbj|AV704400.1|AV704400 AV704400 ADB Homo sapie... 1035 0.0
gi|1424282|gb|W91890.1|W91890 zh47a06.r1 Soares_fetal_liver... 1031 0.0
gi|12613045|gb|BG119539.1|BG119539 602347238F1 NIH_MGC_90 H... 989 0.0
gi|10940429|gb|BF110739.1|BF110739 7n56b09.x1 NCI_CGAP_Lu24... 971 0.0
gi|2657822|gb|AA677300.1|AA677300 zj61f10.s1 Soares_fetal_l... 900 0.0
gi|2584140|gb|AA652488.1|AA652488 ns70b08.s1 NCI_CGAP_Pr2 H... 890 0.0
gi|1472212|gb|AA011185.1|AA011185 ze22d01.s1 Soares_fetal_h... 793 0.0
gi|14320377|gb|BG925854.1|BG925854 HNC21-1-B1.R HNC (Human ... 773 0.0
gi|1388213|gb|W78181.1|W78181 zd68a06.r1 Soares_fetal_heart... 763 0.0
gi|1406088|gb|W90098.1|W90098 zh77e04.s1 Soares_fetal_liver... 714 0.0
gi|2657062|gb|AA676540.1|AA676540 zi38c04.s1 Soares_fetal_l... 698 0.0
gi|14166353|gb|BG818766.1|BG818766 602779096F2 NCI_CGAP_Brn... 642 0.0
gi|1406186|gb|W90196.1|W90196 zh77e04.r1 Soares_fetal_liver... 636 e-180

>gi|14782791|ref|XP_042583.1| FabG (beta-ketoacyl-[acyl-carrier-protein] reductase, E coli) like [Homo sapiens]

EST Search:

Tissues: Organ: lung
Tissue type: small cell carcinoma
Cell line: MGC3

Organ: pancreas
Tissue type: adenocarcinoma

Tissue type: placenta

Organ: placenta
Tissue type: choriocarcinoma

Tissue type: cervical carcinoma cell line

Organ: pancreas
Tissue type: epithelioid carcinoma cell line

Sequences producing significant alignments: (bits) Value

gi|10214178|gb|BE792980.1|BE792980 601585653F1 NIH_MGC_7 Ho... 1384 0.0
gi|10149821|gb|BE735829.1|BE735829 601305146F1 NIH_MGC_39 H... 1352 0.0
gi|12897211|emb|AL555459.1|AL555459 AL555459 LTI_NFL006_PL2... 1344 0.0
gi|10391209|gb|BE901734.1|BE901734 601675345F1 NIH_MGC_21 H... 1285 0.0
gi|14805093|gb|BI253554.1|BI253554 602973478F1 NIH_MGC_12 H... 1251 0.0
gi|14619885|gb|BI159884.1|BI159884 602863711F1 NIH_MGC_42 H... 1245 0.0
gi|2703586|gb|AA700623.1|AA700623 zi43a04.s1 Soares_fetal_l... 1203 0.0
gi|12897209|emb|AL555458.1|AL555458 AL555458 LTI_NFL006_PL2... 1183 0.0
gi|11613994|gb|BF526631.1|BF526631 602070755F1 NCI_CGAP_Brn... 1181 0.0
gi|5394035|gb|AI807469.1|AI807469 wf48b08.x1 Soares_NFL_T_G... 1170 0.0
gi|12345465|gb|BF978250.1|BF978250 602148205F1 NIH_MGC_62 H... 1142 0.0
gi|5878587|gb|AW025057.1|AW025057 wu93f03.x1 NCI_CGAP_Kid3 ... 1120 0.0
gi|5839154|gb|AI992249.1|AI992249 ws41d10.x1 NCI_CGAP_Brn25... 1067 0.0
gi|12411526|gb|BG025183.1|BG025183 602276160F1 NIH_MGC_85 H... 1027 0.0
gi|3766024|gb|AI207352.1|AI207352 qg26d10.x1 NCI_CGAP_Kid3 ... 1027 0.0
gi|4268048|gb|AI422117.1|AI422117 tf40g03.x1 NCI_CGAP_Brn23... 989 0.0
gi|2568438|gb|AA643220.1|AA643220 nr96h03.s1 NCI_CGAP_Pr25 ... 983 0.0
gi|4110767|gb|AI359146.1|AI359146 qy26b08.x1 NCI_CGAP_Brn23... 906 0.0
gi|5838543|gb|AI991715.1|AI991715 wt48a04.x1 NCI_CGAP_Pan1 ... 850 0.0
gi|5397037|gb|AI810471.1|AI810471 wb89a09.x1 NCI_CGAP_Pr28 ... 801 0.0
gi|2942259|gb|AA854721.1|AA854721 aj76h02.s1 Soares_parathy... 797 0.0
gi|4190811|gb|AI380946.1|AI380946 tg18c12.x1 NCI_CGAP_CLL1 ... 779 0.0
gi|3425472|gb|AI087049.1|AI087049 oy70b11.x1 NCI_CGAP_CLL1 ... 761 0.0
gi|6039316|gb|AW084164.1|AW084164 xc48b09.x1 NCI_CGAP_Eso2 ... 755 0.0
gi|3202509|gb|AI002175.1|AI002175 oq85b06.s1 NCI_CGAP_Kid6 ... 747 0.0
gi|2785843|gb|AA745857.1|AA745857 ny93f03.s1 NCI_CGAP_GCB1 ... 745 0.0
gi|1422483|gb|W93361.1|W93361 zd94g06.s1 Soares_fetal_heart... 731 0.0

>gi|14754051|ref|XP_003611.3| similar to oxidoreductase UCPA (H. sapiens) [Homo sapiens]

EST Search:

Organ: brain
Tissue type: neuroblastoma cells

Tissue type: placenta

Organ: kidney

Organ: lung
Tissue type: large cell carcinoma

Organ: brain
Tissue type: hypothalamus

Organ: parathyroid gland
Tissue type: parathyroid tumor

Sequences producing significant alignments: (bits) Value

gi|12786589|emb|AL523096.1|AL523096 AL523096 LTI_NFL003_NBC... 1550 0.0
gi|12889983|emb|AL551741.1|AL551741 AL551741 LTI_NFL006_PL2... 1457 0.0
gi|12936195|emb|AL575230.1|AL575230 AL575230 LTI_NFL006_PL2... 1296 0.0
gi|12793625|emb|AL530132.1|AL530132 AL530132 LTI_NFL001_NBC... 1289 0.0
gi|13294054|gb|BG400606.1|BG400606 602464263F1 NIH_MGC_75 H... 1271 0.0
gi|13452667|gb|BG491155.1|BG491155 602518792F1 NIH_MGC_18 H... 1237 0.0
gi|13982652|gb|BG706873.1|BG706873 602672037F1 NIH_MGC_96 H... 1229 0.0
gi|3281013|gb|AI041819.1|AI041819 oy34a10.x1 Soares_parathy... 1191 0.0
gi|13976480|gb|BG703780.1|BG703780 602686804F1 NIH_MGC_95 H... 1176 0.0
gi|14051133|gb|BG740480.1|BG740480 602633875F1 NCI_CGAP_Skn... 1170 0.0
gi|13545674|gb|BG547009.1|BG547009 602573805F1 NIH_MGC_77 H... 1168 0.0
gi|12793624|emb|AL530131.1|AL530131 AL530131 LTI_NFL001_NBC... 1168 0.0
gi|13039621|gb|BG286600.1|BG286600 602381608F1 NIH_MGC_93 H... 1152 0.0
gi|11257955|gb|BF310393.1|BF310393 601895043F1 NIH_MGC_19 H... 1146 0.0
gi|2839375|gb|AA780044.1|AA780044 zj24e12.s1 Soares_fetal_l... 1142 0.0
gi|8154981|gb|AW965145.1|AW965145 EST377218 MAGE resequence... 1138 0.0
gi|11265005|gb|BF316648.1|BF316648 601903206F1 NIH_MGC_19 H... 1134 0.0
gi|3238050|gb|AI022809.1|AI022809 ow55f02.x1 Soares_parathy... 1104 0.0
gi|4073201|gb|AI336274.1|AI336274 qt45e02.x1 Soares_fetal_l... 1096 0.0
gi|13544541|gb|BG545876.1|BG545876 602573161F1 NIH_MGC_77 H... 1094 0.0
gi|12598260|gb|BG104418.1|BG104418 602311036F1 NIH_MGC_20 H... 1086 0.0
gi|12598014|gb|BG104172.1|BG104172 602310736F1 NIH_MGC_20 H... 1080 0.0
gi|12606210|gb|BG112704.1|BG112704 602282264F1 NIH_MGC_86 H... 1065 0.0
gi|2877836|gb|AA808430.1|AA808430 oe53b08.s1 NCI_CGAP_Lu5 H... 1057 0.0
gi|6471396|gb|AW192697.1|AW192697 xl48h04.x1 NCI_CGAP_Pan1 ... 1037 0.0
gi|9323894|gb|BE378429.1|BE378429 601236767F1 NIH_MGC_44 Ho... 1035 0.0
gi|5109073|gb|AI740785.1|AI740785 wg24b10.x1 Soares_NSF_F8_... 997 0.0
gi|5813571|gb|AI986294.1|AI986294 wz64c08.x1 NCI_CGAP_Mel15... 987 0.0
gi|3400111|gb|AI073467.1|AI073467 ov45a08.x1 Soares_testis_... 983 0.0
gi|6228615|gb|AW157214.1|AW157214 au92h07.x1 Schneider feta... 981 0.0
gi|12910323|emb|AL562168.1|AL562168 AL562168 LTI_NFL003_NBC... 979 0.0
gi|9186202|gb|BE302454.1|BE302454 ba65f04.y1 NIH_MGC_20 Hom... 979 0.0
gi|9186195|gb|BE302447.1|BE302447 ba65e04.y1 NIH_MGC_20 Hom... 963 0.0
gi|12875811|emb|AL543333.1|AL543333 AL543333 LTI_NFL006_PL2... 957 0.0
gi|2993433|gb|AA883903.1|AA883903 aj13a01.s1 Soares_parathy... 946 0.0
gi|4435368|gb|AI521233.1|AI521233 to66f02.x1 NCI_CGAP_Gas4 ... 940 0.0
gi|10350081|gb|BE891095.1|BE891095 601432208F1 NIH_MGC_72 H... 922 0.0
gi|8750771|gb|BE207373.1|BE207373 ba65e04.x1 NIH_MGC_20 Hom... 920 0.0
gi|5858190|gb|AW009412.1|AW009412 ws82c11.x1 NCI_CGAP_Co3 H... 920 0.0
gi|3255193|gb|AI034240.1|AI034240 ow09h12.x1 Soares_parathy... 916 0.0
gi|2324986|gb|AA554447.1|AA554447 nl14h10.s1 NCI_CGAP_Br2 H... 916 0.0
gi|5546002|gb|AI871953.1|AI871953 wm53h05.x1 NCI_CGAP_Ut2 H... 914 0.0

gi|2955773|gb|AA863294.1|AA863294 og93b12.s1 NCI_CGAP_Kid5 ... 904 0.0
gi|4598887|gb|AI589839.1|AI589839 tm81a02.x1 NCI_CGAP_Brn25... 900 0.0

>gi|13278690|gb|AAH04126.1|AAH04126 (BC004126) DKFZP566O084 protein

EST search:

99% identities to ESTs found in small cell lung cancer (tissue, cell line), ovary adenocarcinoma (cell line); pancreas adenocarcinoma (tissue); kidney hypernephroma (cell line); skin/melanotic melanoma

Sequences producing significant alignments: (bits) Value

gi|10219393|gb|BE798195.1|BE798195 601582662F1 NIH_MGC_7 Ho... 1441 0.0
gi|10156033|gb|BE742041.1|BE742041 601594721F1 NIH_MGC_9 Ho... 1423 0.0
gi|10150854|gb|BE736951.1|BE736951 601306912F1 NIH_MGC_39 H... 1415 0.0
gi|10216541|gb|BE795343.1|BE795343 601586662F1 NIH_MGC_7 Ho... 1392 0.0
gi|12678574|gb|BG171871.1|BG171871 602322675F1 NIH_MGC_89 H... 1287 0.0
gi|9331772|gb|BE386407.1|BE386407 601273578F1 NIH_MGC_20 Ho... 1265 0.0
gi|9148949|gb|BE274012.1|BE274012 601104628F1 NIH_MGC_14 Ho... 1255 0.0
gi|9334357|gb|BE388992.1|BE388992 601284814F1 NIH_MGC_44 Ho... 1237 0.0
gi|5674161|gb|AI935291.1|AI935291 wp16e06.x1 NCI_CGAP_Lu19 ... 1209 0.0
gi|13409767|gb|BG477488.1|BG477488 602521540F1 NIH_MGC_20 H... 1180 0.0
gi|9335068|gb|BE389703.1|BE389703 601281945F1 NIH_MGC_44 Ho... 1180 0.0
gi|10206923|gb|BE785725.1|BE785725 601475291F1 NIH_MGC_68 H... 1160 0.0
gi|5920966|gb|AW055263.1|AW055263 wz16b09.x1 NCI_CGAP_Ut4 H... 1148 0.0
gi|14073190|gb|BG762537.1|BG762537 602733994F1 NIH_MGC_49 H... 1122 0.0
gi|4524063|gb|AI565606.1|AI565606 to16g08.x1 NCI_CGAP_Ut2 H... 1090 0.0
gi|9335871|gb|BE390506.1|BE390506 601284123F1 NIH_MGC_44 Ho... 1072 0.0
gi|1696026|gb|AA134925.1|AA134925 zo23c07.s1 Stratagene col... 1023 0.0
gi|2900361|gb|AA827998.1|AA827998 of10c11.s1 NCI_CGAP_Co12 ... 1021 0.0
gi|1383218|gb|W73084.1|W73084 zd54a11.r1 Soares_fetal_heart... 1013 0.0
gi|1319356|gb|W37623.1|W37623 zc12d10.r1 Soares_parathyroid... 963 0.0
gi|6026819|gb|AW071733.1|AW071733 ws54h10.x1 NCI_CGAP_Brn25... 959 0.0
gi|4176147|gb|AI376157.1|AI376157 ta59e06.x1 Soares_total_f... 940 0.0
gi|844959|gb|R71442.1|R71442 yi51f01.r1 Soares placenta Nb2... 940 0.0
gi|6039788|gb|AW084636.1|AW084636 xa45f07.x1 NCI_CGAP_Sar4 ... 924 0.0
gi|2809799|gb|AA760869.1|AA760869 nz14h12.s1 NCI_CGAP_GCB1 ... 912 0.0
gi|6039287|gb|AW084135.1|AW084135 xc37f09.x1 NCI_CGAP_Co20 ... 910 0.0
gi|1319357|gb|W37624.1|W37624 zc12d10.s1 Soares_parathyroid... 910 0.0
gi|2525832|gb|AA621956.1|AA621956 nq24a06.s1 NCI_CGAP_Co10 ... 902 0.0

>gi|14424501|gb|AAH09269.1|AAH09269 Unknown (protein for IMAGE:3140944) [Homo sapiens]

EST search:

97-99% identities to unknown cDNAs from lung carcinoid, neuroblastoma and mainly placenta

Sequences producing significant alignments: (bits) Value

gi|12790502|emb|AL527009.1|AL527009 AL527009 LTI_NFL003_NBC... 1893 0.0
gi|12790549|emb|AL527056.1|AL527056 AL527056 LTI_NFL003_NBC... 1709 0.0

gi|12937462|emb|AL575872.1|AL575872 AL575872 LTI_NFL006_PL2... 1639 0.0
gi|12891750|emb|AL552647.1|AL552647 AL552647 LTI_NFL006_PL2... 1485 0.0
gi|12882168|emb|AL547782.1|AL547782 AL547782 LTI_NFL006_PL2... 1441 0.0
gi|8907775|gb|BE220457.1|BE220457 hv39e05.x1 NCI_CGAP_Lu24 ... 1251 0.0
gi|11448101|gb|BF435786.1|BF435786 nab41g04.x1 Soares_NSF_F... 1229 0.0
gi|10322956|gb|BE874180.1|BE874180 601484366F1 NIH_MGC_69 H... 1213 0.0
gi|13326948|gb|BG420442.1|BG420442 602452476F1 NIH_MGC_14 H... 1195 0.0
gi|10321982|gb|BE873206.1|BE873206 601451732F1 NIH_MGC_65 H... 1170 0.0
gi|11511078|gb|BF445940.1|BF445940 7p16f08.x1 NCI_CGAP_Br22... 1164 0.0
gi|10939112|gb|BF109422.1|BF109422 7l62g12.x1 Soares_NSF_F8... 1158 0.0
gi|5127852|gb|AI749588.1|AI749588 at30h03.x1 Barstead colon... 1148 0.0
gi|9146194|gb|BE271998.1|BE271998 601141171F1 NIH_MGC_9 Hom... 1122 0.0
gi|10821551|gb|BF062641.1|BF062641 7h63b10.x1 NCI_CGAP_Co16... 1067 0.0
gi|10030710|gb|BE670169.1|BE670169 7e31b01.x1 NCI_CGAP_Lu24... 1039 0.0
gi|12882218|emb|AL547808.1|AL547808 AL547808 LTI_NFL006_PL2... 1023 0.0
gi|5232056|gb|AI765547.1|AI765547 wi81d04.x1 NCI_CGAP_Kid12... 987 0.0
gi|3539100|gb|AI123334.1|AI123334 qa48b12.x1 Soares_NhHMPu_... 987 0.0
gi|9706839|gb|BE504431.1|BE504431 hz86d06.x1 NCI_CGAP_Lu24 ... 975 0.0
gi|8278043|gb|BE017981.1|BE017981 bb74b11.y1 NIH_MGC_12 Hom... 973 0.0
gi|10813021|gb|BF059125.1|BF059125 7k66c05.x1 NCI_CGAP_GC6 ... 928 0.0
gi|8155988|gb|AW966152.1|AW966152 EST378225 MAGE resequence... 924 0.0
gi|9185243|gb|BE301495.1|BE301495 bb74b11.x1 NIH_MGC_12 Hom... 914 0.0
gi|5235374|gb|AI768865.1|AI768865 wj12g12.x1 NCI_CGAP_Kid12... 912 0.0
gi|12387026|gb|BF984214.1|BF984214 602307642F1 NIH_MGC_88 H... 906 0.0
gi|9512266|gb|BE466404.1|BE466404 hz21c10.x1 NCI_CGAP_GC6 H... 900 0.0

>gi|13543367|gb|AAH05844.1|AAH05844 Unknown (protein for MGC:2723) [Homo sapiens]

EST search: fetal and adult brain; neuroblastoma; leiomyosarcoma; pancreas carcinoma (cellline); Burkitt B cell lumphoma

Sequences producing significant alignments: (bits) Value

gi|12783362|emb|AL519869.1|AL519869 AL519869 LTI_NFL004_NBC... 1776 0.0
gi|12783361|emb|AL519868.1|AL519868 AL519868 LTI_NFL004_NBC... 1758 0.0
gi|12797239|emb|AL533746.1|AL533746 AL533746 LTI_FL013_FBm... 1739 0.0
gi|12916262|emb|AL565162.1|AL565162 AL565162 LTI_FL015_Bm1... 1542 0.0
gi|12797054|emb|AL533561.1|AL533561 AL533561 LTI_FL015_Bm1... 1443 0.0
gi|11971146|gb|BF685738.1|BF685738 602140418F1 NIH_MGC_46 H... 1338 0.0
gi|14178399|gb|BG830812.1|BG830812 602767532F1 NIH_MGC_42 H... 1304 0.0
gi|12951379|emb|AL582918.1|AL582918 AL582918 LTI_NFL010_BC2... 1269 0.0
gi|10201129|gb|BE779931.1|BE779931 601467958F1 NIH_MGC_67 H... 1229 0.0
gi|5664763|gb|AI928864.1|AI928864 au64c05.x1 Schneider feta... 1207 0.0
gi|13913479|gb|BG682082.1|BG682082 602630059F1 NCI_CGAP_Skn... 1191 0.0
gi|12417863|gb|BG028768.1|BG028768 602292961F1 NIH_MGC_86 H... 1180 0.0
gi|12797240|emb|AL533747.1|AL533747 AL533747 LTI_FL013_FBm... 1172 0.0
gi|12412351|gb|BG025595.1|BG025595 602274520F1 NIH_MGC_85 H... 1154 0.0
gi|2716956|gb|AA707038.1|AA707038 zj32c08.s1 Soares_fetal_l... 1120 0.0
gi|10203449|gb|BE782251.1|BE782251 601466684F1 NIH_MGC_67 H... 1102 0.0
gi|7376813|gb|AW630023.1|AW630023 hh74c04.y1 NCI_CGAP_GU1 H... 1102 0.0
gi|2357785|gb|AA579601.1|AA579601 nm71h09.s1 NCI_CGAP_Co9 H... 1086 0.0
gi|10740475|gb|BF032763.1|BF032763 601453471F1 NIH_MGC_66 H... 1084 0.0
gi|3253464|gb|AI032767.1|AI032767 ox13h06.x1 Soares_fetal_l... 1070 0.0
gi|13968664|gb|BG699891.1|BG699891 602681245F1 NIH_MGC_95 H... 1051 0.0

gi|2397741|gb|AA586927.1|AA586927 nn68g03.s1 NCI_CGAP_Lar1 ... 1013 0.0
gi|11592515|gb|BF509217.1|BF509217 UI-H-BI4-aov-h-02-0-UI.s... 1001 0.0
gi|5664992|gb|AI929028.1|AI929028 au64c05.y1 Schneider feta... 985 0.0
gi|2908208|gb|AA834609.1|AA834609 od64c08.s1 NCI_CGAP_GCB1 ... 981 0.0
gi|6589783|gb|AW246790.1|AW246790 2822178.3prime NIH_MGC_7 ... 975 0.0
gi|13987461|gb|BG709280.1|BG709280 602674673F1 NIH_MGC_96 H... 954 0.0
gi|6086780|gb|AW118196.1|AW118196 xd91b01.x1 Soares_NFL_T_G... 950 0.0
gi|13987880|gb|BG709491.1|BG709491 602674765F1 NIH_MGC_96 H... 938 0.0
gi|1633828|gb|AA088298.1|AA088298 zl84d09.r1 Stratagene col... 934 0.0
gi|2875181|gb|AA806431.1|AA806431 oc23a07.s1 NCI_CGAP_GCB1 ... 910 0.0

>gi|10439230|dbj|BAB15467.1| unnamed protein product [Homo sapiens]

EST search: testis, melanotic melanoma, adenocarcinoma (cellline)

Sequences producing significant alignments: (bits) Value

gi|13999456|gb|BG720269.1|BG720269 602692330F1 NIH_MGC_97 H... 1217 0.0
gi|11975300|gb|BF689892.1|BF689892 602186442F1 NIH_MGC_49 H... 1209 0.0
gi|10350124|gb|BE891116.1|BE891116 601432231F1 NIH_MGC_72 H... 1118 0.0
gi|10161479|gb|BE747487.1|BE747487 601573861F1 NIH_MGC_9 Ho... 965 0.0

>gi|14764177|ref|XP_044864.1| hypothetical protein FLJ10462 [Homo sapiens]

EST search: neuroblastoma; skin; lung

Sequences producing significant alignments: (bits) Value

gi|12792604|emb|AL529111.1|AL529111 AL529111 LTI_NFL001_NBC... 1663 0.0
gi|14052499|gb|BG741846.1|BG741846 602634860F1 NCI_CGAP_Skn... 1562 0.0
gi|12792603|emb|AL529110.1|AL529110 AL529110 LTI_NFL001_NBC... 1505 0.0
gi|13544215|gb|BG545550.1|BG545550 602572801F1 NIH_MGC_77 H... 1417 0.0
gi|13459313|gb|BG497796.1|BG497796 602543069F1 NIH_MGC_60 H... 1310 0.0
gi|13983654|gb|BG707372.1|BG707372 602672776F1 NIH_MGC_96 H... 1239 0.0
gi|4684870|gb|AI633540.1|AI633540 th68d07.x1 Soares_NhHMPu_... 1229 0.0
gi|13342208|gb|BG435702.1|BG435702 602506802F1 NIH_MGC_79 H... 1207 0.0
gi|10700212|gb|BE999936.1|BE999936 7h20b10.x1 NCI_CGAP_Co16... 1197 0.0
gi|9810737|gb|BE567017.1|BE567017 601341163F1 NIH_MGC_53 Ho... 1180 0.0
gi|11985103|gb|BF699695.1|BF699695 602127115F1 NIH_MGC_56 H... 1160 0.0
gi|13521358|gb|BG529821.1|BG529821 602558905F1 NIH_MGC_61 H... 1120 0.0
gi|10997231|dbj|AU136692.1|AU136692 AU136692 PLACE1 Homo sa... 1072 0.0
gi|2207965|gb|AA479409.1|AA479409 zv21g08.r1 Soares_NhHMPu_... 1057 0.0
gi|5631452|gb|AI911597.1|AI911597 wc86a01.x1 NCI_CGAP_Co3 H... 1029 0.0
gi|2207864|gb|AA479308.1|AA479308 zv21g08.s1 Soares_NhHMPu_... 932 0.0
gi|5865542|gb|AW016785.1|AW016785 UI-H-BI0p-abm-g-01-0-UI.s... 926 0.0

>gi|14041699|emb|CAC38443.1| dJ1033B10.9.2 (FabG (beta-ketoacyl-[acyl-carrier-protein] reductase, E coli) like, isoform 2) [Homo sapiens]

97% identical to DHB8; EST search not performed: only 180 Kbp available

>gi|14041946|dbj|BAB55045.1| (AK027337) unnamed protein product

EST search with poor annotated entry: weak similarities with cDNAs expressed in adrenal gland, colon tumor, liver, spleen,lung

Sequences producing significant alignments: (bits) Value

gi|10721718|dbj|AV704400.1|AV704400 AV704400 ADB Homo sapie... 1059 0.0
gi|8165991|gb|AW974788.1|AW974788 EST386893 MAGE resequence... 1057 0.0
gi|1424282|gb|W91890.1|W91890 zh47a06.r1 Soares_fetal_liver... 1029 0.0
gi|10940429|gb|BF110739.1|BF110739 7n56b09.x1 NCI_CGAP_Lu24... 971 0.0
gi|12613045|gb|BG119539.1|BG119539 602347238F1 NIH_MGC_90 H... 950 0.0
gi|2657822|gb|AA677300.1|AA677300 zj61f10.s1 Soares_fetal_l... 900 0.0

putative SDRs identified with no obvious annotation as SDRs in NCBI database and/or referenced Medline/PubMed-link

>gi|11435147|ref|XP_006732.1| retinol dehydrogenase 5 (11-cis and 9-cis) [Homo sapiens]

EST Search:

Sequences producing significant alignments: (bits) Value

gi|8908990|gb|BE221672.1|BE221672 hu27e10.x1 NCI_CGAP_Mel15... 1146 0.0
gi|4900121|gb|AI688827.1|AI688827 wd41d07.x1 Soares_NFL_T_G... 969 0.0
gi|4618930|gb|AI609763.1|AI609763 tf83a04.x1 NCI_CGAP_Brn23... 959 0.0
gi|11081688|gb|BF195132.1|BF195132 7n15f01.x1 NCI_CGAP_Brn2... 950 0.0
gi|4264406|gb|AI418475.1|AI418475 tf74h03.x1 NCI_CGAP_Brn23... 946 0.0
gi|14292293|gb|BG911817.1|BG911817 602810064F1 NCI_CGAP_Brn... 938 0.0
gi|11593828|gb|BF510530.1|BF510530 UI-H-BI4-apa-e-11-0-UI.s... 846 0.0
gi|4114767|gb|AI363146.1|AI363146 qy55a02.x1 NCI_CGAP_Brn23... 799 0.0
gi|5854635|gb|AW005857.1|AW005857 wz80d08.x1 NCI_CGAP_Gas4 ... 797 0.0
gi|6661708|gb|AW274678.1|AW274678 xv32d08.x1 Soares_NFL_T_G... 783 0.0
gi|2525787|gb|AA621911.1|AA621911 nq30b08.s1 NCI_CGAP_Co10 ... 781 0.0
gi|5527702|gb|AI863595.1|AI863595 wj18h11.x1 NCI_CGAP_Kid12... 688 0.0
gi|1190064|gb|N48898.1|N48898 yy77e08.s1 Soares_multiple_sc... 688 0.0
gi|2505366|gb|AA618161.1|AA618161 nq14d10.s1 NCI_CGAP_Thy1 ... 686 0.0
gi|2656640|gb|AA680173.1|AA680173 zi11b06.s1 Soares_fetal_l... 684 0.0
gi|5396293|gb|AI809727.1|AI809727 wh77a07.x1 NCI_CGAP_CLL1 ... 682 0.0
gi|3279324|gb|AI040130.1|AI040130 ox08h01.x1 Soares_fetal_l... 664 0.0
gi|1448549|gb|AA004494.1|AA004494 zh87b01.r1 Soares_fetal_l... 650 0.0
gi|1018746|gb|H63945.1|H63945 yr55b01.s1 Soares fetal liver... 632 e-179
gi|1716962|gb|AA147453.1|AA147453 zl51h03.r1 Soares_pregnan... 613 e-173
gi|1524527|gb|AA046629.1|AA046629 zk62h02.r1 Soares_pregnan... 611 e-172
gi|1188267|gb|N47101.1|N47101 yy85f02.s1 Soares_multiple_sc... 601 e-169

>gi|13655317|ref|XP_007380.2| CGI-86 protein [Homo sapiens]

EST Search:

Sequences producing significant alignments: (bits) Value

gi|12908926|emb|AL561466.1|AL561466 AL561466 LTI_NFL010_BC2... 1475 0.0
gi|12908868|emb|AL561437.1|AL561437 AL561437 LTI_NFL010_BC2... 1457 0.0
gi|13705885|gb|BG184198.1|BG184198 RST3119 Athersys RAGE Li... 1455 0.0
gi|10161043|gb|BE747051.1|BE747051 601580610F1 NIH_MGC_9 Ho... 1382 0.0
gi|9141043|gb|BE267452.1|BE267452 601189745F2 NIH_MGC_7 Hom... 1285 0.0
gi|14080921|gb|BG770268.1|BG770268 602744858F1 NIH_MGC_49 H... 1281 0.0
gi|3308715|gb|AI052724.1|AI052724 oz27a12.x1 Soares_total_f... 1227 0.0
gi|6300903|gb|AW161870.1|AW161870 au71a04.x1 Schneider feta... 1215 0.0
gi|13583649|gb|BG575996.1|BG575996 602597341F1 NIH_MGC_87 H... 1189 0.0
gi|13135151|gb|BG328713.1|BG328713 602427988F1 NIH_MGC_15 H... 1181 0.0
gi|12337285|gb|BF970070.1|BF970070 602272338F1 NIH_MGC_84 H... 1164 0.0
gi|11649289|gb|BF575655.1|BF575655 602133057F1 NIH_MGC_81 H... 1162 0.0
gi|10149412|gb|BE735420.1|BE735420 601304204F1 NIH_MGC_39 H... 1160 0.0
gi|13134589|gb|BG328151.1|BG328151 602427216F1 NIH_MGC_15 H... 1152 0.0
gi|5633042|gb|AI913268.1|AI913268 wa10f08.x1 NCI_CGAP_Kid11... 1148 0.0
gi|13405005|gb|BG472730.1|BG472730 602514555F1 NIH_MGC_16 H... 1114 0.0
gi|13411959|gb|BG479680.1|BG479680 602527142F1 NIH_MGC_21 H... 1102 0.0
gi|10888750|gb|BF106224.1|BF106224 601823412F1 NIH_MGC_77 H... 1098 0.0
gi|10700778|gb|BF000503.1|BF000503 7h32a01.x1 NCI_CGAP_Co16... 1084 0.0
gi|6709918|gb|AW300318.1|AW300318 xs59g06.x1 NCI_CGAP_Kid11... 1078 0.0
gi|11947563|gb|BF673668.1|BF673668 602136388F1 NIH_MGC_83 H... 1072 0.0
gi|11685208|gb|BF592884.1|BF592884 7j95h06.x1 NCI_CGAP_GC6 ... 1070 0.0
gi|10984835|gb|BF115433.1|BF115433 7n81h06.x1 NCI_CGAP_Ov18... 1070 0.0
gi|13544202|gb|BG545537.1|BG545537 602572781F1 NIH_MGC_77 H... 1061 0.0
gi|13404427|gb|BG472241.1|BG472241 602513753F1 NIH_MGC_16 H... 1059 0.0
gi|11951687|gb|BF677792.1|BF677792 602085496F1 NIH_MGC_83 H... 1039 0.0
gi|10940810|gb|BF111120.1|BF111120 7n43g10.x1 NCI_CGAP_Lu24... 1027 0.0
gi|13137281|gb|BG330843.1|BG330843 602431480F1 NIH_MGC_18 H... 1017 0.0
gi|13971790|gb|BG701448.1|BG701448 602682670F1 NIH_MGC_95 H... 1013 0.0
gi|11952455|gb|BF678560.1|BF678560 602086022F1 NIH_MGC_83 H... 1011 0.0
gi|11450749|gb|BF438232.1|BF438232 7q68g12.x1 NCI_CGAP_Lu24... 1009 0.0
gi|11060866|gb|BF182723.1|BF182723 601809222F1 NIH_MGC_18 H... 1005 0.0
gi|6197433|gb|AW149537.1|AW149537 xf39b12.x1 NCI_CGAP_Brn50... 997 0.0
gi|9510747|gb|BE464972.1|BE464972 hv76a11.x1 NCI_CGAP_Lu24 ... 995 0.0
gi|13290415|gb|BG396967.1|BG396967 602433879F1 NIH_MGC_20 H... 991 0.0
gi|9333920|gb|BE388555.1|BE388555 601281843F1 NIH_MGC_44 Ho... 975 0.0
gi|3056175|gb|AA916783.1|AA916783 on10d05.s1 NCI_CGAP_Lu5 H... 973 0.0
gi|10209987|gb|BE788800.1|BE788800 601475705F1 NIH_MGC_68 H... 965 0.0
gi|6710858|gb|AW301181.1|AW301181 xs57d11.x1 NCI_CGAP_Kid11... 959 0.0
gi|9335147|gb|BE389782.1|BE389782 601282967F1 NIH_MGC_44 Ho... 957 0.0
gi|4985638|gb|AI697738.1|AI697738 we16g07.x1 NCI_CGAP_Lu24 ... 954 0.0
gi|9334997|gb|BE389632.1|BE389632 601283343F1 NIH_MGC_44 Ho... 952 0.0
gi|11649406|gb|BF575694.1|BF575694 602135311F1 NIH_MGC_81 H... 942 0.0
gi|1371301|gb|W63721.1|W63721 zc58g09.r1 Soares_parathyroid... 934 0.0
gi|10821341|gb|BF062431.1|BF062431 7h59a01.x1 NCI_CGAP_Co16... 926 0.0
gi|9126816|gb|BE256444.1|BE256444 601108430F1 NIH_MGC_16 Ho... 924 0.0
gi|11979410|gb|BF694002.1|BF694002 602082590F1 NIH_MGC_81 H... 920 0.0
gi|9123725|gb|BE253566.1|BE253566 601108683F1 NIH_MGC_16 Ho... 914 0.0
gi|5424673|gb|AI813458.1|AI813458 wj06f03.x1 NCI_CGAP_Kid12... 912 0.0
gi|3419256|gb|AI082464.1|AI082464 os71e10.x1 NCI_CGAP_GC2 H... 912 0.0
gi|13326319|gb|BG419813.1|BG419813 602453265F1 NIH_MGC_14 H... 906 0.0
gi|11945543|gb|BF671648.1|BF671648 602151504F1 NIH_MGC_81 H... 902 0.0
gi|5934152|gb|AW058513.1|AW058513 wx21h07.x1 NCI_CGAP_Kid11... 900 0.0
gi|12356787|gb|BF939467.1|BF939467 nac76d02.x1 NCI_CGAP_Brn... 898 0.0
gi|5235327|gb|AI768818.1|AI768818 wj03f04.x1 NCI_CGAP_Kid12... 890 0.0
gi|4069463|gb|AI332904.1|AI332904 qq27e11.x1 Soares_NhHMPu_... 882 0.0
gi|11085132|gb|BF196789.1|BF196789 7n05h02.x1 NCI_CGAP_Brn2... 880 0.0

gi|2261683|gb|AA521140.1|AA521140 aa73a10.s1 NCI_CGAP_GCB1 ... 880 0.0
gi|4393211|gb|AI492208.1|AI492208 tg07h04.x1 NCI_CGAP_CLL1 ... 874 0.0
gi|11949993|gb|BF676098.1|BF676098 602084079F1 NIH_MGC_83 H... 866 0.0
gi|9129213|gb|BE258720.1|BE258720 601107578F1 NIH_MGC_16 Ho... 866 0.0
gi|6717096|gb|AW304893.1|AW304893 xv90f05.x1 NCI_CGAP_Brn53... 862 0.0
gi|3736353|gb|AI185715.1|AI185715 qe33a05.s1 Soares_fetal_l... 856 0.0
gi|11450810|gb|BF438293.1|BF438293 7q07e04.x1 NCI_CGAP_Pr28... 852 0.0
gi|4985507|gb|AI697607.1|AI697607 we15d01.x1 NCI_CGAP_Lu24 ... 842 0.0
gi|5437513|gb|AI818434.1|AI818434 wk52f11.x1 NCI_CGAP_Pr22 ... 839 0.0
gi|3675611|gb|AI147929.1|AI147929 qb38g05.x1 Soares_pregnan... 837 0.0
gi|2350395|gb|AA575880.1|AA575880 nm55b04.s1 NCI_CGAP_Br3 H... 837 0.0
gi|1849358|gb|AA227813.1|AA227813 zr56d01.r1 Soares_NhHMPu_... 837 0.0
gi|13326406|gb|BG419900.1|BG419900 602453365F1 NIH_MGC_14 H... 831 0.0
gi|8427731|gb|BE077176.1|BE077176 RC5-BT0605-150200-031-E02... 831 0.0
gi|4080985|gb|AI343779.1|AI343779 qp12a05.x1 NCI_CGAP_Kid5 ... 831 0.0
gi|10703173|gb|BF002898.1|BF002898 7g50f10.x1 NCI_CGAP_Pr28... 827 0.0
gi|4075900|gb|AI338973.1|AI338973 qq29d06.x1 Soares_NhHMPu_... 823 0.0
gi|1306303|gb|W26018.1|W26018 18b7 Human retina cDNA random... 815 0.0
gi|5863353|gb|AW014596.1|AW014596 UI-H-BI0p-aaw-f-06-0-UI.s... 813 0.0
gi|5451513|gb|AI830757.1|AI830757 wj10h09.x1 NCI_CGAP_Kid12... 807 0.0
gi|14567892|gb|BI116991.1|BI116991 602867759F1 NIH_MGC_7 Ho... 803 0.0
gi|5365704|gb|AI800232.1|AI800232 ti76c08.x1 NCI_CGAP_Kid11... 803 0.0
gi|12079946|gb|BF753361.1|BF753361 QV0-CT0581-021000-421-c0... 801 0.0
gi|3933769|gb|AI290995.1|AI290995 qm09e06.x1 NCI_CGAP_Lu5 H... 801 0.0

>gi|12734537|ref|XP_005309.2| 2,4-dienoyl CoA reductase 1 precursor [Homo sapiens]

EST Search:

Sequences producing significant alignments: (bits) Value

gi|12787985|emb|AL524492.1|AL524492 AL524492 LTI_NFL003_NBC... 1859 0.0
gi|12787984|emb|AL524491.1|AL524491 AL524491 LTI_NFL003_NBC... 1626 0.0
gi|13996626|gb|BG717439.1|BG717439 602689790F1 NIH_MGC_97 H... 1495 0.0
gi|14650504|gb|BI195484.1|BI195484 602755036F1 NIH_MGC_19 H... 1469 0.0
gi|10162948|gb|BE748956.1|BE748956 601571895T1 NIH_MGC_55 H... 1469 0.0
gi|14071764|gb|BG761111.1|BG761111 602717444F1 NIH_MGC_49 H... 1453 0.0
gi|12672608|gb|BG165905.1|BG165905 602344213F1 NIH_MGC_89 H... 1423 0.0
gi|13466606|gb|BG505089.1|BG505089 602551544F1 NIH_MGC_61 H... 1404 0.0
gi|5128317|gb|AI750053.1|AI750053 at35b09.x1 Barstead colon... 1400 0.0
gi|10813760|dbj|AV716608.1|AV716608 AV716608 DCB Homo sapie... 1392 0.0
gi|13576811|gb|BG569158.1|BG569158 602588419F1 NIH_MGC_76 H... 1370 0.0
gi|13336042|gb|BG429536.1|BG429536 602501205F1 NIH_MGC_75 H... 1360 0.0
gi|13571121|gb|BG563469.1|BG563469 602582557F1 NIH_MGC_76 H... 1346 0.0
gi|14047081|gb|BG776764.1|BG776764 602663939F1 NIH_MGC_59 H... 1344 0.0
gi|13524113|gb|BG532574.1|BG532574 602562137F1 NIH_MGC_61 H... 1344 0.0
gi|10319791|gb|BE871015.1|BE871015 601449051F1 NIH_MGC_65 H... 1344 0.0
gi|10210166|gb|BE788968.1|BE788968 601481053F1 NIH_MGC_68 H... 1344 0.0
gi|10206721|gb|BE785523.1|BE785523 601475329F1 NIH_MGC_68 H... 1320 0.0
gi|13669956|gb|BG618585.1|BG618585 602646010F1 NIH_MGC_76 H... 1306 0.0
gi|12674840|gb|BG168137.1|BG168137 602341524F1 NIH_MGC_89 H... 1294 0.0
gi|13574458|gb|BG566805.1|BG566805 602585688F1 NIH_MGC_76 H... 1291 0.0
gi|5393464|gb|AI806898.1|AI806898 wf36f02.x1 Soares_NFL_T_G... 1291 0.0
gi|13336546|gb|BG430040.1|BG430040 602499409F1 NIH_MGC_75 H... 1287 0.0
gi|10916765|dbj|AV758917.1|AV758917 AV758917 MDS Homo sapie... 1279 0.0

gi|11648055|gb|BF574343.1|BF574343 602131537F1 NIH_MGC_81 H... 1271 0.0
gi|14047349|gb|BG777032.1|BG777032 602664238F1 NIH_MGC_59 H... 1269 0.0
gi|13524448|gb|BG532909.1|BG532909 602580556F1 NIH_MGC_61 H... 1263 0.0
gi|13669025|gb|BG617654.1|BG617654 602615762F1 NIH_MGC_76 H... 1257 0.0
gi|13295060|gb|BG401612.1|BG401612 602466262F1 NIH_MGC_75 H... 1257 0.0
gi|11648020|gb|BF574308.1|BF574308 602131489F1 NIH_MGC_81 H... 1251 0.0
gi|13670107|gb|BG618736.1|BG618736 602645192F1 NIH_MGC_76 H... 1245 0.0
gi|10162429|gb|BE748437.1|BE748437 601571895F1 NIH_MGC_55 H... 1243 0.0
gi|10207538|gb|BE786340.1|BE786340 601474505F1 NIH_MGC_68 H... 1233 0.0
gi|13543379|gb|BG545240.1|BG545240 602572450F1 NIH_MGC_77 H... 1221 0.0
gi|13283602|gb|BG390056.1|BG390056 602415784F1 NIH_MGC_92 H... 1207 0.0
gi|11105794|gb|BF212221.1|BF212221 601813443F1 NIH_MGC_54 H... 1203 0.0
gi|9134418|gb|BE313925.1|BE313925 601146583F1 NIH_MGC_19 Ho... 1199 0.0
gi|13519342|gb|BG527805.1|BG527805 602556753F1 NIH_MGC_59 H... 1189 0.0
gi|6196683|gb|AW148787.1|AW148787 xf04d02.x1 NCI_CGAP_Brn35... 1181 0.0
gi|9810255|gb|BE566431.1|BE566431 601340156F1 NIH_MGC_53 Ho... 1170 0.0
gi|11650783|gb|BF577071.1|BF577071 602135542F1 NIH_MGC_81 H... 1166 0.0
gi|11986472|gb|BF701064.1|BF701064 602128120F1 NIH_MGC_56 H... 1160 0.0
gi|5674987|gb|AI936117.1|AI936117 wo62a01.x1 NCI_CGAP_Pr22 ... 1150 0.0
gi|10888864|gb|BF106338.1|BF106338 601823556F1 NIH_MGC_77 H... 1140 0.0
gi|4079311|gb|AI342384.1|AI342384 qt27f04.x1 Soares_pregnan... 1140 0.0
gi|13522631|gb|BG531094.1|BG531094 602560995F1 NIH_MGC_61 H... 1136 0.0
gi|13337092|gb|BG430484.1|BG430484 602502057F1 NIH_MGC_75 H... 1136 0.0
gi|9809967|gb|BE566247.1|BE566247 601339193F1 NIH_MGC_53 Ho... 1134 0.0
gi|9808670|gb|BE564950.1|BE564950 601343662F1 NIH_MGC_53 Ho... 1132 0.0
gi|4391359|gb|AI499377.1|AI499377 to11a08.x1 NCI_CGAP_Ut2 H... 1114 0.0
gi|13333323|gb|BG426817.1|BG426817 602492994F1 NIH_MGC_75 H... 1100 0.0
gi|3245241|gb|AI027932.1|AI027932 ov99h12.x1 Soares_testis_... 1100 0.0
gi|10814759|dbj|AV717607.1|AV717607 AV717607 DCB Homo sapie... 1098 0.0
gi|10723616|dbj|AV706331.1|AV706331 AV706331 ADB Homo sapie... 1098 0.0
gi|10851958|dbj|AV734413.1|AV734413 AV734413 cdA Homo sapie... 1082 0.0
gi|10579243|gb|BE968538.1|BE968538 601649641F1 NIH_MGC_74 H... 1080 0.0
gi|11104025|gb|BF210439.1|BF210439 601875143F1 NIH_MGC_54 H... 1072 0.0
gi|6199884|gb|AW151899.1|AW151899 xf72e05.x1 NCI_CGAP_Gas4 ... 1068 0.0
gi|13573893|gb|BG566240.1|BG566240 602585102F1 NIH_MGC_76 H... 1065 0.0
gi|10402036|gb|BE907952.1|BE907952 601497316F1 NIH_MGC_70 H... 1061 0.0
gi|10717509|dbj|AV701179.1|AV701179 AV701179 ADA Homo sapie... 1057 0.0
gi|11102130|gb|BF208544.1|BF208544 601871843F1 NIH_MGC_53 H... 1041 0.0
gi|12512188|gb|BG054950.1|BG054950 nac92g03.x1 NCI_CGAP_Brn... 1039 0.0
gi|2630456|gb|AA668957.1|AA668957 ab92c10.s1 Stratagene lun... 1039 0.0
gi|10315023|gb|BE866260.1|BE866260 601679059F1 NIH_MGC_53 H... 1035 0.0
gi|12676884|gb|BG170256.1|BG170256 602321782F1 NIH_MGC_89 H... 1033 0.0
gi|11629247|gb|BF541938.1|BF541938 602068441F1 NIH_MGC_58 H... 1023 0.0
gi|3735925|gb|AI185287.1|AI185287 qe36a10.s1 Soares_fetal_l... 1021 0.0
gi|11108277|gb|BF214691.1|BF214691 601846069F1 NIH_MGC_55 H... 1017 0.0
gi|4650178|gb|AI625247.1|AI625247 ts42e09.x1 NCI_CGAP_Ut1 H... 1017 0.0
gi|3750677|gb|AI198071.1|AI198071 qi54a04.x1 NCI_CGAP_Brn25... 1015 0.0
gi|4286957|gb|AI433121.1|AI433121 th41f10.x1 NCI_CGAP_Lym12... 1011 0.0
gi|9808193|gb|BE564473.1|BE564473 601343803F1 NIH_MGC_53 Ho... 1009 0.0
gi|10797532|dbj|AV716015.1|AV716015 AV716015 DCB Homo sapie... 999 0.0
gi|4070539|gb|AI333980.1|AI333980 qq32f10.x1 Soares_NhHMPu_... 999 0.0
gi|1679318|gb|AA121670.1|AA121670 zn80d01.s1 Stratagene lun... 995 0.0
gi|2165551|gb|AA451882.1|AA451882 zx16e12.s1 Soares_total_f... 993 0.0
gi|11977705|gb|BF692297.1|BF692297 602249180F1 NIH_MGC_62 H... 983 0.0
gi|9812695|gb|BE568975.1|BE568975 601342357F1 NIH_MGC_53 Ho... 981 0.0
gi|2165746|gb|AA452077.1|AA452077 zx16e11.r1 Soares_total_f... 979 0.0
gi|6040380|gb|AW085228.1|AW085228 xe07d10.x1 Soares_NFL_T_G... 973 0.0

gi|6921257|gb|AW402560.1|AW402560 UI-HF-BK0-aax-a-08-0-UI.r... 969 0.0
gi|2229702|gb|AA496381.1|AA496381 zv31a09.r1 Soares ovary t... 969 0.0
gi|4898710|gb|AI687416.1|AI687416 tp95g10.x1 NCI_CGAP_Ut3 H... 942 0.0
gi|10797969|dbj|AV716452.1|AV716452 AV716452 DCB Homo sapie... 934 0.0
gi|3075651|gb|AA926754.1|AA926754 om25b04.s1 Soares_NFL_T_G... 934 0.0
gi|2884854|gb|AA815258.1|AA815258 ai64d09.s1 Soares_testis_... 932 0.0
gi|11154787|gb|BF240863.1|BF240863 601875406F2 NIH_MGC_55 H... 922 0.0
gi|2156294|gb|AA443619.1|AA443619 zw35d11.s1 Soares ovary t... 920 0.0
gi|2525613|gb|AA621674.1|AA621674 af48e02.s1 Soares_total_f... 906 0.0
gi|10736097|gb|BF028385.1|BF028385 601765181F1 NIH_MGC_53 H... 904 0.0
gi|2959001|gb|AA864688.1|AA864688 oh02c01.s1 NCI_CGAP_Kid3 ... 900 0.0
gi|11648352|gb|BF574640.1|BF574640 602132107F1 NIH_MGC_81 H... 898 0.0
gi|3330805|gb|AI057016.1|AI057016 oy75a01.x1 NCI_CGAP_CLL1 ... 884 0.0
gi|4081099|gb|AI343893.1|AI343893 qp12h02.x1 NCI_CGAP_Kid5 ... 882 0.0
gi|3428450|gb|AI089391.1|AI089391 qb09g07.x1 Soares_pregnan... 878 0.0
gi|3051606|gb|AA912214.1|AA912214 ol92b03.s1 NCI_CGAP_PNS1 ... 878 0.0
gi|4084859|gb|AI347653.1|AI347653 qp01b03.x1 NCI_CGAP_Kid5 ... 858 0.0
gi|2884432|gb|AA814836.1|AA814836 oc05e05.s1 NCI_CGAP_GCB1 ... 858 0.0
gi|10314694|gb|BE865918.1|BE865918 601678332F1 NIH_MGC_53 H... 854 0.0

>gi|14198251|gb|AAH08185.1|AAH08185 Unknown (protein for MGC:17181) [Homo sapiens]

EST Search:

Sequences producing significant alignments: (bits) Value

gi|10214178|gb|BE792980.1|BE792980 601585653F1 NIH_MGC_7 Ho... 1384 0.0
gi|10149821|gb|BE735829.1|BE735829 601305146F1 NIH_MGC_39 H... 1352 0.0
gi|12897211|emb|AL555459.1|AL555459 AL555459 LTI_NFL006_PL2... 1344 0.0
gi|10391209|gb|BE901734.1|BE901734 601675345F1 NIH_MGC_21 H... 1285 0.0
gi|14805093|gb|BI253554.1|BI253554 602973478F1 NIH_MGC_12 H... 1251 0.0
gi|14619885|gb|BI159884.1|BI159884 602863711F1 NIH_MGC_42 H... 1245 0.0
gi|2703586|gb|AA700623.1|AA700623 zi43a04.s1 Soares_fetal_l... 1203 0.0
gi|12897209|emb|AL555458.1|AL555458 AL555458 LTI_NFL006_PL2... 1183 0.0
gi|11613994|gb|BF526631.1|BF526631 602070755F1 NCI_CGAP_Brn... 1181 0.0
gi|5394035|gb|AI807469.1|AI807469 wf48b08.x1 Soares_NFL_T_G... 1170 0.0
gi|12345465|gb|BF978250.1|BF978250 602148205F1 NIH_MGC_62 H... 1142 0.0
gi|5878587|gb|AW025057.1|AW025057 wu93f03.x1 NCI_CGAP_Kid3 ... 1120 0.0
gi|5839154|gb|AI992249.1|AI992249 ws41d10.x1 NCI_CGAP_Brn25... 1067 0.0
gi|12411526|gb|BG025183.1|BG025183 602276160F1 NIH_MGC_85 H... 1027 0.0
gi|3766024|gb|AI207352.1|AI207352 qg26d10.x1 NCI_CGAP_Kid3 ... 1027 0.0
gi|4268048|gb|AI422117.1|AI422117 tf40g03.x1 NCI_CGAP_Brn23... 989 0.0
gi|2568438|gb|AA643220.1|AA643220 nr96h03.s1 NCI_CGAP_Pr25 ... 983 0.0
gi|4110767|gb|AI359146.1|AI359146 qy26b08.x1 NCI_CGAP_Brn23... 906 0.0
gi|5838543|gb|AI991715.1|AI991715 wt48a04.x1 NCI_CGAP_Pan1 ... 850 0.0
gi|5397037|gb|AI810471.1|AI810471 wb89a09.x1 NCI_CGAP_Pr28 ... 801 0.0

>gi|5531815|gb|AAD44482.1| steroid dehydrogenase homolog [Homo sapiens]

EST Search:

Sequences producing significant alignments: (bits) Value

gi|14052291|gb|BG741638.1|BG741638 602635486F1 NCI_CGAP_Skn... 1558 0.0

gi|13906836|gb|BG675440.1|BG675440 602621769F1 NCI_CGAP_Skn... 1526 0.0

gi|13913842|gb|BG682445.1|BG682445 602630189F1 NCI_CGAP_Skn... 1425 0.0
gi|14049580|gb|BG779263.1|BG779263 602665945F1 NIH_MGC_60 H... 1413 0.0
gi|13996568|gb|BG717381.1|BG717381 602689723F1 NIH_MGC_97 H... 1404 0.0
gi|13995178|gb|BG715991.1|BG715991 602674063F1 NIH_MGC_96 H... 1370 0.0
gi|14511171|gb|BI092841.1|BI092841 602858662F1 NIH_MGC_10 H... 1346 0.0
gi|12670128|gb|BG163425.1|BG163425 602338406F1 NIH_MGC_89 H... 1346 0.0
gi|14511086|gb|BI092756.1|BI092756 602858554F1 NIH_MGC_10 H... 1332 0.0
gi|13987330|gb|BG709215.1|BG709215 602675095F1 NIH_MGC_96 H... 1332 0.0
gi|13910534|gb|BG679137.1|BG679137 602627203F1 NCI_CGAP_Skn... 1328 0.0
gi|13662470|gb|BG611099.1|BG611099 602612052F1 NIH_MGC_60 H... 1314 0.0
gi|13045302|gb|BG289447.1|BG289447 602381485F1 NIH_MGC_93 H... 1314 0.0
gi|13047173|gb|BG290374.1|BG290374 602388212F1 NIH_MGC_93 H... 1302 0.0
gi|13339353|gb|BG432847.1|BG432847 602496055F1 NIH_MGC_75 H... 1285 0.0
gi|10321791|gb|BE872911.1|BE872911 601451505F1 NIH_MGC_65 H... 1261 0.0
gi|13546503|gb|BG547838.1|BG547838 602576130F1 NIH_MGC_77 H... 1259 0.0
gi|13532633|gb|BG540400.1|BG540400 602568710F1 NIH_MGC_77 H... 1253 0.0
gi|13464096|gb|BG502579.1|BG502579 602549403F1 NIH_MGC_61 H... 1253 0.0
gi|12673441|gb|BG166738.1|BG166738 602339258F1 NIH_MGC_89 H... 1237 0.0
gi|13047275|gb|BG290433.1|BG290433 602388282F1 NIH_MGC_93 H... 1231 0.0
gi|12425026|gb|BG033087.1|BG033087 602300210F1 NIH_MGC_87 H... 1227 0.0
gi|12383684|gb|BF980872.1|BF980872 602304083F1 NIH_MGC_88 H... 1227 0.0
gi|9890063|gb|BE619038.1|BE619038 601472854F1 NIH_MGC_68 Ho... 1225 0.0
gi|12758336|gb|BG248520.1|BG248520 602400680F1 NIH_MGC_15 H... 1219 0.0
gi|13995758|gb|BG716571.1|BG716571 602677825F1 NIH_MGC_96 H... 1215 0.0
gi|9896933|gb|BE615334.1|BE615334 601280732F1 NIH_MGC_39 Ho... 1211 0.0
gi|12387354|gb|BF984542.1|BF984542 602307730F1 NIH_MGC_88 H... 1170 0.0
gi|13717172|gb|BG195485.1|BG195485 RST14677 Athersys RAGE L... 1168 0.0
gi|10401855|gb|BE907862.1|BE907862 601501989F1 NIH_MGC_70 H... 1166 0.0
gi|12670948|gb|BG164245.1|BG164245 602341256F1 NIH_MGC_89 H... 1152 0.0
gi|11331761|gb|BF369736.1|BF369736 QV4-GN0120-250900-427-c1... 1150 0.0
gi|2321379|gb|AA551127.1|AA551127 nk75g03.s1 NCI_CGAP_Sch1 ... 1150 0.0
gi|10744866|gb|BF036769.1|BF036769 601459836F1 NIH_MGC_66 H... 1146 0.0
gi|13528208|gb|BG536662.1|BG536662 602566285F1 NIH_MGC_77 H... 1144 0.0
gi|8147555|gb|AW957872.1|AW957872 EST369942 MAGE resequence... 1142 0.0
gi|12344922|gb|BF977707.1|BF977707 602148324F1 NIH_MGC_62 H... 1130 0.0
gi|11944012|gb|BF670117.1|BF670117 602119443F1 NIH_MGC_56 H... 1122 0.0
gi|13546026|gb|BG547348.1|BG547348 602574782F1 NIH_MGC_77 H... 1118 0.0
gi|12676722|gb|BG170019.1|BG170019 602323391F1 NIH_MGC_89 H... 1088 0.0
gi|11649900|gb|BF576188.1|BF576188 602132627F1 NIH_MGC_81 H... 1078 0.0
gi|14512380|gb|BI094050.1|BI094050 602860005F1 NIH_MGC_10 H... 1074 0.0
gi|13050007|gb|BG291790.1|BG291790 602386010F1 NIH_MGC_93 H... 1068 0.0
gi|13460516|gb|BG498986.1|BG498986 602544674F1 NIH_MGC_60 H... 1067 0.0
gi|10796504|dbj|AV714987.1|AV714987 AV714987 DCB Homo sapie... 1065 0.0
gi|12604885|gb|BG111281.1|BG111281 602283354F1 NIH_MGC_86 H... 1047 0.0
gi|14049576|gb|BG779259.1|BG779259 602665938F1 NIH_MGC_60 H... 1045 0.0
gi|11111634|gb|BF218048.1|BF218048 601882836F1 NIH_MGC_57 H... 1045 0.0
gi|12383548|gb|BF980736.1|BF980736 602303884F1 NIH_MGC_88 H... 1035 0.0
gi|14049921|gb|BG779604.1|BG779604 602668351F1 NIH_MGC_60 H... 1033 0.0
gi|11252265|gb|BF305371.1|BF305371 601892847F1 NIH_MGC_17 H... 1021 0.0
gi|13041668|gb|BG287637.1|BG287637 602384460F1 NIH_MGC_93 H... 1019 0.0
gi|12677991|gb|BG171288.1|BG171288 602322318F1 NIH_MGC_89 H... 1015 0.0
gi|4435867|gb|AI521732.1|AI521732 ti82c06.x1 NCI_CGAP_Kid11... 1007 0.0
gi|7136231|gb|AW498488.1|AW498488 EST0021 Human Fetal Brain... 1001 0.0
gi|12097334|gb|BF792280.1|BF792280 602252790F1 NIH_MGC_84 H... 991 0.0
gi|1522055|gb|AA044198.1|AA044198 zk50e08.r1 Soares_pregnan... 991 0.0

gi|14049653|gb|BG779336.1|BG779336 602665853F1 NIH_MGC_60 H... 973 0.0
gi|14049581|gb|BG779264.1|BG779264 602665946F1 NIH_MGC_60 H... 961 0.0
gi|1371208|gb|W63627.1|W63627 zc56f09.r1 Soares_parathyroid... 961 0.0
gi|7136229|gb|AW498487.1|AW498487 EST0020 Human Fetal Brain... 959 0.0
gi|11629318|gb|BF541849.1|BF541849 602069042F1 NIH_MGC_58 H... 954 0.0
gi|14003292|gb|BG724105.1|BG724105 602697407F1 NIH_MGC_97 H... 950 0.0
gi|14070365|gb|BG759712.1|BG759712 602711109F1 NIH_MGC_48 H... 940 0.0
gi|1735571|gb|AA161274.1|AA161274 zq38f09.r1 Stratagene hNT... 940 0.0
gi|12066633|gb|BF739957.1|BF739957 7o41d12.x1 NCI_CGAP_Kid1... 932 0.0

gi|11112382|gb|BF218886.1|BF218886 601885044F1 NIH_MGC_57 H... 928 0.0
gi|11977542|gb|BF692134.1|BF692134 602248727F1 NIH_MGC_62 H... 920 0.0
gi|11767406|gb|BE963886.2|BE963886 601657654R1 NIH_MGC_68 H... 912 0.0
gi|3920107|gb|AI281874.1|AI281874 qt68g10.x1 NCI_CGAP_Eso2 ... 910 0.0
gi|10970869|gb|BF131829.1|BF131829 601820750F1 NIH_MGC_58 H... 906 0.0
gi|13043036|gb|BG288319.1|BG288319 602383655F1 NIH_MGC_93 H... 900 0.0
gi|12345982|gb|BF978767.1|BF978767 602149103F2 NIH_MGC_62 H... 898 0.0
gi|5113976|gb|AI745688.1|AI745688 tr24h04.x1 NCI_CGAP_Ov23 ... 894 0.0
gi|1694006|gb|AA132312.1|AA132312 zo17g05.s1 Stratagene col... 874 0.0
gi|5875725|gb|AW022195.1|AW022195 df34b10.y1 Morton Fetal C... 870 0.0
gi|2113174|gb|AA429830.1|AA429830 zw60g07.r1 Soares_total_f... 868 0.0
gi|11257080|gb|BF309649.1|BF309649 601891975F1 NIH_MGC_17 H... 866 0.0
gi|11649499|gb|BF575787.1|BF575787 602134824F1 NIH_MGC_81 H... 858 0.0
gi|12339937|gb|BF972722.1|BF972722 602240976F1 NIH_MGC_46 H... 856 0.0
gi|5113967|gb|AI745679.1|AI745679 tr24g03.x1 NCI_CGAP_Ov23 ... 856 0.0
gi|4486633|gb|AI554270.1|AI554270 tq05b03.x1 NCI_CGAP_Ut3 H... 852 0.0
gi|9771262|gb|BE542617.1|BE542617 601067112F1 NIH_MGC_10 Ho... 848 0.0
gi|7043218|gb|AW473112.1|AW473112 xp68h08.x2 NCI_CGAP_Ov39 ... 848 0.0
gi|4372411|gb|AI479243.1|AI479243 tm56b07.x1 NCI_CGAP_Kid11... 844 0.0
gi|1138607|gb|N24457.1|N24457 yx15a03.r1 Soares melanocyte ... 837 0.0
gi|1577675|gb|AA070298.1|AA070298 zm68c06.r1 Stratagene neu... 831 0.0
gi|8909315|gb|BE221906.1|BE221906 hu04d07.x1 NCI_CGAP_Lu24 ... 821 0.0
gi|6975014|gb|AW439708.1|AW439708 hb87f06.x1 NCI_CGAP_Ut2 H... 809 0.0
gi|12077114|gb|BF750438.1|BF750438 RC1-BN0410-261000-013-a0... 803 0.0
gi|5232026|gb|AI765517.1|AI765517 wi81a05.x1 NCI_CGAP_Kid12... 803 0.0
gi|4969797|gb|AI692457.1|AI692457 wd70f09.x1 NCI_CGAP_Lu24 ... 803 0.0
gi|7667944|gb|AW753012.1|AW753012 QV0-CT0225-011199-041-h01... 801 0.0

>gi|13183088|gb|AAK15047.1|AF237684_1 steroid dehydrogenase-like protein [Homo sapiens]

EST Search:

Sequences producing significant alignments: (bits) Value

gi|10142026|gb|BE728034.1|BE728034 601561322F1 NIH_MGC_20 H... 1233 0.0
gi|13030446|gb|BG281521.1|BG281521 602402054F1 NIH_MGC_20 H... 1209 0.0
gi|9143340|gb|BE269715.1|BE269715 601185872F1 NIH_MGC_8 Hom... 1108 0.0
gi|9142938|gb|BE269319.1|BE269319 601186383F1 NIH_MGC_8 Hom... 1070 0.0
gi|10809436|gb|BF055540.1|BF055540 7j81f05.x1 Soares_NSF_F8... 1068 0.0
gi|13996002|gb|BG716815.1|BG716815 602677928F1 NIH_MGC_96 H... 1045 0.0
gi|10938754|gb|BF109143.1|BF109143 7l57d11.x1 Soares_NSF_F8... 1039 0.0
gi|10721512|dbj|AV704193.1|AV704193 AV704193 ADB Homo sapie... 1033 0.0
gi|9180067|gb|BE296505.1|BE296505 601174783F1 NIH_MGC_17 Ho... 1009 0.0
gi|13968438|gb|BG699782.1|BG699782 602681486F1 NIH_MGC_95 H... 985 0.0
gi|11682562|gb|BF590238.1|BF590238 nab21g09.x1 Soares_NSF_F... 983 0.0

gi|9145595|gb|BE271650.1|BE271650 601141215F1 NIH_MGC_9 Hom... 965 0.0
gi|9121356|gb|BE251234.1|BE251234 601116339F1 NIH_MGC_16 Ho... 954 0.0
gi|11647948|gb|BF574236.1|BF574236 602131406F1 NIH_MGC_81 H... 952 0.0
gi|8148410|gb|AW958726.1|AW958726 EST370796 MAGE resequence... 936 0.0
gi|2154380|gb|AA442502.1|AA442502 zv59c01.r1 Soares_testis_... 862 0.0
gi|2141613|gb|AA436699.1|AA436699 zv59c01.s1 Soares_testis_... 842 0.0

>gi|6523809|gb|AAF14864.1|AF113123_1 carbonyl reductase [Homo sapiens]

EST Search:

Sequences producing significant alignments: (bits) Value

gi|13413874|gb|BG481595.1|BG481595 602528316F1 NIH_MGC_21 H... 1511 0.0
gi|14178945|gb|BG831358.1|BG831358 602766220F1 NIH_MGC_42 H... 1491 0.0
gi|14177680|gb|BG830093.1|BG830093 602764845F1 NIH_MGC_42 H... 1491 0.0
gi|13404430|gb|BG472244.1|BG472244 602513756F1 NIH_MGC_16 H... 1443 0.0
gi|14568476|gb|BI117575.1|BI117575 602866754F1 NIH_MGC_7 Ho... 1419 0.0
gi|13982131|gb|BG706614.1|BG706614 602674104F1 NIH_MGC_96 H... 1380 0.0
gi|13976241|gb|BG703674.1|BG703674 602686647F1 NIH_MGC_95 H... 1368 0.0
gi|10390490|gb|BE901372.1|BE901372 601674675F1 NIH_MGC_21 H... 1354 0.0
gi|12343809|gb|BF976594.1|BF976594 602244271F1 NIH_MGC_48 H... 1326 0.0
gi|11641972|gb|BF568592.1|BF568592 602184218F1 NIH_MGC_42 H... 1326 0.0
gi|11970704|gb|BF685296.1|BF685296 602141648F1 NIH_MGC_46 H... 1304 0.0
gi|11252161|gb|BF305282.1|BF305282 601892747F1 NIH_MGC_17 H... 1304 0.0
gi|11098442|gb|BF204856.1|BF204856 601867158F1 NIH_MGC_17 H... 1300 0.0
gi|9137251|gb|BE263706.1|BE263706 601192146F1 NIH_MGC_7 Hom... 1279 0.0
gi|10404479|gb|BE909167.1|BE909167 601501782F1 NIH_MGC_70 H... 1277 0.0
gi|11151599|gb|BF237681.1|BF237681 601841865F1 NIH_MGC_46 H... 1275 0.0
gi|9156256|gb|BE281240.1|BE281240 601155341F1 NIH_MGC_21 Ho... 1275 0.0
gi|12342418|gb|BF975203.1|BF975203 602244705F1 NIH_MGC_48 H... 1269 0.0
gi|14058856|gb|BG748203.1|BG748203 602705827F1 NIH_MGC_43 H... 1263 0.0
gi|11263622|gb|BF315274.1|BF315274 601902672F1 NIH_MGC_19 H... 1239 0.0
gi|11098117|gb|BF204531.1|BF204531 601868138F1 NIH_MGC_17 H... 1237 0.0
gi|9133208|gb|BE313377.1|BE313377 601147921F1 NIH_MGC_19 Ho... 1237 0.0
gi|12683322|gb|BG176619.1|BG176619 602313206F1 NIH_MGC_85 H... 1235 0.0
gi|9882826|dbj|AV661812.1|AV661812 AV661812 GLC Homo sapien... 1233 0.0
gi|12615652|gb|BG122143.1|BG122143 602349585F1 NIH_MGC_90 H... 1227 0.0
gi|11251336|gb|BF304588.1|BF304588 601887980F1 NIH_MGC_17 H... 1199 0.0
gi|4536632|gb|AI573258.1|AI573258 tn03e05.x1 NCI_CGAP_Brn25... 1197 0.0
gi|13032709|gb|BG283133.1|BG283133 602406785F1 NIH_MGC_91 H... 1195 0.0
gi|10346623|gb|BE889373.1|BE889373 601513264F1 NIH_MGC_71 H... 1189 0.0
gi|13137904|gb|BG331552.1|BG331552 602433326F1 NIH_MGC_18 H... 1187 0.0
gi|8167102|gb|AW975880.1|AW975880 EST387989 MAGE resequence... 1185 0.0
gi|9155643|gb|BE280635.1|BE280635 601155778F1 NIH_MGC_21 Ho... 1183 0.0
gi|11258150|gb|BF310575.1|BF310575 601895295F2 NIH_MGC_19 H... 1174 0.0
gi|8147508|gb|AW957825.1|AW957825 EST369895 MAGE resequence... 1158 0.0
gi|13340715|gb|BG434209.1|BG434209 602506154F1 NIH_MGC_79 H... 1128 0.0
gi|10216172|gb|BE794974.1|BE794974 601589746F1 NIH_MGC_7 Ho... 1118 0.0
gi|11949082|gb|BF675187.1|BF675187 602138110F1 NIH_MGC_83 H... 1116 0.0
gi|8147585|gb|AW957902.1|AW957902 EST369972 MAGE resequence... 1112 0.0
gi|14620169|gb|BI160168.1|BI160168 602864026F1 NIH_MGC_42 H... 1104 0.0
gi|4194952|gb|AI382182.1|AI382182 te70b01.x1 Soares_NFL_T_G... 1098 0.0
gi|6588561|gb|AW245568.1|AW245568 2822726.5prime NIH_MGC_7 ... 1092 0.0
gi|11617689|gb|BF530338.1|BF530338 602071618F1 NCI_CGAP_Brn... 1082 0.0
gi|9137978|gb|BE264422.1|BE264422 601191730F1 NIH_MGC_7 Hom... 1080 0.0

gi|6588571|gb|AW245578.1|AW245578 2822726.3prime NIH_MGC_7 ... 1072 0.0
gi|14320386|gb|BG925863.1|BG925863 HNC21-1-B11.R HNC (Human... 1068 0.0
gi|2726589|gb|AA714315.1|AA714315 nw06c05.s1 NCI_CGAP_SS1 H... 1027 0.0
gi|2537901|gb|AA625514.1|AA625514 af72e06.r1 Soares_NhHMPu_... 1023 0.0
gi|1211129|gb|N63300.1|N63300 yy71a11.s1 Soares_multiple_sc... 1021 0.0
gi|2155441|gb|AA442766.1|AA442766 zv60c08.s1 Soares_testis_... 1019 0.0
gi|1148734|gb|N30214.1|N30214 yw83h09.s1 Soares_placenta_8t... 1017 0.0
gi|13137575|gb|BG331137.1|BG331137 602431839F1 NIH_MGC_18 H... 1013 0.0
gi|9866354|dbj|AV645340.1|AV645340 AV645340 GLA Homo sapien... 1011 0.0
gi|2464707|gb|AA613669.1|AA613669 no39h10.s1 NCI_CGAP_Pr23 ... 1009 0.0
gi|12412330|gb|BG025585.1|BG025585 602274505F1 NIH_MGC_85 H... 997 0.0
gi|9882981|dbj|AV661967.1|AV661967 AV661967 GLC Homo sapien... 997 0.0
gi|14058983|gb|BG748330.1|BG748330 602706579F1 NIH_MGC_43 H... 991 0.0
gi|3230271|gb|AI015935.1|AI015935 ov26c11.x1 Soares_testis_... 989 0.0
gi|6399823|gb|AW168298.1|AW168298 xg62g11.x1 NCI_CGAP_Ut4 H... 987 0.0
gi|2243999|gb|AA507560.1|AA507560 ng88h09.s1 NCI_CGAP_Pr6 H... 977 0.0
gi|3840076|gb|AI244679.1|AI244679 qj97c09.x1 NCI_CGAP_Kid3 ... 973 0.0
gi|5838015|gb|AI991112.1|AI991112 wu38c07.x1 Soares_Dieckgr... 969 0.0
gi|9140017|gb|BE266440.1|BE266440 601193195F1 NIH_MGC_7 Hom... 965 0.0
gi|10216094|gb|BE794896.1|BE794896 601589638F1 NIH_MGC_7 Ho... 954 0.0
gi|1210879|gb|N63050.1|N63050 yy70g11.s1 Soares_multiple_sc... 938 0.0
gi|8750451|gb|BE207053.1|BE207053 ba09d08.y1 NIH_MGC_7 Homo... 936 0.0
gi|10144813|gb|BE730821.1|BE730821 601570791F1 NIH_MGC_21 H... 934 0.0
gi|5395010|gb|AI808444.1|AI808444 wf94h12.x1 Soares_NSF_F8_... 930 0.0
gi|10813709|dbj|AV716557.1|AV716557 AV716557 DCB Homo sapie... 926 0.0
gi|2883312|gb|AA813327.1|AA813327 ai81a07.s1 Soares_testis_... 920 0.0
gi|1193558|gb|N52392.1|N52392 yv49g09.s1 Soares fetal liver... 910 0.0
gi|2138860|gb|AA433946.1|AA433946 zw52g09.s1 Soares_total_f... 900 0.0
gi|4489892|gb|AI557529.1|AI557529 pt2.1-06.D05.r tumor2 Hom... 896 0.0
gi|11955171|gb|BF681276.1|BF681276 602155553F1 NIH_MGC_83 H... 894 0.0
gi|5591001|gb|AI885837.1|AI885837 wl62c01.x1 NCI_CGAP_Brn25... 894 0.0
gi|12431844|gb|BG036553.1|BG036553 602326326F1 NIH_MGC_91 H... 892 0.0
gi|2221812|gb|AA492250.1|AA492250 ng79d12.s1 NCI_CGAP_Pr6 H... 888 0.0
gi|3803259|gb|AI221056.1|AI221056 qg09c12.x1 Soares_placent... 886 0.0
gi|3422302|gb|AI083879.1|AI083879 qf22c05.x1 NCI_CGAP_Brn25... 886 0.0
gi|2159247|gb|AA446582.1|AA446582 zw84d08.s1 Soares_total_f... 874 0.0
gi|2341742|gb|AA568688.1|AA568688 nm06f08.s1 NCI_CGAP_Co10 ... 868 0.0
gi|4833888|gb|AI669114.1|AI669114 wb80e10.x1 NCI_CGAP_Pr28 ... 858 0.0
gi|10293455|dbj|AV691592.1|AV691592 AV691592 GKC Homo sapie... 854 0.0
gi|1965893|gb|AA313563.1|AA313563 EST185441 Colon carcinoma... 846 0.0
gi|3988221|gb|AI304532.1|AI304532 qo55a06.x1 NCI_CGAP_Co8 H... 844 0.0
gi|2731990|gb|AA720021.1|AA720021 zh22e05.s1 Soares_pineal_... 842 0.0
gi|7316134|gb|AW615416.1|AW615416 ba09d08.x1 NIH_MGC_7 Homo... 833 0.0
gi|9875231|dbj|AV654217.1|AV654217 AV654217 GLC Homo sapien... 831 0.0
gi|4598919|gb|AI589871.1|AI589871 tm81d01.x1 NCI_CGAP_Brn25... 823 0.0
gi|4489893|gb|AI557530.1|AI557530 pt2.1-06.D05b.r tumor2 Ho... 823 0.0
gi|9874547|dbj|AV653533.1|AV653533 AV653533 GLC Homo sapien... 803 0.0
gi|3988144|gb|AI304455.1|AI304455 qo54a10.x1 NCI_CGAP_Co8 H... 801 0.0

>gi|7023407|dbj|BAA91953.1| unnamed protein product [Homo sapiens]

EST Search:

Sequences producing significant alignments: (bits) Value

gi|10220190|gb|BE798992.1|BE798992 601583126F1 NIH_MGC_7 Ho... 1487 0.0

gi|9149748|gb|BE274802.1|BE274802 601122492F1 NIH_MGC_20 Ho... 1483 0.0
gi|10158478|gb|BE744486.1|BE744486 601576764F1 NIH_MGC_9 Ho... 1433 0.0
gi|15018843|gb|BI334186.1|BI334186 602997649F1 NIH_MGC_12 H... 1427 0.0
gi|10155434|gb|BE741442.1|BE741442 601594426F1 NIH_MGC_9 Ho... 1392 0.0
gi|12767656|gb|BG257840.1|BG257840 602377359F1 NIH_MGC_92 H... 1360 0.0
gi|2555545|gb|AA632131.1|AA632131 np74e04.s1 NCI_CGAP_Br2 H... 1344 0.0
gi|13961948|gb|BG696620.1|BG696620 602658918F1 NCI_CGAP_Skn... 1340 0.0
gi|13293198|gb|BG399750.1|BG399750 602441351F1 NIH_MGC_75 H... 1340 0.0
gi|13343333|gb|BG436827.1|BG436827 602488812F1 NIH_MGC_18 H... 1336 0.0
gi|15020179|gb|BI335522.1|BI335522 602997109F1 NIH_MGC_12 H... 1318 0.0
gi|12616196|gb|BG122687.1|BG122687 602351815F1 NIH_MGC_90 H... 1306 0.0
gi|5848066|gb|AW001150.1|AW001150 wu25a06.x1 Soares_Dieckgr... 1287 0.0
gi|9807602|gb|BE563882.1|BE563882 601335069F1 NIH_MGC_39 Ho... 1283 0.0
gi|5544472|gb|AI870504.1|AI870504 wi74d11.x1 NCI_CGAP_Brn25... 1275 0.0
gi|14620794|gb|BI160793.1|BI160793 602864883F1 NIH_MGC_42 H... 1249 0.0
gi|11972158|gb|BF686750.1|BF686750 602143895F1 NIH_MGC_46 H... 1249 0.0
gi|3887481|gb|AI268314.1|AI268314 qm04c02.x1 NCI_CGAP_Lu5 H... 1241 0.0
gi|10206517|gb|BE785319.1|BE785319 601474695F1 NIH_MGC_68 H... 1231 0.0
gi|10996420|dbj|AU135881.1|AU135881 AU135881 PLACE1 Homo sa... 1227 0.0
gi|6588855|gb|AW245862.1|AW245862 2822884.5prime NIH_MGC_7 ... 1140 0.0
gi|3425727|gb|AI087304.1|AI087304 oz77h11.x1 Soares_senesce... 1136 0.0
gi|3400045|gb|AI073401.1|AI073401 ov46a12.x1 Soares_testis_... 1128 0.0
gi|3601194|gb|AI131178.1|AI131178 qc15d06.x1 Soares_fetal_h... 1118 0.0
gi|2269422|gb|AA527353.1|AA527353 ng40a12.s1 NCI_CGAP_Co3 H... 1104 0.0
gi|10811999|gb|BF058103.1|BF058103 7k38d05.x1 NCI_CGAP_Ov18... 1102 0.0
gi|9323511|gb|BE378146.1|BE378146 601237876F1 NIH_MGC_44 Ho... 1084 0.0
gi|3917423|gb|AI279189.1|AI279189 qm24a07.x1 NCI_CGAP_Lu5 H... 1076 0.0
gi|6947123|gb|AW419191.1|AW419191 hb73d11.x1 NCI_CGAP_Ut2 H... 1039 0.0
gi|1941184|gb|AA293161.1|AA293161 zt55e02.s1 Soares ovary t... 1029 0.0
gi|9260951|gb|BE349176.1|BE349176 ht49c06.x1 NCI_CGAP_Mel15... 1015 0.0
gi|8147307|gb|AW957624.1|AW957624 EST369694 MAGE resequence... 1015 0.0
gi|3751973|gb|AI199367.1|AI199367 qi47g02.x1 NCI_CGAP_Brn25... 1013 0.0
gi|13793809|gb|BG656400.1|BG656400 ib36h12.x1 HR85 islet Ho... 1009 0.0
gi|2837067|gb|AA777588.1|AA777588 zi98d03.s1 Soares_fetal_l... 1003 0.0
gi|1382848|gb|W72175.1|W72175 zd61e02.s1 Soares_fetal_heart... 995 0.0
gi|11514695|gb|BF448575.1|BF448575 7n73d05.x1 NCI_CGAP_Ov18... 991 0.0
gi|5675100|gb|AI936230.1|AI936230 wo63e06.x1 NCI_CGAP_Pr22 ... 987 0.0
gi|2879104|gb|AA809698.1|AA809698 nk96e07.s1 NCI_CGAP_Co3 H... 983 0.0
gi|2563616|gb|AA639837.1|AA639837 nq85a11.s1 NCI_CGAP_Co9 H... 983 0.0
gi|6026748|gb|AW071823.1|AW071823 ws54b01.x1 NCI_CGAP_Brn25... 981 0.0
gi|2270176|gb|AA528107.1|AA528107 nj15a09.s1 NCI_CGAP_Pr22 ... 957 0.0
gi|12098389|gb|BF793335.1|BF793335 602254749F1 NIH_MGC_84 H... 955 0.0
gi|3755391|gb|AI202785.1|AI202785 qi39b06.x1 NCI_CGAP_Brn25... 940 0.0
gi|4070443|gb|AI333884.1|AI333884 qq17e01.x1 Soares_NhHMPu_... 928 0.0
gi|3958752|gb|AI299098.1|AI299098 qn14e10.x1 NCI_CGAP_Lu5 H... 912 0.0
gi|2732328|gb|AA719229.1|AA719229 ah45g05.s1 Soares_testis_... 912 0.0
gi|2878736|gb|AA809330.1|AA809330 ob70c08.s1 NCI_CGAP_GCB1 ... 910 0.0
gi|1153479|gb|N33080.1|N33080 yy33d10.s1 Soares melanocyte ... 908 0.0
gi|5513052|gb|AI859436.1|AI859436 wm11e11.x1 NCI_CGAP_Ut4 H... 906 0.0
gi|5447444|gb|AI826773.1|AI826773 wk56a11.x1 NCI_CGAP_Pr22 ... 892 0.0
gi|3241643|gb|AI026030.1|AI026030 ow03f06.s1 Soares_parathy... 890 0.0
gi|10920186|dbj|AV762338.1|AV762338 AV762338 MDS Homo sapie... 878 0.0
gi|1471524|gb|AA010478.1|AA010478 zi09e01.r1 Soares_fetal_l... 878 0.0
gi|2269399|gb|AA527330.1|AA527330 ng36c09.s1 NCI_CGAP_Co3 H... 870 0.0
gi|12161980|gb|BF822251.1|BF822251 MR1-RT0041-051200-007-f1... 862 0.0
gi|9175770|gb|BE304542.1|BE304542 601105911F1 NIH_MGC_15 Ho... 854 0.0
gi|1959201|gb|AA306873.1|AA306873 EST177798 Jurkat T-cells ... 848 0.0

gi|3934019|gb|AI291245.1|AI291245 qm11c01.x1 NCI_CGAP_Lu5 H... 844 0.0
gi|2842062|gb|AA782731.1|AA782731 aj08a05.s1 Soares_parathy... 835 0.0
gi|13916648|gb|BG685251.1|BG685251 602637158F1 NIH_MGC_48 H... 833 0.0
gi|3086142|gb|AA931756.1|AA931756 oo77f06.s1 NCI_CGAP_Kid5 ... 827 0.0
gi|1349991|gb|W51877.1|W51877 zc36c10.s1 Soares_senescent_f... 827 0.0
gi|14001369|gb|BG722182.1|BG722182 602698423F1 NIH_MGC_97 H... 825 0.0
gi|3154538|gb|AA977092.1|AA977092 oq24a03.s1 NCI_CGAP_GC4 H... 819 0.0
gi|2113245|gb|AA429946.1|AA429946 zw67f12.s1 Soares_testis_... 819 0.0
gi|11970016|gb|BF684608.1|BF684608 602140946F1 NIH_MGC_46 H... 815 0.0
gi|14564968|gb|BI114067.1|BI114067 602861166F2 NIH_MGC_17 H... 813 0.0
gi|1696541|gb|AA135492.1|AA135492 zo28h02.s1 Stratagene col... 805 0.0
gi|10159931|gb|BE745939.1|BE745939 601573574F1 NIH_MGC_9 Ho... 801 0.0

>gi|11360148|pir||T46363 hypothetical protein DKFZp434O0916.1 - human (fragment)

EST Search:

Sequences producing significant alignments: (bits) Value

gi|7848800|gb|AW796930.1|AW796930 CM3-UM0034-230300-126-d05... 38 2.8
gi|7844653|gb|AW792874.1|AW792874 CM3-UM0001-280100-082-e12... 38 2.8
gi|7111080|gb|AW466324.1|AW466324 bbc1g1b52 Neuronal Differ... 38 2.8
gi|772618|gb|R19008.1|R19008 yg26d09.r1 Soares infant brain... 38 2.8

>gi|7023407|dbj|BAA91953.1| unnamed protein product [Homo sapiens]

EST Search:

Sequences producing significant alignments: (bits) Value

gi|10220190|gb|BE798992.1|BE798992 601583126F1 NIH_MGC_7 Ho... 1487 0.0
gi|9149748|gb|BE274802.1|BE274802 601122492F1 NIH_MGC_20 Ho... 1483 0.0
gi|10158478|gb|BE744486.1|BE744486 601576764F1 NIH_MGC_9 Ho... 1433 0.0
gi|15018843|gb|BI334186.1|BI334186 602997649F1 NIH_MGC_12 H... 1427 0.0
gi|10155434|gb|BE741442.1|BE741442 601594426F1 NIH_MGC_9 Ho... 1392 0.0
gi|12767656|gb|BG257840.1|BG257840 602377359F1 NIH_MGC_92 H... 1360 0.0
gi|2555545|gb|AA632131.1|AA632131 np74e04.s1 NCI_CGAP_Br2 H... 1344 0.0
gi|13961948|gb|BG696620.1|BG696620 602658918F1 NCI_CGAP_Skn... 1340 0.0
gi|13293198|gb|BG399750.1|BG399750 602441351F1 NIH_MGC_75 H... 1340 0.0
gi|13343333|gb|BG436827.1|BG436827 602488812F1 NIH_MGC_18 H... 1336 0.0

gi|15020179|gb|BI335522.1|BI335522 602997109F1 NIH_MGC_12 H... 1318 0.0
gi|12616196|gb|BG122687.1|BG122687 602351815F1 NIH_MGC_90 H... 1306 0.0
gi|5848066|gb|AW001150.1|AW001150 wu25a06.x1 Soares_Dieckgr... 1287 0.0
gi|9807602|gb|BE563882.1|BE563882 601335069F1 NIH_MGC_39 Ho... 1283 0.0
gi|5544472|gb|AI870504.1|AI870504 wi74d11.x1 NCI_CGAP_Brn25... 1275 0.0
gi|14620794|gb|BI160793.1|BI160793 602864883F1 NIH_MGC_42 H... 1249 0.0
gi|11972158|gb|BF686750.1|BF686750 602143895F1 NIH_MGC_46 H... 1249 0.0
gi|3887481|gb|AI268314.1|AI268314 qm04c02.x1 NCI_CGAP_Lu5 H... 1241 0.0
gi|10206517|gb|BE785319.1|BE785319 601474695F1 NIH_MGC_68 H... 1231 0.0
gi|10996420|dbj|AU135881.1|AU135881 AU135881 PLACE1 Homo sa... 1227 0.0
gi|6588855|gb|AW245862.1|AW245862 2822884.5prime NIH_MGC_7 ... 1140 0.0
gi|3425727|gb|AI087304.1|AI087304 oz77h11.x1 Soares_senesce... 1136 0.0
gi|3400045|gb|AI073401.1|AI073401 ov46a12.x1 Soares_testis_... 1128 0.0

gi|3601194|gb|AI131178.1|AI131178 qc15d06.x1 Soares_fetal_h... 1118 0.0
gi|2269422|gb|AA527353.1|AA527353 ng40a12.s1 NCI_CGAP_Co3 H... 1104 0.0
gi|10811999|gb|BF058103.1|BF058103 7k38d05.x1 NCI_CGAP_Ov18... 1102 0.0
gi|9323511|gb|BE378146.1|BE378146 601237876F1 NIH_MGC_44 Ho... 1084 0.0
gi|3917423|gb|AI279189.1|AI279189 qm24a07.x1 NCI_CGAP_Lu5 H... 1076 0.0
gi|6947123|gb|AW419191.1|AW419191 hb73d11.x1 NCI_CGAP_Ut2 H... 1039 0.0
gi|1941184|gb|AA293161.1|AA293161 zt55e02.s1 Soares ovary t... 1029 0.0
gi|9260951|gb|BE349176.1|BE349176 ht49c06.x1 NCI_CGAP_Mel15... 1015 0.0
gi|8147307|gb|AW957624.1|AW957624 EST369694 MAGE resequence... 1015 0.0
gi|3751973|gb|AI199367.1|AI199367 qi47g02.x1 NCI_CGAP_Brn25... 1013 0.0
gi|13793809|gb|BG656400.1|BG656400 ib36h12.x1 HR85 islet Ho... 1009 0.0
gi|2837067|gb|AA777588.1|AA777588 zi98d03.s1 Soares_fetal_l... 1003 0.0
gi|1382848|gb|W72175.1|W72175 zd61e02.s1 Soares_fetal_heart... 995 0.0
gi|11514695|gb|BF448575.1|BF448575 7n73d05.x1 NCI_CGAP_Ov18... 991 0.0
gi|5675100|gb|AI936230.1|AI936230 wo63e06.x1 NCI_CGAP_Pr22 ... 987 0.0
gi|2879104|gb|AA809698.1|AA809698 nk96e07.s1 NCI_CGAP_Co3 H... 983 0.0
gi|2563616|gb|AA639837.1|AA639837 nq85a11.s1 NCI_CGAP_Co9 H... 983 0.0
gi|6026748|gb|AW071823.1|AW071823 ws54b01.x1 NCI_CGAP_Brn25... 981 0.0
gi|2270176|gb|AA528107.1|AA528107 nj15a09.s1 NCI_CGAP_Pr22 ... 957 0.0
gi|12098389|gb|BF793335.1|BF793335 602254749F1 NIH_MGC_84 H... 955 0.0
gi|3755391|gb|AI202785.1|AI202785 qi39b06.x1 NCI_CGAP_Brn25... 940 0.0
gi|4070443|gb|AI333884.1|AI333884 qq17e01.x1 Soares_NhHMPu_... 928 0.0
gi|3958752|gb|AI299098.1|AI299098 qn14e10.x1 NCI_CGAP_Lu5 H... 912 0.0
gi|2732328|gb|AA719229.1|AA719229 ah45g05.s1 Soares_testis_... 912 0.0
gi|2878736|gb|AA809330.1|AA809330 ob70c08.s1 NCI_CGAP_GCB1 ... 910 0.0
gi|1153479|gb|N33080.1|N33080 yy33d10.s1 Soares melanocyte ... 908 0.0
gi|5513052|gb|AI859436.1|AI859436 wm11e11.x1 NCI_CGAP_Ut4 H... 906 0.0
gi|5447444|gb|AI826773.1|AI826773 wk56a11.x1 NCI_CGAP_Pr22 ... 892 0.0
gi|3241643|gb|AI026030.1|AI026030 ow03f06.s1 Soares_parathy... 890 0.0
gi|10920186|dbj|AV762338.1|AV762338 AV762338 MDS Homo sapie... 878 0.0
gi|1471524|gb|AA010478.1|AA010478 zi09e01.r1 Soares_fetal_l... 878 0.0
gi|2269399|gb|AA527330.1|AA527330 ng36c09.s1 NCI_CGAP_Co3 H... 870 0.0
gi|12161980|gb|BF822251.1|BF822251 MR1-RT0041-051200-007-f1... 862 0.0
gi|9175770|gb|BE304542.1|BE304542 601105911F1 NIH_MGC_15 Ho... 854 0.0
gi|1959201|gb|AA306873.1|AA306873 EST177798 Jurkat T-cells ... 848 0.0
gi|3934019|gb|AI291245.1|AI291245 qm11c01.x1 NCI_CGAP_Lu5 H... 844 0.0
gi|2842062|gb|AA782731.1|AA782731 aj08a05.s1 Soares_parathy... 835 0.0
gi|13916648|gb|BG685251.1|BG685251 602637158F1 NIH_MGC_48 H... 833 0.0
gi|3086142|gb|AA931756.1|AA931756 oo77f06.s1 NCI_CGAP_Kid5 ... 827 0.0
gi|1349991|gb|W51877.1|W51877 zc36c10.s1 Soares_senescent_f... 827 0.0
gi|14001369|gb|BG722182.1|BG722182 602698423F1 NIH_MGC_97 H... 825 0.0
gi|3154538|gb|AA977092.1|AA977092 oq24a03.s1 NCI_CGAP_GC4 H... 819 0.0
gi|2113245|gb|AA429946.1|AA429946 zw67f12.s1 Soares_testis_... 819 0.0
gi|11970016|gb|BF684608.1|BF684608 602140946F1 NIH_MGC_46 H... 815 0.0
gi|14564968|gb|BI114067.1|BI114067 602861166F2 NIH_MGC_17 H... 813 0.0
gi|1696541|gb|AA135492.1|AA135492 zo28h02.s1 Stratagene col... 805 0.0
gi|10159931|gb|BE745939.1|BE745939 601573574F1 NIH_MGC_9 Ho... 801 0.0

>gi|14734800|ref|XP_002640.3| peroxisomal trans 2-enoyl CoA reductase; putative short chain al [Homo sapiens]

EST Search:

Sequences producing significant alignments: (bits) Value

gi|12789234|emb|AL525741.1|AL525741 AL525741 LTI_NFL003_NBC... 1826 0.0

gi|12791177|emb|AL527684.1|AL527684 AL527684 LTI_NFL003_NBC... 1663 0.0
gi|12786798|emb|AL523305.1|AL523305 AL523305 LTI_NFL003_NBC... 1532 0.0
gi|14053003|gb|BG742350.1|BG742350 602631722F1 NCI_CGAP_Skn... 1503 0.0
gi|14045131|gb|BG774814.1|BG774814 602662684F1 NIH_MGC_21 H... 1415 0.0
gi|14052853|gb|BG742200.1|BG742200 602634087F1 NCI_CGAP_Skn... 1396 0.0
gi|9873450|dbj|AV652436.1|AV652436 AV652436 GLC Homo sapien... 1348 0.0
gi|12786797|emb|AL523304.1|AL523304 AL523304 LTI_NFL003_NBC... 1336 0.0
gi|13722475|gb|BG200900.1|BG200900 RST20108 Athersys RAGE L... 1336 0.0
gi|12911098|emb|AL562558.1|AL562558 AL562558 LTI_NFL003_NBC... 1166 0.0
gi|5232357|gb|AI765848.1|AI765848 wi85c03.x1 NCI_CGAP_Kid12... 1134 0.0
gi|10914602|dbj|AV756754.1|AV756754 AV756754 BM Homo sapien... 1100 0.0
gi|8907537|gb|BE220231.1|BE220231 hv69f02.x1 NCI_CGAP_Lu24 ... 1017 0.0
gi|14053002|gb|BG742349.1|BG742349 602631721F1 NCI_CGAP_Skn... 995 0.0
gi|10938068|gb|BF108369.1|BF108369 7n62f05.x1 NCI_CGAP_Lu24... 993 0.0
gi|4303253|gb|AI435448.1|AI435448 th94e11.x1 Soares_NSF_F8_... 906 0.0
gi|11363688|gb|BF382385.1|BF382385 601815316F2 NIH_MGC_56 H... 896 0.0
gi|9792594|gb|BE550902.1|BE550902 7b65g01.x1 NCI_CGAP_Lu24 ... 894 0.0
gi|9184025|gb|BE300277.1|BE300277 600944051T1 NIH_MGC_17 Ho... 858 0.0
gi|9155968|gb|BE280956.1|BE280956 601155875F1 NIH_MGC_21 Ho... 852 0.0
gi|12041930|gb|BF726019.1|BF726019 bx23a05.y1 Human Iris cD... 844 0.0
gi|12135102|gb|BF806113.1|BF806113 MR1-CI0183-071100-001-f0... 841 0.0
gi|4312182|gb|AI458176.1|AI458176 tj94c11.x1 NCI_CGAP_Lu24 ... 807 0.0

SDRs identified with "SDR region" mostly by automated alignement (BLAST Domain) and unreviewed description in NCBI database (identification might be" putative" SDR or "putative" protein); substrate and/or function might be unknown. Exceptions may be for example known hydroxysteroid dehydrogenases like 17-beta HSD1-10 and 11-beta-HSD1-2 and retinol/retinal dehydrogenases

>gi¦65913¦pir¦¦DEHUE7 estradiol 17beta-dehydrogenase (EC 1.1.1.62) type 1 - human

EST Search:

Sequences producing significant alignments: (bits) Value

gi¦12887229¦emb¦AL550345.1¦AL550345 AL550345 LTI_NFL006_PL2... 1675 0.0
gi¦12874252¦emb¦AL542322.1¦AL542322 AL542322 LTI_FL002_PL1 ... 1665 0.0
gi¦12877696¦emb¦AL545215.1¦AL545215 AL545215 LTI_NFL006_PL2... 1663 0.0
gi¦12878160¦emb¦AL545678.1¦AL545678 AL545678 LTI_NFL006_PL2... 1651 0.0
gi¦12889399¦emb¦AL551445.1¦AL551445 AL551445 LTI_NFL006_PL2... 1641 0.0
gi¦12893008¦emb¦AL553301.1¦AL553301 AL553301 LTI_NFL006_PL2... 1639 0.0
gi¦12875567¦emb¦AL543089.1¦AL543089 AL543089 LTI_NFL006_PL2... 1618 0.0
gi¦12894623¦emb¦AL554134.1¦AL554134 AL554134 LTI_NFL006_PL2... 1564 0.0
gi¦12880090¦emb¦AL546712.1¦AL546712 AL546712 LTI_NFL006_PL2... 1524 0.0
gi¦12884123¦emb¦AL548779.1¦AL548779 AL548779 LTI_NFL006_PL2... 1451 0.0
gi¦12882682¦emb¦AL548045.1¦AL548045 AL548045 LTI_NFL006_PL2... 1417 0.0
gi¦12928450¦emb¦AL571296.1¦AL571296 AL571296 LTI_NFL006_PL2... 1300 0.0
gi¦10995327¦dbj¦AU134788.1¦AU134788 AU134788 PLACE1 Homo sa... 1231 0.0
gi¦11000660¦dbj¦AU139139.1¦AU139139 AU139139 PLACE1 Homo sa... 1215 0.0
gi¦12876594¦emb¦AL544115.1¦AL544115 AL544115 LTI_NFL006_PL2... 1191 0.0
gi¦11000409¦dbj¦AU138888.1¦AU138888 AU138888 PLACE1 Homo sa... 1185 0.0
gi¦10996612¦dbj¦AU136073.1¦AU136073 AU136073 PLACE1 Homo sa... 1185 0.0
gi¦12935757¦emb¦AL575009.1¦AL575009 AL575009 LTI_NFL006_PL2... 1176 0.0
gi¦12929750¦emb¦AL571950.1¦AL571950 AL571950 LTI_NFL006_PL2... 1160 0.0
gi¦11000929¦dbj¦AU139408.1¦AU139408 AU139408 PLACE1 Homo sa... 1154 0.0
gi¦12925425¦emb¦AL569763.1¦AL569763 AL569763 LTI_NFL006_PL2... 1118 0.0
gi¦12938593¦emb¦AL576443.1¦AL576443 AL576443 LTI_NFL006_PL2... 1110 0.0
gi¦12874250¦emb¦AL542321.1¦AL542321 AL542321 LTI_FL002_PL1 ... 1078 0.0
gi¦12887536¦emb¦AL550503.1¦AL550503 AL550503 LTI_NFL006_PL2... 1023 0.0
gi¦12927925¦emb¦AL571031.1¦AL571031 AL571031 LTI_NFL006_PL2... 983 0.0
gi¦12884042¦emb¦AL548739.1¦AL548739 AL548739 LTI_NFL006_PL2... 981 0.0
gi¦11001082¦dbj¦AU139561.1¦AU139561 AU139561 PLACE1 Homo sa... 979 0.0
gi¦12882968¦emb¦AL548193.1¦AL548193 AL548193 LTI_NFL006_PL2... 952 0.0
gi¦10996347¦dbj¦AU135808.1¦AU135808 AU135808 PLACE1 Homo sa... 902 0.0
gi¦10996163¦dbj¦AU135624.1¦AU135624 AU135624 PLACE1 Homo sa... 896 0.0
gi¦11000650¦dbj¦AU139129.1¦AU139129 AU139129 PLACE1 Homo sa... 894 0.0
gi¦11000302¦dbj¦AU138781.1¦AU138781 AU138781 PLACE1 Homo sa... 894 0.0
gi¦10999181¦dbj¦AU137660.1¦AU137660 AU137660 PLACE1 Homo sa... 894 0.0
gi¦11000400¦dbj¦AU138879.1¦AU138879 AU138879 PLACE1 Homo sa... 886 0.0
gi¦10941914¦gb¦BF112224.1¦BF112224 7l42c05.x1 Soares_NSF_F8... 825 0.0
gi¦12872814¦emb¦AL541595.1¦AL541595 AL541595 LTI_FL002_PL1 ... 799 0.0
gi¦10941804¦gb¦BF112114.1¦BF112114 7l40e05.x1 Soares_NSF_F8... 779 0.0
gi¦10999521¦dbj¦AU138000.1¦AU138000 AU138000 PLACE1 Homo sa... 696 0.0
gi¦12939576¦emb¦AL576938.1¦AL576938 AL576938 LTI_NFL006_PL2... 686 0.0
gi¦10997013¦dbj¦AU136474.1¦AU136474 AU136474 PLACE1 Homo sa... 682 0.0
gi¦1571801¦dbj¦C17094.1¦C17094 C17094 Clontech human aorta ... 682 0.0
gi¦1722365¦gb¦AA150854.1¦AA150854 zl44b07.r1 Soares_pregnan... 666 0.0
gi¦1579212¦dbj¦C17609.1¦C17609 C17609 Human placenta cDNA (... 660 0.0
gi¦11018663¦dbj¦AU157142.1¦AU157142 AU157142 PLACE1 Homo sa... 652 0.0

gi|2718881|gb|AA708963.1|AA708963 zl58g02.s1 Soares_pregnan... 648 0.0
gi|12875835|emb|AL543357.1|AL543357 AL543357 LTI_NFL006_PL2... 626 e-177
gi|10941920|gb|BF112230.1|BF112230 7l42d05.x1 Soares_NSF_F8... 618 e-174
gi|2715031|gb|AA705113.1|AA705113 zj94h11.s1 Soares_fetal_l... 597 e-168
gi|12442104|gb|BG002508.1|BG002508 MR3-GN0186-171100-005-e0... 595 e-167
gi|1722257|gb|AA150545.1|AA150545 zl44b07.s1 Soares_pregnan... 593 e-167
gi|12396831|gb|BF990506.1|BF990506 RC0-GN0133-261000-031-c0... 585 e-164
gi|1722312|gb|AA150800.1|AA150800 zl46b07.r1 Soares_pregnan... 581 e-163
gi|4435924|gb|AI521789.1|AI521789 ti77d11.x1 NCI_CGAP_Kid11... 579 e-163
gi|12923868|emb|AL568983.1|AL568983 AL568983 LTI_FL002_PL1 ... 575 e-161
gi|12926714|emb|AL570422.1|AL570422 AL570422 LTI_NFL006_PL2... 557 e-156
gi|4665448|gb|AI628648.1|AI628648 ty77e09.x1 NCI_CGAP_Kid11... 553 e-155
gi|848714|gb|R74344.1|R74344 yl01f08.s1 Soares breast 2NbHB... 551 e-154

>gi|4504503|ref|NP_002144.1| hydroxysteroid (17-beta) dehydrogenase 2 [Homo sapiens]

EST Search:
Sequences producing significant alignments: (bits) Value

gi|12927087|emb|AL570611.1|AL570611 AL570611 LTI_NFL006_PL2... 2095 0.0
gi|12876988|emb|AL544508.1|AL544508 AL544508 LTI_NFL006_PL2... 2074 0.0
gi|12928176|emb|AL571159.1|AL571159 AL571159 LTI_NFL006_PL2... 1832 0.0
gi|12938929|emb|AL576614.1|AL576614 AL576614 LTI_NFL006_PL2... 1818 0.0
gi|12891054|emb|AL552292.1|AL552292 AL552292 LTI_NFL006_PL2... 1810 0.0
gi|12879139|emb|AL546227.1|AL546227 AL546227 LTI_NFL006_PL2... 1806 0.0
gi|12890884|emb|AL552206.1|AL552206 AL552206 LTI_NFL006_PL2... 1764 0.0
gi|12936979|emb|AL575629.1|AL575629 AL575629 LTI_NFL006_PL2... 1760 0.0
gi|12893833|emb|AL553729.1|AL553729 AL553729 LTI_NFL006_PL2... 1746 0.0
gi|12927335|emb|AL570735.1|AL570735 AL570735 LTI_NFL006_PL2... 1719 0.0
gi|12877918|emb|AL545437.1|AL545437 AL545437 LTI_NFL006_PL2... 1719 0.0
gi|12937110|emb|AL575695.1|AL575695 AL575695 LTI_NFL006_PL2... 1673 0.0
gi|12928206|emb|AL571174.1|AL571174 AL571174 LTI_NFL006_PL2... 1631 0.0
gi|12877180|emb|AL544700.1|AL544700 AL544700 LTI_NFL006_PL2... 1600 0.0
gi|12877944|emb|AL545463.1|AL545463 AL545463 LTI_NFL006_PL2... 1582 0.0
gi|12893532|emb|AL553572.1|AL553572 AL553572 LTI_NFL006_PL2... 1542 0.0
gi|12886959|emb|AL550209.1|AL550209 AL550209 LTI_NFL006_PL2... 1532 0.0
gi|12934254|emb|AL574239.1|AL574239 AL574239 LTI_NFL006_PL2... 1507 0.0
gi|12933073|emb|AL573641.1|AL573641 AL573641 LTI_NFL006_PL2... 1489 0.0
gi|12940371|emb|AL577339.1|AL577339 AL577339 LTI_NFL006_PL2... 1459 0.0
gi|12939042|emb|AL576670.1|AL576670 AL576670 LTI_NFL006_PL2... 1435 0.0

gi|13580329|gb|BG572676.1|BG572676 602593783F1 NIH_MGC_79 H... 1425 0.0
gi|12885339|emb|AL549395.1|AL549395 AL549395 LTI_NFL006_PL2... 1404 0.0
gi|13669901|gb|BG618530.1|BG618530 602645433F2 NIH_MGC_76 H... 1382 0.0
gi|13575119|gb|BG567466.1|BG567466 602585994F1 NIH_MGC_76 H... 1354 0.0
gi|11000555|dbj|AU139034.1|AU139034 AU139034 PLACE1 Homo sa... 1338 0.0
gi|13670494|gb|BG619123.1|BG619123 602616490F1 NIH_MGC_79 H... 1332 0.0
gi|9719951|gb|BE512678.1|BE512678 601171639F1 NIH_MGC_15 Ho... 1310 0.0
gi|10995811|dbj|AU135272.1|AU135272 AU135272 PLACE1 Homo sa... 1294 0.0
gi|13519989|gb|BG528452.1|BG528452 602579896F1 NIH_MGC_60 H... 1279 0.0
gi|12940459|emb|AL577384.1|AL577384 AL577384 LTI_NFL006_PL2... 1191 0.0
gi|9869431|dbj|AV648417.1|AV648417 AV648417 GLC Homo sapien... 1148 0.0
gi|10286850|dbj|AV684987.1|AV684987 AV684987 GKC Homo sapie... 1138 0.0
gi|9871386|dbj|AV650372.1|AV650372 AV650372 GLC Homo sapien... 1128 0.0
gi|8141093|gb|AW951420.1|AW951420 EST363490 MAGE resequence... 1094 0.0
gi|9874839|dbj|AV653825.1|AV653825 AV653825 GLC Homo sapien... 1076 0.0
gi|9812898|gb|BE569178.1|BE569178 601338993F2 NIH_MGC_53 Ho... 1037 0.0
gi|12041605|gb|BF725694.1|BF725694 bx18g03.y1 Human Iris cD... 1013 0.0
gi|12940352|emb|AL577329.1|AL577329 AL577329 LTI_NFL006_PL2... 999 0.0
gi|10300921|dbj|AV698950.1|AV698950 AV698950 GKC Homo sapie... 989 0.0
gi|10297535|dbj|AV695672.1|AV695672 AV695672 GKC Homo sapie... 989 0.0
gi|10289123|dbj|AV687260.1|AV687260 AV687260 GKC Homo sapie... 989 0.0
gi|13572512|gb|BG564859.1|BG564859 602589807F1 NIH_MGC_76 H... 977 0.0
gi|10301035|dbj|AV699064.1|AV699064 AV699064 GKC Homo sapie... 959 0.0
gi|5436727|gb|AI817648.1|AI817648 td15a06.x1 NCI_CGAP_Co16 ... 950 0.0
gi|13669619|gb|BG618248.1|BG618248 602645981F1 NIH_MGC_76 H... 942 0.0
gi|3734912|gb|AI184274.1|AI184274 qc63f10.x1 Soares_placent... 942 0.0
gi|3601482|gb|AI131466.1|AI131466 qc09c01.x1 Soares_fetal_h... 936 0.0
gi|1137815|gb|N23665.1|N23665 yw40b12.s1 Weizmann Olfactory... 910 0.0
gi|4223511|gb|AI393964.1|AI393964 tg11d10.x1 NCI_CGAP_CLL1 ... 906 0.0
gi|10297172|dbj|AV695309.1|AV695309 AV695309 GKC Homo sapie... 898 0.0
gi|10822421|gb|BF063511.1|BF063511 7h81e04.x1 NCI_CGAP_Co16... 860 0.0
gi|11107323|gb|BF213737.1|BF213737 601847627F1 NIH_MGC_55 H... 858 0.0
gi|11107339|gb|BF213753.1|BF213753 601847652F1 NIH_MGC_55 H... 852 0.0
gi|10289096|dbj|AV687233.1|AV687233 AV687233 GKC Homo sapie... 848 0.0
gi|6039642|gb|AW084490.1|AW084490 wz24e10.x1 Soares_Dieckgr... 837 0.0
gi|9881634|dbj|AV660620.1|AV660620 AV660620 GLC Homo sapien... 829 0.0
gi|9719903|gb|BE512784.1|BE512784 601171544F1 NIH_MGC_15 Ho... 823 0.0
gi|10297603|dbj|AV695740.1|AV695740 AV695740 GKC Homo sapie... 813 0.0
gi|11108307|gb|BF214721.1|BF214721 601846621F1 NIH_MGC_55 H... 801 0.0

>gi|4557649|ref|NP_000188.1| estradiol 17 beta-dehydrogenase 3; 17-beta-HSD3 [Homo sapiens]

EST Search:

N62871 multiple sclerosis lesion

N77777 multiple sclerosis lesion

Sequences producing significant alignments: (bits) Value

gi|3429912|gb|AI090853.1|AI090853 ov44f05.x1 Soares_testis_... 1380 0.0
gi|2154248|gb|AA442370.1|AA442370 zv62c08.r1 Soares_testis_... 1053 0.0
gi|2154226|gb|AA442348.1|AA442348 zv62a08.r1 Soares_testis_... 1043 0.0
gi|2142185|gb|AA437271.1|AA437271 zv62a08.s1 Soares_testis_... 1017 0.0

gi|2142205|gb|AA437291.1|AA437291 zv62c08.s1 Soares_testis_... 1003 0.0
gi|1210700|gb|N62871.1|N62871 yz83e04.s1 Soares_multiple_sc... 797 0.0
gi|1783826|gb|AA194135.1|AA194135 zr37f08.r1 Soares_NhHMPu_... 769 0.0
gi|6073356|gb|AW102743.1|AW102743 xd70e10.x1 Soares_NFL_T_G... 718 0.0

gi|2993224|gb|AA883694.1|AA883694 al58b05.s1 Soares_NFL_T_G... 626 e-177
gi|2837959|gb|AA778628.1|AA778628 af87b08.s1 Soares_testis_... 517 e-144
gi|5446033|gb|AI825362.1|AI825362 wb17e09.x1 NCI_CGAP_GC6 H... 507 e-141
gi|4682494|gb|AI631164.1|AI631164 ts93d10.x1 NCI_CGAP_GC6 H... 500 e-139

>gi|1706396|sp|P51659|DHB4_HUMAN ESTRADIOL 17 BETA-DEHYDROGENASE 4 (17-BETA-HSD 4) (17-BETA-HYDROXYSTEROID DEHYDROGENASE 4)

EST Search:

Sequences producing significant alignments: (bits) Value

gi|12797915|emb|AL534422.1|AL534422 AL534422 LTI_FL013_FBrn... 1741 0.0
gi|12929551|emb|AL571847.1|AL571847 AL571847 LTI_NFL006_PL2... 1731 0.0
gi|12795330|emb|AL531837.1|AL531837 AL531837 LTI_NFL001_NBC... 1659 0.0
gi|13908294|gb|BG676897.1|BG676897 602623506F1 NCI_CGAP_Skn... 1631 0.0
gi|12914346|emb|AL564189.1|AL564189 AL564189 LTI_NFL001_NBC... 1586 0.0
gi|12879740|emb|AL546532.1|AL546532 AL546532 LTI_NFL006_PL2... 1524 0.0
gi|10949847|dbj|AU125131.1|AU125131 AU125131 NT2RM4 Homo sa... 1479 0.0
gi|10948684|dbj|AU123968.1|AU123968 AU123968 NT2RM2 Homo sa... 1479 0.0
gi|10992681|dbj|AU132327.1|AU132327 AU132327 NT2RP3 Homo sa... 1437 0.0
gi|3214525|gb|AI005015.1|AI005015 ou91a01.x1 NCI_CGAP_Kid3 ... 1427 0.0
gi|13721603|gb|BG199916.1|BG199916 RST19212 Athersys RAGE L... 1413 0.0
gi|3674126|gb|AI146444.1|AI146444 qb93a03.x1 Soares_fetal_h... 1402 0.0
gi|13911524|gb|BG680127.1|BG680127 602628285F1 NCI_CGAP_Skn... 1394 0.0
gi|3412550|gb|AI078142.1|AI078142 oz30b04.x1 Soares_total_f... 1394 0.0
gi|10991451|dbj|AU131097.1|AU131097 AU131097 NT2RP3 Homo sa... 1374 0.0
gi|5409861|emb|AL040917.1|AL040917 DKFZp434J2215_s1 434 (sy... 1372 0.0
gi|10795143|dbj|AV713626.1|AV713626 AV713626 DCB Homo sapie... 1348 0.0
gi|10991758|dbj|AU131404.1|AU131404 AU131404 NT2RP3 Homo sa... 1346 0.0
gi|10932266|dbj|AU117308.1|AU117308 AU117308 HEMBA1 Homo sa... 1346 0.0
gi|10996985|dbj|AU136446.1|AU136446 AU136446 PLACE1 Homo sa... 1344 0.0
gi|11004302|dbj|AU142781.1|AU142781 AU142781 Y79AA1 Homo sa... 1328 0.0
gi|10144826|gb|BE730834.1|BE730834 601569914F1 NIH_MGC_21 H... 1316 0.0
gi|9769065|gb|BE540420.1|BE540420 601065826F1 NIH_MGC_10 Ho... 1308 0.0
gi|12429277|gb|BG035291.1|BG035291 602324913F1 NIH_MGC_90 H... 1304 0.0
gi|10992834|dbj|AU132480.1|AU132480 AU132480 NT2RP3 Homo sa... 1292 0.0
gi|10365912|gb|BE898933.1|BE898933 601682360F1 NIH_MGC_9 Ho... 1292 0.0
gi|3002065|gb|AA886957.1|AA886957 oi14e10.s1 NCI_CGAP_GC4 H... 1291 0.0
gi|8169585|gb|AW978321.1|AW978321 EST390430 MAGE resequence... 1283 0.0
gi|10579372|gb|BE968667.1|BE968667 601650086F1 NIH_MGC_74 H... 1279 0.0
gi|10352702|gb|BE892403.1|BE892403 601433879F1 NIH_MGC_72 H... 1273 0.0
gi|14512082|gb|BI093752.1|BI093752 602860460F1 NIH_MGC_10 H... 1269 0.0
gi|6439061|gb|AW173113.1|AW173113 xj83d12.x1 Soares_NFL_T_G... 1247 0.0
gi|11264224|gb|BF315938.1|BF315938 601895882F1 NIH_MGC_19 H... 1231 0.0

gi|10321137|gb|BE872361.1|BE872361 601448614F1 NIH_MGC_65 H... 1223 0.0
gi|10355660|gb|BE893865.1|BE893865 601436228F1 NIH_MGC_72 H... 1221 0.0
gi|10098245|gb|BE710071.1|BE710071 IL3-HT0618-030800-233-G0... 1217 0.0
gi|11283822|gb|BF337571.1|BF337571 602035323F1 NCI_CGAP_Brn... 1191 0.0
gi|10038238|gb|BE677697.1|BE677697 7d90e10.x1 Lupski_dorsal... 1187 0.0
gi|10098237|gb|BE710063.1|BE710063 IL3-HT0618-030800-233-C0... 1180 0.0
gi|10725045|dbj|AV707780.1|AV707780 AV707780 ADB Homo sapie... 1178 0.0
gi|12416699|gb|BG027664.1|BG027664 602294679F1 NIH_MGC_86 H... 1176 0.0
gi|12101942|gb|BF796888.1|BF796888 602258274F1 NIH_MGC_85 H... 1174 0.0
gi|1799096|gb|AA203386.1|AA203386 zx57f11.r1 Soares_fetal_l... 1170 0.0
gi|13704200|gb|BG182513.1|BG182513 RST1389 Athersys RAGE Li... 1168 0.0
gi|5393242|gb|AI806676.1|AI806676 wf35d04.x1 Soares_NFL_T_G... 1168 0.0
gi|4875177|gb|AI674697.1|AI674697 wd19d06.x1 Soares_NFL_T_G... 1160 0.0
gi|10965228|gb|BF126270.1|BF126270 601650451F1 NIH_MGC_76 H... 1154 0.0
gi|6661159|gb|AW274129.1|AW274129 xv27b02.x1 Soares_NFL_T_G... 1148 0.0
gi|5393220|gb|AI806654.1|AI806654 wf35b04.x1 Soares_NFL_T_G... 1144 0.0
gi|13050584|gb|BG292110.1|BG292110 602386409F1 NIH_MGC_93 H... 1134 0.0
gi|11968943|gb|BF683535.1|BF683535 602139737F1 NIH_MGC_46 H... 1128 0.0
gi|12614085|gb|BG120576.1|BG120576 602346709F1 NIH_MGC_90 H... 1126 0.0
gi|11978501|gb|BF693093.1|BF693093 602080115F1 NIH_MGC_81 H... 1126 0.0
gi|10951089|dbj|AU126373.1|AU126373 AU126373 NT2RP1 Homo sa... 1122 0.0
gi|10995386|dbj|AU134847.1|AU134847 AU134847 PLACE1 Homo sa... 1114 0.0
gi|2992678|gb|AA883079.1|AA883079 am24a03.s1 Soares_NFL_T_G... 1114 0.0
gi|10823746|dbj|AV721848.1|AV721848 AV721848 HTB Homo sapie... 1112 0.0
gi|4893253|gb|AI683071.1|AI683071 tx01b04.x1 NCI_CGAP_Ut4 H... 1110 0.0
gi|4610274|gb|AI601245.1|AI601245 ar88b08.x1 Barstead colon... 1098 0.0
gi|10825009|dbj|AV722480.1|AV722480 AV722480 HTB Homo sapie... 1096 0.0
gi|9132373|gb|BE312992.1|BE312992 601150276F1 NIH_MGC_19 Ho... 1094 0.0
gi|13980573|gb|BG705833.1|BG705833 602669317F1 NIH_MGC_96 H... 1090 0.0
gi|6451107|gb|AW182647.1|AW182647 xj45a04.x1 Soares_NFL_T_G... 1088 0.0
gi|12674928|gb|BG168225.1|BG168225 602339543F1 NIH_MGC_89 H... 1082 0.0
gi|12040732|gb|BF724821.1|BF724821 bx09b01.y1 Human Iris cD... 1082 0.0
gi|10299269|dbj|AV697406.1|AV697406 AV697406 GKC Homo sapie... 1080 0.0
gi|2185694|gb|AA460574.1|AA460574 zx60a12.r1 Soares_testis_... 1080 0.0
gi|8149925|gb|AW960241.1|AW960241 EST372312 MAGE resequence... 1076 0.0
gi|2261844|gb|AA521301.1|AA521301 aa79f07.s1 NCI_CGAP_GCB1 ... 1061 0.0
gi|12768489|gb|BG258673.1|BG258673 602379803F1 NIH_MGC_92 H... 1051 0.0
gi|3922551|gb|AI284318.1|AI284318 qj65c07.x1 NCI_CGAP_Kid3 ... 1047 0.0
gi|6881860|gb|AW377197.1|AW377197 IL3-CT0220-111199-028-D09... 1041 0.0
gi|4833752|gb|AI668978.1|AI668978 wb82g01.x1 NCI_CGAP_Pr28 ... 1033 0.0
gi|12916948|emb|AL565505.1|AL565505 AL565505 LTI_FL013_FBrn... 1031 0.0
gi|10990261|dbj|AU129907.1|AU129907 AU129907 NT2RP2 Homo sa... 1031 0.0
gi|1350109|gb|W52530.1|W52530 zc54d04.r1 Soares_senescent_f... 1025 0.0
gi|10203989|gb|BE782791.1|BE782791 601471972F1 NIH_MGC_67 H... 1015 0.0
gi|9871380|dbj|AV650366.1|AV650366 AV650366 GLC Homo sapien... 1011 0.0
gi|1961448|gb|AA309123.1|AA309123 EST179897 Colon carcinoma... 1011 0.0
gi|14403997|gb|BG999925.1|BG999925 MR1-HN0069-040101-015-g1... 999 0.0
gi|5036667|gb|AI719411.1|AI719411 as64c11.x1 Barstead colon... 993 0.0
gi|10299583|dbj|AV697720.1|AV697720 AV697720 GKC Homo sapie... 991 0.0
gi|2335271|gb|AA563632.1|AA563632 ng47f08.s1 NCI_CGAP_Co3 H... 983 0.0
gi|11263172|gb|BF314998.1|BF314998 601899017F1 NIH_MGC_19 H... 977 0.0
gi|2933392|gb|AA845633.1|AA845633 ai90c08.s1 Soares_parathy... 969 0.0
gi|14172393|gb|BG824806.1|BG824806 602725101F1 NIH_MGC_15 H... 963 0.0
gi|6038150|gb|AW082998.1|AW082998 xb72d12.x1 Soares_NFL_T_G... 959 0.0
gi|3844111|gb|AI248714.1|AI248714 qh72c04.x1 Soares_fetal_l... 959 0.0
gi|11012858|dbj|AU151337.1|AU151337 AU151337 NT2RP2 Homo sa... 957 0.0
gi|9877013|dbj|AV655999.1|AV655999 AV655999 GLC Homo sapien... 957 0.0

gi|5449606|gb|AI828935.1|AI828935 wj37h08.x1 NCI_CGAP_Lu19 ... 952 0.0
gi|11015393|dbj|AU153872.1|AU153872 AU153872 NT2RP3 Homo sa... 948 0.0
gi|2838179|gb|AA778848.1|AA778848 zj42a03.s1 Soares_fetal_l... 946 0.0
gi|10200888|gb|BE779690.1|BE779690 601465210F1 NIH_MGC_67 H... 942 0.0
gi|3742671|gb|AI191462.1|AI191462 qe32f11.s1 Soares_fetal_l... 940 0.0
gi|3596240|gb|AI127726.1|AI127726 qc26h03.x1 Soares_pregnan... 940 0.0
gi|4270907|gb|AI424976.1|AI424976 tg38g11.x1 Soares_NFL_T_G... 936 0.0
gi|2704986|gb|AA701873.1|AA701873 zi56b08.s1 Soares_fetal_l... 932 0.0
gi|4073260|gb|AI336333.1|AI336333 qt43f09.x1 Soares_fetal_l... 924 0.0
gi|4073310|gb|AI336383.1|AI336383 qt51c08.x1 Soares_fetal_l... 916 0.0

>gi|7705421|ref|NP_057455.1| hydroxysteroid (17-beta) dehydrogenase 7; 17 beta-hydroxysteroid dehydrogenase type VII [Homo sapiens]

EST Search:

Sequences producing significant alignments: (bits) Value

AA381145 activated T cells

AA381143 activated T cells

Sequences producing significant alignments: (bits) Value

gi|12795928|emb|AL532435.1|AL532435 AL532435 LTI_NFL001_NBC... 1871 0.0
gi|12914735|emb|AL564384.1|AL564384 AL564384 LTI_NFL001_NBC... 1683 0.0
gi|12385016|gb|BF982204.1|BF982204 602306244F1 NIH_MGC_88 H... 1302 0.0
gi|12097882|gb|BF792897.1|BF792897 602253394F1 NIH_MGC_84 H... 1221 0.0
gi|13403023|gb|BG470748.1|BG470748 602511688F1 NIH_MGC_16 H... 1168 0.0
gi|2881531|gb|AA811920.1|AA811920 ob72e11.s1 NCI_CGAP_GCB1 ... 1051 0.0
gi|14169203|gb|BG821616.1|BG821616 602727619F1 NIH_MGC_15 H... 1027 0.0
gi|13721684|gb|BG199997.1|BG199997 RST19294 Athersys RAGE L... 993 0.0
gi|10737010|gb|BF029298.1|BF029298 601765528F1 NIH_MGC_53 H... 977 0.0
gi|12327098|gb|BF928970.1|BF928970 QV3-NT0217-071200-518-e0... 934 0.0
gi|4334333|gb|AI472243.1|AI472243 tj86g08.x1 Soares_NSF_F8_... 934 0.0
gi|11162286|gb|BF247157.1|BF247157 601857822F1 NIH_MGC_58 H... 906 0.0
gi|10989791|dbj|AU129437.1|AU129437 AU129437 NT2RP2 Homo sa... 890 0.0
gi|13703900|gb|BG182213.1|BG182213 RST1077 Athersys RAGE Li... 884 0.0
gi|10992118|dbj|AU131764.1|AU131764 AU131764 NT2RP3 Homo sa... 876 0.0
gi|10988921|dbj|AU128567.1|AU128567 AU128567 NT2RP2 Homo sa... 868 0.0
gi|11363939|gb|BF382636.1|BF382636 601816836F1 NIH_MGC_56 H... 848 0.0
gi|8144565|gb|AW954882.1|AW954882 EST366952 MAGE resequence... 835 0.0
gi|9128432|gb|BE257950.1|BE257950 601109786F1 NIH_MGC_16 Ho... 801 0.0
gi|1844803|gb|AA224260.1|AA224260 zr15a04.r1 Stratagene NT2... 799 0.0
gi|9128029|gb|BE257566.1|BE257566 601109643F1 NIH_MGC_16 Ho... 797 0.0
gi|928055|gb|R83178.1|R83178 yp87e11.r1 Soares fetal liver ... 791 0.0
gi|12270902|gb|BF880776.1|BF880776 QV3-ET0174-011200-513-f0... 765 0.0
gi|10921244|dbj|AV763396.1|AV763396 AV763396 MDS Homo sapie... 700 0.0

>gi|12643402|sp|Q92506|DHB8_HUMAN ESTRADIOL 17 BETA-DEHYDROGENASE 8 (17-BETA-HSD 8) (17-BETA-HYDROXYSTEROID DEHYDROGENASE 8) (KE6 PROTEIN) (KE-6)

EST Search :

N47726 multiple sclerosis lesion

N47727 multiple sclerosis lesion

N98941 multiple sclerosis lesion

Sequences producing significant alignments: (bits) Value

gi|10214178|gb|BE792980.1|BE792980 601585653F1 NIH_MGC_7 Ho... 1336 0.0
gi|10149821|gb|BE735829.1|BE735829 601305146F1 NIH_MGC_39 H... 1304 0.0
gi|12897211|emb|AL555459.1|AL555459 AL555459 LTI_NFL006_PL2... 1296 0.0
gi|10391209|gb|BE901734.1|BE901734 601675345F1 NIH_MGC_21 H... 1237 0.0
gi|14805093|gb|BI253554.1|BI253554 602973478F1 NIH_MGC_12 H... 1203 0.0
gi|14619885|gb|BI159884.1|BI159884 602863711F1 NIH_MGC_42 H... 1197 0.0
gi|2703586|gb|AA700623.1|AA700623 zl43a04.s1 Soares_fetal_l... 1156 0.0
gi|12897209|emb|AL555458.1|AL555458 AL555458 LTI_NFL006_PL2... 1136 0.0
gi|5394035|gb|AI807469.1|AI807469 wf48b08.x1 Soares_NFL_T_G... 1120 0.0
gi|5878587|gb|AW025057.1|AW025057 wu93f03.x1 NCI_CGAP_Kid3 ... 1104 0.0
gi|11613994|gb|BF526631.1|BF526631 602070755F1 NCI_CGAP_Brn... 1102 0.0
gi|12345465|gb|BF978250.1|BF978250 602148205F1 NIH_MGC_62 H... 1084 0.0
gi|5839154|gb|AI992249.1|AI992249 ws41d10.x1 NCI_CGAP_Brn25... 1027 0.0
gi|12411526|gb|BG025183.1|BG025183 602276160F1 NIH_MGC_85 H... 995 0.0
gi|3766024|gb|AI207352.1|AI207352 qg26d10.x1 NCI_CGAP_Kid3 ... 995 0.0
gi|4268048|gb|AI422117.1|AI422117 tf40g03.x1 NCI_CGAP_Brn23... 954 0.0
gi|2568438|gb|AA643220.1|AA643220 nr96h03.s1 NCI_CGAP_Pr25 ... 948 0.0
gi|4110767|gb|AI359146.1|AI359146 qy26b08.x1 NCI_CGAP_Brn23... 890 0.0
gi|5838543|gb|AI991715.1|AI991715 wt48a04.x1 NCI_CGAP_Pan1 ... 819 0.0
gi|2942259|gb|AA854721.1|AA854721 aj76h02.s1 Soares_parathy... 765 0.0
gi|5397037|gb|AI810471.1|AI810471 wb89a09.x1 NCI_CGAP_Pr28 ... 757 0.0
gi|4190811|gb|AI380946.1|AI380946 tg18c12.x1 NCI_CGAP_CLL1 ... 747 0.0
gi|3425472|gb|AI087049.1|AI087049 oy70b11.x1 NCI_CGAP_CLL1 ... 745 0.0
gi|2785843|gb|AA745857.1|AA745857 ny93f03.s1 NCI_CGAP_GCB1 ... 730 0.0
gi|6039316|gb|AW084164.1|AW084164 xc48b09.x1 NCI_CGAP_Eso2 ... 718 0.0
gi|3202509|gb|AI002175.1|AI002175 oq85b06.s1 NCI_CGAP_Kid6 ... 714 0.0
gi|1422483|gb|W93361.1|W93361 zd94g06.s1 Soares_fetal_heart... 700 0.0
gi|3891188|gb|AI272021.1|AI272021 qj83h01.x1 NCI_CGAP_Kid3 ... 654 0.0
gi|3040584|gb|AA905461.1|AA905461 ok01e08.s1 Soares_NFL_T_G... 563 e-158
gi|1188892|gb|N47726.1|N47726 yy92h12.r1 Soares_multiple_sc... 555 e-156
gi|8139732|gb|AW950194.1|AW950194 EST362159 MAGE resequence... 551 e-154
gi|1378970|gb|W69711.1|W69711 zd47e09.s1 Soares_fetal_heart... 551 e-154
gi|1664996|gb|AA113291.1|AA113291 zm28d01.s1 Stratagene pan... 549 e-154
gi|3058465|gb|AA918575.1|AA918575 ol42h06.s1 Soares_NFL_T_G... 517 e-144
gi|1547517|gb|AA055098.1|AA055098 zf17a01.s1 Soares_fetal_h... 517 e-144

gi|6138458|gb|AW134912.1|AW134912 UI-H-BI1-abr-c-10-0-UI.s1... 515 e-144
gi|13664562|gb|BG613191.1|BG613191 602640738F1 NIH_MGC_61 H... 507 e-141
gi|5233304|gb|AI766795.1|AI766795 wi88e08.x1 NCI_CGAP_Kid12... 504 e-140

>gi|2558754|gb|AAC51812.1| amyloid beta-peptide binding protein [Homo sapiens]; similar 17-beta-hydroxysteroid dehydrogenase type 10

EST Search:

Sequences producing significant alignments: (bits) Value

AI 672661 spleen

AI572890 lymphoma

Sequences producing significant alignments: (bits) Value

gi|12952470|emb|AL583473.1|AL583473 AL583473 LTI_NFL004_NBC... 1784 0.0
gi|12903888|emb|AL558907.1|AL558907 AL558907 LTI_NFL008_TC2... 1756 0.0
gi|12783279|emb|AL519786.1|AL519786 AL519786 LTI_NFL004_NBC... 1756 0.0
gi|12897788|emb|AL555756.1|AL555756 AL555756 LTI_NFL006_PL2... 1723 0.0
gi|12900345|emb|AL557084.1|AL557084 AL557084 LTI_FL012_TC1 ... 1701 0.0
gi|12790972|emb|AL527479.1|AL527479 AL527479 LTI_NFL003_NBC... 1699 0.0
gi|12903886|emb|AL558906.1|AL558906 AL558906 LTI_NFL008_TC2... 1677 0.0
gi|14177068|gb|BG829481.1|BG829481 602763779F1 NIH_MGC_42 H... 1612 0.0
gi|13515355|gb|BG519629.1|BG519629 602578744F1 NIH_MGC_19 H... 1578 0.0
gi|13515189|gb|BG519532.1|BG519532 602578613F1 NIH_MGC_19 H... 1576 0.0
gi|10212533|gb|BE791335.1|BE791335 601582717F1 NIH_MGC_7 Ho... 1530 0.0
gi|14177225|gb|BG829638.1|BG829638 602763994F1 NIH_MGC_42 H... 1526 0.0
gi|10161376|gb|BE747384.1|BE747384 601580434F1 NIH_MGC_9 Ho... 1505 0.0
gi|13980226|gb|BG705661.1|BG705661 602668874F1 NIH_MGC_96 H... 1495 0.0
gi|12340198|gb|BF972983.1|BF972983 602241285F1 NIH_MGC_46 H... 1491 0.0
gi|12900344|emb|AL557083.1|AL557083 AL557083 LTI_FL012_TC1 ... 1485 0.0
gi|12786487|emb|AL522994.1|AL522994 AL522994 LTI_NFL003_NBC... 1477 0.0
gi|9806674|gb|BE562954.1|BE562954 601336395F1 NIH_MGC_44 Ho... 1471 0.0
gi|14060190|gb|BG749537.1|BG749537 602707687F1 NIH_MGC_43 H... 1463 0.0
gi|10993386|dbj|AU132847.1|AU132847 AU132847 NT2RP4 Homo sa... 1427 0.0
gi|10213089|gb|BE791891.1|BE791891 601586179F1 NIH_MGC_7 Ho... 1427 0.0
gi|12686237|gb|BG179544.1|BG179544 602328141F1 NIH_MGC_91 H... 1405 0.0
gi|13143793|gb|BG337355.1|BG337355 602434902F1 NIH_MGC_46 H... 1398 0.0
gi|11290698|gb|BF343424.1|BF343424 602014537F1 NCI_CGAP_Brn... 1390 0.0
gi|13583928|gb|BG576275.1|BG576275 602595778F1 NIH_MGC_87 H... 1384 0.0
gi|10141135|gb|BE727143.1|BE727143 601563585F1 NIH_MGC_20 H... 1384 0.0
gi|14651188|gb|BI196168.1|BI196168 602754680F1 NIH_MGC_19 H... 1366 0.0
gi|9130990|gb|BE260026.1|BE260026 601150544F1 NIH_MGC_19 Ho... 1354 0.0
gi|13328527|gb|BG422021.1|BG422021 602448619F1 NIH_MGC_14 H... 1344 0.0
gi|10157401|gb|BE743409.1|BE743409 601573650F1 NIH_MGC_9 Ho... 1338 0.0
gi|13144448|gb|BG338010.1|BG338010 602435826F1 NIH_MGC_46 H... 1334 0.0
gi|12897787|emb|AL555755.1|AL555755 AL555755 LTI_NFL006_PL2... 1334 0.0
gi|2929646|gb|AA843128.1|AA843128 ak06b01.s1 Soares_parathy... 1334 0.0
gi|13144112|gb|BG337674.1|BG337674 602435234F1 NIH_MGC_46 H... 1330 0.0
gi|10984794|gb|BF115392.1|BF115392 7n81c10.x1 NCI_CGAP_Ov18... 1312 0.0
gi|10160758|gb|BE746766.1|BE746766 601579220F1 NIH_MGC_9 Ho... 1308 0.0
gi|10207861|gb|BE786663.1|BE786663 601475007F1 NIH_MGC_68 H... 1306 0.0
gi|9328027|gb|BE382662.1|BE382662 601297319F1 NIH_MGC_19 Ho... 1298 0.0
gi|12786554|emb|AL523061.1|AL523061 AL523061 LTI_NFL003_NBC... 1292 0.0
gi|10159290|gb|BE745298.1|BE745298 601574074F1 NIH_MGC_9 Ho... 1292 0.0
gi|2557125|gb|AA633911.1|AA633911 ac73b06.s1 Stratagene lun... 1287 0.0
gi|12600433|gb|BG106587.1|BG106587 602290404F1 NIH_MGC_85 H... 1285 0.0

gi|13325474|gb|BG418969.1|BG418969 602446586F1 NIH_MGC_14 H... 1283 0.0
gi|2930155|gb|AA843637.1|AA843637 ak08e05.s1 Soares_parathy... 1281 0.0
gi|9721817|gb|BE514603.1|BE514603 601316950F1 NIH_MGC_9 Hom... 1277 0.0
gi|13143209|gb|BG336771.1|BG336771 602405512F1 NIH_MGC_21 H... 1275 0.0
gi|12786486|emb|AL522993.1|AL522993 AL522993 LTI_NFL003_NBC... 1269 0.0
gi|12677545|gb|BG170842.1|BG170842 602323784F1 NIH_MGC_89 H... 1269 0.0
gi|11970276|gb|BF684868.1|BF684868 602142585F1 NIH_MGC_46 H... 1267 0.0
gi|13142863|gb|BG336425.1|BG336425 602405366F1 NIH_MGC_21 H... 1261 0.0
gi|10938598|gb|BF108908.1|BF108908 7l54a06.x1 Soares_NSF_F8... 1257 0.0
gi|9775533|gb|BE546888.1|BE546888 601073928F1 NIH_MGC_12 Ho... 1257 0.0
gi|11452182|gb|BF439665.1|BF439665 nab69d05.x1 Soares_NSF_F... 1235 0.0
gi|11126323|gb|BF220229.1|BF220229 601296789T1 NIH_MGC_7 Ho... 1235 0.0
gi|11125937|gb|BF219843.1|BF219843 601296789F1 NIH_MGC_7 Ho... 1223 0.0
gi|9132309|gb|BE260753.1|BE260753 601150179F1 NIH_MGC_19 Ho... 1219 0.0
gi|13579025|gb|BG571372.1|BG571372 602592643F1 NIH_MGC_79 H... 1217 0.0
gi|10352672|gb|BE892388.1|BE892388 601433863F1 NIH_MGC_72 H... 1215 0.0
gi|12414601|gb|BG026711.1|BG026711 602293559F1 NIH_MGC_86 H... 1211 0.0
gi|10209561|gb|BE788363.1|BE788363 601480193F1 NIH_MGC_68 H... 1211 0.0
gi|10157261|gb|BE743269.1|BE743269 601574865F1 NIH_MGC_9 Ho... 1203 0.0
gi|9338006|gb|BE392641.1|BE392641 601307482F1 NIH_MGC_44 Ho... 1191 0.0
gi|11262743|gb|BF314610.1|BF314610 601900635F1 NIH_MGC_19 H... 1187 0.0
gi|5512308|gb|AI858692.1|AI858692 wl41c01.x1 NCI_CGAP_Ut1 H... 1181 0.0
gi|9146544|gb|BE272203.1|BE272203 601126161F1 NIH_MGC_9 Hom... 1170 0.0
gi|11985061|gb|BF699653.1|BF699653 602127064F1 NIH_MGC_56 H... 1168 0.0
gi|12790938|emb|AL527445.1|AL527445 AL527445 LTI_NFL003_NBC... 1166 0.0
gi|11260701|gb|BF312822.1|BF312822 601896961F1 NIH_MGC_19 H... 1162 0.0
gi|6591193|gb|AW248200.1|AW248200 2819721.5prime NIH_MGC_7 ... 1158 0.0
gi|8169874|gb|AW978604.1|AW978604 EST390713 MAGE resequence... 1156 0.0
gi|6590163|gb|AW247170.1|AW247170 2819721.3prime NIH_MGC_7 ... 1152 0.0
gi|10397018|gb|BE904601.1|BE904601 601498691F1 NIH_MGC_70 H... 1150 0.0
gi|13293601|gb|BG400153.1|BG400153 602440936F1 NIH_MGC_75 H... 1144 0.0
gi|4330014|gb|AI467924.1|AI467924 tj84b08.x1 Soares_NSF_F8_... 1142 0.0
gi|11263591|gb|BF315353.1|BF315353 601902636F1 NIH_MGC_19 H... 1138 0.0
gi|9324464|gb|BE379099.1|BE379099 601237744F1 NIH_MGC_44 Ho... 1138 0.0
gi|9134960|gb|BE314169.1|BE314169 601150413F1 NIH_MGC_19 Ho... 1134 0.0
gi|12431144|gb|BG036213.1|BG036213 602326967F1 NIH_MGC_91 H... 1116 0.0
gi|10349600|gb|BE890858.1|BE890858 601431314F1 NIH_MGC_72 H... 1110 0.0
gi|5905050|gb|AW044521.1|AW044521 wy73a12.x1 Soares_NSF_F8_... 1110 0.0
gi|9130493|gb|BE312164.1|BE312164 601152459F1 NIH_MGC_19 Ho... 1106 0.0
gi|7538454|gb|AW673219.1|AW673219 ba64b02.x1 NIH_MGC_12 Hom... 1094 0.0
gi|4437833|gb|AI523698.1|AI523698 th18c11.x1 NCI_CGAP_Pr28 ... 1088 0.0
gi|4852392|gb|AI672661.1|AI672661 we57b07.x1 Soares_thymus_... 1084 0.0
gi|8152566|gb|AW962730.1|AW962730 EST374803 MAGE resequence... 1076 0.0
gi|11940734|gb|BF666839.1|BF666839 602121161F1 NIH_MGC_56 H... 1067 0.0
gi|11261865|gb|BF313796.1|BF313796 601900471F1 NIH_MGC_19 H... 1067 0.0
gi|11015820|dbj|AU154299.1|AU154299 AU154299 NT2RP4 Homo sa... 1067 0.0
gi|14654647|gb|BI199626.1|BI199626 602763205F1 NIH_MGC_19 H... 1057 0.0
gi|6898801|gb|AW394142.1|AW394142 MR2-TT0013-151299-211-a01... 1045 0.0
gi|5511698|gb|AI858082.1|AI858082 wj70b06.x1 NCI_CGAP_Lu19 ... 1043 0.0
gi|4244537|gb|AI401450.1|AI401450 tg64c01.x1 Soares_NhHMPu_... 1037 0.0
gi|11446450|gb|BF434178.1|BF434178 7o99g04.x1 NCI_CGAP_Ov18... 1029 0.0
gi|11682416|gb|BF590092.1|BF590092 nab18g11.x1 Soares_NSF_F... 1015 0.0
gi|1959225|gb|AA306825.1|AA306825 EST177820 Jurkat T-cells ... 1015 0.0
gi|10319956|gb|BE871180.1|BE871180 601448752F1 NIH_MGC_65 H... 1001 0.0
gi|4536264|gb|AI572890.1|AI572890 tn63d09.x1 NCI_CGAP_Lym12... 999 0.0
gi|7540188|gb|AW674953.1|AW674953 ba60c02.y1 NIH_MGC_10 Hom... 995 0.0
gi|10587007|gb|BE973671.1|BE973671 601680849F1 NIH_MGC_83 H... 989 0.0

gi|5933240|gb|AW057601.1|AW057601 wy61d07.x1 Soares_NSF_F8_... 989 0.0
gi|3086338|gb|AA931952.1|AA931952 om88g07.s1 NCI_CGAP_Kid3 ... 985 0.0
gi|2713875|gb|AA703957.1|AA703957 ag79f03.r1 Stratagene hNT... 971 0.0
gi|5512644|gb|AI859028.1|AI859028 wl66a04.x1 NCI_CGAP_Brn25... 965 0.0
gi|9776820|gb|BE548175.1|BE548175 601073180F1 NIH_MGC_12 Ho... 963 0.0
gi|3674555|gb|AI146873.1|AI146873 oy22g02.s1 Soares_senesce... 961 0.0
gi|5914335|gb|AW051976.1|AW051976 wy86a08.x1 Soares_NSF_F8_... 926 0.0
gi|3050720|gb|AA911356.1|AA911356 oe76c12.s1 NCI_CGAP_Lu5 H... 926 0.0
gi|1728098|gb|AA156357.1|AA156357 zo33a08.s1 Stratagene col... 918 0.0
gi|1885828|gb|AA250805.1|AA250805 zs06a02.r1 NCI_CGAP_GCB1 ... 910 0.0
gi|2840960|gb|AA781629.1|AA781629 ai56g06.s1 Soares_parathy... 908 0.0
gi|1885771|gb|AA250790.1|AA250790 zs06a02.s1 NCI_CGAP_GCB1 ... 900 0.0
gi|11947190|gb|BF673295.1|BF673295 602136147F1 NIH_MGC_83 H... 892 0.0
gi|1765501|gb|AA182000.1|AA182000 zp62f09.s1 Stratagene end... 886 0.0
gi|3895935|gb|AI273667.1|AI273667 qi61g05.x1 Soares_NhHMPu_... 884 0.0
gi|10569025|gb|BE958320.1|BE958320 601644804F1 NIH_MGC_56 H... 878 0.0
gi|2524747|gb|AA620808.1|AA620808 af95c08.s1 Soares_testis_... 872 0.0
gi|7412872|gb|AW651626.1|AW651626 ba60c02.x1 NIH_MGC_10 Hom... 870 0.0
gi|1958522|gb|AA306194.1|AA306194 EST177168 Jurkat T-cells ... 866 0.0
gi|3145278|gb|AA972514.1|AA972514 op15d03.s1 NCI_CGAP_Co12 ... 864 0.0
gi|7412881|gb|AW651635.1|AW651635 ba60d01.x1 NIH_MGC_10 Hom... 856 0.0
gi|3835691|gb|AI240294.1|AI240294 qi11h12.x1 Soares_NhHMPu_... 850 0.0
gi|2805809|gb|AA757946.1|AA757946 zg44h11.s1 Soares_pineal_... 850 0.0
gi|3659170|gb|AI142811.1|AI142811 qa26e02.s1 Soares_NhHMPu_... 848 0.0
gi|1962410|gb|AA310009.1|AA310009 EST180922 Jurkat T-cells ... 842 0.0
gi|14647912|gb|BI192892.1|BI192892 602945296F1 NIH_MGC_42 H... 839 0.0
gi|5450543|gb|AI829872.1|AI829872 wj58c10.x1 NCI_CGAP_Lu19 ... 835 0.0
gi|3895220|gb|AI272952.1|AI272952 qi56h03.x1 Soares_NhHMPu_... 825 0.0
gi|3836511|gb|AI241114.1|AI241114 qj96b06.x1 NCI_CGAP_Kid3 ... 825 0.0
gi|4852404|gb|AI672673.1|AI672673 we57c08.x1 Soares_thymus_... 819 0.0
gi|5855096|gb|AW006318.1|AW006318 wt04a10.x1 NCI_CGAP_Co3 H... 805 0.0
gi|4489773|gb|AI557410.1|AI557410 PT2.1_7_A05.r tumor2 Homo... 801 0.0

>gi|9622124|gb|AAF89632.1|AF167438_1 androgen-regulated short-chain dehydrogenase/reductase 1 [Homo sapiens]

EST Search:

Sequences producing significant alignments: (bits) Value

gi|13401922|gb|BG469647.1|BG469647 602534103F1 NIH_MGC_15 H... 1550 0.0
gi|13746560|gb|BG220539.1|BG220539 RST40325 Athersys RAGE L... 1483 0.0
gi|14053553|gb|BG742900.1|BG742900 602632481F1 NCI_CGAP_Skn... 1457 0.0
gi|13967002|gb|BG699072.1|BG699072 602678713F1 NIH_MGC_95 H... 1439 0.0
gi|14053781|gb|BG743128.1|BG743128 602634270F1 NCI_CGAP_Skn... 1427 0.0
gi|13410718|gb|BG478523.1|BG478523 602524002F1 NIH_MGC_20 H... 1419 0.0
gi|9146489|gb|BE272160.1|BE272160 601141656F1 NIH_MGC_9 Hom... 1409 0.0
gi|14047524|gb|BG777207.1|BG777207 602664432F1 NIH_MGC_59 H... 1402 0.0
gi|13963233|gb|BG697241.1|BG697241 602660481F1 NCI_CGAP_Skn... 1394 0.0
gi|14651659|gb|BI196639.1|BI196639 602755427F1 NIH_MGC_19 H... 1388 0.0
gi|14059064|gb|BG748411.1|BG748411 602705974F1 NIH_MGC_43 H... 1380 0.0
gi|13336094|gb|BG429588.1|BG429588 602501268F1 NIH_MGC_75 H... 1368 0.0
gi|9124275|gb|BE253854.1|BE253854 601112818F1 NIH_MGC_16 Ho... 1364 0.0
gi|12604238|gb|BG110732.1|BG110732 602279029F1 NIH_MGC_86 H... 1358 0.0
gi|14064290|gb|BG753637.1|BG753637 602732827F1 NIH_MGC_43 H... 1348 0.0
gi|13527202|gb|BG535657.1|BG535657 602563366F1 NIH_MGC_77 H... 1344 0.0
gi|13289966|gb|BG396518.1|BG396518 602459353F1 NIH_MGC_16 H... 1342 0.0
gi|10399800|gb|BE906369.1|BE906369 601498517F1 NIH_MGC_70 H... 1340 0.0
gi|10156435|gb|BE742443.1|BE742443 601575210F1 NIH_MGC_9 Ho... 1330 0.0
gi|6361758|gb|AI305108.1|AI305108 HA2404 Human fetal liver ... 1316 0.0
gi|13570738|gb|BG563086.1|BG563086 602581878F1 NIH_MGC_76 H... 1314 0.0
gi|12607924|gb|BG114418.1|BG114418 602285710F1 NIH_MGC_86 H... 1314 0.0
gi|14809963|gb|BI255993.1|BI255993 602976353F1 NIH_MGC_12 H... 1306 0.0
gi|14565107|gb|BI114206.1|BI114206 602862564F1 NIH_MGC_17 H... 1302 0.0
gi|14566335|gb|BI115434.1|BI115434 602863311F1 NIH_MGC_17 H... 1296 0.0
gi|6359266|gb|AI064994.1|AI064994 HA0821 Human fetal liver ... 1296 0.0
gi|9186637|gb|BE302889.1|BE302889 ba70g10.y1 NIH_MGC_20 Hom... 1289 0.0
gi|14566302|gb|BI115401.1|BI115401 602863260F1 NIH_MGC_17 H... 1279 0.0
gi|9328145|gb|BE382780.1|BE382780 601298459F1 NIH_MGC_19 Ho... 1259 0.0
gi|10160188|gb|BE746196.1|BE746196 601578644F1 NIH_MGC_9 Ho... 1253 0.0
gi|12761697|gb|BG251881.1|BG251881 602364502F1 NIH_MGC_90 H... 1251 0.0
gi|13969001|gb|BG700048.1|BG700048 602681055F1 NIH_MGC_95 H... 1241 0.0
gi|12678524|gb|BG171821.1|BG171821 602322603F1 NIH_MGC_89 H... 1237 0.0
gi|9179232|gb|BE295680.1|BE295680 601175688F1 NIH_MGC_17 Ho... 1235 0.0
gi|4763039|gb|AI659469.1|AI659469 tu30g07.x1 NCI_CGAP_Pr28 ... 1229 0.0
gi|13523981|gb|BG532442.1|BG532442 602561968F1 NIH_MGC_61 H... 1227 0.0
gi|9346825|gb|BE410375.1|BE410375 601302363F1 NIH_MGC_21 Ho... 1219 0.0
gi|12609069|gb|BG115563.1|BG115563 602317253F1 NIH_MGC_88 H... 1213 0.0
gi|2398040|gb|AA587226.1|AA587226 nn82b08.s1 NCI_CGAP_Co9 H... 1213 0.0
gi|13534026|gb|BG541793.1|BG541793 602569677F1 NIH_MGC_77 H... 1211 0.0
gi|13459320|gb|BG497803.1|BG497803 602543080F1 NIH_MGC_60 H... 1209 0.0
gi|10741086|gb|BF033374.1|BF033374 601458081F1 NIH_MGC_66 H... 1199 0.0
gi|9722042|gb|BE514828.1|BE514828 601316764F1 NIH_MGC_9 Hom... 1191 0.0
gi|9339021|gb|BE393656.1|BE393656 601310379F1 NIH_MGC_44 Ho... 1187 0.0
gi|13406852|gb|BG474575.1|BG474575 602517363F1 NIH_MGC_16 H... 1185 0.0
gi|11952823|gb|BF678928.1|BF678928 602153555F1 NIH_MGC_83 H... 1166 0.0
gi|12770117|gb|BG260301.1|BG260301 602371417F1 NIH_MGC_93 H... 1162 0.0
gi|13972135|gb|BG701616.1|BG701616 602682503F1 NIH_MGC_95 H... 1158 0.0
gi|9323581|gb|BE378216.1|BE378216 601237991F1 NIH_MGC_44 Ho... 1158 0.0
gi|14471561|gb|BI064034.1|BI064034 IL3-UT0119-120401-430-G0... 1156 0.0

gi|8144363|gb|AW954680.1|AW954680 EST366750 MAGE resequence... 1150 0.0
gi|9331236|gb|BE385871.1|BE385871 601275933F1 NIH_MGC_20 Ho... 1144 0.0
gi|12687397|gb|BG180694.1|BG180694 602329481F1 NIH_MGC_91 H... 1142 0.0
gi|11953928|gb|BF680033.1|BF680033 602154752F1 NIH_MGC_83 H... 1132 0.0
gi|13458797|gb|BG497280.1|BG497280 602537844F1 NIH_MGC_59 H... 1128 0.0
gi|9179583|gb|BE296026.1|BE296026 601175058F1 NIH_MGC_17 Ho... 1128 0.0
gi|9770617|gb|BE541972.1|BE541972 601064273F1 NIH_MGC_10 Ho... 1126 0.0
gi|6568025|gb|AW235636.1|AW235636 xn20g09.x1 NCI_CGAP_Kid11... 1126 0.0
gi|12612166|gb|BG118660.1|BG118660 602348226F1 NIH_MGC_90 H... 1124 0.0
gi|13282164|gb|BG388718.1|BG388718 602414406F1 NIH_MGC_92 H... 1108 0.0
gi|11952959|gb|BF679064.1|BF679064 602153322F1 NIH_MGC_83 H... 1094 0.0
gi|11954261|gb|BF680366.1|BF680366 602154150F1 NIH_MGC_83 H... 1092 0.0
gi|13336068|gb|BG429562.1|BG429562 602501238F1 NIH_MGC_75 H... 1076 0.0
gi|11613456|gb|BF526180.1|BF526180 602071089F1 NCI_CGAP_Brn... 1076 0.0
gi|1544739|gb|AA053804.1|AA053804 ze25e09.s1 Soares_fetal_h... 1076 0.0
gi|11954238|gb|BF680343.1|BF680343 602154124F1 NIH_MGC_83 H... 1070 0.0
gi|2154395|gb|AA442517.1|AA442517 zv68a01.r1 Soares_total_f... 1068 0.0
gi|13727617|gb|BG205930.1|BG205930 RST25365 Athersys RAGE L... 1067 0.0
gi|11947983|gb|BF674088.1|BF674088 602137489F1 NIH_MGC_83 H... 1059 0.0
gi|14178068|gb|BG830481.1|BG830481 602767043F1 NIH_MGC_42 H... 1057 0.0
gi|11954070|gb|BF680175.1|BF680175 602154923F1 NIH_MGC_83 H... 1055 0.0
gi|11947422|gb|BF673610.1|BF673610 602136021F1 NIH_MGC_83 H... 1055 0.0
gi|9135943|gb|BE262703.1|BE262703 601146057F1 NIH_MGC_19 Ho... 1055 0.0
gi|12523600|gb|BG057848.1|BG057848 naf13d09.x1 Soares_NPBMC... 1051 0.0
gi|11107340|gb|BF213754.1|BF213754 601847654F1 NIH_MGC_55 H... 1051 0.0
gi|11947265|gb|BF673370.1|BF673370 602135837F1 NIH_MGC_83 H... 1047 0.0
gi|13714218|gb|BG192531.1|BG192531 RST11646 Athersys RAGE L... 1043 0.0
gi|9189288|gb|BE336903.1|BE336903 bb68f05.y1 NIH_MGC_9 Homo... 1043 0.0
gi|10348906|gb|BE890514.1|BE890514 601431585F1 NIH_MGC_72 H... 1037 0.0
gi|12158715|gb|BF820301.1|BF820301 CM0-RT0018-181100-706-e0... 1029 0.0
gi|2167857|gb|AA454188.1|AA454188 zx48a12.s1 Soares_testis_... 1029 0.0
gi|12062595|gb|BF735895.1|BF735895 QV1-KT0023-131100-480-b0... 1027 0.0
gi|12062768|gb|BF736094.1|BF736094 QV1-KT0023-131100-475-h0... 1025 0.0
gi|5080879|gb|AF063505.1|AF063505 AF063505 Homo sapiens lib... 1023 0.0
gi|6359496|gb|AI110631.1|AI110631 HA0057 Human fetal liver ... 1023 0.0
gi|14471624|gb|BI064110.1|BI064110 IL3-UT0119-170401-458-F0... 1021 0.0
gi|10587293|gb|BE973957.1|BE973957 601680275F1 NIH_MGC_83 H... 1021 0.0
gi|14565160|gb|BI114259.1|BI114259 602862449F1 NIH_MGC_17 H... 1017 0.0
gi|11947398|gb|BF673586.1|BF673586 602136287F1 NIH_MGC_83 H... 1017 0.0
gi|11948042|gb|BF674147.1|BF674147 602137658F1 NIH_MGC_83 H... 1009 0.0
gi|11948071|gb|BF674176.1|BF674176 602137695F1 NIH_MGC_83 H... 1007 0.0
gi|12062604|gb|BF735904.1|BF735904 QV1-KT0023-131100-480-h0... 1005 0.0
gi|2703194|gb|AA700231.1|AA700231 zj52f03.s1 Soares_fetal_l... 1003 0.0
gi|5663000|gb|AI927036.1|AI927036 wo87b07.x1 NCI_CGAP_Kid11... 997 0.0
gi|11949270|gb|BF675375.1|BF675375 602138336F1 NIH_MGC_83 H... 993 0.0
gi|11107263|gb|BF213677.1|BF213677 601847527F1 NIH_MGC_55 H... 993 0.0
gi|5839186|gb|AI992281.1|AI992281 ws41g11.x1 NCI_CGAP_Brn25... 991 0.0
gi|4897519|gb|AI686225.1|AI686225 tu40f05.x1 NCI_CGAP_Pr28 ... 991 0.0
gi|5364540|gb|AI799068.1|AI799068 we98b05.x1 Soares_NFL_T_G... 989 0.0
gi|14471659|gb|BI064132.1|BI064132 IL3-UT0119-170401-459-H0... 983 0.0
gi|5864305|gb|AW015548.1|AW015548 UI-H-BI0p-aau-e-01-0-UI.s... 983 0.0
gi|11943604|gb|BF669709.1|BF669709 602118259F1 NIH_MGC_56 H... 981 0.0
gi|12062547|gb|BF735964.1|BF735964 QV1-KT0023-111100-479-b0... 979 0.0
gi|2167856|gb|AA454187.1|AA454187 zx48a12.r1 Soares_testis_... 977 0.0
gi|9969904|gb|BE645593.1|BE645593 7e72g02.x1 NCI_CGAP_Pr28 ... 975 0.0
gi|7280592|gb|AW593334.1|AW593334 hg13d03.x1 Soares_NFL_T_G... 975 0.0
gi|11954107|gb|BF680212.1|BF680212 602154965F1 NIH_MGC_83 H... 971 0.0

gi|13335825|gb|BG429319.1|BG429319 602494022F1 NIH_MGC_75 H... 967 0.0
gi|10578047|gb|BE967342.1|BE967342 601649342F1 NIH_MGC_73 H... 967 0.0
gi|1686108|gb|AA126515.1|AA126515 zn85c12.s1 Stratagene lun... 965 0.0
gi|5913719|gb|AW051449.1|AW051449 wy95h11.x1 NCI_CGAP_Brn23... 961 0.0
gi|9156141|gb|BE281127.1|BE281127 601157756F1 NIH_MGC_21 Ho... 959 0.0
gi|2584691|gb|AA653039.1|AA653039 ns71e08.s1 NCI_CGAP_Pr2 H... 959 0.0
gi|11449515|gb|BF437182.1|BF437182 7p67e11.x1 NCI_CGAP_Pr28... 957 0.0
gi|7632890|gb|AW732557.1|AW732557 bb08c01.y1 NIH_MGC_14 Hom... 955 0.0
gi|11107822|gb|BF214236.1|BF214236 601848414F1 NIH_MGC_55 H... 946 0.0
gi|5632015|gb|AI912160.1|AI912160 wd71a09.x1 NCI_CGAP_Lu24 ... 938 0.0
gi|9156661|gb|BE281638.1|BE281638 601155146F1 NIH_MGC_21 Ho... 934 0.0
gi|5886621|gb|AW027865.1|AW027865 ws62b11.x1 NCI_CGAP_Brn23... 932 0.0
gi|9186545|gb|BE302797.1|BE302797 ba69a06.y1 NIH_MGC_20 Hom... 928 0.0
gi|8364368|gb|BE047315.1|BE047315 hq78g07.x1 NCI_CGAP_Ov41 ... 928 0.0
gi|6361052|gb|AI174674.1|AI174674 HA2365 Human fetal liver ... 928 0.0
gi|10367360|gb|BE855387.1|BE855387 7g13b06.x1 NCI_CGAP_Brn2... 922 0.0
gi|13970318|gb|BG700707.1|BG700707 602682353F1 NIH_MGC_95 H... 916 0.0
gi|1507636|gb|AA035790.1|AA035790 ze25e09.r1 Soares_fetal_h... 916 0.0
gi|1679019|gb|AA121396.1|AA121396 zn77h06.s1 Stratagene NT2... 914 0.0
gi|5768230|gb|AI971404.1|AI971404 wr04e08.x1 NCI_CGAP_GC6 H... 912 0.0
gi|11681877|gb|BF589553.1|BF589553 naa05g08.x1 NCI_CGAP_Pr2... 910 0.0
gi|10887537|gb|BF105011.1|BF105011 601822785F1 NIH_MGC_75 H... 908 0.0
gi|5767638|gb|AI970812.1|AI970812 wr20b02.x1 NCI_CGAP_Pr28 ... 906 0.0
gi|11950417|gb|BF676522.1|BF676522 602084429F1 NIH_MGC_83 H... 904 0.0
gi|11108871|gb|BF215285.1|BF215285 601846338F1 NIH_MGC_55 H... 900 0.0
gi|1383082|gb|W72327.1|W72327 zd62b11.s1 Soares_fetal_heart... 900 0.0

>gi|7705907|ref|NP_057330.1| retinal short-chain dehydrogenase/reductase retSDR3 [Homo sapiens]

EST Search:

Sequences producing significant alignments: (bits) Value

gi|14077603|gb|BG766950.1|BG766950 602740653F1 NIH_MGC_49 H... 1437 0.0
gi|10370049|gb|BE856729.1|BE856729 7f66h09.x1 Soares_NSF_F8... 1183 0.0
gi|3180757|gb|AA994212.1|AA994212 ou49b10.s1 NCI_CGAP_Br2 H... 1104 0.0
gi|12102027|gb|BF796973.1|BF796973 602258193F1 NIH_MGC_85 H... 1055 0.0
gi|4334141|gb|AI472051.1|AI472051 tj85e10.x1 Soares_NSF_F8_... 1047 0.0
gi|5394770|gb|AI808204.1|AI808204 wf93f01.x1 Soares_NSF_F8_... 1045 0.0
gi|8156902|gb|AW967066.1|AW967066 EST379140 MAGE resequence... 1023 0.0
gi|9706163|gb|BE503755.1|BE503755 hz51b10.x1 NCI_CGAP_Lu24 ... 1013 0.0
gi|4971779|gb|AI694439.1|AI694439 wd83g04.x1 NCI_CGAP_Lu24 ... 1005 0.0
gi|5110372|gb|AI742084.1|AI742084 wg38g06.x1 Soares_NSF_F8_... 957 0.0
gi|3214671|gb|AI005161.1|AI005161 ou13c05.x1 Soares_NFL_T_G... 940 0.0
gi|1523029|gb|AA044826.1|AA044826 zk72b09.s1 Soares_pregnan... 918 0.0
gi|3594921|gb|AI126407.1|AI126407 qc55g09.x1 Soares_placent... 902 0.0
gi|10964840|gb|BF125800.1|BF125800 601763002F1 NIH_MGC_20 H... 894 0.0
gi|4523233|gb|AI564776.1|AI564776 tn37b01.x1 NCI_CGAP_Brn25... 882 0.0
gi|4189789|gb|AI379936.1|AI379936 tc53c09.x1 Soares_NhHMPu_... 872 0.0
gi|10718270|dbj|AV701940.1|AV701940 AV701940 ADB Homo sapie... 835 0.0
gi|10941621|gb|BF112008.1|BF112008 7l37e08.x1 Soares_NSF_F8... 817 0.0
gi|6946828|gb|AW418896.1|AW418896 ha15c03.x1 NCI_CGAP_Kid12... 817 0.0

>gi¦3372592¦gb¦AAC39922.1¦ sterol/retinol dehydrogenase [Homo sapiens]

EST Search:

Sequences producing significant alignments: (bits) Value

gi¦9882195¦dbj¦AV661181.1¦AV661181 AV661181 GLC Homo sapien... 987 0.0
gi¦9882144¦dbj¦AV661130.1¦AV661130 AV661130 GLC Homo sapien... 928 0.0
gi¦10297142¦dbj¦AV695279.1¦AV695279 AV695279 GKC Homo sapie... 611 e-172
gi¦10290555¦dbj¦AV688692.1¦AV688692 AV688692 GKC Homo sapie... 595 e-167
gi¦9868702¦dbj¦AV647688.1¦AV647688 AV647688 GLC Homo sapien... 543 e-152
gi¦9868612¦dbj¦AV647598.1¦AV647598 AV647598 GLC Homo sapien... 543 e-152
gi¦9868272¦dbj¦AV647258.1¦AV647258 AV647258 GLC Homo sapien... 543 e-152
gi¦9868493¦dbj¦AV647479.1¦AV647479 AV647479 GLC Homo sapien... 504 e-140

Jurkat Tcells: AA312392

gb¦AA381769.1¦AA381769 EST94887 Activated T-cells I Homo sa... 36 9.9
gb¦AA381726.1¦AA381726 EST94873 Activated T-cells I Homo sa... 36 9.9
gb¦AA381649.1¦AA381649 EST94823 Activated T-cells I Homo sa... 36 9.9
gb¦AA381695.1¦AA381695 EST94806 Activated T-cells I Homo sa... 36 9.9
gb¦AA381691.1¦AA381691 EST94801 Activated T-cells I Homo sa... 36 9.9
gb¦AA381683.1¦AA381683 EST94792 Activated T-cells I Homo sa... 36 9.9
gb¦AA381621.1¦AA381621 EST94733 Activated T-cells I Homo sa... 36 9.9
gb¦AA381348.1¦AA381348 EST94418 Activated T-cells I Homo sa... 36 9.9

>gi¦5031765¦ref¦NP_005516.1¦ hydroxysteroid (11-beta) dehydrogenase 1 [Homo sapiens]

EST Search :

N59147 multiple sclerosis lesion

N75182 multiple sclerosis lesion

Sequences producing significant alignments: (bits) Value

gi¦13906209¦gb¦BG674813.1¦BG674813 602620946F1 NCI_CGAP_Skn... 1685 0.0
gi¦13905643¦gb¦BG674247.1¦BG674247 602620212F1 NCI_CGAP_Skn... 1635 0.0
gi¦13961308¦gb¦BG696304.1¦BG696304 602659453F1 NCI_CGAP_Skn... 1614 0.0
gi¦14052781¦gb¦BG742128.1¦BG742128 602634002F1 NCI_CGAP_Skn... 1564 0.0
gi¦14052023¦gb¦BG741370.1¦BG741370 602631924F1 NCI_CGAP_Skn... 1562 0.0
gi¦13966183¦gb¦BG698667.1¦BG698667 602703031F1 NCI_CGAP_Skn... 1469 0.0
gi¦14051962¦gb¦BG741309.1¦BG741309 602634443F1 NCI_CGAP_Skn... 1437 0.0
gi¦13543809¦gb¦BG545364.1¦BG545364 602572590F1 NIH_MGC_77 H... 1382 0.0

gi|13964039|gb|BG697623.1|BG697623 602660865F1 NCI_CGAP_Skn... 1376 0.0
gi|13972710|gb|BG701903.1|BG701903 602683260F1 NIH_MGC_95 H... 1350 0.0
gi|13573357|gb|BG565704.1|BG565704 602589036F1 NIH_MGC_76 H... 1336 0.0
gi|9438885|gb|BE439403.1|BE439403 HTM1-018F1 HTM1 Homo sapi... 1255 0.0
gi|9872526|dbj|AV651512.1|AV651512 AV651512 GLC Homo sapien... 1223 0.0
gi|14053029|gb|BG742376.1|BG742376 602631760F1 NCI_CGAP_Skn... 1219 0.0
gi|11987203|gb|BF701795.1|BF701795 602129255F2 NIH_MGC_56 H... 1219 0.0
gi|13673667|gb|BG622296.1|BG622296 602646960F1 NIH_MGC_79 H... 1215 0.0
gi|13531288|gb|BG539055.1|BG539055 602568425F1 NIH_MGC_77 H... 1168 0.0
gi|10911141|dbj|AV753293.1|AV753293 AV753293 NPD Homo sapie... 1045 0.0
gi|12512467|gb|BG055093.1|BG055093 nac99e06.x1 NCI_CGAP_Pr2... 1039 0.0
gi|11984275|gb|BF698867.1|BF698867 602126436F1 NIH_MGC_56 H... 1021 0.0
gi|13670422|gb|BG619051.1|BG619051 602616588F1 NIH_MGC_79 H... 997 0.0
gi|14051178|gb|BG740525.1|BG740525 602633033F1 NCI_CGAP_Skn... 971 0.0
gi|9876959|dbj|AV655945.1|AV655945 AV655945 GLC Homo sapien... 957 0.0
gi|9872114|dbj|AV651100.1|AV651100 AV651100 GLC Homo sapien... 955 0.0
gi|9871963|dbj|AV650949.1|AV650949 AV650949 GLC Homo sapien... 955 0.0
gi|10291657|dbj|AV689794.1|AV689794 AV689794 GKC Homo sapie... 932 0.0
gi|9439140|gb|BE439658.1|BE439658 HTM1-325F HTM1 Homo sapie... 926 0.0
gi|3752813|gb|AI200207.1|AI200207 qf92a08.x1 Soares_placent... 902 0.0
gi|1679084|gb|AA121470.1|AA121470 zk91d05.r1 Soares_pregnan... 842 0.0
gi|1237760|gb|N75182.1|N75182 yz62g12.r1 Soares_multiple_sc... 827 0.0
gi|3645147|gb|AI139163.1|AI139163 qc23f09.x1 Soares_pregnan... 811 0.0

>gi|14776198|ref|XP_043103.1| hydroxysteroid (11-beta) dehydrogenase 2 [Homo sapiens]

EST Search :

Sequences producing significant alignments: (bits) Value

gi|12883011|emb|AL548215.1|AL548215 AL548215 LTI_NFL006_PL2... 1709 0.0
gi|12888948|emb|AL551216.1|AL551216 AL551216 LTI_NFL006_PL2... 1673 0.0
gi|12935463|emb|AL574858.1|AL574858 AL574858 LTI_NFL006_PL2... 1612 0.0
gi|12931533|emb|AL572859.1|AL572859 AL572859 LTI_NFL006_PL2... 1610 0.0
gi|14506196|gb|BI087866.1|BI087866 602852664F1 NIH_MGC_10 H... 1328 0.0
gi|12924205|emb|AL569153.1|AL569153 AL569153 LTI_FL002_PL1 ... 1201 0.0
gi|12894985|emb|AL554320.1|AL554320 AL554320 LTI_NFL006_PL2... 1197 0.0
gi|12444516|gb|BG003850.1|BG003850 MR3-GN0187-201100-010-g0... 1138 0.0
gi|5111814|gb|AI743526.1|AI743526 wf72c10.x2 Soares_NFL_T_G... 1126 0.0
gi|11767117|gb|BE963698.2|BE963698 601657032R1 NIH_MGC_67 H... 1078 0.0
gi|2280229|gb|AA535976.1|AA535976 nf95a05.s1 NCI_CGAP_Co3 H... 1017 0.0
gi|2278552|gb|AA534299.1|AA534299 nf73d11.s1 NCI_CGAP_Co3 H... 1015 0.0
gi|12446016|gb|BG004736.1|BG004736 MR3-GN0187-211100-009-f0... 1007 0.0
gi|12939828|emb|AL577064.1|AL577064 AL577064 LTI_NFL006_PL2... 981 0.0
gi|3840588|gb|AI245191.1|AI245191 qk22d10.x1 NCI_CGAP_Kid3 ... 963 0.0
gi|4111819|gb|AI360198.1|AI360198 qy84a11.x1 NCI_CGAP_Brn25... 924 0.0
gi|3057842|gb|AA917952.1|AA917952 ol68g12.s1 NCI_CGAP_Kid3 ... 918 0.0
gi|12441996|gb|BG002650.1|BG002650 MR3-GN0187-171100-003-c0... 910 0.0
gi|4329685|gb|AI476640.1|AI476640 tm23a04.x1 Soares_NFL_T_G... 890 0.0
gi|12758118|gb|BG248303.1|BG248303 602400339F1 NIH_MGC_15 H... 878 0.0
gi|1776122|gb|AA189088.1|AA189088 zq45c08.s1 Stratagene hNT... 874 0.0
gi|12393991|gb|BF987669.1|BF987669 QV0-GN0141-121000-433-a0... 866 0.0
gi|5128365|gb|AI750101.1|AI750101 at35h04.x1 Barstead colon... 866 0.0
gi|3801491|gb|AI219288.1|AI219288 qg18c11.x1 Soares_placent... 823 0.0
gi|14253306|gb|BG876216.1|BG876216 QV4-CT0361-140200-101-a0... 819 0.0
gi|13139762|gb|BG333324.1|BG333324 602431361F1 NIH_MGC_18 H... 817 0.0
gi|3679683|gb|AI151214.1|AI151214 qc73h09.x1 Soares_placent... 811 0.0
gi|3741199|gb|AI189990.1|AI189990 qd25a10.x1 Soares_placent... 803 0.0
gi|12401269|gb|BF994842.1|BF994842 QV0-GN0211-031100-471-a0... 795 0.0
gi|12162695|gb|BF822586.1|BF822586 CM2-RT0009-071200-604-a0... 793 0.0
gi|3595626|gb|AI127112.1|AI127112 qb98a09.x1 Soares_fetal_h... 793 0.0
gi|10893038|gb|BF087328.1|BF087328 QV2-HT0540-120900-356-b0... 787 0.0
gi|3307586|gb|AI050781.1|AI050781 ov12a05.x1 NCI_CGAP_Kid3 ... 787 0.0
gi|12370277|gb|BF953002.1|BF953002 QV3-NN0198-111100-373-f0... 765 0.0
gi|7956033|gb|AW860340.1|AW860340 RC0-CT0380-210300-035-g09... 757 0.0
gi|14385887|gb|BG983048.1|BG983048 IL5-CN0068-060301-381-d0... 749 0.0
gi|4568562|gb|AI582665.1|AI582665 tn16b05.x1 NCI_CGAP_Brn25... 737 0.0
gi|4567538|gb|AI581641.1|AI581641 as03f05.x1 Barstead colon... 726 0.0
gi|2694936|gb|AA693998.1|AA693998 zi48b09.s1 Soares_fetal_l... 724 0.0
gi|856647|gb|R80366.1|R80366 yi96g01.r1 Soares placenta Nb2... 724 0.0
gi|2716774|gb|AA706856.1|AA706856 zi21c10.s1 Soares_fetal_l... 720 0.0

>gi¦4504479¦ref¦NP_000851.1¦ hydroxyprostaglandin dehydrogenase 15-(NAD) [Homo sapiens]

EST Search:

Sequences producing significant alignments: (bits) Value

gi¦12874897¦emb¦AL542647.1¦AL542647 AL542647 LTI_FL002_PL1 ... 1931 0.0
gi¦12925069¦emb¦AL569585.1¦AL569585 AL569585 LTI_FL002_PL1 ... 1905 0.0
gi¦12873492¦emb¦AL541940.1¦AL541940 AL541940 LTI_FL002_PL1 ... 1877 0.0
gi¦12875081¦emb¦AL542740.1¦AL542740 AL542740 LTI_FL002_PL1 ... 1855 0.0
gi¦10932989¦dbj¦AU117975.1¦AU117975 AU117975 HEMBA1 Homo sa... 1419 0.0
gi¦10995644¦dbj¦AU135105.1¦AU135105 AU135105 PLACE1 Homo sa... 1415 0.0
gi¦10996543¦dbj¦AU136004.1¦AU136004 AU136004 PLACE1 Homo sa... 1409 0.0
gi¦13040302¦gb¦BG286949.1¦BG286949 602382834F1 NIH_MGC_93 H... 1400 0.0
gi¦11001299¦dbj¦AU139778.1¦AU139778 AU139778 PLACE1 Homo sa... 1388 0.0
gi¦10997253¦dbj¦AU136714.1¦AU136714 AU136714 PLACE1 Homo sa... 1382 0.0
gi¦13669926¦gb¦BG618555.1¦BG618555 602645464F2 NIH_MGC_76 H... 1364 0.0
gi¦13578224¦gb¦BG570571.1¦BG570571 602591255F1 NIH_MGC_77 H... 1354 0.0
gi¦10996695¦dbj¦AU136156.1¦AU136156 AU136156 PLACE1 Homo sa... 1354 0.0
gi¦10995511¦dbj¦AU134972.1¦AU134972 AU134972 PLACE1 Homo sa... 1354 0.0
gi¦10997831¦dbj¦AU137292.1¦AU137292 AU137292 PLACE1 Homo sa... 1352 0.0
gi¦13039192¦gb¦BG286372.1¦BG286372 602383144F1 NIH_MGC_93 H... 1350 0.0
gi¦13048908¦gb¦BG291198.1¦BG291198 602388639F1 NIH_MGC_93 H... 1344 0.0
gi¦13546833¦gb¦BG548168.1¦BG548168 602575324F1 NIH_MGC_77 H... 1342 0.0
gi¦10999798¦dbj¦AU138277.1¦AU138277 AU138277 PLACE1 Homo sa... 1340 0.0
gi¦14048877¦gb¦BG778560.1¦BG778560 602668005F1 NIH_MGC_60 H... 1338 0.0
gi¦13574910¦gb¦BG567257.1¦BG567257 602589738F1 NIH_MGC_76 H... 1330 0.0
gi¦13715496¦gb¦BG193809.1¦BG193809 RST12945 Athersys RAGE L... 1330 0.0
gi¦12924251¦emb¦AL569176.1¦AL569176 AL569176 LTI_FL002_PL1 ... 1328 0.0
gi¦10998094¦dbj¦AU137555.1¦AU137555 AU137555 PLACE1 Homo sa... 1320 0.0
gi¦13572596¦gb¦BG564943.1¦BG564943 602583911F1 NIH_MGC_76 H... 1310 0.0
gi¦13528136¦gb¦BG536590.1¦BG536590 602566204F1 NIH_MGC_77 H... 1298 0.0
gi¦13044260¦gb¦BG288929.1¦BG288929 602383878F1 NIH_MGC_93 H... 1296 0.0
gi¦11000464¦dbj¦AU138943.1¦AU138943 AU138943 PLACE1 Homo sa... 1292 0.0
gi¦10997016¦dbj¦AU136477.1¦AU136477 AU136477 PLACE1 Homo sa... 1289 0.0
gi¦10151099¦gb¦BE737107.1¦BE737107 601304459F1 NIH_MGC_39 H... 1281 0.0
gi¦11000653¦dbj¦AU139132.1¦AU139132 AU139132 PLACE1 Homo sa... 1279 0.0
gi¦13039746¦gb¦BG286666.1¦BG286666 602381684F1 NIH_MGC_93 H... 1267 0.0
gi¦10932798¦dbj¦AU117801.1¦AU117801 AU117801 HEMBA1 Homo sa... 1261 0.0
gi¦10995272¦dbj¦AU134733.1¦AU134733 AU134733 PLACE1 Homo sa... 1253 0.0
gi¦13049252¦gb¦BG291389.1¦BG291389 602387263F1 NIH_MGC_93 H... 1235 0.0
gi¦13045000¦gb¦BG289298.1¦BG289298 602387415F1 NIH_MGC_93 H... 1233 0.0
gi¦11001529¦dbj¦AU140008.1¦AU140008 AU140008 PLACE1 Homo sa... 1231 0.0
gi¦13044292¦gb¦BG288945.1¦BG288945 602383896F1 NIH_MGC_93 H... 1223 0.0
gi¦10997197¦dbj¦AU136658.1¦AU136658 AU136658 PLACE1 Homo sa... 1221 0.0
gi¦10996351¦dbj¦AU135812.1¦AU135812 AU135812 PLACE1 Homo sa... 1219 0.0
gi¦14050602¦gb¦BG739949.1¦BG739949 602630904F1 NCI_CGAP_Skn... 1213 0.0
gi¦13521654¦gb¦BG530117.1¦BG530117 602558603F1 NIH_MGC_61 H... 1211 0.0
gi¦13294287¦gb¦BG400839.1¦BG400839 602464062F1 NIH_MGC_75 H... 1193 0.0
gi¦10996117¦dbj¦AU135578.1¦AU135578 AU135578 PLACE1 Homo sa... 1187 0.0
gi¦10995111¦dbj¦AU134572.1¦AU134572 AU134572 PLACE1 Homo sa... 1187 0.0
gi¦13416849¦gb¦BG484570.1¦BG484570 602505736F1 NIH_MGC_77 H... 1185 0.0
gi¦13342897¦gb¦BG436391.1¦BG436391 602509051F1 NIH_MGC_79 H... 1183 0.0
gi¦12934190¦emb¦AL574206.1¦AL574206 AL574206 LTI_NFL006_PL2... 1183 0.0
gi¦13340956¦gb¦BG434450.1¦BG434450 602506473F1 NIH_MGC_79 H... 1156 0.0
gi¦13342591¦gb¦BG436085.1¦BG436085 602508877F1 NIH_MGC_79 H... 1154 0.0

gi|13460521|gb|BG498991.1|BG498991 602544679F1 NIH_MGC_60 H... 1152 0.0
gi|9324951|gb|BE379586.1|BE379586 601159319T1 NIH_MGC_53 Ho... 1150 0.0
gi|4153537|gb|AI373671.1|AI373671 qz53h05.x1 NCI_CGAP_Kid11... 1148 0.0
gi|13416352|gb|BG484073.1|BG484073 602504677F1 NIH_MGC_77 H... 1146 0.0
gi|12938589|emb|AL576441.1|AL576441 AL576441 LTI_NFL006_PL2... 1146 0.0
gi|10997472|dbj|AU136933.1|AU136933 AU136933 PLACE1 Homo sa... 1136 0.0
gi|13041924|gb|BG287765.1|BG287765 602384115F1 NIH_MGC_93 H... 1134 0.0
gi|13530725|gb|BG538492.1|BG538492 602567213F1 NIH_MGC_77 H... 1132 0.0
gi|13545497|gb|BG546832.1|BG546832 602574013F1 NIH_MGC_77 H... 1124 0.0
gi|13415427|gb|BG483148.1|BG483148 602503084F1 NIH_MGC_77 H... 1122 0.0
gi|10141065|gb|BE727073.1|BE727073 601563751F1 NIH_MGC_20 H... 1120 0.0
gi|13673902|gb|BG622531.1|BG622531 602647264F1 NIH_MGC_79 H... 1118 0.0
gi|9325374|gb|BE380009.1|BE380009 601159319F2 NIH_MGC_53 Ho... 1118 0.0
gi|10995892|dbj|AU135353.1|AU135353 AU135353 PLACE1 Homo sa... 1094 0.0
gi|10142996|gb|BE729004.1|BE729004 601562266F1 NIH_MGC_20 H... 1090 0.0
gi|13341323|gb|BG434817.1|BG434817 602507341F1 NIH_MGC_79 H... 1084 0.0
gi|4850556|gb|AI670825.1|AI670825 wa04f11.x1 NCI_CGAP_Kid11... 1084 0.0
gi|9810249|gb|BE566425.1|BE566425 601340150F1 NIH_MGC_53 Ho... 1070 0.0
gi|6658819|gb|AW271789.1|AW271789 xs18d09.x1 NCI_CGAP_Kid11... 1067 0.0
gi|4738059|gb|AI654080.1|AI654080 ty61e04.x1 NCI_CGAP_Kid11... 1067 0.0
gi|11081229|gb|BF194909.1|BF194909 7o90b11.x1 NCI_CGAP_Kid1... 1061 0.0
gi|12934146|emb|AL574184.1|AL574184 AL574184 LTI_NFL006_PL2... 1059 0.0
gi|12769742|gb|BG259926.1|BG259926 602371888F1 NIH_MGC_93 H... 1053 0.0
gi|10372563|gb|BE857988.1|BE857988 7f73g06.x1 Soares_NSF_F8... 1053 0.0
gi|13544140|gb|BG545475.1|BG545475 602572711F1 NIH_MGC_77 H... 1039 0.0
gi|11001068|dbj|AU139547.1|AU139547 AU139547 PLACE1 Homo sa... 1039 0.0
gi|5812803|gb|AI985526.1|AI985526 ws08f05.x1 NCI_CGAP_Kid11... 1039 0.0
gi|9810998|gb|BE567278.1|BE567278 601340881F1 NIH_MGC_53 Ho... 1027 0.0
gi|13712893|gb|BG191206.1|BG191206 RST10293 Athersys RAGE L... 1023 0.0
gi|11001465|dbj|AU139944.1|AU139944 AU139944 PLACE1 Homo sa... 1021 0.0
gi|9509268|gb|BE463495.1|BE463495 hw24c08.x1 NCI_CGAP_Kid11... 1011 0.0
gi|5100597|gb|AI738616.1|AI738616 wi11b03.x1 NCI_CGAP_Co16 ... 1005 0.0
gi|10315127|gb|BE866442.1|BE866442 601678681F1 NIH_MGC_53 H... 997 0.0
gi|11017265|dbj|AU155744.1|AU155744 AU155744 PLACE1 Homo sa... 991 0.0
gi|10997723|dbj|AU137184.1|AU137184 AU137184 PLACE1 Homo sa... 987 0.0
gi|13342905|gb|BG436399.1|BG436399 602509061F1 NIH_MGC_79 H... 965 0.0
gi|10735967|gb|BF028255.1|BF028255 601765033F1 NIH_MGC_53 H... 957 0.0
gi|13673548|gb|BG622177.1|BG622177 602646815F1 NIH_MGC_79 H... 954 0.0
gi|6576242|gb|AW242488.1|AW242488 xm99e10.x1 NCI_CGAP_Kid11... 948 0.0
gi|4334187|gb|AI472097.1|AI472097 tj80e11.x1 Soares_NSF_F8_... 944 0.0
gi|11155126|gb|BF241201.1|BF241201 601880081F1 NIH_MGC_55 H... 940 0.0
gi|2834557|gb|AA775223.1|AA775223 ac79e08.s1 Stratagene lun... 940 0.0
gi|13342718|gb|BG436212.1|BG436212 602508629F1 NIH_MGC_79 H... 936 0.0
gi|12893004|emb|AL553299.1|AL553299 AL553299 LTI_NFL006_PL2... 936 0.0
gi|3888220|gb|AI269053.1|AI269053 qi24f07.x1 Soares_NhHMPu_... 930 0.0
gi|12041908|gb|BF725997.1|BF725997 bx22g02.y1 Human Iris cD... 926 0.0
gi|10996590|dbj|AU136051.1|AU136051 AU136051 PLACE1 Homo sa... 920 0.0
gi|10735132|gb|BF027420.1|BF027420 601672490F1 NIH_MGC_20 H... 920 0.0
gi|11000958|dbj|AU139437.1|AU139437 AU139437 PLACE1 Homo sa... 916 0.0
gi|10584213|gb|BE971156.1|BE971156 601651108F1 NIH_MGC_81 H... 914 0.0

>gi|7705925|ref|NP_057370.1| carbonyl reductase [Homo sapiens]

EST Search:

Sequences producing significant alignments: (bits) Value

gi|13413874|gb|BG481595.1|BG481595 602528316F1 NIH_MGC_21 H... 1511 0.0
gi|14178945|gb|BG831358.1|BG831358 602766220F1 NIH_MGC_42 H... 1491 0.0
gi|14177680|gb|BG830093.1|BG830093 602764845F1 NIH_MGC_42 H... 1491 0.0
gi|13404430|gb|BG472244.1|BG472244 602513756F1 NIH_MGC_16 H... 1443 0.0
gi|14568476|gb|BI117575.1|BI117575 602866754F1 NIH_MGC_7 Ho... 1419 0.0
gi|13982131|gb|BG706614.1|BG706614 602674104F1 NIH_MGC_96 H... 1380 0.0
gi|13976241|gb|BG703674.1|BG703674 602686647F1 NIH_MGC_95 H... 1368 0.0
gi|10390490|gb|BE901372.1|BE901372 601674675F1 NIH_MGC_21 H... 1354 0.0
gi|12343809|gb|BF976594.1|BF976594 602244271F1 NIH_MGC_48 H... 1326 0.0
gi|11641972|gb|BF568592.1|BF568592 602184218F1 NIH_MGC_42 H... 1326 0.0
gi|11970704|gb|BF685296.1|BF685296 602141648F1 NIH_MGC_46 H... 1304 0.0
gi|11252161|gb|BF305282.1|BF305282 601892747F1 NIH_MGC_17 H... 1304 0.0
gi|11098442|gb|BF204856.1|BF204856 601867158F1 NIH_MGC_17 H... 1300 0.0
gi|9137251|gb|BE263706.1|BE263706 601192146F1 NIH_MGC_7 Hom... 1279 0.0
gi|10404479|gb|BE909167.1|BE909167 601501782F1 NIH_MGC_70 H... 1277 0.0
gi|11151599|gb|BF237681.1|BF237681 601841865F1 NIH_MGC_46 H... 1275 0.0
gi|9156256|gb|BE281240.1|BE281240 601155341F1 NIH_MGC_21 Ho... 1275 0.0
gi|12342418|gb|BF975203.1|BF975203 602244705F1 NIH_MGC_48 H... 1269 0.0
gi|14058856|gb|BG748203.1|BG748203 602705827F1 NIH_MGC_43 H... 1263 0.0
gi|11263622|gb|BF315274.1|BF315274 601902672F1 NIH_MGC_19 H... 1239 0.0
gi|11098117|gb|BF204531.1|BF204531 601868138F1 NIH_MGC_17 H... 1237 0.0
gi|9133208|gb|BE313377.1|BE313377 601147921F1 NIH_MGC_19 Ho... 1237 0.0
gi|12683322|gb|BG176619.1|BG176619 602313206F1 NIH_MGC_85 H... 1235 0.0
gi|9882826|dbj|AV661812.1|AV661812 AV661812 GLC Homo sapien... 1233 0.0
gi|12615652|gb|BG122143.1|BG122143 602349585F1 NIH_MGC_90 H... 1227 0.0
gi|11251336|gb|BF304588.1|BF304588 601887980F1 NIH_MGC_17 H... 1199 0.0
gi|4536632|gb|AI573258.1|AI573258 tn03e05.x1 NCI_CGAP_Brn25... 1197 0.0
gi|13032709|gb|BG283133.1|BG283133 602406785F1 NIH_MGC_91 H... 1195 0.0
gi|10346623|gb|BE889373.1|BE889373 601513264F1 NIH_MGC_71 H... 1189 0.0
gi|13137904|gb|BG331552.1|BG331552 602433326F1 NIH_MGC_18 H... 1187 0.0
gi|8167102|gb|AW975880.1|AW975880 EST387989 MAGE resequence... 1185 0.0
gi|9155643|gb|BE280635.1|BE280635 601155778F1 NIH_MGC_21 Ho... 1183 0.0
gi|11258150|gb|BF310575.1|BF310575 601895295F2 NIH_MGC_19 H... 1174 0.0
gi|8147508|gb|AW957825.1|AW957825 EST369895 MAGE resequence... 1158 0.0
gi|13340715|gb|BG434209.1|BG434209 602506154F1 NIH_MGC_79 H... 1128 0.0
gi|10216172|gb|BE794974.1|BE794974 601589746F1 NIH_MGC_7 Ho... 1118 0.0
gi|11949082|gb|BF675187.1|BF675187 602138110F1 NIH_MGC_83 H... 1116 0.0
gi|8147585|gb|AW957902.1|AW957902 EST369972 MAGE resequence... 1112 0.0
gi|14620169|gb|BI160168.1|BI160168 602864026F1 NIH_MGC_42 H... 1104 0.0
gi|4194952|gb|AI382182.1|AI382182 te70b01.x1 Soares_NFL_T_G... 1098 0.0
gi|6588561|gb|AW245568.1|AW245568 2822726.5prime NIH_MGC_7 ... 1092 0.0
gi|11617689|gb|BF530338.1|BF530338 602071618F1 NCI_CGAP_Brn... 1082 0.0
gi|9137978|gb|BE264422.1|BE264422 601191730F1 NIH_MGC_7 Hom... 1080 0.0
gi|6588571|gb|AW245578.1|AW245578 2822726.3prime NIH_MGC_7 ... 1072 0.0
gi|14320386|gb|BG925863.1|BG925863 HNC21-1-B11.R HNC (Human... 1068 0.0
gi|2726589|gb|AA714315.1|AA714315 nw06c05.s1 NCI_CGAP_SS1 H... 1027 0.0
gi|2537901|gb|AA625514.1|AA625514 af72e06.r1 Soares_NhHMPu_... 1023 0.0
gi|1211129|gb|N63300.1|N63300 yy71a11.s1 Soares_multiple_sc... 1021 0.0
gi|2155441|gb|AA442766.1|AA442766 zv60c08.s1 Soares_testis_... 1019 0.0
gi|1148734|gb|N30214.1|N30214 yw83h09.s1 Soares_placenta_8t... 1017 0.0
gi|13137575|gb|BG331137.1|BG331137 602431839F1 NIH_MGC_18 H... 1013 0.0

gi|9866354|dbj|AV645340.1|AV645340 AV645340 GLA Homo sapien... 1011 0.0
gi|2464707|gb|AA613669.1|AA613669 no39h10.s1 NCI_CGAP_Pr23 ... 1009 0.0
gi|12412330|gb|BG025585.1|BG025585 602274505F1 NIH_MGC_85 H... 997 0.0
gi|9882981|dbj|AV661967.1|AV661967 AV661967 GLC Homo sapien... 997 0.0
gi|14058983|gb|BG748330.1|BG748330 602706579F1 NIH_MGC_43 H... 991 0.0
gi|3230271|gb|AI015935.1|AI015935 ov26c11.x1 Soares_testis_... 989 0.0
gi|6399823|gb|AW168298.1|AW168298 xg62g11.x1 NCI_CGAP_Ut4 H... 987 0.0
gi|2243999|gb|AA507560.1|AA507560 ng88h09.s1 NCI_CGAP_Pr6 H... 977 0.0
gi|3840076|gb|AI244679.1|AI244679 qj97c09.x1 NCI_CGAP_Kid3 ... 973 0.0
gi|5838015|gb|AI991112.1|AI991112 wu38c07.x1 Soares_Dieckgr... 969 0.0
gi|9140017|gb|BE266440.1|BE266440 601193195F1 NIH_MGC_7 Hom... 965 0.0
gi|10216094|gb|BE794896.1|BE794896 601589638F1 NIH_MGC_7 Ho... 954 0.0
gi|1210879|gb|N63050.1|N63050 yy70g11.s1 Soares_multiple_sc... 938 0.0
gi|8750451|gb|BE207053.1|BE207053 ba09d08.y1 NIH_MGC_7 Homo... 936 0.0
gi|10144813|gb|BE730821.1|BE730821 601570791F1 NIH_MGC_21 H... 934 0.0
gi|5395010|gb|AI808444.1|AI808444 wf94h12.x1 Soares_NSF_F8_... 930 0.0
gi|10813709|dbj|AV716557.1|AV716557 AV716557 DCB Homo sapie... 926 0.0
gi|2883312|gb|AA813327.1|AA813327 ai81a07.s1 Soares_testis_... 920 0.0
gi|1193558|gb|N52392.1|N52392 yv49g09.s1 Soares fetal liver... 910 0.0
gi|2138860|gb|AA433946.1|AA433946 zw52g09.s1 Soares_total_f... 900 0.0
gi|4489892|gb|AI557529.1|AI557529 pt2.1-06.D05.r tumor2 Hom... 896 0.0
gi|11955171|gb|BF681276.1|BF681276 602155553F1 NIH_MGC_83 H... 894 0.0
gi|5591001|gb|AI885837.1|AI885837 wl62c01.x1 NCI_CGAP_Brn25... 894 0.0
gi|12431844|gb|BG036553.1|BG036553 602326326F1 NIH_MGC_91 H... 892 0.0
gi|2221812|gb|AA492250.1|AA492250 ng79d12.s1 NCI_CGAP_Pr6 H... 888 0.0
gi|3803259|gb|AI221056.1|AI221056 qg09c12.x1 Soares_placent... 886 0.0
gi|3422302|gb|AI083879.1|AI083879 qf22c05.x1 NCI_CGAP_Brn25... 886 0.0
gi|2159247|gb|AA446582.1|AA446582 zw84d08.s1 Soares_total_f... 874 0.0
gi|2341742|gb|AA568688.1|AA568688 nm06f08.s1 NCI_CGAP_Co10 ... 868 0.0
gi|4833888|gb|AI669114.1|AI669114 wb80e10.x1 NCI_CGAP_Pr28 ... 858 0.0
gi|10293455|dbj|AV691592.1|AV691592 AV691592 GKC Homo sapie... 854 0.0
gi|1965893|gb|AA313563.1|AA313563 EST185441 Colon carcinoma... 846 0.0
gi|3988221|gb|AI304532.1|AI304532 qo55a06.x1 NCI_CGAP_Co8 H... 844 0.0
gi|2731990|gb|AA720021.1|AA720021 zh22e05.s1 Soares_pineal_... 842 0.0
gi|7316134|gb|AW615416.1|AW615416 ba09d08.x1 NIH_MGC_7 Homo... 833 0.0
gi|9875231|dbj|AV654217.1|AV654217 AV654217 GLC Homo sapien... 831 0.0
gi|4598919|gb|AI589871.1|AI589871 tm81d01.x1 NCI_CGAP_Brn25... 823 0.0
gi|4489893|gb|AI557530.1|AI557530 pt2.1-06.D05b.r tumor2 Ho... 823 0.0
gi|9874547|dbj|AV653533.1|AV653533 AV653533 GLC Homo sapien... 803 0.0
gi|3988144|gb|AI304455.1|AI304455 qo54a10.x1 NCI_CGAP_Co8 H... 801 0.0

>gi|4503817|ref|NP_002026.1| follicular lymphoma variant translocation 1 [Homo sapiens]

EST Search:

Sequences producing significant alignments: (bits) Value

gi|12783826|emb|AL520333.1|AL520333 AL520333 LTI_NFL004_NBC... 1647 0.0
gi|10936759|dbj|AU121524.1|AU121524 AU121524 MAMMA1 Homo sa... 1628 0.0
gi|13913049|gb|BG681652.1|BG681652 602627957F1 NCI_CGAP_Skn... 1477 0.0
gi|12893255|emb|AL553429.1|AL553429 AL553429 LTI_NFL006_PL2... 1360 0.0
gi|11000513|dbj|AU138992.1|AU138992 AU138992 PLACE1 Homo sa... 1326 0.0
gi|10994408|dbj|AU133869.1|AU133869 AU133869 OVARC1 Homo sa... 1316 0.0
gi|14063903|gb|BG753250.1|BG753250 602731650F1 NIH_MGC_43 H... 1281 0.0

gi|12383693|gb|BF980881.1|BF980881 602304095F1 NIH_MGC_88 H... 1275 0.0
gi|13049086|gb|BG291280.1|BG291280 602388439F1 NIH_MGC_93 H... 1265 0.0
gi|13289457|gb|BG396009.1|BG396009 602458738F1 NIH_MGC_16 H... 1223 0.0
gi|13999988|gb|BG720801.1|BG720801 602692025F1 NIH_MGC_97 H... 1203 0.0
gi|10293319|dbj|AV691456.1|AV691456 AV691456 GKC Homo sapie... 1130 0.0
gi|10936667|dbj|AU121432.1|AU121432 AU121432 MAMMA1 Homo sa... 1126 0.0
gi|14511044|gb|BI092714.1|BI092714 602858508F1 NIH_MGC_10 H... 1090 0.0
gi|13526132|gb|BG534590.1|BG534590 602553441F1 NIH_MGC_77 H... 1090 0.0
gi|10995473|dbj|AU134934.1|AU134934 AU134934 PLACE1 Homo sa... 1045 0.0
gi|8278290|gb|BE018271.1|BE018271 bb77h08.y1 NIH_MGC_12 Hom... 1009 0.0
gi|9347181|gb|BE410731.1|BE410731 601301615F1 NIH_MGC_21 Ho... 1001 0.0
gi|14439727|gb|BI033101.1|BI033101 MR4-NN0205-310101-201-d0... 989 0.0
gi|13994779|gb|BG715592.1|BG715592 602675925F1 NIH_MGC_96 H... 977 0.0
gi|14439726|gb|BI033100.1|BI033100 MR4-NN0205-310101-201-d0... 975 0.0
gi|1358334|gb|W56476.1|W56476 zc59b03.r1 Soares_parathyroid... 965 0.0
gi|10202721|gb|BE781523.1|BE781523 601467126F1 NIH_MGC_67 H... 959 0.0
gi|13905677|gb|BG674281.1|BG674281 602620250F1 NCI_CGAP_Skn... 950 0.0
gi|11285372|gb|BF338952.1|BF338952 602036022F1 NCI_CGAP_Brn... 912 0.0
gi|2788091|gb|AA748133.1|AA748133 nx79h02.s1 NCI_CGAP_Ew1 H... 912 0.0
gi|9512306|gb|BE466531.1|BE466531 hz21h07.x1 NCI_CGAP_GC6 H... 910 0.0.
gi|11686102|gb|BF593778.1|BF593778 nac08h08.x1 NCI_CGAP_Brn... 876 0.0
gi|11016564|dbj|AU155043.1|AU155043 AU155043 OVARC1 Homo sa... 876 0.0
gi|9185496|gb|BE301748.1|BE301748 bb77h08.x1 NIH_MGC_12 Hom... 876 0.0
gi|5397891|gb|AI811325.1|AI811325 tw38d08.x1 NCI_CGAP_Ut1 H... 876 0.0
gi|4176027|gb|AI376037.1|AI376037 ta57h08.x1 Soares_total_f... 876 0.0
gi|2933339|gb|AA845580.1|AA845580 ak04f02.s1 Soares_parathy... 876 0.0
gi|5132786|gb|AI754522.1|AI754522 cr26d08.x1 Jia bone marro... 870 0.0
gi|4113305|gb|AI361684.1|AI361684 qy90h03.x1 NCI_CGAP_Brn25... 868 0.0
gi|3959459|gb|AI300113.1|AI300113 qn59h09.x1 NCI_CGAP_Kid5 ... 868 0.0
gi|3601540|gb|AI131524.1|AI131524 qc13h09.x1 Soares_fetal_h... 868 0.0
gi|2336669|gb|AA565030.1|AA565030 nj11g07.s1 NCI_CGAP_Pr22 ... 868 0.0
gi|2265380|gb|AA524452.1|AA524452 ng45b01.s1 NCI_CGAP_Co3 H... 868 0.0
gi|12336897|gb|BF969682.1|BF969682 602272067F1 NIH_MGC_84 H... 862 0.0
gi|3596148|gb|AI127634.1|AI127634 qc30f11.x1 Soares_pregnan... 862 0.0
gi|4264050|gb|AI418119.1|AI418119 tf73h07.x1 NCI_CGAP_Brn23... 860 0.0
gi|3934574|gb|AI291800.1|AI291800 qm75d07.x1 Soares_placent... 860 0.0
gi|5133017|gb|AI754753.1|AI754753 cr29f09.x1 Jia bone marro... 858 0.0
gi|1157254|gb|N36112.1|N36112 yy32f04.s1 Soares melanocyte ... 854 0.0
gi|6200565|gb|AW152665.1|AW152665 xf77g03.x1 NCI_CGAP_Gas4 ... 852 0.0
gi|3110443|gb|AA947048.1|AA947048 oq57d09.s1 NCI_CGAP_Kid6 ... 852 0.0
gi|11008839|dbj|AU147318.1|AU147318 AU147318 MAMMA1 Homo sa... 850 0.0
gi|5854880|gb|AW006102.1|AW006102 wz92d03.x1 NCI_CGAP_Brn25... 850 0.0
gi|6463721|gb|AW189265.1|AW189265 xl03f02.x1 NCI_CGAP_Ut4 H... 848 0.0
gi|9873394|dbj|AV652380.1|AV652380 AV652380 GLC Homo sapien... 842 0.0
gi|1219078|gb|N66953.1|N66953 za48g10.s1 Soares fetal liver... 842 0.0
gi|3844217|gb|AI248820.1|AI248820 qh72e03.x1 Soares_fetal_l... 829 0.0
gi|7038930|gb|AW468824.1|AW468824 hd28f02.x1 Soares_NFL_T_G... 821 0.0
gi|3752125|gb|AI199519.1|AI199519 qi56h10.x1 NCI_CGAP_Brn25... 819 0.0
gi|11017247|dbj|AU155726.1|AU155726 AU155726 PLACE1 Homo sa... 817 0.0
gi|10314879|gb|BE866103.1|BE866103 601679103F1 NIH_MGC_53 H... 817 0.0
gi|1350226|gb|W52783.1|W52783 zd13h07.r1 Soares_fetal_heart... 813 0.0
gi|3429339|gb|AI090280.1|AI090280 qb28f11.x1 Soares_pregnan... 809 0.0
gi|1156184|gb|N35042.1|N35042 yy17e01.s1 Soares melanocyte ... 807 0.0
gi|4153051|gb|AI373185.1|AI373185 qz13e06.x1 NCI_CGAP_CLL1 ... 803 0.0

>gi|4503891|ref|NP_000394.1| UDP-galactose-4-epimerase; UDP galactose-4-epimerase; galactowaldenase [Homo sapiens]

EST Search:

Sequences producing significant alignments: (bits) Value

gi|12899882|emb|AL556844.1|AL556844 AL556844 LTI_NFL006_PL2... 1739 0.0
gi|12943580|emb|AL578982.1|AL578982 AL578982 LTI_NFL006_PL2... 1699 0.0
gi|12791395|emb|AL527902.1|AL527902 AL527902 LTI_NFL003_NBC... 1657 0.0
gi|12935014|emb|AL574629.1|AL574629 AL574629 LTI_NFL006_PL2... 1643 0.0
gi|12884919|emb|AL549184.1|AL549184 AL549184 LTI_NFL006_PL2... 1570 0.0
gi|12800245|emb|AL536752.1|AL536752 AL536752 LTI_FL013_FBm... 1554 0.0
gi|13582317|gb|BG574664.1|BG574664 602596666F1 NIH_MGC_87 H... 1475 0.0
gi|13401772|gb|BG469497.1|BG469497 602532809F1 NIH_MGC_15 H... 1457 0.0
gi|13909656|gb|BG678259.1|BG678259 602624574F1 NCI_CGAP_Skn... 1443 0.0
gi|12759023|gb|BG249207.1|BG249207 602361637F1 NIH_MGC_89 H... 1404 0.0
gi|12787709|emb|AL524216.1|AL524216 AL524216 LTI_NFL003_NBC... 1394 0.0
gi|10146723|gb|BE732731.1|BE732731 601565201F1 NIH_MGC_21 H... 1386 0.0
gi|12918864|emb|AL566474.1|AL566474 AL566474 LTI_FL013_FBm... 1380 0.0
gi|10141023|gb|BE727031.1|BE727031 601563701F1 NIH_MGC_20 H... 1378 0.0
gi|12419290|gb|BG030193.1|BG030193 602297382F1 NIH_MGC_87 H... 1372 0.0
gi|12601828|gb|BG107982.1|BG107982 602278281F1 NIH_MGC_86 H... 1370 0.0
gi|12793968|emb|AL530475.1|AL530475 AL530475 LTI_NFL001_NBC... 1362 0.0
gi|12426779|gb|BG033962.1|BG033962 602301070F1 NIH_MGC_87 H... 1330 0.0
gi|13144832|gb|BG338394.1|BG338394 602436183F1 NIH_MGC_46 H... 1324 0.0
gi|14505450|gb|BI087120.1|BI087120 602850790F1 NIH_MGC_10 H... 1306 0.0
gi|13461976|gb|BG500459.1|BG500459 602544981F1 NIH_MGC_60 H... 1304 0.0
gi|13140715|gb|BG334277.1|BG334277 602461781F1 NIH_MGC_20 H... 1298 0.0
gi|3087051|gb|AA932009.1|AA932009 om84a11.s1 NCI_CGAP_Kid3 ... 1287 0.0
gi|10144377|gb|BE730385.1|BE730385 601563872F1 NIH_MGC_20 H... 1279 0.0
gi|13328160|gb|BG421654.1|BG421654 602449748F1 NIH_MGC_14 H... 1277 0.0
gi|5768204|gb|AI971378.1|AI971378 wr04a10.x1 NCI_CGAP_GC6 H... 1261 0.0
gi|10142036|gb|BE728044.1|BE728044 601561335F1 NIH_MGC_20 H... 1249 0.0
gi|12913462|emb|AL563756.1|AL563756 AL563756 LTI_NFL001_NBC... 1247 0.0
gi|12788023|emb|AL524530.1|AL524530 AL524530 LTI_NFL003_NBC... 1241 0.0
gi|14061340|gb|BG750674.1|BG750674 602708562F1 NIH_MGC_43 H... 1223 0.0
gi|2823895|gb|AA772112.1|AA772112 ai40b11.s1 Soares_parathy... 1203 0.0
gi|12932776|emb|AL573485.1|AL573485 AL573485 LTI_NFL006_PL2... 1201 0.0
gi|3959421|gb|AI300075.1|AI300075 qn59e05.x1 NCI_CGAP_Kid5 ... 1183 0.0
gi|14507383|gb|BI089053.1|BI089053 602853414F1 NIH_MGC_10 H... 1178 0.0

gi|11098747|gb|BF205161.1|BF205161 601866902F1 NIH_MGC_17 H... 1174 0.0
gi|4764219|gb|AI660636.1|AI660636 wf23a09.x1 Soares_Dieckgr... 1166 0.0
gi|14071426|gb|BG760786.1|BG760786 602717144F1 NIH_MGC_49 H... 1162 0.0
gi|4328802|gb|AI475757.1|AI475757 tc94a04.x1 NCI_CGAP_CLL1 ... 1140 0.0
gi|2348271|gb|AA573756.1|AA573756 nk07c02.s1 NCI_CGAP_Co2 H... 1124 0.0
gi|2409414|gb|AA594064.1|AA594064 nn16g10.s1 NCI_CGAP_Co12 ... 1088 0.0
gi|9334109|gb|BE388744.1|BE388744 601283824F1 NIH_MGC_44 Ho... 1084 0.0
gi|14255590|gb|BG878500.1|BG878500 RC1-UM0047-290200-011-b0... 1072 0.0
gi|2409413|gb|AA594063.1|AA594063 nn16g09.s1 NCI_CGAP_Co12 ... 1067 0.0
gi|11253252|gb|BF306167.1|BF306167 601893016F1 NIH_MGC_17 H... 1059 0.0
gi|11107300|gb|BF213714.1|BF213714 601847578F1 NIH_MGC_55 H... 1053 0.0
gi|9331897|gb|BE386532.1|BE386532 601273783F1 NIH_MGC_20 Ho... 1051 0.0
gi|6037026|gb|AW081874.1|AW081874 xb56d11.x1 NCI_CGAP_Eso2 ... 1051 0.0
gi|5765666|gb|AI968848.1|AI968848 wt93g02.x1 NCI_CGAP_GC6 H... 1037 0.0

gi|13038030|gb|BG285754.1|BG285754 602380818F1 NIH_MGC_93 H... 1035 0.0
gi|12791394|emb|AL527901.1|AL527901 AL527901 LTI_NFL003_NBC... 1023 0.0
gi|9888038|gb|BE617100.1|BE617100 601441635F1 NIH_MGC_65 Ho... 1013 0.0
gi|4618533|gb|AI609366.1|AI609366 tw30g01.x1 NCI_CGAP_Ov35 ... 1007 0.0
gi|9330183|gb|BE384818.1|BE384818 601276175F1 NIH_MGC_20 Ho... 995 0.0
gi|6131515|gb|AW129910.1|AW129910 xf25a03.x1 NCI_CGAP_Kid8 ... 993 0.0
gi|14079219|gb|BG768566.1|BG768566 602742063F1 NIH_MGC_49 H... 991 0.0
gi|8139993|gb|AW950343.1|AW950343 EST362413 MAGE resequence... 985 0.0
gi|6198635|gb|AW150737.1|AW150737 xg38e05.x1 NCI_CGAP_Ut1 H... 979 0.0
gi|5436394|gb|AI817315.1|AI817315 wk36f10.x1 NCI_CGAP_Pr22 ... 977 0.0
gi|5177406|gb|AI761815.1|AI761815 wi62f10.x1 NCI_CGAP_Co16 ... 973 0.0
gi|12788022|emb|AL524529.1|AL524529 AL524529 LTI_NFL003_NBC... 969 0.0
gi|12345824|gb|BF978609.1|BF978609 602149059F1 NIH_MGC_62 H... 965 0.0
gi|9334794|gb|BE389429.1|BE389429 601284739F1 NIH_MGC_44 Ho... 961 0.0
gi|5594691|gb|AI889527.1|AI889527 wn05f12.x1 NCI_CGAP_Ut1 H... 955 0.0
gi|6656965|gb|AW269935.1|AW269935 xv46b10.x1 Soares_NFL_T_G... 950 0.0
gi|11154277|gb|BF240354.1|BF240354 601905896F1 NIH_MGC_54 H... 942 0.0
gi|3922447|gb|AI284214.1|AI284214 qj70a03.x1 NCI_CGAP_Kid3 ... 940 0.0
gi|4137868|gb|AI368123.1|AI368123 qq44e05.x1 Soares_total_f... 930 0.0
gi|11443110|gb|BF430962.1|BF430962 nab30b09.x1 Soares_NSF_F... 920 0.0
gi|7320035|gb|AW614849.1|AW614849 hh67d05.x1 NCI_CGAP_GU1 H... 912 0.0
gi|9888642|gb|BE617704.1|BE617704 601441635T1 NIH_MGC_65 Ho... 910 0.0
gi|9330040|gb|BE384675.1|BE384675 601276952F1 NIH_MGC_20 Ho... 908 0.0
gi|3539703|gb|AI123937.1|AI123937 qa37f12.x1 Soares_NhHMPu_... 906 0.0
gi|10370419|gb|BE856914.1|BE856914 7f71b01.x1 Soares_NSF_F8... 902 0.0
gi|1687010|gb|AA127721.1|AA127721 zk92b07.s1 Soares_pregnan... 900 0.0
gi|7281553|gb|AW594295.1|AW594295 hg58a07.x1 NCI_CGAP_GC6 H... 898 0.0
gi|5512301|gb|AI858685.1|AI858685 wl41a12.x1 NCI_CGAP_Ut1 H... 898 0.0
gi|3841337|gb|AI245940.1|AI245940 qk45a03.x1 NCI_CGAP_Co8 H... 894 0.0
gi|3077524|gb|AA928368.1|AA928368 on49d11.s1 NCI_CGAP_Co8 H... 894 0.0
gi|1801454|gb|AA206021.1|AA206021 zq54d10.s1 Stratagene neu... 884 0.0
gi|4569117|gb|AI583220.1|AI583220 tq64b02.x1 NCI_CGAP_Lu19 ... 882 0.0
gi|1371254|gb|W63673.1|W63673 zd30a04.s1 Soares_fetal_heart... 882 0.0
gi|1923512|gb|AA280832.1|AA280832 zs99e01.s1 NCI_CGAP_GCB1 ... 880 0.0
gi|3919345|gb|AI281112.1|AI281112 qk71b04.x1 NCI_CGAP_Co8 H... 870 0.0
gi|14564997|gb|BI114096.1|BI114096 602862607F1 NIH_MGC_17 H... 864 0.0
gi|4452505|gb|AI538370.1|AI538370 tp64g07.x1 NCI_CGAP_Ut3 H... 864 0.0
gi|3539691|gb|AI123925.1|AI123925 qa37e12.x1 Soares_NhHMPu_... 862 0.0
gi|1801470|gb|AA206099.1|AA206099 zq54f06.s1 Stratagene neu... 852 0.0
gi|11599887|gb|BF514708.1|BF514708 UI-H-BW1-ans-a-01-0-UI.s... 848 0.0
gi|4852606|gb|AI672875.1|AI672875 we72g11.x1 Soares_Dieckgr... 848 0.0
gi|3743916|gb|AI192707.1|AI192707 qe67b12.x1 Soares_fetal_l... 846 0.0
gi|3277882|gb|AI038688.1|AI038688 ox35b10.s1 Soares_total_f... 841 0.0
gi|5451136|gb|AI830465.1|AI830465 wh51e05.x1 NCI_CGAP_Kid11... 839 0.0
gi|5744908|gb|AI952598.1|AI952598 wx75h09.x1 NCI_CGAP_Ov38 ... 835 0.0
gi|8149904|gb|AW960220.1|AW960220 EST372291 MAGE resequence... 833 0.0
gi|4876466|gb|AI675986.1|AI675986 wd08f08.x1 NCI_CGAP_Co3 H... 833 0.0
gi|12057494|gb|BF732336.1|BF732336 nae10g11.x1 NCI_CGAP_Ov1... 823 0.0
gi|4217587|gb|AI391583.1|AI391583 tg16d04.x1 NCI_CGAP_CLL1 ... 823 0.0
gi|9175795|gb|BE304553.1|BE304553 601105958F1 NIH_MGC_15 Ho... 817 0.0

gi|12888316|emb|AL550893.1|AL550893 AL550893 LTI_NFL006_PL2... 815 0.0
gi|1977901|gb|AA325658.1|AA325658 EST28681 Cerebellum II Ho... 801 0.0

>gi|7705791|ref|NP_057110.1| CGI-82 protein [Homo sapiens]
Prostate short-chain dehydrogenase reductase 1

EST Search:

Organ: colon
Tissue type: adenocarcinoma cell line

Organ: skin

Organ: brain
Tissue type: hippocampus

Organ: skin
Tissue type: melanotic melanoma

Organ: ovary
Tissue type: adenocarcinoma cell line

Sequences producing significant alignments: (bits) Value

gi|13401922|gb|BG469647.1|BG469647 602534103F1 NIH_MGC_15 H... 1550 0.0
gi|13746560|gb|BG220539.1|BG220539 RST40325 Athersys RAGE L... 1467 0.0
gi|14053553|gb|BG742900.1|BG742900 602632481F1 NCI_CGAP_Skn... 1457 0.0
gi|13967002|gb|BG699072.1|BG699072 602678713F1 NIH_MGC_95 H... 1439 0.0
gi|14053781|gb|BG743128.1|BG743128 602634270F1 NCI_CGAP_Skn... 1427 0.0
gi|13410718|gb|BG478523.1|BG478523 602524002F1 NIH_MGC_20 H... 1419 0.0
gi|9146489|gb|BE272160.1|BE272160 601141656F1 NIH_MGC_9 Hom... 1409 0.0
gi|14047524|gb|BG777207.1|BG777207 602664432F1 NIH_MGC_59 H... 1402 0.0
gi|13963233|gb|BG697241.1|BG697241 602660481F1 NCI_CGAP_Skn... 1392 0.0
gi|14651659|gb|BI196639.1|BI196639 602755427F1 NIH_MGC_19 H... 1388 0.0
gi|14059064|gb|BG748411.1|BG748411 602705974F1 NIH_MGC_43 H... 1380 0.0
gi|13336094|gb|BG429588.1|BG429588 602501268F1 NIH_MGC_75 H... 1368 0.0
gi|9124275|gb|BE253854.1|BE253854 601112818F1 NIH_MGC_16 Ho... 1364 0.0
gi|12604238|gb|BG110732.1|BG110732 602279029F1 NIH_MGC_86 H... 1358 0.0
gi|13527202|gb|BG535657.1|BG535657 602563366F1 NIH_MGC_77 H... 1344 0.0
gi|13289966|gb|BG396518.1|BG396518 602459353F1 NIH_MGC_16 H... 1342 0.0
gi|14064290|gb|BG753637.1|BG753637 602732827F1 NIH_MGC_43 H... 1330 0.0
gi|10156435|gb|BE742443.1|BE742443 601575210F1 NIH_MGC_9 Ho... 1330 0.0
gi|13570738|gb|BG563086.1|BG563086 602581878F1 NIH_MGC_76 H... 1314 0.0
gi|10399800|gb|BE906369.1|BE906369 601498517F1 NIH_MGC_70 H... 1308 0.0
gi|14809963|gb|BI255993.1|BI255993 602976353F1 NIH_MGC_12 H... 1306 0.0
gi|12607924|gb|BG114418.1|BG114418 602285710F1 NIH_MGC_86 H... 1298 0.0
gi|14565107|gb|BI114206.1|BI114206 602862564F1 NIH_MGC_17 H... 1292 0.0
gi|9186637|gb|BE302889.1|BE302889 ba70g10.y1 NIH_MGC_20 Hom... 1289 0.0
gi|6361758|gb|AI305108.1|AI305108 HA2404 Human fetal liver ... 1285 0.0
gi|10160188|gb|BE746196.1|BE746196 601578644F1 NIH_MGC_9 Ho... 1283 0.0
gi|14566335|gb|BI115434.1|BI115434 602863311F1 NIH_MGC_17 H... 1281 0.0
gi|14566302|gb|BI115401.1|BI115401 602863260F1 NIH_MGC_17 H... 1273 0.0
gi|12761697|gb|BG251881.1|BG251881 602364502F1 NIH_MGC_90 H... 1267 0.0
gi|6359266|gb|AI064994.1|AI064994 HA0821 Human fetal liver ... 1265 0.0
gi|9328145|gb|BE382780.1|BE382780 601298459F1 NIH_MGC_19 Ho... 1259 0.0
gi|13969001|gb|BG700048.1|BG700048 602681055F1 NIH_MGC_95 H... 1241 0.0
gi|12678524|gb|BG171821.1|BG171821 602322603F1 NIH_MGC_89 H... 1237 0.0
gi|9179232|gb|BE295680.1|BE295680 601175688F1 NIH_MGC_17 Ho... 1235 0.0
gi|13523981|gb|BG532442.1|BG532442 602561968F1 NIH_MGC_61 H... 1227 0.0

gi|9346825|gb|BE410375.1|BE410375 601302363F1 NIH_MGC_21 Ho... 1219 0.0
gi|12609069|gb|BG115563.1|BG115563 602317253F1 NIH_MGC_88 H... 1213 0.0
gi|4763039|gb|AI659469.1|AI659469 tu30g07.x1 NCI_CGAP_Pr28 ... 1205 0.0
gi|10741086|gb|BF033374.1|BF033374 601458081F1 NIH_MGC_66 H... 1199 0.0
gi|9722042|gb|BE514828.1|BE514828 601316764F1 NIH_MGC_9 Hom... 1191 0.0
gi|13459320|gb|BG497803.1|BG497803 602543080F1 NIH_MGC_60 H... 1185 0.0
gi|2398040|gb|AA587226.1|AA587226 nn82b08.s1 NCI_CGAP_Co9 H... 1181 0.0
gi|13534026|gb|BG541793.1|BG541793 602569677F1 NIH_MGC_77 H... 1180 0.0
gi|13406852|gb|BG474575.1|BG474575 602517363F1 NIH_MGC_16 H... 1170 0.0
gi|13972135|gb|BG701616.1|BG701616 602682503F1 NIH_MGC_95 H... 1158 0.0
gi|8144363|gb|AW954680.1|AW954680 EST366750 MAGE resequence... 1158 0.0
gi|9339021|gb|BE393656.1|BE393656 601310379F1 NIH_MGC_44 Ho... 1156 0.0
gi|11952823|gb|BF678928.1|BF678928 602153555F1 NIH_MGC_83 H... 1150 0.0
gi|12770117|gb|BG260301.1|BG260301 602371417F1 NIH_MGC_93 H... 1146 0.0
gi|9331236|gb|BE385871.1|BE385871 601275933F1 NIH_MGC_20 Ho... 1144 0.0
gi|12687397|gb|BG180694.1|BG180694 602329481F1 NIH_MGC_91 H... 1142 0.0
gi|9323581|gb|BE378216.1|BE378216 601237991F1 NIH_MGC_44 Ho... 1140 0.0
gi|14471561|gb|BI064034.1|BI064034 IL3-UT0119-120401-430-G0... 1132 0.0
gi|11953928|gb|BF680033.1|BF680033 602154752F1 NIH_MGC_83 H... 1132 0.0
gi|13458797|gb|BG497280.1|BG497280 602537844F1 NIH_MGC_59 H... 1128 0.0
gi|9179583|gb|BE296026.1|BE296026 601175058F1 NIH_MGC_17 Ho... 1128 0.0
gi|9770617|gb|BE541972.1|BE541972 601064273F1 NIH_MGC_10 Ho... 1126 0.0
gi|12612166|gb|BG118660.1|BG118660 602348226F1 NIH_MGC_90 H... 1108 0.0
gi|6568025|gb|AW235636.1|AW235636 xn20g09.x1 NCI_CGAP_Kid11... 1102 0.0
gi|2154395|gb|AA442517.1|AA442517 zv68a01.r1 Soares_total_f... 1098 0.0
gi|11952959|gb|BF679064.1|BF679064 602153322F1 NIH_MGC_83 H... 1094 0.0
gi|13282164|gb|BG388718.1|BG388718 602414406F1 NIH_MGC_92 H... 1092 0.0
gi|11954261|gb|BF680366.1|BF680366 602154150F1 NIH_MGC_83 H... 1092 0.0
gi|13336068|gb|BG429562.1|BG429562 602501238F1 NIH_MGC_75 H... 1076 0.0
gi|11613456|gb|BF526180.1|BF526180 602071089F1 NCI_CGAP_Brn... 1076 0.0
gi|11954238|gb|BF680343.1|BF680343 602154124F1 NIH_MGC_83 H... 1070 0.0
gi|13727617|gb|BG205930.1|BG205930 RST25365 Athersys RAGE L... 1061 0.0
gi|11947983|gb|BF674088.1|BF674088 602137489F1 NIH_MGC_83 H... 1059 0.0
gi|14178068|gb|BG830481.1|BG830481 602767043F1 NIH_MGC_42 H... 1057 0.0
gi|11954070|gb|BF680175.1|BF680175 602154923F1 NIH_MGC_83 H... 1055 0.0
gi|9135943|gb|BE262703.1|BE262703 601146057F1 NIH_MGC_19 Ho... 1055 0.0
gi|1544739|gb|AA053804.1|AA053804 ze25e09.s1 Soares_fetal_h... 1055 0.0
gi|12523600|gb|BG057848.1|BG057848 naf13d09.x1 Soares_NPBMC... 1051 0.0
gi|11107340|gb|BF213754.1|BF213754 601847654F1 NIH_MGC_55 H... 1051 0.0
gi|11947265|gb|BF673370.1|BF673370 602135837F1 NIH_MGC_83 H... 1047 0.0
gi|9189288|gb|BE336903.1|BE336903 bb68f05.y1 NIH_MGC_9 Homo... 1043 0.0
gi|11947422|gb|BF673610.1|BF673610 602136021F1 NIH_MGC_83 H... 1039 0.0
gi|10348906|gb|BE890514.1|BE890514 601431585F1 NIH_MGC_72 H... 1037 0.0
gi|13714218|gb|BG192531.1|BG192531 RST11646 Athersys RAGE L... 1027 0.0
gi|2167857|gb|AA454188.1|AA454188 zx48a12.s1 Soares_testis_... 1027 0.0
gi|10587293|gb|BE973957.1|BE973957 601680275F1 NIH_MGC_83 H... 1021 0.0
gi|14565160|gb|BI114259.1|BI114259 602862449F1 NIH_MGC_17 H... 1017 0.0
gi|12062768|gb|BF736094.1|BF736094 QV1-KT0023-131100-475-h0... 1017 0.0
gi|11947398|gb|BF673586.1|BF673586 602136287F1 NIH_MGC_83 H... 1017 0.0
gi|12158715|gb|BF820301.1|BF820301 CM0-RT0018-181100-706-e0... 1013 0.0
gi|11948042|gb|BF674147.1|BF674147 602137658F1 NIH_MGC_83 H... 1009 0.0
gi|11948071|gb|BF674176.1|BF674176 602137695F1 NIH_MGC_83 H... 1007 0.0
gi|14471624|gb|BI064110.1|BI064110 IL3-UT0119-170401-458-F0... 1005 0.0
gi|5080879|gb|AF063505.1|AF063505 AF063505 Homo sapiens lib... 1005 0.0
gi|6359496|gb|AI110631.1|AI110631 HA0057 Human fetal liver ... 1005 0.0
gi|12062595|gb|BF735895.1|BF735895 QV1-KT0023-131100-480-b0... 1003 0.0
gi|2703194|gb|AA700231.1|AA700231 zj52f03.s1 Soares_fetal_l... 995 0.0

gi|11949270|gb|BF675375.1|BF675375 602138336F1 NIH_MGC_83 H... 993 0.0
gi|11107263|gb|BF213677.1|BF213677 601847527F1 NIH_MGC_55 H... 993 0.0
gi|2167856|gb|AA454187.1|AA454187 zx48a12.r1 Soares_testis_... 991 0.0
gi|12062604|gb|BF735904.1|BF735904 QV1-KT0023-131100-480-h0... 989 0.0
gi|5839186|gb|AI992281.1|AI992281 ws41g11.x1 NCI_CGAP_Brn25... 989 0.0
gi|5364540|gb|AI799068.1|AI799068 we98b05.x1 Soares_NFL_T_G... 987 0.0
gi|11943604|gb|BF669709.1|BF669709 602118259F1 NIH_MGC_56 H... 981 0.0
gi|5663000|gb|AI927036.1|AI927036 wo87b07.x1 NCI_CGAP_Kid11... 979 0.0

>gi|7706523|ref|NP_057457.1| FOR II; WW domain-containing protein WWOX; fragile site FRA16D oxidoreductase; putative oxidoreductase [Homo sapiens]

EST Search:

Sequences producing significant alignments: (bits) Value

gi|12890387|emb|AL551953.1|AL551953 AL551953 LTI_NFL006_PL2... 1786 0.0
gi|12903293|emb|AL558608.1|AL558608 AL558608 LTI_NFL008_TC2... 1784 0.0
gi|12788142|emb|AL524649.1|AL524649 AL524649 LTI_NFL003_NBC... 1739 0.0
gi|12924548|emb|AL569324.1|AL569324 AL569324 LTI_FL002_PL1 ... 1522 0.0
gi|14044591|gb|BG774292.1|BG774292 602662318F1 NIH_MGC_21 H... 1507 0.0
gi|13980599|gb|BG705846.1|BG705846 602669332F1 NIH_MGC_96 H... 1455 0.0
gi|14082760|gb|BG772107.1|BG772107 602721554F1 NIH_MGC_97 H... 1398 0.0
gi|11643090|gb|BF569710.1|BF569710 602186235F1 NIH_MGC_45 H... 1338 0.0
gi|5849973|gb|AW002967.1|AW002967 wr03h08.x1 NCI_CGAP_GC6 H... 1328 0.0
gi|5886535|gb|AW027779.1|AW027779 wv24d06.x1 NCI_CGAP_Kid11... 1326 0.0
gi|10316595|gb|BE867819.1|BE867819 601443785F1 NIH_MGC_65 H... 1320 0.0
gi|10147851|gb|BE733756.1|BE733756 601568287F1 NIH_MGC_21 H... 1314 0.0
gi|13735635|gb|BG213932.1|BG213932 RST33572 Athersys RAGE L... 1308 0.0
gi|12910724|emb|AL562371.1|AL562371 AL562371 LTI_NFL003_NBC... 1302 0.0
gi|5368521|gb|AI803049.1|AI803049 tj60g08.x1 Soares_NSF_F8_... 1296 0.0
gi|12766396|gb|BG256580.1|BG256580 602370237F1 NIH_MGC_92 H... 1289 0.0
gi|12874081|emb|AL542236.1|AL542236 AL542236 LTI_FL002_PL1 ... 1287 0.0
gi|13746217|gb|BG220196.1|BG220196 RST39968 Athersys RAGE L... 1265 0.0
gi|6473914|gb|AW194946.1|AW194946 xn32e04.x1 NCI_CGAP_Kid11... 1235 0.0
gi|9898118|gb|BE616519.1|BE616519 601281151F1 NIH_MGC_39 Ho... 1223 0.0
gi|7280541|gb|AW593283.1|AW593283 hg12c01.x1 Soares_NFL_T_G... 1181 0.0
gi|13414425|gb|BG482146.1|BG482146 602528052F1 NIH_MGC_21 H... 1176 0.0
gi|14566906|gb|BI116005.1|BI116005 602866590F1 NIH_MGC_7 Ho... 1174 0.0
gi|11295586|gb|BF347991.1|BF347991 602023121F1 NCI_CGAP_Brn... 1172 0.0
gi|6451381|gb|AW182921.1|AW182921 xj65b02.x1 Soares_NFL_T_G... 1170 0.0
gi|10148597|gb|BE734605.1|BE734605 601570003F1 NIH_MGC_21 H... 1136 0.0
gi|9139887|gb|BE266312.1|BE266312 601191934F1 NIH_MGC_7 Hom... 1132 0.0
gi|5810913|gb|AI983694.1|AI983694 wz34a04.x1 NCI_CGAP_Brn53... 1116 0.0
gi|3153960|gb|AA978351.1|AA978351 oq40b04.s1 NCI_CGAP_Kid5 ... 1082 0.0
gi|13137803|gb|BG331365.1|BG331365 602432107F1 NIH_MGC_18 H... 1080 0.0
gi|11683578|gb|BF591254.1|BF591254 7h44b11.x1 NCI_CGAP_Co16... 1033 0.0
gi|14566532|gb|BI115631.1|BI115631 602865966F1 NIH_MGC_7 Ho... 1023 0.0
gi|14568452|gb|BI117551.1|BI117551 602866727F1 NIH_MGC_7 Ho... 1015 0.0
gi|3802061|gb|AI219858.1|AI219858 qg88f04.x1 Soares_NFL_T_G... 989 0.0
gi|4762296|gb|AI658726.1|AI658726 tu22h04.x1 NCI_CGAP_Pr28 ... 967 0.0
gi|13714360|gb|BG192673.1|BG192673 RST11790 Athersys RAGE L... 942 0.0
gi|13748701|gb|BG460195.1|BG460195 RST42664 Athersys RAGE L... 934 0.0
gi|4834104|gb|AI669330.1|AI669330 wb85d11.x1 NCI_CGAP_Pr28 ... 932 0.0
gi|9945265|gb|AW874692.1|AW874692 kdef10 Soares_NFL_T_GBC_S... 918 0.0

gi|8364318|gb|BE047265.1|BE047265 hq77g07.x1 NCI_CGAP_Ov41 ... 912 0.0
gi|7540649|gb|AW675414.1|AW675414 ba49a12.x1 NIH_MGC_10 Hom... 906 0.0
gi|12946366|emb|AL580390.1|AL580390 AL580390 LTI_NFL008_TC2... 898 0.0
gi|6946883|gb|AW418951.1|AW418951 ha24d04.x1 NCI_CGAP_Kid12... 874 0.0
gi|11687028|gb|BF594704.1|BF594704 7o54c01.x1 NCI_CGAP_Kid1... 870 0.0
gi|5812079|gb|AI984802.1|AI984802 wr85e01.x1 NCI_CGAP_Kid11... 862 0.0
gi|5707011|gb|AI942355.1|AI942355 wo80b08.x1 NCI_CGAP_Kid11... 827 0.0
gi|9512753|gb|BE466978.1|BE466978 hz59h08.x1 NCI_CGAP_Lu24 ... 815 0.0
gi|9260409|gb|BE348556.1|BE348556 ht71g08.x1 NCI_CGAP_Lu24 ... 815 0.0
gi|4985674|gb|AI697774.1|AI697774 we17b12.x1 NCI_CGAP_Lu24 ... 815 0.0
gi|10035137|gb|BE674596.1|BE674596 7e09c12.x1 NCI_CGAP_Lu24... 813 0.0
gi|3277850|gb|AI038656.1|AI038656 ox39e11.s1 Soares_total_f... 809 0.0

>gi|4502599|ref|NP_001748.1| carbonyl reductase 1; carbonyl reductase (NADPH); carbonyl reductase (NADPH) 1 [Homo sapiens]

EST Search:

Sequences producing significant alignments: (bits) Value

gi|12787486|emb|AL523993.1|AL523993 AL523993 LTI_NFL003_NBC... 1598 0.0
gi|13911420|gb|BG680023.1|BG680023 602626762F1 NCI_CGAP_Skn... 1522 0.0
gi|12932323|emb|AL573258.1|AL573258 AL573258 LTI_NFL006_PL2... 1515 0.0
gi|12910574|emb|AL562295.1|AL562295 AL562295 LTI_NFL003_NBC... 1513 0.0
gi|12878532|emb|AL545910.1|AL545910 AL545910 LTI_NFL006_PL2... 1505 0.0
gi|14051000|gb|BG740347.1|BG740347 602634102F1 NCI_CGAP_Skn... 1485 0.0
gi|13995976|gb|BG716789.1|BG716789 602678195F1 NIH_MGC_96 H... 1483 0.0
gi|13913215|gb|BG681818.1|BG681818 602629747F1 NCI_CGAP_Skn... 1473 0.0
gi|13409549|gb|BG477270.1|BG477270 602523416F1 NIH_MGC_20 H... 1457 0.0
gi|14061754|gb|BG751101.1|BG751101 602729893F1 NIH_MGC_43 H... 1445 0.0
gi|14567986|gb|BI117085.1|BI117085 602867878F1 NIH_MGC_7 Ho... 1427 0.0
gi|13976186|gb|BG703646.1|BG703646 602686612F1 NIH_MGC_95 H... 1421 0.0
gi|12884266|emb|AL548852.1|AL548852 AL548852 LTI_NFL006_PL2... 1411 0.0
gi|10157335|gb|BE743343.1|BE743343 601573262F1 NIH_MGC_9 Ho... 1388 0.0
gi|12928754|emb|AL571448.1|AL571448 AL571448 LTI_NFL006_PL2... 1382 0.0
gi|13986026|gb|BG708561.1|BG708561 602670460F1 NIH_MGC_96 H... 1378 0.0
gi|12873034|emb|AL541708.1|AL541708 AL541708 LTI_FL002_PL1 ... 1366 0.0
gi|12343309|gb|BF976094.1|BF976094 602244927F1 NIH_MGC_48 H... 1358 0.0
gi|10356604|gb|BE894338.1|BE894338 601432922F1 NIH_MGC_72 H... 1346 0.0
gi|12097845|gb|BF792860.1|BF792860 602253342F1 NIH_MGC_84 H... 1338 0.0
gi|12422069|gb|BG031614.1|BG031614 602299760F1 NIH_MGC_87 H... 1336 0.0
gi|10205944|gb|BE784746.1|BE784746 601473657F1 NIH_MGC_68 H... 1332 0.0
gi|13337465|gb|BG430959.1|BG430959 602500260F1 NIH_MGC_75 H... 1330 0.0
gi|12336923|gb|BF969708.1|BF969708 602272106F1 NIH_MGC_84 H... 1328 0.0
gi|11100906|gb|BF207320.1|BF207320 601870527F1 NIH_MGC_19 H... 1320 0.0
gi|10354151|gb|BE893116.1|BE893116 601437011F1 NIH_MGC_72 H... 1320 0.0
gi|5364351|gb|AI798879.1|AI798879 we93g10.x1 Soares_NFL_T_G... 1292 0.0
gi|10995194|dbj|AU134655.1|AU134655 AU134655 PLACE1 Homo sa... 1277 0.0
gi|9151374|gb|BE276411.1|BE276411 601144086F1 NIH_MGC_20 Ho... 1277 0.0
gi|12419167|gb|BG030070.1|BG030070 602297637F1 NIH_MGC_87 H... 1275 0.0
gi|13040559|gb|BG287078.1|BG287078 602382377F1 NIH_MGC_93 H... 1269 0.0
gi|12512254|gb|BG054983.1|BG054983 nac93d10.x1 NCI_CGAP_Brn... 1267 0.0
gi|14075435|gb|BG764782.1|BG764782 602736387F1 NIH_MGC_49 H... 1261 0.0
gi|4109064|gb|AI357443.1|AI357443 qy13e11.x1 NCI_CGAP_Brn23... 1259 0.0
gi|10321877|gb|BE873101.1|BE873101 601451604F1 NIH_MGC_65 H... 1245 0.0
gi|11261318|gb|BF313339.1|BF313339 601899896F1 NIH_MGC_19 H... 1241 0.0

gi|13414667|gb|BG482388.1|BG482388 602526551F1 NIH_MGC_21 H... 1227 0.0
gi|12793560|emb|AL530067.1|AL530067 AL530067 LTI_NFL001_NBC... 1217 0.0
gi|11444579|gb|BF432430.1|BF432430 nac54h10.x1 NCI_CGAP_Brn... 1213 0.0
gi|12676791|gb|BG170088.1|BG170088 602321554F1 NIH_MGC_89 H... 1183 0.0
gi|12873032|emb|AL541707.1|AL541707 AL541707 LTI_FL002_PL1 ... 1172 0.0
gi|5920889|gb|AW055186.1|AW055186 wz02a08.x1 NCI_CGAP_Brn23... 1164 0.0
gi|10733479|gb|BF025767.1|BF025767 601670465F1 NIH_MGC_20 H... 1150 0.0
gi|5111360|gb|AI743072.1|AI743072 wg85h01.x1 Soares_NSF_F8_... 1132 0.0
gi|9336906|gb|BE391541.1|BE391541 601285082F1 NIH_MGC_44 Ho... 1126 0.0
gi|9333205|gb|BE387840.1|BE387840 601282454F1 NIH_MGC_44 Ho... 1110 0.0
gi|12793559|emb|AL530066.1|AL530066 AL530066 LTI_NFL001_NBC... 1102 0.0
gi|9331116|gb|BE385751.1|BE385751 601276394F1 NIH_MGC_20 Ho... 1092 0.0
gi|9334511|gb|BE389146.1|BE389146 601285937F1 NIH_MGC_44 Ho... 1088 0.0
gi|9331225|gb|BE385860.1|BE385860 601275921F1 NIH_MGC_20 Ho... 1088 0.0
gi|6047445|gb|AW090101.1|AW090101 xc91b04.x1 NCI_CGAP_Brn35... 1084 0.0
gi|4618950|gb|AI609783.1|AI609783 tf83c08.x1 NCI_CGAP_Brn23... 1084 0.0
gi|11546273|gb|BF475446.1|BF475446 nac44h11.x1 Lupski_sciat... 1082 0.0
gi|13578051|gb|BG570398.1|BG570398 602590838F1 NIH_MGC_77 H... 1078 0.0
gi|5813280|gb|AI986003.1|AI986003 wu43a07.x1 Soares_Dieckgr... 1078 0.0
gi|2436789|gb|AA602855.1|AA602855 np20d07.s1 NCI_CGAP_Br3 H... 1076 0.0
gi|5447543|gb|AI826872.1|AI826872 wk75e01.x1 NCI_CGAP_Pan1 ... 1061 0.0
gi|10359089|gb|BE895565.1|BE895565 601438358F1 NIH_MGC_72 H... 1059 0.0
gi|12332915|gb|BF965700.1|BF965700 602276810F1 NIH_MGC_86 H... 1051 0.0
gi|12042635|gb|BF726724.1|BF726724 by11a05.y1 Human Lens cD... 1043 0.0
gi|13970816|gb|BG700956.1|BG700956 602682126F1 NIH_MGC_95 H... 1033 0.0
gi|5452311|gb|AI831640.1|AI831640 wj50b09.x1 NCI_CGAP_Lu19 ... 1029 0.0
gi|3254892|gb|AI033939.1|AI033939 ox09e05.x1 Soares_fetal_l... 1027 0.0
gi|9151920|gb|BE276858.1|BE276858 601178418F1 NIH_MGC_20 Ho... 1023 0.0
gi|13525487|gb|BG533947.1|BG533947 602553048F1 NIH_MGC_77 H... 1005 0.0
gi|1157922|gb|N36780.1|N36780 yy34e02.s1 Soares melanocyte ... 1005 0.0
gi|7318453|gb|AW613267.1|AW613267 hh69b02.x1 NCI_CGAP_GU1 H... 997 0.0
gi|4079449|gb|AI342522.1|AI342522 qt28g12.x1 Soares_pregnan... 991 0.0
gi|6836803|gb|AW340177.1|AW340177 hd02h06.x1 Soares_NFL_T_G... 989 0.0
gi|13407132|gb|BG474855.1|BG474855 602490904F1 NIH_MGC_20 H... 987 0.0
gi|10209552|gb|BE788354.1|BE788354 601480184F1 NIH_MGC_68 H... 981 0.0
gi|9133572|gb|BE313540.1|BE313540 601147169F1 NIH_MGC_19 Ho... 975 0.0
gi|3843568|gb|AI248160.1|AI248160 qh64e12.x1 Soares_fetal_l... 965 0.0
gi|1187855|gb|N46689.1|N46689 yy50e05.r1 Soares_multiple_sc... 955 0.0

>gi|4502601|ref|NP_001227.1| carbonyl reductase 3; carbonyl reductase (NADPH) 3 [Homo sapiens]

EST Search:

Sequences producing significant alignments: (bits) Value

gi|4762402|gb|AI658832.1|AI658832 tu29g04.x1 NCI_CGAP_Pr28 ... 1265 0.0
gi|4897979|gb|AI686685.1|AI686685 tu35g06.x1 NCI_CGAP_Pr28 ... 1191 0.0
gi|9344743|gb|BE408293.1|BE408293 601302679F1 NIH_MGC_21 Ho... 1108 0.0
gi|14502813|gb|BI084483.1|BI084483 602869227T1 NIH_MGC_102 ... 1086 0.0
gi|12672477|gb|BG165774.1|BG165774 602344434F1 NIH_MGC_89 H... 1086 0.0
gi|13992978|gb|BG714047.1|BG714047 602674460F1 NIH_MGC_96 H... 1043 0.0
gi|14075958|gb|BG765305.1|BG765305 602738744F1 NIH_MGC_49 H... 1023 0.0
gi|10141391|gb|BE727298.1|BE727298 601560989F1 NIH_MGC_20 H... 1011 0.0
gi|10228958|gb|BE775303.1|BE775303 QV0-UM0091-260500-245-f1... 1009 0.0
gi|5451368|gb|AI830785.1|AI830785 wj41e04.x1 NCI_CGAP_Lu19 ... 926 0.0
gi|13732235|gb|BG210468.1|BG210468 RST30093 Athersys RAGE L... 906 0.0
gi|4175510|gb|AI375520.1|AI375520 tc23b01.x1 Soares_total_f... 906 0.0
gi|4736532|gb|AI652553.1|AI652553 wb61e09.x1 NCI_CGAP_GC6 H... 856 0.0
gi|6991764|gb|AW450998.1|AW450998 UI-H-BI3-ala-c-09-0-UI.s1... 839 0.0
gi|7253791|gb|AW578742.1|AW578742 RC1-CT0279-070100-021-h06... 825 0.0
gi|4089551|gb|AI352345.1|AI352345 qt19h03.x1 NCI_CGAP_GC4 H... 819 0.0
gi|6886298|gb|AW381639.1|AW381639 QV0-HT0309-071299-068-g01... 805 0.0

>gi|5031737|ref|NP_005785.1| short-chain alcohol dehydrogenase family member [Homo sapiens]

EST Search:

Sequences producing significant alignments: (bits) Value

gi|13408914|gb|BG476635.1|BG476635 602524915F1 NIH_MGC_20 H... 1568 0.0
gi|10141769|gb|BE727777.1|BE727777 601564116F1 NIH_MGC_20 H... 1431 0.0
gi|13410948|gb|BG478669.1|BG478669 602525561F1 NIH_MGC_20 H... 1411 0.0
gi|14802215|gb|BI252096.1|BI252096 602952761F1 NIH_MGC_100 ... 1388 0.0
gi|14802992|gb|BI252487.1|BI252487 602952951F1 NIH_MGC_100 ... 1356 0.0
gi|10360386|gb|BE896211.1|BE896211 601438923F1 NIH_MGC_72 H... 1344 0.0
gi|13408303|gb|BG476024.1|BG476024 602521168F1 NIH_MGC_20 H... 1312 0.0
gi|13047921|gb|BG290697.1|BG290697 602388991F1 NIH_MGC_93 H... 1300 0.0
gi|10964687|gb|BF125647.1|BF125647 601763219F1 NIH_MGC_20 H... 1296 0.0
gi|14801948|gb|BI251960.1|BI251960 602952582F1 NIH_MGC_100 ... 1292 0.0
gi|13048916|gb|BG291202.1|BG291202 602388644F1 NIH_MGC_93 H... 1271 0.0
gi|14802560|gb|BI252269.1|BI252269 602953178F1 NIH_MGC_100 ... 1263 0.0
gi|13407753|gb|BG475474.1|BG475474 602491469F1 NIH_MGC_20 H... 1261 0.0
gi|9331795|gb|BE386430.1|BE386430 601273627F1 NIH_MGC_20 Ho... 1255 0.0
gi|10318914|gb|BE870138.1|BE870138 601449851F1 NIH_MGC_65 H... 1251 0.0
gi|11001027|dbj|AU139506.1|AU139506 AU139506 PLACE1 Homo sa... 1249 0.0
gi|13297151|gb|BG403703.1|BG403703 602419531F1 NIH_MGC_93 H... 1247 0.0
gi|13050383|gb|BG291998.1|BG291998 602388569F1 NIH_MGC_93 H... 1213 0.0
gi|14802908|gb|BI252445.1|BI252445 602952901F1 NIH_MGC_100 ... 1209 0.0
gi|13038500|gb|BG285990.1|BG285990 602381170F1 NIH_MGC_93 H... 1185 0.0
gi|14803672|gb|BI252829.1|BI252829 602953214T1 NIH_MGC_100 ... 1181 0.0
gi|10144041|gb|BE730049.1|BE730049 601562688F1 NIH_MGC_20 H... 1168 0.0

gi|14802770|gb|BI252376.1|BI252376 602953214F1 NIH_MGC_100 ... 1152 0.0
gi|10733962|gb|BF026250.1|BF026250 601672857F1 NIH_MGC_20 H... 1148 0.0
gi|13409965|gb|BG477686.1|BG477686 602522370F1 NIH_MGC_20 H... 1124 0.0
gi|14803944|gb|BI252967.1|BI252967 602953015T1 NIH_MGC_100 ... 1118 0.0
gi|9150493|gb|BE275537.1|BE275537 601121206F1 NIH_MGC_20 Ho... 1098 0.0
gi|14804186|gb|BI253093.1|BI253093 602953178T1 NIH_MGC_100 ... 1074 0.0
gi|14802614|gb|BI252296.1|BI252296 602953015F1 NIH_MGC_100 ... 1037 0.0
gi|10144259|gb|BE730267.1|BE730267 601563674F1 NIH_MGC_20 H... 1027 0.0
gi|7376376|gb|AW629586.1|AW629586 hh67c01.y1 NCI_CGAP_GU1 H... 985 0.0
gi|9150554|gb|BE275597.1|BE275597 601121106F1 NIH_MGC_20 Ho... 954 0.0
gi|2825544|gb|AA774246.1|AA774246 af66a05.r1 Soares_NhHMPu_... 946 0.0
gi|14802393|gb|BI252185.1|BI252185 602952878F1 NIH_MGC_100 ... 936 0.0
gi|14803206|gb|BI252593.1|BI252593 602952582T1 NIH_MGC_100 ... 912 0.0
gi|4991284|gb|AI703384.1|AI703384 wd93f03.x1 NCI_CGAP_Lu24 ... 906 0.0
gi|14803859|gb|BI252924.1|BI252924 602952951T1 NIH_MGC_100 ... 900 0.0
gi|14803620|gb|BI252803.1|BI252803 602952878T1 NIH_MGC_100 ... 898 0.0
gi|14803446|gb|BI252716.1|BI252716 602952761T1 NIH_MGC_100 ... 898 0.0
gi|5663486|gb|AI927522.1|AI927522 wo90h11.x1 NCI_CGAP_Kid11... 894 0.0
gi|9510775|gb|BE465000.1|BE465000 hv76d05.x1 NCI_CGAP_Lu24 ... 866 0.0

>gi|4504507|ref|NP_000853.1| hydroxy-delta-5-steroid dehydrogenase, 3 beta- and steroid delta-isomerase 1; Hydroxy-delta-5-steroid dehydrogenase, 3 beta- and steroid [Homo sapiens]

EST Search:

Sequences producing significant alignments: (bits) Value

gi|12927162|emb|AL570648.1|AL570648 AL570648 LTI_NFL006_PL2... 1966 0.0
gi|12928250|emb|AL571196.1|AL571196 AL571196 LTI_NFL006_PL2... 1939 0.0
gi|12887155|emb|AL550307.1|AL550307 AL550307 LTI_NFL006_PL2... 1927 0.0
gi|12877991|emb|AL545509.1|AL545509 AL545509 LTI_NFL006_PL2... 1925 0.0
gi|12893183|emb|AL553392.1|AL553392 AL553392 LTI_NFL006_PL2... 1911 0.0
gi|12895448|emb|AL554554.1|AL554554 AL554554 LTI_NFL006_PL2... 1909 0.0
gi|12931487|emb|AL572835.1|AL572835 AL572835 LTI_NFL006_PL2... 1905 0.0
gi|12940115|emb|AL577210.1|AL577210 AL577210 LTI_NFL006_PL2... 1903 0.0
gi|12937740|emb|AL576013.1|AL576013 AL576013 LTI_NFL006_PL2... 1871 0.0
gi|12882457|emb|AL547931.1|AL547931 AL547931 LTI_NFL006_PL2... 1861 0.0
gi|12871910|emb|AL541135.1|AL541135 AL541135 LTI_FL002_PL1 ... 1852 0.0
gi|12886860|emb|AL550160.1|AL550160 AL550160 LTI_NFL006_PL2... 1850 0.0
gi|12938513|emb|AL576403.1|AL576403 AL576403 LTI_NFL006_PL2... 1842 0.0
gi|12882827|emb|AL548117.1|AL548117 AL548117 LTI_NFL006_PL2... 1838 0.0
gi|12895626|emb|AL554645.1|AL554645 AL554645 LTI_NFL006_PL2... 1836 0.0
gi|12935937|emb|AL575100.1|AL575100 AL575100 LTI_NFL006_PL2... 1826 0.0
gi|12882752|emb|AL548079.1|AL548079 AL548079 LTI_NFL006_PL2... 1826 0.0
gi|12889651|emb|AL551573.1|AL551573 AL551573 LTI_NFL006_PL2... 1816 0.0
gi|12888448|emb|AL550960.1|AL550960 AL550960 LTI_NFL006_PL2... 1808 0.0
gi|12935106|emb|AL574677.1|AL574677 AL574677 LTI_NFL006_PL2... 1806 0.0
gi|12872853|emb|AL541617.1|AL541617 AL541617 LTI_FL002_PL1 ... 1776 0.0
gi|12939546|emb|AL576923.1|AL576923 AL576923 LTI_NFL006_PL2... 1774 0.0
gi|12929393|emb|AL571768.1|AL571768 AL571768 LTI_NFL006_PL2... 1764 0.0
gi|12934688|emb|AL574461.1|AL574461 AL574461 LTI_NFL006_PL2... 1762 0.0
gi|12894585|emb|AL554113.1|AL554113 AL554113 LTI_NFL006_PL2... 1758 0.0
gi|12877435|emb|AL544954.1|AL544954 AL544954 LTI_NFL006_PL2... 1754 0.0
gi|12877044|emb|AL544564.1|AL544564 AL544564 LTI_NFL006_PL2... 1742 0.0
gi|12892145|emb|AL552859.1|AL552859 AL552859 LTI_NFL006_PL2... 1719 0.0

gi|12937367|emb|AL575824.1|AL575824 AL575824 LTI_NFL006_PL2... 1697 0.0
gi|12871127|emb|AL540716.1|AL540716 AL540716 LTI_FL002_PL1 ... 1689 0.0
gi|12885872|emb|AL549664.1|AL549664 AL549664 LTI_NFL006_PL2... 1679 0.0
gi|12893547|emb|AL553580.1|AL553580 AL553580 LTI_NFL006_PL2... 1677 0.0
gi|12882951|emb|AL548184.1|AL548184 AL548184 LTI_NFL006_PL2... 1677 0.0
gi|12884358|emb|AL548898.1|AL548898 AL548898 LTI_NFL006_PL2... 1661 0.0
gi|12938939|emb|AL576619.1|AL576619 AL576619 LTI_NFL006_PL2... 1649 0.0
gi|12933347|emb|AL573779.1|AL573779 AL573779 LTI_NFL006_PL2... 1626 0.0
gi|12878205|emb|AL545723.1|AL545723 AL545723 LTI_NFL006_PL2... 1604 0.0
gi|12881974|emb|AL547683.1|AL547683 AL547683 LTI_NFL006_PL2... 1600 0.0
gi|12871823|emb|AL541089.1|AL541089 AL541089 LTI_FL002_PL1 ... 1594 0.0
gi|12879228|emb|AL546272.1|AL546272 AL546272 LTI_NFL006_PL2... 1572 0.0
gi|14053316|gb|BG742663.1|BG742663 602633265F1 NCI_CGAP_Skn... 1568 0.0
gi|12877300|emb|AL544820.1|AL544820 AL544820 LTI_NFL006_PL2... 1558 0.0
gi|12884046|emb|AL548741.1|AL548741 AL548741 LTI_NFL006_PL2... 1552 0.0
gi|12923409|emb|AL568754.1|AL568754 AL568754 LTI_FL002_PL1 ... 1528 0.0
gi|12878320|emb|AL545804.1|AL545804 AL545804 LTI_NFL006_PL2... 1524 0.0
gi|12931409|emb|AL572796.1|AL572796 AL572796 LTI_NFL006_PL2... 1485 0.0
gi|14052078|gb|BG741425.1|BG741425 602632206F1 NCI_CGAP_Skn... 1475 0.0
gi|12887220|emb|AL550340.1|AL550340 AL550340 LTI_NFL006_PL2... 1475 0.0
gi|12923357|emb|AL568728.1|AL568728 AL568728 LTI_FL002_PL1 ... 1459 0.0
gi|13906575|gb|BG675192.1|BG675192 602621456F1 NCI_CGAP_Skn... 1405 0.0
gi|12891598|emb|AL552571.1|AL552571 AL552571 LTI_NFL006_PL2... 1390 0.0
gi|12923025|emb|AL568562.1|AL568562 AL568562 LTI_FL002_PL1 ... 1356 0.0
gi|4312074|gb|AI458056.1|AI458056 tj64a01.x1 Soares_NSF_F8_... 1352 0.0
gi|12887294|emb|AL550378.1|AL550378 AL550378 LTI_NFL006_PL2... 1334 0.0
gi|14051781|gb|BG741128.1|BG741128 602631689F1 NCI_CGAP_Skn... 1302 0.0
gi|12931361|emb|AL572772.1|AL572772 AL572772 LTI_NFL006_PL2... 1289 0.0
gi|13961102|gb|BG696201.1|BG696201 602659327F1 NCI_CGAP_Skn... 1281 0.0
gi|12884855|emb|AL549152.1|AL549152 AL549152 LTI_NFL006_PL2... 1281 0.0
gi|12934204|emb|AL574213.1|AL574213 AL574213 LTI_NFL006_PL2... 1269 0.0
gi|13578387|gb|BG570734.1|BG570734 602591849F1 NIH_MGC_79 H... 1267 0.0
gi|12885649|emb|AL549552.1|AL549552 AL549552 LTI_NFL006_PL2... 1267 0.0
gi|12886858|emb|AL550159.1|AL550159 AL550159 LTI_NFL006_PL2... 1265 0.0
gi|12872851|emb|AL541616.1|AL541616 AL541616 LTI_FL002_PL1 ... 1229 0.0
gi|12928875|emb|AL571509.1|AL571509 AL571509 LTI_NFL006_PL2... 1225 0.0
gi|12884913|emb|AL549181.1|AL549181 AL549181 LTI_NFL006_PL2... 1225 0.0
gi|14054469|gb|BG743816.1|BG743816 602631735F1 NCI_CGAP_Skn... 1193 0.0
gi|13674098|gb|BG622727.1|BG622727 602647503F1 NIH_MGC_79 H... 1156 0.0
gi|8140987|gb|AW951317.1|AW951317 EST363387 MAGE resequence... 1148 0.0
gi|12875988|emb|AL543510.1|AL543510 AL543510 LTI_NFL006_PL2... 1140 0.0
gi|3803768|gb|AI221565.1|AI221565 qg15d10.x1 Soares_placent... 1114 0.0
gi|12925861|emb|AL569984.1|AL569984 AL569984 LTI_NFL006_PL2... 1106 0.0
gi|12930920|emb|AL572546.1|AL572546 AL572546 LTI_NFL006_PL2... 1096 0.0
gi|12879171|emb|AL546243.1|AL546243 AL546243 LTI_NFL006_PL2... 1078 0.0
gi|12927889|emb|AL571013.1|AL571013 AL571013 LTI_NFL006_PL2... 1072 0.0
gi|12877667|emb|AL545186.1|AL545186 AL545186 LTI_NFL006_PL2... 1053 0.0
gi|12392723|gb|BF986403.1|BF986403 QV4-GN0143-031000-445-f0... 1031 0.0
gi|1445235|gb|AA001626.1|AA001626 zh85e10.r1 Soares_fetal_l... 1017 0.0

>gi|4504509|ref|NP_000189.1| hydroxy-delta-5-steroid dehydrogenase, 3 beta- and steroid delta-isomerase 2; Hydroxy-delta-5-steroid dehydrogenase, 3 beta- and steroid [Homo sapiens]

EST Search:

Sequences producing significant alignments: (bits) Value

gi|12875988|emb|AL543510.1|AL543510 AL543510 LTI_NFL006_PL2... 1733 0.0
gi|12925861|emb|AL569984.1|AL569984 AL569984 LTI_NFL006_PL2... 1717 0.0
gi|10730833|dbj|AV711527.1|AV711527 AV711527 Cu Homo sapien... 1415 0.0
gi|12887155|emb|AL550307.1|AL550307 AL550307 LTI_NFL006_PL2... 1400 0.0
gi|12877991|emb|AL545509.1|AL545509 AL545509 LTI_NFL006_PL2... 1392 0.0
gi|12895448|emb|AL554554.1|AL554554 AL554554 LTI_NFL006_PL2... 1374 0.0
gi|12893183|emb|AL553392.1|AL553392 AL553392 LTI_NFL006_PL2... 1352 0.0
gi|12882457|emb|AL547931.1|AL547931 AL547931 LTI_NFL006_PL2... 1334 0.0
gi|12871910|emb|AL541135.1|AL541135 AL541135 LTI_FL002_PL1 ... 1332 0.0
gi|12886860|emb|AL550160.1|AL550160 AL550160 LTI_NFL006_PL2... 1330 0.0
gi|10730542|dbj|AV711236.1|AV711236 AV711236 Cu Homo sapien... 1326 0.0
gi|12882827|emb|AL548117.1|AL548117 AL548117 LTI_NFL006_PL2... 1324 0.0
gi|12882752|emb|AL548079.1|AL548079 AL548079 LTI_NFL006_PL2... 1316 0.0
gi|12895626|emb|AL554645.1|AL554645 AL554645 LTI_NFL006_PL2... 1314 0.0
gi|12889651|emb|AL551573.1|AL551573 AL551573 LTI_NFL006_PL2... 1294 0.0
gi|12888448|emb|AL550960.1|AL550960 AL550960 LTI_NFL006_PL2... 1294 0.0
gi|10730656|dbj|AV711350.1|AV711350 AV711350 Cu Homo sapien... 1285 0.0
gi|10730523|dbj|AV711217.1|AV711217 AV711217 Cu Homo sapien... 1279 0.0
gi|10728926|dbj|AV710297.1|AV710297 AV710297 Cu Homo sapien... 1275 0.0
gi|12872853|emb|AL541617.1|AL541617 AL541617 LTI_FL002_PL1 ... 1271 0.0
gi|10730030|dbj|AV710724.1|AV710724 AV710724 Cu Homo sapien... 1271 0.0
gi|10725428|dbj|AV708163.1|AV708163 AV708163 ADC Homo sapie... 1271 0.0
gi|10730059|dbj|AV710753.1|AV710753 AV710753 Cu Homo sapien... 1269 0.0
gi|10728958|dbj|AV710329.1|AV710329 AV710329 Cu Homo sapien... 1265 0.0
gi|10730175|dbj|AV710869.1|AV710869 AV710869 Cu Homo sapien... 1261 0.0
gi|12877044|emb|AL544564.1|AL544564 AL544564 LTI_NFL006_PL2... 1257 0.0
gi|10728954|dbj|AV710325.1|AV710325 AV710325 Cu Homo sapien... 1257 0.0
gi|10722430|dbj|AV705124.1|AV705124 AV705124 ADB Homo sapie... 1257 0.0
gi|10730370|dbj|AV711064.1|AV711064 AV711064 Cu Homo sapien... 1255 0.0
gi|10730249|dbj|AV710943.1|AV710943 AV710943 Cu Homo sapien... 1255 0.0
gi|12894585|emb|AL554113.1|AL554113 AL554113 LTI_NFL006_PL2... 1253 0.0
gi|10823643|dbj|AV721796.1|AV721796 AV721796 HTB Homo sapie... 1253 0.0
gi|10730859|dbj|AV711553.1|AV711553 AV711553 Cu Homo sapien... 1249 0.0
gi|10730058|dbj|AV710752.1|AV710752 AV710752 Cu Homo sapien... 1247 0.0
gi|10730382|dbj|AV711076.1|AV711076 AV711076 Cu Homo sapien... 1243 0.0
gi|10721736|dbj|AV704418.1|AV704418 AV704418 ADB Homo sapie... 1241 0.0
gi|10720632|dbj|AV703303.1|AV703303 AV703303 ADB Homo sapie... 1241 0.0
gi|10729167|dbj|AV710538.1|AV710538 AV710538 Cu Homo sapien... 1239 0.0
gi|12927162|emb|AL570648.1|AL570648 AL570648 LTI_NFL006_PL2... 1237 0.0
gi|10729922|dbj|AV710616.1|AV710616 AV710616 Cu Homo sapien... 1237 0.0
gi|10725209|dbj|AV707944.1|AV707944 AV707944 ADB Homo sapie... 1237 0.0
gi|10717788|dbj|AV701458.1|AV701458 AV701458 ADA Homo sapie... 1233 0.0
gi|10818240|dbj|AV721088.1|AV721088 AV721088 HTB Homo sapie... 1231 0.0
gi|10730255|dbj|AV710949.1|AV710949 AV710949 Cu Homo sapien... 1231 0.0
gi|10729996|dbj|AV710690.1|AV710690 AV710690 Cu Homo sapien... 1231 0.0
gi|10724631|dbj|AV707364.1|AV707364 AV707364 ADB Homo sapie... 1231 0.0
gi|12892145|emb|AL552859.1|AL552859 AL552859 LTI_NFL006_PL2... 1229 0.0
gi|10729084|dbj|AV710455.1|AV710455 AV710455 Cu Homo sapien... 1227 0.0
gi|10728984|dbj|AV710355.1|AV710355 AV710355 Cu Homo sapien... 1227 0.0
gi|10728930|dbj|AV710301.1|AV710301 AV710301 Cu Homo sapien... 1227 0.0
gi|10730470|dbj|AV711164.1|AV711164 AV711164 Cu Homo sapien... 1221 0.0
gi|10720681|dbj|AV703353.1|AV703353 AV703353 ADB Homo sapie... 1221 0.0
gi|10717625|dbj|AV701295.1|AV701295 AV701295 ADA Homo sapie... 1221 0.0
gi|10730748|dbj|AV711442.1|AV711442 AV711442 Cu Homo sapien... 1219 0.0
gi|10724044|dbj|AV706766.1|AV706766 AV706766 ADB Homo sapie... 1217 0.0

gi|10729931|dbj|AV710625.1|AV710625 AV710625 Cu Homo sapien... 1215 0.0
gi|10717918|dbj|AV701588.1|AV701588 AV701588 ADB Homo sapie... 1215 0.0
gi|10728798|dbj|AV710236.1|AV710236 AV710236 Cu Homo sapien... 1211 0.0
gi|10730083|dbj|AV710777.1|AV710777 AV710777 Cu Homo sapien... 1209 0.0
gi|10721372|dbj|AV704052.1|AV704052 AV704052 ADB Homo sapie... 1209 0.0
gi|10720663|dbj|AV703334.1|AV703334 AV703334 ADB Homo sapie... 1209 0.0
gi|12940115|emb|AL577210.1|AL577210 AL577210 LTI_NFL006_PL2... 1203 0.0
gi|10729927|dbj|AV710621.1|AV710621 AV710621 Cu Homo sapien... 1203 0.0
gi|12885872|emb|AL549664.1|AL549664 AL549664 LTI_NFL006_PL2... 1201 0.0
gi|10730418|dbj|AV711112.1|AV711112 AV711112 Cu Homo sapien... 1199 0.0
gi|12928250|emb|AL571196.1|AL571196 AL571196 LTI_NFL006_PL2... 1197 0.0
gi|10730638|dbj|AV711332.1|AV711332 AV711332 Cu Homo sapien... 1195 0.0
gi|10730252|dbj|AV710946.1|AV710946 AV710946 Cu Homo sapien... 1195 0.0
gi|10728707|dbj|AV710181.1|AV710181 AV710181 Cu Homo sapien... 1195 0.0
gi|10728775|dbj|AV710220.1|AV710220 AV710220 Cu Homo sapien... 1193 0.0
gi|12871127|emb|AL540716.1|AL540716 AL540716 LTI_FL002_PL1 ... 1191 0.0
gi|10717763|dbj|AV701433.1|AV701433 AV701433 ADA Homo sapie... 1191 0.0
gi|10728810|dbj|AV710244.1|AV710244 AV710244 Cu Homo sapien... 1189 0.0
gi|10728686|dbj|AV710172.1|AV710172 AV710172 Cu Homo sapien... 1189 0.0
gi|10728432|dbj|AV710048.1|AV710048 AV710048 Cu Homo sapien... 1189 0.0
gi|10728736|dbj|AV710195.1|AV710195 AV710195 Cu Homo sapien... 1187 0.0
gi|12882951|emb|AL548184.1|AL548184 AL548184 LTI_NFL006_PL2... 1185 0.0
gi|10836637|dbj|AV727216.1|AV727216 AV727216 HTC Homo sapie... 1185 0.0
gi|12931487|emb|AL572835.1|AL572835 AL572835 LTI_NFL006_PL2... 1183 0.0
gi|10730541|dbj|AV711235.1|AV711235 AV711235 Cu Homo sapien... 1183 0.0
gi|10717498|dbj|AV701168.1|AV701168 AV701168 ADA Homo sapie... 1183 0.0
gi|10729910|dbj|AV710604.1|AV710604 AV710604 Cu Homo sapien... 1181 0.0
gi|10728903|dbj|AV710282.1|AV710282 AV710282 Cu Homo sapien... 1181 0.0
gi|10728792|dbj|AV710233.1|AV710233 AV710233 Cu Homo sapien... 1181 0.0
gi|12937740|emb|AL576013.1|AL576013 AL576013 LTI_NFL006_PL2... 1180 0.0
gi|12893547|emb|AL553580.1|AL553580 AL553580 LTI_NFL006_PL2... 1180 0.0
gi|10729951|dbj|AV710645.1|AV710645 AV710645 Cu Homo sapien... 1180 0.0
gi|10724073|dbj|AV706795.1|AV706795 AV706795 ADB Homo sapie... 1178 0.0
gi|10728319|dbj|AV710016.1|AV710016 AV710016 Cu Homo sapien... 1174 0.0
gi|10723602|dbj|AV706317.1|AV706317 AV706317 ADB Homo sapie... 1170 0.0
gi|10722640|dbj|AV705335.1|AV705335 AV705335 ADB Homo sapie... 1170 0.0
gi|10721164|dbj|AV703837.1|AV703837 AV703837 ADB Homo sapie... 1170 0.0
gi|10728931|dbj|AV710302.1|AV710302 AV710302 Cu Homo sapien... 1168 0.0
gi|10724584|dbj|AV707317.1|AV707317 AV707317 ADB Homo sapie... 1168 0.0
gi|10723870|dbj|AV706592.1|AV706592 AV706592 ADB Homo sapie... 1168 0.0
gi|10721084|dbj|AV703757.1|AV703757 AV703757 ADB Homo sapie... 1168 0.0
gi|10717794|dbj|AV701464.1|AV701464 AV701464 ADA Homo sapie... 1168 0.0
gi|12938513|emb|AL576403.1|AL576403 AL576403 LTI_NFL006_PL2... 1166 0.0
gi|10730789|dbj|AV711483.1|AV711483 AV711483 Cu Homo sapien... 1166 0.0
gi|10722122|dbj|AV704810.1|AV704810 AV704810 ADB Homo sapie... 1166 0.0

>gi|4507185|ref|NP_003115.1| sepiapterin reductase (7,8-dihydrobiopterin:NADP+ oxidoreductase); Sepiapterin reductase [Homo sapiens]

EST Search:

Sequences producing significant alignments: (bits) Value

gi|14078647|gb|BG767994.1|BG767994 602743750F1 NIH_MGC_49 H... 1479 0.0
gi|14074318|gb|BG763665.1|BG763665 602735883F1 NIH_MGC_49 H... 1443 0.0

gi|11060920|gb|BF182777.1|BF182777 601809284F1 NIH_MGC_18 H... 1402 0.0
gi|14178938|gb|BG831351.1|BG831351 602766203F1 NIH_MGC_42 H... 1392 0.0
gi|13143827|gb|BG337389.1|BG337389 602434948F1 NIH_MGC_46 H... 1378 0.0
gi|12430554|gb|BG035928.1|BG035928 602326035F1 NIH_MGC_90 H... 1372 0.0
gi|14077523|gb|BG766870.1|BG766870 602740993F1 NIH_MGC_49 H... 1336 0.0
gi|12427743|gb|BG034435.1|BG034435 602302839F1 NIH_MGC_87 H... 1320 0.0
gi|10396046|gb|BE904122.1|BE904122 601494330F2 NIH_MGC_70 H... 1318 0.0
gi|13337173|gb|BG430667.1|BG430667 602498463F1 NIH_MGC_75 H... 1292 0.0
gi|11003989|dbj|AU142468.1|AU142468 AU142468 Y79AA1 Homo sa... 1285 0.0
gi|14648668|gb|BI193648.1|BI193648 602946558F1 NIH_MGC_42 H... 1253 0.0
gi|13450197|gb|BG488690.1|BG488690 602534629F1 NIH_MGC_18 H... 1205 0.0
gi|12671640|gb|BG164847.1|BG164847 602340567F1 NIH_MGC_89 H... 1195 0.0
gi|13289136|gb|BG395688.1|BG395688 602458332F1 NIH_MGC_16 H... 1189 0.0
gi|10398692|gb|BE905423.1|BE905423 601495014F1 NIH_MGC_70 H... 1185 0.0
gi|9335041|gb|BE389676.1|BE389676 601281907F1 NIH_MGC_44 Ho... 1132 0.0
gi|13344731|gb|BG438225.1|BG438225 602490133F1 NIH_MGC_18 H... 1120 0.0
gi|14812620|gb|BI257340.1|BI257340 602967404F1 NIH_MGC_12 H... 1100 0.0
gi|14179931|gb|BG832344.1|BG832344 602765285F1 NIH_MGC_42 H... 1100 0.0
gi|14052217|gb|BG741564.1|BG741564 602635181F1 NCI_CGAP_Skn... 1082 0.0
gi|10734687|gb|BF026975.1|BF026975 601671150F1 NIH_MGC_20 H... 1005 0.0
gi|9341224|gb|BE395859.1|BE395859 601312905F1 NIH_MGC_44 Ho... 993 0.0
gi|9323592|gb|BE378227.1|BE378227 601238014F1 NIH_MGC_44 Ho... 993 0.0
gi|12677110|gb|BG170407.1|BG170407 602322738F1 NIH_MGC_89 H... 967 0.0
gi|12041099|gb|BF725188.1|BF725188 bx13b08.y1 Human Iris cD... 904 0.0
gi|9890172|gb|BE619234.1|BE619234 601472991F1 NIH_MGC_68 Ho... 868 0.0
gi|14061495|gb|BG750842.1|BG750842 602707368F1 NIH_MGC_43 H... 839 0.0
gi|8750114|gb|BE206716.1|BE206716 bb26f11.x1 NIH_MGC_5 Homo... 809 0.0
gi|1633911|gb|AA088398.1|AA088398 zl82h01.r1 Stratagene col... 741 0.0
gi|2269710|gb|AA527641.1|AA527641 ni29g12.s1 NCI_CGAP_Ew1 H... 680 0.0
gi|2212939|gb|AA484126.1|AA484126 ne77g09.s1 NCI_CGAP_Ew1 H... 672 0.0
gi|11614477|gb|BF527114.1|BF527114 602039563F2 NCI_CGAP_Brn... 642 0.0
gi|5854647|gb|AW005869.1|AW005869 wz90a12.x1 NCI_CGAP_Brn25... 642 0.0
gi|2211891|gb|AA483046.1|AA483046 ne71c01.s1 NCI_CGAP_Ew1 H... 638 0.0

>gi|177198|gb|AAA58352.1| (R)-3-hydroxybutyrate dehydrogenase

EST Search:

Sequences producing significant alignments: (bits) Value

gi|12783361|emb|AL519868.1|AL519868 AL519868 LTI_NFL004_NBC... 1675 0.0
gi|12797239|emb|AL533746.1|AL533746 AL533746 LTI_FL013_FBrn... 1620 0.0
gi|12916262|emb|AL565162.1|AL565162 AL565162 LTI_FL015_Brn1... 1493 0.0
gi|12783362|emb|AL519869.1|AL519869 AL519869 LTI_NFL004_NBC... 1285 0.0
gi|11971146|gb|BF685738.1|BF685738 602140418F1 NIH_MGC_46 H... 1269 0.0
gi|14178399|gb|BG830812.1|BG830812 602767532F1 NIH_MGC_42 H... 1235 0.0
gi|12951379|emb|AL582918.1|AL582918 AL582918 LTI_NFL010_BC2... 1203 0.0
gi|10201129|gb|BE779931.1|BE779931 601467958F1 NIH_MGC_67 H... 1160 0.0
gi|5664763|gb|AI928864.1|AI928864 au64c05.x1 Schneider feta... 1128 0.0
gi|13913479|gb|BG682082.1|BG682082 602630059F1 NCI_CGAP_Skn... 1122 0.0
gi|12797240|emb|AL533747.1|AL533747 AL533747 LTI_FL013_FBrn... 1110 0.0
gi|2716956|gb|AA707038.1|AA707038 zj32c08.s1 Soares_fetal_l... 1063 0.0
gi|2357785|gb|AA579601.1|AA579601 nm71h09.s1 NCI_CGAP_Co9 H... 1029 0.0
gi|3253464|gb|AI032767.1|AI032767 ox13h06.x1 Soares_fetal_l... 1017 0.0
gi|12797054|emb|AL533561.1|AL533561 AL533561 LTI_FL015_Brn1... 983 0.0
gi|2397741|gb|AA586927.1|AA586927 nn68g03.s1 NCI_CGAP_Lar1 ... 955 0.0

gi|11592515|gb|BF509217.1|BF509217 UI-H-BI4-aov-h-02-0-UI.s... 942 0.0
gi|6589783|gb|AW246790.1|AW246790 2822178.3prime NIH_MGC_7 ... 902 0.0
gi|6086780|gb|AW118196.1|AW118196 xd91b01.x1 Soares_NFL_T_G... 892 0.0
gi|2908208|gb|AA834609.1|AA834609 od64c08.s1 NCI_CGAP_GCB1 ... 888 0.0
gi|2713499|gb|AA703581.1|AA703581 zj14e02.s1 Soares_fetal_l... 839 0.0
gi|3934411|gb|AI291637.1|AI291637 qm85b07.x1 NCI_CGAP_Lu5 H... 835 0.0
gi|2875181|gb|AA806431.1|AA806431 oc23a07.s1 NCI_CGAP_GCB1 ... 817 0.0
gi|5810898|gb|AI983679.1|AI983679 wt50g04.x1 NCI_CGAP_Pan1 ... 801 0.0
gi|3182604|gb|AA996115.1|AA996115 ou98g04.s1 NCI_CGAP_Kid3 ... 801 0.0

gi|1964997|gb|AA312648.1|AA312648 EST183324 Jurkat T-cells ... 797 0.0

>gi|2338748|gb|AAB67236.1| oxidoreductase [Homo sapiens]

EST Search:

Sequences producing significant alignments: (bits) Value

gi|10300929|dbj|AV698958.1|AV698958 AV698958 GKC Homo sapie... 1100 0.0
gi|13669994|gb|BG618623.1|BG618623 602646057F1 NIH_MGC_76 H... 1088 0.0
gi|9876625|dbj|AV655611.1|AV655611 AV655611 GLC Homo sapien... 1043 0.0
gi|13542818|gb|BG545075.1|BG545075 602572263F1 NIH_MGC_77 H... 987 0.0
gi|13669741|gb|BG618370.1|BG618370 602645735F1 NIH_MGC_76 H... 932 0.0
gi|13669621|gb|BG618250.1|BG618250 602645983F1 NIH_MGC_76 H... 864 0.0
gi|9874191|dbj|AV653177.1|AV653177 AV653177 GLC Homo sapien... 860 0.0
gi|13574972|gb|BG567319.1|BG567319 602585811F1 NIH_MGC_76 H... 819 0.0
gi|6993788|gb|AW453012.1|AW453012 UI-H-BW1-ama-b-05-0-UI.s1... 809 0.0
gi|9878346|dbj|AV657332.1|AV657332 AV657332 GLC Homo sapien... 785 0.0
gi|10289690|dbj|AV687827.1|AV687827 AV687827 GKC Homo sapie... 728 0.0
gi|10294040|dbj|AV692177.1|AV692177 AV692177 GKC Homo sapie... 710 0.0
gi|10285234|dbj|AV683371.1|AV683371 AV683371 GKC Homo sapie... 690 0.0
gi|10293387|dbj|AV691524.1|AV691524 AV691524 GKC Homo sapie... 684 0.0
gi|4762302|gb|AI658732.1|AI658732 tu22h11.x1 NCI_CGAP_Pr28 ... 672 0.0
gi|13711093|gb|BG189406.1|BG189406 RST8451 Athersys RAGE Li... 664 0.0
gi|10285582|dbj|AV683719.1|AV683719 AV683719 GKC Homo sapie... 644 0.0

>gi|4506359|ref|NP_000311.1| quinoid dihydropteridine reductase; dihydropteridine reductase [Homo sapiens]

EST Search:

Sequences producing significant alignments: (bits) Value

gi|12908475|emb|AL561241.1|AL561241 AL561241 LTI_NFL010_BC2... 1816 0.0
gi|12781312|emb|AL517819.1|AL517819 AL517819 LTI_NFL011_NBC... 1774 0.0
gi|12788167|emb|AL524674.1|AL524674 AL524674 LTI_NFL003_NBC... 1768 0.0
gi|12797002|emb|AL533509.1|AL533509 AL533509 LTI_FL015_Brn1... 1764 0.0
gi|12899944|emb|AL556877.1|AL556877 AL556877 LTI_NFL006_PL2... 1752 0.0
gi|12790624|emb|AL527131.1|AL527131 AL527131 LTI_NFL003_NBC... 1713 0.0
gi|13981336|gb|BG706213.1|BG706213 602669493F1 NIH_MGC_96 H... 1596 0.0
gi|12790052|emb|AL526559.1|AL526559 AL526559 LTI_NFL003_NBC... 1590 0.0
gi|14062755|gb|BG752102.1|BG752102 602732090F1 NIH_MGC_43 H... 1586 0.0
gi|12781311|emb|AL517818.1|AL517818 AL517818 LTI_NFL011_NBC... 1570 0.0
gi|12950590|emb|AL582524.1|AL582524 AL582524 LTI_NFL010_BC2... 1552 0.0
gi|12899880|emb|AL556843.1|AL556843 AL556843 LTI_NFL006_PL2... 1530 0.0
gi|13979564|gb|BG705333.1|BG705333 602687849F1 NIH_MGC_95 H... 1495 0.0

gi|12916230|emb|AL565146.1|AL565146 AL565146 LTI_FL015_Brn1... 1463 0.0
gi|9132175|gb|BE312903.1|BE312903 601153331F1 NIH_MGC_19 Ho... 1461 0.0
gi|13980908|gb|BG706000.1|BG706000 602669137F1 NIH_MGC_96 H... 1441 0.0
gi|14651085|gb|BI196065.1|BI196065 602754509F1 NIH_MGC_19 H... 1439 0.0
gi|9133114|gb|BE261182.1|BE261182 601147690F1 NIH_MGC_19 Ho... 1431 0.0
gi|13406319|gb|BG474042.1|BG474042 602516601F1 NIH_MGC_16 H... 1417 0.0
gi|10149956|gb|BE735964.1|BE735964 601305311F1 NIH_MGC_39 H... 1415 0.0
gi|11099812|gb|BF206226.1|BF206226 601869219F1 NIH_MGC_19 H... 1409 0.0
gi|11641766|gb|BF568386.1|BF568386 602184579F1 NIH_MGC_42 H... 1402 0.0
gi|13988103|gb|BG709599.1|BG709599 602673640F1 NIH_MGC_96 H... 1400 0.0

gi|13987762|gb|BG709432.1|BG709432 602673489F1 NIH_MGC_96 H... 1392 0.0
gi|14654693|gb|BI199672.1|BI199672 602763290F1 NIH_MGC_19 H... 1380 0.0
gi|12339131|gb|BF971916.1|BF971916 602240318F1 NIH_MGC_46 H... 1368 0.0
gi|12338770|gb|BF971542.1|BF971542 602239795F1 NIH_MGC_46 H... 1368 0.0
gi|13994815|gb|BG715628.1|BG715628 602675965F1 NIH_MGC_96 H... 1364 0.0
gi|14081358|gb|BG770705.1|BG770705 602734055F1 NIH_MGC_49 H... 1350 0.0
gi|14073363|gb|BG762710.1|BG762710 602734619F1 NIH_MGC_49 H... 1340 0.0
gi|3666090|gb|AI144281.1|AI144281 qb59f10.x1 NCI_CGAP_Brn23... 1340 0.0
gi|12911388|emb|AL562705.1|AL562705 AL562705 LTI_NFL003_NBC... 1336 0.0
gi|9131800|gb|BE312725.1|BE312725 601149689F1 NIH_MGC_19 Ho... 1336 0.0
gi|13994083|gb|BG715150.1|BG715150 602675603F1 NIH_MGC_96 H... 1332 0.0
gi|11258064|gb|BF310495.1|BF310495 601894981F1 NIH_MGC_19 H... 1332 0.0
gi|12340581|gb|BF973366.1|BF973366 602242316F1 NIH_MGC_46 H... 1320 0.0
gi|13145363|gb|BG338925.1|BG338925 602436725F1 NIH_MGC_46 H... 1318 0.0
gi|14072266|gb|BG761613.1|BG761613 602717857F1 NIH_MGC_49 H... 1310 0.0
gi|14655059|gb|BI200038.1|BI200038 602763190F1 NIH_MGC_19 H... 1302 0.0
gi|13983017|gb|BG707042.1|BG707042 602670372F1 NIH_MGC_96 H... 1302 0.0
gi|14074488|gb|BG763835.1|BG763835 602735680F1 NIH_MGC_49 H... 1298 0.0
gi|12785791|emb|AL522298.1|AL522298 AL522298 LTI_NFL004_NBC... 1283 0.0
gi|12432839|gb|BG037025.1|BG037025 602287379F1 NIH_MGC_96 H... 1245 0.0
gi|14654739|gb|BI199718.1|BI199718 602760580F1 NIH_MGC_19 H... 1241 0.0
gi|9136444|gb|BE314836.1|BE314836 601147576F1 NIH_MGC_19 Ho... 1241 0.0
gi|13995161|gb|BG715974.1|BG715974 602674039F1 NIH_MGC_96 H... 1233 0.0
gi|11261670|gb|BF313632.1|BF313632 601900280F1 NIH_MGC_19 H... 1231 0.0
gi|10158621|gb|BE744629.1|BE744629 601577461F1 NIH_MGC_9 Ho... 1225 0.0
gi|9126143|gb|BE255699.1|BE255699 601110541F1 NIH_MGC_16 Ho... 1225 0.0
gi|10364341|gb|BE898155.1|BE898155 601440285F1 NIH_MGC_72 H... 1223 0.0
gi|10356002|gb|BE894035.1|BE894035 601437848F1 NIH_MGC_72 H... 1223 0.0
gi|13993594|gb|BG714663.1|BG714663 602677014F1 NIH_MGC_96 H... 1217 0.0
gi|13981830|gb|BG706461.1|BG706461 602670011F1 NIH_MGC_96 H... 1211 0.0
gi|13329170|gb|BG422664.1|BG422664 602449167F1 NIH_MGC_14 H... 1205 0.0
gi|11642541|gb|BF569161.1|BF569161 602184579T1 NIH_MGC_42 H... 1205 0.0
gi|10143373|gb|BE729381.1|BE729381 601561403F1 NIH_MGC_20 H... 1193 0.0
gi|12334642|gb|BF967427.1|BF967427 602287347F1 NIH_MGC_96 H... 1189 0.0
gi|13030449|gb|BG281524.1|BG281524 602402059F1 NIH_MGC_20 H... 1183 0.0
gi|13143494|gb|BG337056.1|BG337056 602434324F1 NIH_MGC_46 H... 1176 0.0
gi|13985863|gb|BG708479.1|BG708479 602672457F1 NIH_MGC_96 H... 1172 0.0
gi|12334371|gb|BF967156.1|BF967156 602287724F1 NIH_MGC_96 H... 1172 0.0
gi|10143660|gb|BE729668.1|BE729668 601562815F1 NIH_MGC_20 H... 1166 0.0
gi|13408539|gb|BG476260.1|BG476260 602525123F1 NIH_MGC_20 H... 1164 0.0
gi|10964924|gb|BF125884.1|BF125884 601763094F1 NIH_MGC_20 H... 1164 0.0
gi|3739860|gb|AI188651.1|AI188651 qd15g07.x1 Soares_placent... 1162 0.0
gi|13985115|gb|BG708103.1|BG708103 602671554F1 NIH_MGC_96 H... 1156 0.0
gi|9332444|gb|BE387079.1|BE387079 601275165F1 NIH_MGC_20 Ho... 1142 0.0
gi|9124995|gb|BE254566.1|BE254566 601115188F1 NIH_MGC_16 Ho... 1142 0.0
gi|12334862|gb|BF967647.1|BF967647 602287347T1 NIH_MGC_96 H... 1140 0.0
gi|11100810|gb|BF207224.1|BF207224 601870669F1 NIH_MGC_19 H... 1132 0.0
gi|12334887|gb|BF967672.1|BF967672 602287379T1 NIH_MGC_96 H... 1130 0.0
gi|13030971|gb|BG282045.1|BG282045 602402758F1 NIH_MGC_20 H... 1124 0.0
gi|13973958|gb|BG702530.1|BG702530 602684418F1 NIH_MGC_95 H... 1120 0.0
gi|11098635|gb|BF205049.1|BF205049 601866676F1 NIH_MGC_17 H... 1116 0.0
gi|6399286|gb|AW167761.1|AW167761 xn48g05.x1 Soares_NHCe_ce... 1110 0.0
gi|14052120|gb|BG741467.1|BG741467 602632257F1 NCI_CGAP_Skn... 1108 0.0
gi|9136756|gb|BE263218.1|BE263218 601145094F2 NIH_MGC_19 Ho... 1096 0.0

gi|9330889|gb|BE385524.1|BE385524 601278046F1 NIH_MGC_20 Ho... 1086 0.0
gi|8122899|gb|AW945148.1|AW945148 EST361341 MAGE resequence... 1076 0.0

gi|9126167|gb|BE255723.1|BE255723 601110574F1 NIH_MGC_16 Ho... 1067 0.0
gi|14075337|gb|BG764684.1|BG764684 602736768F1 NIH_MGC_49 H... 1065 0.0
gi|12335107|gb|BF967892.1|BF967892 602287724T1 NIH_MGC_96 H... 1045 0.0
gi|12415647|gb|BG027229.1|BG027229 602295923F1 NIH_MGC_86 H... 1043 0.0
gi|9335076|gb|BE389711.1|BE389711 601281955F1 NIH_MGC_44 Ho... 1039 0.0
gi|3658900|gb|AI142541.1|AI142541 qb47a12.x1 NCI_CGAP_Brn23... 1037 0.0
gi|12339043|gb|BF971828.1|BF971828 602240414F1 NIH_MGC_46 H... 1033 0.0
gi|9893798|gb|BE622858.1|BE622858 601441025T1 NIH_MGC_72 Ho... 1021 0.0
gi|3960473|gb|AI301127.1|AI301127 qo16f02.x1 NCI_CGAP_Lu5 H... 1011 0.0
gi|14407119|gb|BI003045.1|BI003045 MR3-HN0152-020201-007-c0... 1007 0.0
gi|6025803|gb|AW070805.1|AW070805 xa30e09.x1 NCI_CGAP_Br18 ... 999 0.0
gi|14172587|gb|BG825000.1|BG825000 602747441F1 NIH_MGC_17 H... 997 0.0
gi|10221442|gb|BE767784.1|BE767784 RC5-GN0046-040800-031-D0... 979 0.0
gi|5920706|gb|AW055003.1|AW055003 wy98c01.x1 NCI_CGAP_Brn23... 979 0.0
gi|5436685|gb|AI817606.1|AI817606 wk39d09.x1 NCI_CGAP_Pr22 ... 952 0.0
gi|11642937|gb|BF569557.1|BF569557 602186057F1 NIH_MGC_45 H... 928 0.0
gi|6798913|gb|AW328417.1|AW328417 ds02d10.x1 NIH_MGC_4 Homo... 926 0.0
gi|9869668|dbj|AV648654.1|AV648654 AV648654 GLC Homo sapien... 922 0.0
gi|14654708|gb|BI199687.1|BI199687 602760523F1 NIH_MGC_19 H... 916 0.0
gi|9869672|dbj|AV648658.1|AV648658 AV648658 GLC Homo sapien... 916 0.0
gi|7041436|gb|AW471330.1|AW471330 xw57h08.x1 NCI_CGAP_Pan1 ... 910 0.0

>gi|4506571|ref|NP_003699.1| microsomal NAD+-dependent retinol dehydrogenase 4 [Homo sapiens]

EST Search:

Sequences producing significant alignments: (bits) Value

gi|9882195|dbj|AV661181.1|AV661181 AV661181 GLC Homo sapien... 987 0.0
gi|9882144|dbj|AV661130.1|AV661130 AV661130 GLC Homo sapien... 928 0.0
gi|10297142|dbj|AV695279.1|AV695279 AV695279 GKC Homo sapie... 611 e-172
gi|10290555|dbj|AV688692.1|AV688692 AV688692 GKC Homo sapie... 595 e-167
gi|9868702|dbj|AV647688.1|AV647688 AV647688 GLC Homo sapien... 543 e-152
gi|9868612|dbj|AV647598.1|AV647598 AV647598 GLC Homo sapien... 543 e-152
gi|9868272|dbj|AV647258.1|AV647258 AV647258 GLC Homo sapien... 543 e-152
gi|9868493|dbj|AV647479.1|AV647479 AV647479 GLC Homo sapien... 504 e-140

>gi|7705855|ref|NP_057226.1| steroid dehydrogenase homolog [Homo sapiens]

EST Search:

Sequences producing significant alignments: (bits) Value

gi|14052291|gb|BG741638.1|BG741638 602635486F1 NCI_CGAP_Skn... 1558 0.0
gi|13906836|gb|BG675440.1|BG675440 602621769F1 NCI_CGAP_Skn... 1526 0.0
gi|13913842|gb|BG682445.1|BG682445 602630189F1 NCI_CGAP_Skn... 1425 0.0
gi|14049580|gb|BG779263.1|BG779263 602665945F1 NIH_MGC_60 H... 1413 0.0
gi|13996568|gb|BG717381.1|BG717381 602689723F1 NIH_MGC_97 H... 1404 0.0

gi|13995178|gb|BG715991.1|BG715991 602674063F1 NIH_MGC_96 H... 1370 0.0
gi|14511171|gb|BI092841.1|BI092841 602858662F1 NIH_MGC_10 H... 1346 0.0
gi|12670128|gb|BG163425.1|BG163425 602338406F1 NIH_MGC_89 H... 1346 0.0
gi|14511086|gb|BI092756.1|BI092756 602858554F1 NIH_MGC_10 H... 1332 0.0
gi|13987330|gb|BG709215.1|BG709215 602675095F1 NIH_MGC_96 H... 1332 0.0
gi|13910534|gb|BG679137.1|BG679137 602627203F1 NCI_CGAP_Skn... 1328 0.0
gi|13662470|gb|BG611099.1|BG611099 602612052F1 NIH_MGC_60 H... 1314 0.0
gi|13045302|gb|BG289447.1|BG289447 602381485F1 NIH_MGC_93 H... 1314 0.0
gi|13047173|gb|BG290374.1|BG290374 602388212F1 NIH_MGC_93 H... 1302 0.0
gi|13339353|gb|BG432847.1|BG432847 602496055F1 NIH_MGC_75 H... 1285 0.0
gi|10321791|gb|BE872911.1|BE872911 601451505F1 NIH_MGC_65 H... 1261 0.0
gi|13546503|gb|BG547838.1|BG547838 602576130F1 NIH_MGC_77 H... 1259 0.0
gi|13532633|gb|BG540400.1|BG540400 602568710F1 NIH_MGC_77 H... 1253 0.0
gi|13464096|gb|BG502579.1|BG502579 602549403F1 NIH_MGC_61 H... 1253 0.0
gi|12673441|gb|BG166738.1|BG166738 602339258F1 NIH_MGC_89 H... 1237 0.0
gi|13047275|gb|BG290433.1|BG290433 602388282F1 NIH_MGC_93 H... 1231 0.0
gi|12425026|gb|BG033087.1|BG033087 602300210F1 NIH_MGC_87 H... 1227 0.0
gi|12383684|gb|BF980872.1|BF980872 602304083F1 NIH_MGC_88 H... 1227 0.0
gi|9890063|gb|BE619038.1|BE619038 601472854F1 NIH_MGC_68 Ho... 1225 0.0
gi|12758336|gb|BG248520.1|BG248520 602400680F1 NIH_MGC_15 H... 1219 0.0
gi|13995758|gb|BG716571.1|BG716571 602677825F1 NIH_MGC_96 H... 1215 0.0
gi|9896933|gb|BE615334.1|BE615334 601280732F1 NIH_MGC_39 Ho... 1211 0.0
gi|12387354|gb|BF984542.1|BF984542 602307730F1 NIH_MGC_88 H... 1170 0.0
gi|13717172|gb|BG195485.1|BG195485 RST14677 Athersys RAGE L... 1168 0.0
gi|10401855|gb|BE907862.1|BE907862 601501989F1 NIH_MGC_70 H... 1166 0.0
gi|12670948|gb|BG164245.1|BG164245 602341256F1 NIH_MGC_89 H... 1152 0.0
gi|11331761|gb|BF369736.1|BF369736 QV4-GN0120-250900-427-c1... 1150 0.0
gi|2321379|gb|AA551127.1|AA551127 nk75g03.s1 NCI_CGAP_Sch1 ... 1150 0.0
gi|10744866|gb|BF036769.1|BF036769 601459836F1 NIH_MGC_66 H... 1146 0.0
gi|13528208|gb|BG536662.1|BG536662 602566285F1 NIH_MGC_77 H... 1144 0.0
gi|8147555|gb|AW957872.1|AW957872 EST369942 MAGE resequence... 1142 0.0
gi|12344922|gb|BF977707.1|BF977707 602148324F1 NIH_MGC_62 H... 1130 0.0
gi|11944012|gb|BF670117.1|BF670117 602119443F1 NIH_MGC_56 H... 1122 0.0
gi|13546026|gb|BG547348.1|BG547348 602574782F1 NIH_MGC_77 H... 1118 0.0
gi|12676722|gb|BG170019.1|BG170019 602323391F1 NIH_MGC_89 H... 1088 0.0
gi|11649900|gb|BF576188.1|BF576188 602132627F1 NIH_MGC_81 H... 1078 0.0
gi|14512380|gb|BI094050.1|BI094050 602860005F1 NIH_MGC_10 H... 1074 0.0
gi|13050007|gb|BG291790.1|BG291790 602386010F1 NIH_MGC_93 H... 1068 0.0
gi|13460516|gb|BG498986.1|BG498986 602544674F1 NIH_MGC_60 H... 1067 0.0
gi|10796504|dbj|AV714987.1|AV714987 AV714987 DCB Homo sapie... 1065 0.0
gi|12604885|gb|BG111281.1|BG111281 602283354F1 NIH_MGC_86 H... 1047 0.0
gi|14049576|gb|BG779259.1|BG779259 602665938F1 NIH_MGC_60 H... 1045 0.0
gi|11111634|gb|BF218048.1|BF218048 601882836F1 NIH_MGC_57 H... 1045 0.0
gi|12383548|gb|BF980736.1|BF980736 602303884F1 NIH_MGC_88 H... 1035 0.0
gi|14049921|gb|BG779604.1|BG779604 602668351F1 NIH_MGC_60 H... 1033 0.0
gi|11252265|gb|BF305371.1|BF305371 601892847F1 NIH_MGC_17 H... 1021 0.0
gi|13041668|gb|BG287637.1|BG287637 602384460F1 NIH_MGC_93 H... 1019 0.0
gi|12677991|gb|BG171288.1|BG171288 602322318F1 NIH_MGC_89 H... 1015 0.0
gi|4435867|gb|AI521732.1|AI521732 ti82c06.x1 NCI_CGAP_Kid11... 1007 0.0
gi|7136231|gb|AW498488.1|AW498488 EST0021 Human Fetal Brain... 1001 0.0
gi|12097334|gb|BF792280.1|BF792280 602252790F1 NIH_MGC_84 H... 991 0.0
gi|1522055|gb|AA044198.1|AA044198 zk50e08.r1 Soares_pregnan... 991 0.0
gi|14049653|gb|BG779336.1|BG779336 602665853F1 NIH_MGC_60 H... 973 0.0
gi|14049581|gb|BG779264.1|BG779264 602665946F1 NIH_MGC_60 H... 961 0.0
gi|1371208|gb|W63627.1|W63627 zc56f09.r1 Soares_parathyroid... 961 0.0
gi|7136229|gb|AW498487.1|AW498487 EST0020 Human Fetal Brain... 959 0.0
gi|11629318|gb|BF541849.1|BF541849 602069042F1 NIH_MGC_58 H... 954 0.0

gi|14003292|gb|BG724105.1|BG724105 602697407F1 NIH_MGC_97 H... 950 0.0
gi|14070365|gb|BG759712.1|BG759712 602711109F1 NIH_MGC_48 H... 940 0.0
gi|1735571|gb|AA161274.1|AA161274 zq38f09.r1 Stratagene hNT... 940 0.0
gi|12066633|gb|BF739957.1|BF739957 7o41d12.x1 NCI_CGAP_Kid1... 932 0.0
gi|11112382|gb|BF218886.1|BF218886 601885044F1 NIH_MGC_57 H... 928 0.0
gi|11977542|gb|BF692134.1|BF692134 602248727F1 NIH_MGC_62 H... 920 0.0
gi|11767406|gb|BE963886.2|BE963886 601657654R1 NIH_MGC_68 H... 912 0.0
gi|3920107|gb|AI281874.1|AI281874 qt68g10.x1 NCI_CGAP_Eso2 ... 910 0.0
gi|10970869|gb|BF131829.1|BF131829 601820750F1 NIH_MGC_58 H... 906 0.0
gi|13043036|gb|BG288319.1|BG288319 602383655F1 NIH_MGC_93 H... 900 0.0
gi|12345982|gb|BF978767.1|BF978767 602149103F2 NIH_MGC_62 H... 898 0.0
gi|5113976|gb|AI745688.1|AI745688 tr24h04.x1 NCI_CGAP_Ov23 ... 894 0.0
gi|1694006|gb|AA132312.1|AA132312 zo17g05.s1 Stratagene col... 874 0.0
gi|5875725|gb|AW022195.1|AW022195 df34b10.y1 Morton Fetal C... 870 0.0
gi|2113174|gb|AA429830.1|AA429830 zw60g07.r1 Soares_total_f... 868 0.0
gi|11257080|gb|BF309649.1|BF309649 601891975F1 NIH_MGC_17 H... 866 0.0
gi|11649499|gb|BF575787.1|BF575787 602134824F1 NIH_MGC_81 H... 858 0.0
gi|12339937|gb|BF972722.1|BF972722 602240976F1 NIH_MGC_46 H... 856 0.0
gi|5113967|gb|AI745679.1|AI745679 tr24g03.x1 NCI_CGAP_Ov23 ... 856 0.0
gi|4486633|gb|AI554270.1|AI554270 tq05b03.x1 NCI_CGAP_Ut3 H... 852 0.0
gi|9771262|gb|BE542617.1|BE542617 601067112F1 NIH_MGC_10 Ho... 848 0.0
gi|7043218|gb|AW473112.1|AW473112 xp68h08.x2 NCI_CGAP_Ov39 ... 848 0.0
gi|4372411|gb|AI479243.1|AI479243 tm56b07.x1 NCI_CGAP_Kid11... 844 0.0
gi|1138607|gb|N24457.1|N24457 yx15a03.r1 Soares melanocyte ... 837 0.0
gi|1577675|gb|AA070298.1|AA070298 zm68c06.r1 Stratagene neu... 831 0.0
gi|8909315|gb|BE221906.1|BE221906 hu04d07.x1 NCI_CGAP_Lu24 ... 821 0.0
gi|6975014|gb|AW439708.1|AW439708 hb87f06.x1 NCI_CGAP_Ut2 H... 809 0.0
gi|12077114|gb|BF750438.1|BF750438 RC1-BN0410-261000-013-a0... 803 0.0
gi|5232026|gb|AI765517.1|AI765517 wi81a05.x1 NCI_CGAP_Kid12... 803 0.0
gi|4969797|gb|AI692457.1|AI692457 wd70f09.x1 NCI_CGAP_Lu24 ... 803 0.0
gi|7667944|gb|AW753012.1|AW753012 QV0-CT0225-011199-041-h01... 801 0.0

>gi|3859946|gb|AAC72923.1| retinol dehydrogenase [Homo sapiens]

EST Search:

Sequences producing significant alignments: (bits) Value

gi|9868612|dbj|AV647598.1|AV647598 AV647598 GLC Homo sapien... 1041 0.0
gi|9868702|dbj|AV647688.1|AV647688 AV647688 GLC Homo sapien... 1017 0.0
gi|9882195|dbj|AV661181.1|AV661181 AV661181 GLC Homo sapien... 955 0.0
gi|9882144|dbj|AV661130.1|AV661130 AV661130 GLC Homo sapien... 928 0.0
gi|7310181|gb|AW605440.1|AW605440 PM1-DT0063-170100-002-h11... 880 0.0
gi|3432904|gb|AI093928.1|AI093928 qa27e04.s1 Soares_NhHMPu_... 825 0.0

>gi|8393516|ref|NP_057006.1| NAD(P) dependent steroid dehydrogenase-like; H105e3 [Homo sapiens]

EST Search:

Sequences producing significant alignments: (bits) Value

gi|12798924|emb|AL535431.1|AL535431 AL535431 LTI_FL013_FBrn... 1852 0.0
gi|12795943|emb|AL532450.1|AL532450 AL532450 LTI_NFL001_NBC... 1800 0.0
gi|12798925|emb|AL535432.1|AL535432 AL535432 LTI_FL013_FBrn... 1758 0.0

gi|12783081|emb|AL519588.1|AL519588 AL519588 LTI_NFL004_NBC... 1721 0.0
gi|12791348|emb|AL527855.1|AL527855 AL527855 LTI_NFL003_NBC... 1687 0.0
gi|12787933|emb|AL524440.1|AL524440 AL524440 LTI_NFL003_NBC... 1639 0.0
gi|12783082|emb|AL519589.1|AL519589 AL519589 LTI_NFL004_NBC... 1614 0.0
gi|12914749|emb|AL564391.1|AL564391 AL564391 LTI_NFL001_NBC... 1590 0.0
gi|14051016|gb|BG740363.1|BG740363 602634122F1 NCI_CGAP_Skn... 1550 0.0
gi|12787932|emb|AL524439.1|AL524439 AL524439 LTI_NFL003_NBC... 1548 0.0
gi|12890777|emb|AL552152.1|AL552152 AL552152 LTI_NFL006_PL2... 1542 0.0
gi|13402737|gb|BG470462.1|BG470462 602511345F1 NIH_MGC_16 H... 1509 0.0
gi|14053579|gb|BG742926.1|BG742926 602632016F1 NCI_CGAP_Skn... 1487 0.0
gi|12791349|emb|AL527856.1|AL527856 AL527856 LTI_NFL003_NBC... 1475 0.0
gi|13995873|gb|BG716686.1|BG716686 602678065F1 NIH_MGC_96 H... 1469 0.0
gi|13969104|gb|BG700101.1|BG700101 602679482F1 NIH_MGC_95 H... 1453 0.0
gi|12912123|emb|AL563072.1|AL563072 AL563072 LTI_NFL003_NBC... 1447 0.0
gi|14620007|gb|BI160006.1|BI160006 602864207F1 NIH_MGC_42 H... 1439 0.0
gi|13287087|gb|BG393639.1|BG393639 602412043F1 NIH_MGC_92 H... 1384 0.0
gi|12098534|gb|BF793480.1|BF793480 602254967F1 NIH_MGC_84 H... 1366 0.0
gi|12347277|gb|BF980062.1|BF980062 602288651T1 NIH_MGC_97 H... 1360 0.0
gi|13450037|gb|BG488530.1|BG488530 602534430F1 NIH_MGC_18 H... 1344 0.0
gi|10321873|gb|BE873097.1|BE873097 601451595F1 NIH_MGC_65 H... 1342 0.0
gi|12936786|emb|AL575531.1|AL575531 AL575531 LTI_NFL006_PL2... 1336 0.0
gi|12098227|gb|BF793173.1|BF793173 602253005F1 NIH_MGC_84 H... 1332 0.0
gi|9894650|gb|BE613053.1|BE613053 601451936T1 NIH_MGC_66 Ho... 1324 0.0
gi|13994535|gb|BG715352.1|BG715352 602677379F1 NIH_MGC_96 H... 1322 0.0
gi|9893974|gb|BE612377.1|BE612377 601451936F1 NIH_MGC_66 Ho... 1300 0.0
gi|4740315|gb|AI656336.1|AI656336 tt44h04.x1 NCI_CGAP_GC6 H... 1298 0.0
gi|12673903|gb|BG167200.1|BG167200 602345338F1 NIH_MGC_89 H... 1237 0.0
gi|9125384|gb|BE254951.1|BE254951 601115211F1 NIH_MGC_16 Ho... 1231 0.0
gi|10728677|dbj|AV710167.1|AV710167 AV710167 Cu Homo sapien... 1229 0.0
gi|12409317|gb|BG024095.1|BG024095 602303147F1 NIH_MGC_88 H... 1227 0.0
gi|12672161|gb|BG165458.1|BG165458 602345840F1 NIH_MGC_89 H... 1225 0.0
gi|12358345|gb|BF941025.1|BF941025 hu63d04.x1 NCI_CGAP_Brn4... 1213 0.0
gi|13521645|gb|BG530108.1|BG530108 602558776F1 NIH_MGC_61 H... 1209 0.0
gi|10035195|gb|BE674654.1|BE674654 7e10c08.x1 NCI_CGAP_Lu24... 1185 0.0
gi|12428756|gb|BG035023.1|BG035023 602325104F1 NIH_MGC_90 H... 1172 0.0
gi|6039708|gb|AW084556.1|AW084556 wz26e04.x1 Soares_Dieckgr... 1162 0.0
gi|4373215|gb|AI480047.1|AI480047 tm71e11.x1 NCI_CGAP_Brn25... 1138 0.0
gi|4289089|gb|AI433425.1|AI433425 ti65d04.x1 NCI_CGAP_Kid11... 1090 0.0
gi|11106808|gb|BF213222.1|BF213222 601844705F1 NIH_MGC_55 H... 1078 0.0
gi|10215890|gb|BE794692.1|BE794692 601590508F1 NIH_MGC_7 Ho... 1074 0.0
gi|14002691|gb|BG723504.1|BG723504 602694207F1 NIH_MGC_97 H... 1067 0.0
gi|8006977|gb|AW872924.1|AW872924 hq20a04.x1 NCI_CGAP_Adr1 ... 1059 0.0
gi|10328016|gb|BE879240.1|BE879240 601486988F1 NIH_MGC_69 H... 1047 0.0
gi|12346975|gb|BF979760.1|BF979760 602288651F1 NIH_MGC_97 H... 1027 0.0
gi|8139772|gb|AW950007.1|AW950007 EST362197 MAGE resequence... 1011 0.0
gi|12901543|emb|AL557690.1|AL557690 AL557690 LTI_FL012_TC1 ... 1005 0.0
gi|7236923|gb|AW572192.1|AW572192 xt75h04.x2 NCI_CGAP_Ut2 H... 975 0.0
gi|3446399|gb|AI096817.1|AI096817 qb35f07.x1 Soares_pregnan... 973 0.0
gi|14649236|gb|BI194216.1|BI194216 602945971F1 NIH_MGC_42 H... 961 0.0
gi|13141924|gb|BG335486.1|BG335486 602403957F1 NIH_MGC_21 H... 946 0.0
gi|12132238|gb|BF803249.1|BF803249 IL5-CI0149-011100-224-h0... 934 0.0
gi|4111947|gb|AI360326.1|AI360326 qy89e03.x1 NCI_CGAP_Brn25... 930 0.0
gi|2162963|gb|AA448943.1|AA448943 zx07a07.r1 Soares_total_f... 926 0.0
gi|12070667|gb|BF743991.1|BF743991 RC0-BT0812-181000-035-a0... 916 0.0
gi|7913755|gb|AW820761.1|AW820761 RC5-ST0300-270300-014-B08... 916 0.0
gi|2411270|gb|AA595924.1|AA595924 nn15h12.s1 NCI_CGAP_Co12 ... 904 0.0
gi|1802687|gb|AA207195.1|AA207195 zq73h05.r1 Stratagene neu... 900 0.0

gi|10829806|dbj|AV724928.1|AV724928 AV724928 HTB Homo sapie... 894 0.0
gi|3405877|gb|AI076699.1|AI076699 oz16f12.x1 Soares_fetal_l... 872 0.0
gi|14471711|gb|BI064184.1|BI064184 IL3-UT0119-180401-476-B0... 870 0.0
gi|5130990|gb|AI752726.1|AI752726 cn18d06.y1 Normal Human T... 839 0.0
gi|3418300|gb|AI081508.1|AI081508 oz53h08.x1 Soares_senesce... 833 0.0
gi|9323549|gb|BE378184.1|BE378184 601237939F1 NIH_MGC_44 Ho... 827 0.0
gi|10719367|dbj|AV703037.1|AV703037 AV703037 ADB Homo sapie... 823 0.0
gi|3434745|gb|AI095769.1|AI095769 qb30c05.x1 Soares_pregnan... 815 0.0

>gi|7661658|ref|NP_056325.1| DKFZP566O084 protein [Homo sapiens]

EST Search:

Sequences producing significant alignments: (bits) Value

gi|15019948|gb|BI335291.1|BI335291 602998213F1 NIH_MGC_12 H... 1463 0.0
gi|10219393|gb|BE798195.1|BE798195 601582662F1 NIH_MGC_7 Ho... 1411 0.0
gi|10156033|gb|BE742041.1|BE742041 601594721F1 NIH_MGC_9 Ho... 1400 0.0
gi|10150854|gb|BE736951.1|BE736951 601306912F1 NIH_MGC_39 H... 1392 0.0
gi|10216541|gb|BE795343.1|BE795343 601586662F1 NIH_MGC_7 Ho... 1376 0.0
gi|12678574|gb|BG171871.1|BG171871 602322675F1 NIH_MGC_89 H... 1279 0.0
gi|9331772|gb|BE386407.1|BE386407 601273578F1 NIH_MGC_20 Ho... 1249 0.0
gi|9148949|gb|BE274012.1|BE274012 601104628F1 NIH_MGC_14 Ho... 1239 0.0
gi|9334357|gb|BE388992.1|BE388992 601284814F1 NIH_MGC_44 Ho... 1229 0.0
gi|9335068|gb|BE389703.1|BE389703 601281945F1 NIH_MGC_44 Ho... 1172 0.0
gi|13409767|gb|BG477488.1|BG477488 602521540F1 NIH_MGC_20 H... 1164 0.0
gi|10206923|gb|BE785725.1|BE785725 601475291F1 NIH_MGC_68 H... 1160 0.0
gi|14073190|gb|BG762537.1|BG762537 602733994F1 NIH_MGC_49 H... 1098 0.0
gi|9335871|gb|BE390506.1|BE390506 601284123F1 NIH_MGC_44 Ho... 1072 0.0
gi|1383218|gb|W73084.1|W73084 zd54a11.r1 Soares_fetal_heart... 952 0.0
gi|5674161|gb|AI935291.1|AI935291 wp16e06.x1 NCI_CGAP_Lu19 ... 924 0.0
gi|844959|gb|R71442.1|R71442 yi51f01.r1 Soares placenta Nb2... 908 0.0
gi|1163805|gb|N40260.1|N40260 yx99g06.r1 Soares melanocyte ... 892 0.0
gi|5920966|gb|AW055263.1|AW055263 wz16b09.x1 NCI_CGAP_Ut4 H... 872 0.0
gi|12240526|gb|BF852782.1|BF852782 MR3-EN0087-151200-012-f0... 864 0.0
gi|1319356|gb|W37623.1|W37623 zc12d10.r1 Soares_parathyroid... 839 0.0
gi|1319173|gb|W37568.1|W37568 zc10c03.r1 Soares_parathyroid... 821 0.0

>gi|12804999|gb|AAH01953.1|AAH01953 oxidoreductase UCPA [Homo sapiens]

EST Search:

Sequences producing significant alignments: (bits) Value

gi|12786589|emb|AL523096.1|AL523096 AL523096 LTI_NFL003_NBC... 1764 0.0
gi|12889983|emb|AL551741.1|AL551741 AL551741 LTI_NFL006_PL2... 1675 0.0
gi|12793625|emb|AL530132.1|AL530132 AL530132 LTI_NFL001_NBC... 1481 0.0
gi|12936195|emb|AL575230.1|AL575230 AL575230 LTI_NFL006_PL2... 1477 0.0
gi|13294054|gb|BG400606.1|BG400606 602464263F1 NIH_MGC_75 H... 1451 0.0
gi|13452667|gb|BG491155.1|BG491155 602518792F1 NIH_MGC_18 H... 1392 0.0
gi|14051133|gb|BG740480.1|BG740480 602633875F1 NCI_CGAP_Skn... 1390 0.0
gi|13982652|gb|BG706873.1|BG706873 602672037F1 NIH_MGC_96 H... 1378 0.0
gi|3281013|gb|AI041819.1|AI041819 oy34a10.x1 Soares_parathy... 1354 0.0
gi|13545674|gb|BG547009.1|BG547009 602573805F1 NIH_MGC_77 H... 1336 0.0
gi|12793624|emb|AL530131.1|AL530131 AL530131 LTI_NFL001_NBC... 1336 0.0
gi|13976480|gb|BG703780.1|BG703780 602686804F1 NIH_MGC_95 H... 1328 0.0
gi|13039621|gb|BG286600.1|BG286600 602381608F1 NIH_MGC_93 H... 1304 0.0
gi|13544541|gb|BG545876.1|BG545876 602573161F1 NIH_MGC_77 H... 1302 0.0
gi|2839375|gb|AA780044.1|AA780044 zj24e12.s1 Soares_fetal_l... 1300 0.0
gi|11257955|gb|BF310393.1|BF310393 601895043F1 NIH_MGC_19 H... 1294 0.0
gi|12598260|gb|BG104418.1|BG104418 602311036F1 NIH_MGC_20 H... 1291 0.0
gi|12598014|gb|BG104172.1|BG104172 602310736F1 NIH_MGC_20 H... 1287 0.0
gi|4073201|gb|AI336274.1|AI336274 qt45e02.x1 Soares_fetal_l... 1277 0.0
gi|12606210|gb|BG112704.1|BG112704 602282264F1 NIH_MGC_86 H... 1263 0.0

gi|11265005|gb|BF316648.1|BF316648 601903206F1 NIH_MGC_19 H... 1263 0.0
gi|8154981|gb|AW965145.1|AW965145 EST377218 MAGE resequence... 1263 0.0
gi|3238050|gb|AI022809.1|AI022809 ow55f02.x1 Soares_parathy... 1255 0.0
gi|2877836|gb|AA808430.1|AA808430 oe53b08.s1 NCI_CGAP_Lu5 H... 1209 0.0
gi|6471396|gb|AW192697.1|AW192697 xl48h04.x1 NCI_CGAP_Pan1 ... 1193 0.0
gi|12910323|emb|AL562168.1|AL562168 AL562168 LTI_NFL003_NBC... 1178 0.0
gi|9186202|gb|BE302454.1|BE302454 ba65f04.y1 NIH_MGC_20 Hom... 1164 0.0
gi|5813571|gb|AI986294.1|AI986294 wz64c08.x1 NCI_CGAP_Mel15... 1156 0.0
gi|9323894|gb|BE378429.1|BE378429 601236767F1 NIH_MGC_44 Ho... 1142 0.0
gi|5109073|gb|AI740785.1|AI740785 wg24b10.x1 Soares_NSF_F8_... 1138 0.0
gi|3400111|gb|AI073467.1|AI073467 ov45a08.x1 Soares_testis_... 1126 0.0
gi|6228615|gb|AW157214.1|AW157214 au92h07.x1 Schneider feta... 1124 0.0
gi|9186195|gb|BE302447.1|BE302447 ba65e04.y1 NIH_MGC_20 Hom... 1120 0.0
gi|4435368|gb|AI521233.1|AI521233 to66f02.x1 NCI_CGAP_Gas4 ... 1080 0.0
gi|12875811|emb|AL543333.1|AL543333 AL543333 LTI_NFL006_PL2... 1068 0.0
gi|8750771|gb|BE207373.1|BE207373 ba65e04.x1 NIH_MGC_20 Hom... 1063 0.0
gi|2993433|gb|AA883903.1|AA883903 aj13a01.s1 Soares_parathy... 1061 0.0
gi|3255193|gb|AI034240.1|AI034240 ow09h12.x1 Soares_parathy... 1059 0.0
gi|10350081|gb|BE891095.1|BE891095 601432208F1 NIH_MGC_72 H... 1053 0.0
gi|8750775|gb|BE207377.1|BE207377 ba65f04.x1 NIH_MGC_20 Hom... 1035 0.0
gi|5858190|gb|AW009412.1|AW009412 ws82c11.x1 NCI_CGAP_Co3 H... 1035 0.0
gi|5546002|gb|AI871953.1|AI871953 wm53h05.x1 NCI_CGAP_Ut2 H... 1029 0.0
gi|2324986|gb|AA554447.1|AA554447 nl14h10.s1 NCI_CGAP_Br2 H... 1027 0.0
gi|4598887|gb|AI589839.1|AI589839 tm81a02.x1 NCI_CGAP_Brn25... 1017 0.0
gi|6200155|gb|AW152255.1|AW152255 xg40e03.x1 NCI_CGAP_Ut1 H... 1015 0.0
gi|2955773|gb|AA863294.1|AA863294 og93b12.s1 NCI_CGAP_Kid5 ... 1015 0.0
gi|2690528|gb|AA689601.1|AA689601 nv66b12.s1 NCI_CGAP_GCB1 ... 1013 0.0
gi|4834180|gb|AI669406.1|AI669406 ty32b07.x1 NCI_CGAP_Ut2 H... 1007 0.0
gi|9866597|dbj|AV645583.1|AV645583 AV645583 GLC Homo sapien... 999 0.0
gi|3001833|gb|AA886725.1|AA886725 oj52h06.s1 NCI_CGAP_Kid3 ... 999 0.0
gi|13546020|gb|BG547368.1|BG547368 602574776F1 NIH_MGC_77 H... 997 0.0
gi|13294752|gb|BG401304.1|BG401304 602465415F1 NIH_MGC_75 H... 997 0.0
gi|10367680|gb|BE855542.1|BE855542 7g15h08.x1 NCI_CGAP_Brn2... 995 0.0
gi|3086555|gb|AA932317.1|AA932317 oo70g12.s1 NCI_CGAP_GC4 H... 993 0.0
gi|3057816|gb|AA917926.1|AA917926 ol76h08.s1 NCI_CGAP_Kid3 ... 991 0.0
gi|9260891|gb|BE349038.1|BE349038 ht48c06.x1 NCI_CGAP_Mel15... 989 0.0
gi|5110966|gb|AI742678.1|AI742678 wg44h01.x1 Soares_NSF_F8_... 987 0.0
gi|2411344|gb|AA595998.1|AA595998 nn64h09.s1 NCI_CGAP_Lar1 ... 987 0.0
gi|11129201|gb|BF222024.1|BF222024 7p41b04.x1 NCI_CGAP_Pr28... 985 0.0
gi|10891010|gb|BF085209.1|BF085209 MR3-GN0029-110900-004-h0... 983 0.0
gi|1493027|gb|AA026818.1|AA026818 zk02b02.r1 Soares_pregnan... 983 0.0
gi|5661371|gb|AI925407.1|AI925407 wo20h04.x1 NCI_CGAP_Pan1 ... 979 0.0
gi|1320910|gb|W39201.1|W39201 zb35h02.r1 Soares_parathyroid... 979 0.0
gi|4085247|gb|AI348041.1|AI348041 qp56b07.x1 NCI_CGAP_Co8 H... 975 0.0
gi|13336418|gb|BG429912.1|BG429912 602499351F1 NIH_MGC_75 H... 969 0.0
gi|2875248|gb|AA806498.1|AA806498 oc23f11.s1 NCI_CGAP_GCB1 ... 967 0.0
gi|2156117|gb|AA443442.1|AA443442 zw94c04.r1 Soares_total_f... 967 0.0
gi|7412910|gb|AW651660.1|AW651660 ba17d12.y2 NIH_MGC_35 Hom... 965 0.0
gi|3155485|gb|AA978039.1|AA978039 oq55e12.s1 NCI_CGAP_Kid5 ... 965 0.0
gi|13340888|gb|BG434382.1|BG434382 602506384F1 NIH_MGC_79 H... 961 0.0
gi|5592517|gb|AI887353.1|AI887353 wm39c04.x1 NCI_CGAP_Ut4 H... 961 0.0
gi|3645373|gb|AI139401.1|AI139401 qc29a10.x1 Soares_pregnan... 961 0.0
gi|4075385|gb|AI338458.1|AI338458 qq92d04.x1 Soares_total_f... 959 0.0
gi|14083867|gb|BG773214.1|BG773214 602721957F1 NIH_MGC_97 H... 955 0.0
gi|3155394|gb|AA977948.1|AA977948 oq60h10.s1 NCI_CGAP_Kid6 ... 955 0.0
gi|2155983|gb|AA443308.1|AA443308 zw94c04.s1 Soares_total_f... 955 0.0
gi|13337258|gb|BG430752.1|BG430752 602498512F1 NIH_MGC_75 H... 950 0.0

gi|13964507|gb|BG697842.1|BG697842 602661052F1 NCI_CGAP_Skn... 948 0.0
gi|3281636|gb|AI042442.1|AI042442 oy14a03.x1 Soares_senesce... 944 0.0
gi|3179412|gb|AA992867.1|AA992867 ot76b02.s1 Soares_total_f... 940 0.0
gi|6302223|gb|AW163190.1|AW163190 au92h07.y1 Schneider feta... 934 0.0
gi|3423724|gb|AI085301.1|AI085301 qf18g03.x1 NCI_CGAP_Bm25... 934 0.0
gi|3017217|gb|AA890338.1|AA890338 aj94a11.s1 Soares_parathy... 932 0.0
gi|12925499|emb|AL569800.1|AL569800 AL569800 LTI_NFL006_PL2... 928 0.0
gi|10994439|dbj|AU133900.1|AU133900 AU133900 OVARC1 Homo sa... 928 0.0
gi|11016587|dbj|AU155066.1|AU155066 AU155066 OVARC1 Homo sa... 926 0.0
gi|3871543|gb|AI263340.1|AI263340 qq87h07.x1 Soares_total_f... 926 0.0
gi|2359920|gb|AA582560.1|AA582560 nn55c06.s1 NCI_CGAP_Kid6 ... 920 0.0
gi|1281745|gb|W07723.1|W07723 zb03b03.r1 Soares_fetal_lung_... 914 0.0
gi|2941643|gb|AA854105.1|AA854105 aj71a02.s1 Soares_parathy... 908 0.0
gi|12897527|emb|AL555621.1|AL555621 AL555621 LTI_NFL006_PL2... 886 0.0
gi|12875635|emb|AL543157.1|AL543157 AL543157 LTI_NFL006_PL2... 878 0.0
gi|12873084|emb|AL541734.1|AL541734 AL541734 LTI_FL002_PL1 ... 876 0.0
gi|9768144|gb|BE539499.1|BE539499 601060187F1 NIH_MGC_10 Ho... 874 0.0
gi|14653349|gb|BI198328.1|BI198328 602761334F1 NIH_MGC_19 H... 868 0.0
gi|11263603|gb|BF315365.1|BF315365 601902650F1 NIH_MGC_19 H... 868 0.0
gi|12875843|emb|AL543365.1|AL543365 AL543365 LTI_NFL006_PL2... 864 0.0
gi|14653113|gb|BI198092.1|BI198092 602762295F1 NIH_MGC_19 H... 852 0.0
gi|5665179|gb|AI929215.1|AI929215 au58e05.x1 Schneider feta... 848 0.0
gi|3241454|gb|AI025841.1|AI025841 ow12b07.s1 Soares_parathy... 848 0.0

>gi|4507709|ref|NP_003304.1| tissue specific transplantation antigen P35B; p35B; tissue specific transplantation antigen 3; Tissue-specific transplantation antigen-3; GDP-4-keto-6-deoxy-D-mannose epimerase-reductase [Homo sapiens]

EST Search:

Sequences producing significant alignments: (bits) Value

gi|12883797|emb|AL548615.1|AL548615 AL548615 LTI_NFL006_PL2... 1772 0.0
gi|12789331|emb|AL525838.1|AL525838 AL525838 LTI_NFL003_NBC... 1752 0.0
gi|13905346|gb|BG673954.1|BG673954 602620125F1 NCI_CGAP_Skn... 1649 0.0
gi|12792036|emb|AL528543.1|AL528543 AL528543 LTI_NFL001_NBC... 1628 0.0
gi|12789378|emb|AL525885.1|AL525885 AL525885 LTI_NFL003_NBC... 1620 0.0
gi|14060819|gb|BG750166.1|BG750166 602708953F1 NIH_MGC_43 H... 1580 0.0
gi|13584011|gb|BG576358.1|BG576358 602597077F1 NIH_MGC_87 H... 1576 0.0
gi|14808128|gb|BI255073.1|BI255073 602975916F1 NIH_MGC_12 H... 1532 0.0
gi|12932173|emb|AL573182.1|AL573182 AL573182 LTI_NFL006_PL2... 1520 0.0
gi|14170351|gb|BG822764.1|BG822764 602725927F1 NIH_MGC_15 H... 1501 0.0
gi|13582297|gb|BG574644.1|BG574644 602596643F1 NIH_MGC_87 H... 1491 0.0
gi|14504443|gb|BI086113.1|BI086113 602870179T1 NIH_MGC_98 H... 1465 0.0
gi|13031499|gb|BG282607.1|BG282607 602406274F1 NIH_MGC_91 H... 1425 0.0
gi|13987738|gb|BG709420.1|BG709420 602673472F1 NIH_MGC_96 H... 1419 0.0
gi|11974033|gb|BF688625.1|BF688625 602185261F1 NIH_MGC_43 H... 1390 0.0
gi|4997719|gb|AI707943.1|AI707943 as34g07.x1 Barstead aorta... 1372 0.0
gi|10153576|gb|BE739584.1|BE739584 601556554T1 NIH_MGC_58 H... 1362 0.0
gi|14050417|gb|BG739764.1|BG739764 602630479F1 NCI_CGAP_Skn... 1356 0.0
gi|12347310|gb|BF980095.1|BF980095 602288690T1 NIH_MGC_97 H... 1338 0.0
gi|11974420|gb|BF689012.1|BF689012 602185261T1 NIH_MGC_43 H... 1330 0.0
gi|14000222|gb|BG721035.1|BG721035 602692740F1 NIH_MGC_97 H... 1326 0.0
gi|12912349|emb|AL563185.1|AL563185 AL563185 LTI_NFL001_NBC... 1298 0.0
gi|6473452|gb|AW194598.1|AW194598 xn42b05.x1 NCI_CGAP_Kid11... 1285 0.0

gi|12384107|gb|BF981295.1|BF981295 602308539F1 NIH_MGC_88 H... 1283 0.0
gi|5745797|gb|AI953487.1|AI953487 wq29c04.x1 NCI_CGAP_Kid11... 1281 0.0
gi|12418870|gb|BG029773.1|BG029773 602296507F1 NIH_MGC_87 H... 1279 0.0
gi|10812855|gb|BF058959.1|BF058959 7k36d11.x1 NCI_CGAP_Ov18... 1279 0.0
gi|5037850|gb|AI720594.1|AI720594 as70e02.x1 Barstead colon... 1269 0.0
gi|13129704|gb|BG323267.1|BG323267 602421494F1 NIH_MGC_14 H... 1267 0.0
gi|14177350|gb|BG829763.1|BG829763 602764240F1 NIH_MGC_42 H... 1265 0.0
gi|13404586|gb|BG472311.1|BG472311 602513954F1 NIH_MGC_16 H... 1259 0.0
gi|9346533|gb|BE410083.1|BE410083 601302232F1 NIH_MGC_21 Ho... 1259 0.0
gi|4684533|gb|AI633203.1|AI633203 tz07e05.x1 NCI_CGAP_Ut1 H... 1259 0.0
gi|14677298|gb|BI223854.1|BI223854 602942773F1 NIH_MGC_12 H... 1255 0.0
gi|4764562|gb|AI660979.1|AI660979 wf20f11.x1 Soares_Dieckgr... 1253 0.0
gi|13329564|gb|BG423058.1|BG423058 602450261F1 NIH_MGC_14 H... 1247 0.0
gi|11250503|gb|BF303843.1|BF303843 601886640F2 NIH_MGC_17 H... 1241 0.0
gi|5593865|gb|AI888701.1|AI888701 wn34f08.x1 NCI_CGAP_Gas4 ... 1231 0.0
gi|8905436|gb|BE218030.1|BE218030 hv34e04.x1 NCI_CGAP_Lu24 ... 1227 0.0
gi|11971550|gb|BF686142.1|BF686142 602143377F1 NIH_MGC_46 H... 1225 0.0
gi|11130839|gb|BF223661.1|BF223661 7q78e07.x1 NCI_CGAP_Lu24... 1223 0.0
gi|14503965|gb|BI085635.1|BI085635 602870179F1 NIH_MGC_98 H... 1217 0.0
gi|12342081|gb|BF974866.1|BF974866 602245527F1 NIH_MGC_48 H... 1207 0.0
gi|12339751|gb|BF972536.1|BF972536 602242932F1 NIH_MGC_46 H... 1203 0.0
gi|10316825|gb|BE868049.1|BE868049 601444153F1 NIH_MGC_65 H... 1195 0.0
gi|13342831|gb|BG436325.1|BG436325 602508768F1 NIH_MGC_79 H... 1193 0.0
gi|13459197|gb|BG497680.1|BG497680 601859714F1 NIH_MGC_60 H... 1187 0.0
gi|13414805|gb|BG482526.1|BG482526 602527765F1 NIH_MGC_21 H... 1185 0.0
gi|14294354|gb|BG913878.1|BG913878 602810511F1 NCI_CGAP_Brn... 1183 0.0
gi|13451814|gb|BG490304.1|BG490304 602519301F1 NIH_MGC_18 H... 1181 0.0
gi|7704180|gb|AW772117.1|AW772117 hn67f10.x1 NCI_CGAP_Kid11... 1172 0.0
gi|12762969|gb|BG253153.1|BG253153 602363796F1 NIH_MGC_90 H... 1170 0.0
gi|6590433|gb|AW247440.1|AW247440 2819332.5prime NIH_MGC_7 ... 1162 0.0
gi|12603972|gb|BG110466.1|BG110466 602278881F1 NIH_MGC_86 H... 1160 0.0
gi|12426963|gb|BG034049.1|BG034049 602300978F1 NIH_MGC_87 H... 1158 0.0
gi|11443051|gb|BF431015.1|BF431015 7o18a05.x1 NCI_CGAP_Kid1... 1156 0.0
gi|9339602|gb|BE394237.1|BE394237 601311549F1 NIH_MGC_44 Ho... 1146 0.0
gi|6361205|gb|AI174814.1|AI174814 HA2535 Human fetal liver ... 1138 0.0
gi|10389807|gb|BE901034.1|BE901034 601674169F1 NIH_MGC_21 H... 1130 0.0
gi|2933350|gb|AA845591.1|AA845591 ak04g03.s1 Soares_parathy... 1106 0.0
gi|12725613|gb|BG230580.1|BG230580 naf40f04.x1 Soares_NPBMC... 1104 0.0
gi|11263814|gb|BF315551.1|BF315551 601899689F1 NIH_MGC_19 H... 1104 0.0
gi|9346913|gb|BE410463.1|BE410463 601302064F1 NIH_MGC_21 Ho... 1102 0.0
gi|4851563|gb|AI671832.1|AI671832 wb34e03.x1 NCI_CGAP_GC6 H... 1102 0.0
gi|2409463|gb|AA594113.1|AA594113 nm81f09.s1 NCI_CGAP_Co9 H... 1102 0.0
gi|6590289|gb|AW247296.1|AW247296 2819332.3prime NIH_MGC_7 ... 1096 0.0
gi|14252587|gb|BG875594.1|BG875594 RC0-CN0025-010200-012-h0... 1088 0.0
gi|6660479|gb|AW273449.1|AW273449 xr39g05.x1 NCI_CGAP_Ut4 H... 1068 0.0
gi|12344867|gb|BF977652.1|BF977652 602147454F1 NIH_MGC_62 H... 1059 0.0
gi|5767006|gb|AI970180.1|AI970180 wr08c02.x1 NCI_CGAP_Lu19 ... 1045 0.0
gi|9154860|gb|BE279864.1|BE279864 601157218F1 NIH_MGC_21 Ho... 1043 0.0
gi|6043887|gb|AW088082.1|AW088082 xc97c12.x1 NCI_CGAP_Brn35... 1041 0.0
gi|5660644|gb|AI924680.1|AI924680 wn74c04.x1 NCI_CGAP_Ut1 H... 1041 0.0
gi|7320037|gb|AW614851.1|AW614851 hh67d09.x1 NCI_CGAP_GU1 H... 1005 0.0
gi|14374439|gb|BG956268.1|BG956268 QV3-CT0616-190201-553-f1... 993 0.0
gi|5368755|gb|AI803283.1|AI803283 tc17c01.x1 Soares_NhHMPu_... 989 0.0
gi|14569068|gb|BI118167.1|BI118167 602867450F1 NIH_MGC_7 Ho... 977 0.0
gi|7319620|gb|AW614434.1|AW614434 hg83c06.x1 NCI_CGAP_Kid11... 973 0.0
gi|7044918|gb|AW474812.1|AW474812 xy20e11.x1 NCI_CGAP_Ut4 H... 973 0.0
gi|11983366|gb|BF697958.1|BF697958 602130044F1 NIH_MGC_56 H... 963 0.0

gi|7376393|gb|AW629603.1|AW629603 hh67d09.y1 NCI_CGAP_GU1 H... 961 0.0
gi|12908174|emb|AL561089.1|AL561089 AL561089 LTI_NFL010_BC2... 957 0.0
gi|3214460|gb|AI004950.1|AI004950 ot98b10.x1 Soares_total_f... 957 0.0
gi|3756666|gb|AI204060.1|AI204060 qe77h04.x1 Soares_fetal_l... 944 0.0
gi|10964119|gb|BF125079.1|BF125079 601762687F1 NIH_MGC_20 H... 936 0.0
gi|13032697|gb|BG283127.1|BG283127 602406778F1 NIH_MGC_91 H... 932 0.0
gi|13410684|gb|BG478405.1|BG478405 602523747F1 NIH_MGC_20 H... 928 0.0
gi|13030280|gb|BG281355.1|BG281355 602401842F1 NIH_MGC_20 H... 926 0.0
gi|5101285|gb|AI739304.1|AI739304 wi30c03.x1 NCI_CGAP_Co16 ... 924 0.0
gi|3754557|gb|AI201951.1|AI201951 qs77a10.x1 NCI_CGAP_Pr28 ... 922 0.0
gi|8140882|gb|AW951214.1|AW951214 EST363284 MAGE resequence... 920 0.0
gi|12042881|gb|BF726970.1|BF726970 by14h02.y1 Human Lens cD... 918 0.0
gi|7150886|gb|AW512808.1|AW512808 xm04b07.x1 NCI_CGAP_Ut1 H... 916 0.0
gi|9334131|gb|BE388766.1|BE388766 601283865F1 NIH_MGC_44 Ho... 904 0.0
gi|4149912|gb|AI371159.1|AI371159 ta09b06.x1 Soares_total_f... 892 0.0
gi|14505970|gb|BI087640.1|BI087640 602852161F1 NIH_MGC_10 H... 890 0.0
gi|4662870|gb|AI626070.1|AI626070 ar87f06.x1 Barstead colon... 890 0.0
gi|3693002|gb|AI160843.1|AI160843 qb65e01.x1 Soares_fetal_h... 888 0.0
gi|3400763|gb|AI074119.1|AI074119 oz54c02.x1 Soares_senesce... 884 0.0
gi|3735843|gb|AI185205.1|AI185205 qe47a05.x1 Soares_fetal_l... 882 0.0

Table 2: Mouse-SDRs derived from non redundant NCBI Database

EST Searches in human tissue

>gi¦5668733¦dbj¦BAA82656.1¦ UBE-1a [Mus musculus]

EST Search:
Organ: eye
Tissue type: retinoblastoma

Organ: brain
Tissue type: hippocampus

Organ: ovary
Tissue type: adenocarcinoma cell line

Organ: bone
Tissue type: osteosarcoma, cell line

Human Sequences producing significant alignments: (bits) Value

gi¦9124275¦gb¦BE253854.1¦BE253854 601112818F1 NIH_MGC_16 Ho... 454 e-125
gi¦13967002¦gb¦BG699072.1¦BG699072 602678713F1 NIH_MGC_95 H... 430 e-118
gi¦10156435¦gb¦BE742443.1¦BE742443 601575210F1 NIH_MGC_9 Ho... 428 e-117
gi¦12604238¦gb¦BG110732.1¦BG110732 602279029F1 NIH_MGC_86 H... 418 e-114
gi¦13401922¦gb¦BG469647.1¦BG469647 602534103F1 NIH_MGC_15 H... 412 e-112
gi¦12609069¦gb¦BG115563.1¦BG115563 602317253F1 NIH_MGC_88 H... 412 e-112
gi¦9186637¦gb¦BE302889.1¦BE302889 ba70g10.y1 NIH_MGC_20 Hom... 406 e-111
gi¦12761697¦gb¦BG251881.1¦BG251881 602364502F1 NIH_MGC_90 H... 402 e-109
gi¦14809963¦gb¦BI255993.1¦BI255993 602976353F1 NIH_MGC_12 H... 394 e-107
gi¦12678524¦gb¦BG171821.1¦BG171821 602322603F1 NIH_MGC_89 H... 393 e-106
gi¦10160188¦gb¦BE746196.1¦BE746196 601578644F1 NIH_MGC_9 Ho... 391 e-106

gi¦12687397¦gb¦BG180694.1¦BG180694 602329481F1 NIH_MGC_91 H... 373 e-100
gi¦13336094¦gb¦BG429588.1¦BG429588 602501268F1 NIH_MGC_75 H... 371 e-100
gi¦8144363¦gb¦AW954680.1¦AW954680 EST366750 MAGE resequence... 371 e-100
gi¦13999085¦gb¦BG719898.1¦BG719898 602691430F1 NIH_MGC_97 H... 357 7e-96
gi¦11953928¦gb¦BF680033.1¦BF680033 602154752F1 NIH_MGC_83 H... 357 7e-96
gi¦13972135¦gb¦BG701616.1¦BG701616 602682503F1 NIH_MGC_95 H... 345 3e-92
gi¦10348906¦gb¦BE890514.1¦BE890514 601431585F1 NIH_MGC_72 H... 345 3e-92
gi¦13969001¦gb¦BG700048.1¦BG700048 602681055F1 NIH_MGC_95 H... 343 1e-91
gi¦9770617¦gb¦BE541972.1¦BE541972 601064273F1 NIH_MGC_10 Ho... 331 4e-88

>gi¦5668735¦dbj¦BAA82657.1¦ UBE-1b [Mus musculus]

EST Search:

Organ: eye
Tissue type: retinoblastoma

Organ: ovary
Tissue type: adenocarcinoma cell line

Organ: brain
Tissue type: hippocampus

Organ: colon
Tissue type: adenocarcinoma cell line

Human Sequences producing significant alignments: (bits) Value

gi|9124275|gb|BE253854.1|BE253854 601112818F1 NIH_MGC_16 Ho... 438 e-120
gi|10156435|gb|BE742443.1|BE742443 601575210F1 NIH_MGC_9 Ho... 412 e-112
gi|13967002|gb|BG699072.1|BG699072 602678713F1 NIH_MGC_95 H... 400 e-109
gi|13401922|gb|BG469647.1|BG469647 602534103F1 NIH_MGC_15 H... 396 e-108
gi|12604238|gb|BG110732.1|BG110732 602279029F1 NIH_MGC_86 H... 389 e-105
gi|12761697|gb|BG251881.1|BG251881 602364502F1 NIH_MGC_90 H... 387 e-105
gi|12609069|gb|BG115563.1|BG115563 602317253F1 NIH_MGC_88 H... 383 e-103
gi|14809963|gb|BI255993.1|BI255993 602976353F1 NIH_MGC_12 H... 379 e-102
gi|9186637|gb|BE302889.1|BE302889 ba70g10.y1 NIH_MGC_20 Hom... 377 e-102

gi|10160188|gb|BE746196.1|BE746196 601578644F1 NIH_MGC_9 Ho... 375 e-101
gi|12678524|gb|BG171821.1|BG171821 602322603F1 NIH_MGC_89 H... 369 2e-99
gi|8144363|gb|AW954680.1|AW954680 EST366750 MAGE resequence... 355 3e-95
gi|12687397|gb|BG180694.1|BG180694 602329481F1 NIH_MGC_91 H... 349 2e-93
gi|13336094|gb|BG429588.1|BG429588 602501268F1 NIH_MGC_75 H... 341 4e-91
gi|13999085|gb|BG719898.1|BG719898 602691430F1 NIH_MGC_97 H... 327 7e-87
gi|11953928|gb|BF680033.1|BF680033 602154752F1 NIH_MGC_83 H... 327 7e-87
gi|10348906|gb|BE890514.1|BE890514 601431585F1 NIH_MGC_72 H... 323 1e-85
gi|13972135|gb|BG701616.1|BG701616 602682503F1 NIH_MGC_95 H... 315 3e-83
gi|14053553|gb|BG742900.1|BG742900 602632481F1 NCI_CGAP_Skn... 313 1e-82
gi|9770617|gb|BE541972.1|BE541972 601064273F1 NIH_MGC_10 Ho... 305 2e-80

>gi|12835589|dbj|BAB23296.1| putative [Mus musculus]

EST Search:

Organ: eye
Tissue type: retinoblastoma

Organ: brain
Tissue type: hippocampus

Organ: ovary
Tissue type: adenocarcinoma cell line

Organ: bone
Tissue type: osteosarcoma, cell line

Human Sequences producing significant alignments: (bits) Value

gi|9124275|gb|BE253854.1|BE253854 601112818F1 NIH_MGC_16 Ho... 454 e-125
gi|13967002|gb|BG699072.1|BG699072 602678713F1 NIH_MGC_95 H... 430 e-118
gi|10156435|gb|BE742443.1|BE742443 601575210F1 NIH_MGC_9 Ho... 428 e-117
gi|12604238|gb|BG110732.1|BG110732 602279029F1 NIH_MGC_86 H... 418 e-114
gi|13401922|gb|BG469647.1|BG469647 602534103F1 NIH_MGC_15 H... 412 e-112
gi|12609069|gb|BG115563.1|BG115563 602317253F1 NIH_MGC_88 H... 412 e-112

gi¦9186637¦gb¦BE302889.1¦BE302889 ba70g10.y1 NIH_MGC_20 Hom... 406 e-111

gi¦12761697¦gb¦BG251881.1¦BG251881 602364502F1 NIH_MGC_90 H... 402 e-109
gi¦14809963¦gb¦BI255993.1¦BI255993 602976353F1 NIH_MGC_12 H... 394 e-107
gi¦12678524¦gb¦BG171821.1¦BG171821 602322603F1 NIH_MGC_89 H... 393 e-106
gi¦10160188¦gb¦BE746196.1¦BE746196 601578644F1 NIH_MGC_9 Ho... 391 e-106
gi¦12687397¦gb¦BG180694.1¦BG180694 602329481F1 NIH_MGC_91 H... 373 e-100
gi¦13336094¦gb¦BG429588.1¦BG429588 602501268F1 NIH_MGC_75 H... 371 e-100
gi¦8144363¦gb¦AW954680.1¦AW954680 EST366750 MAGE resequence... 371 e-100
gi¦13999085¦gb¦BG719898.1¦BG719898 602691430F1 NIH_MGC_97 H... 357 7e-96
gi¦11953928¦gb¦BF680033.1¦BF680033 602154752F1 NIH_MGC_83 H... 357 7e-96
gi¦13972135¦gb¦BG701616.1¦BG701616 602682503F1 NIH_MGC_95 H... 345 3e-92
gi¦10348906¦gb¦BE890514.1¦BE890514 601431585F1 NIH_MGC_72 H... 345 3e-92
gi¦13969001¦gb¦BG700048.1¦BG700048 602681055F1 NIH_MGC_95 H... 343 1e-91
gi¦9770617¦gb¦BE541972.1¦BE541972 601064273F1 NIH_MGC_10 Ho... 331 4e-88

>gi¦12848558¦dbj¦BAB27997.1¦ putative [Mus musculus]

EST Search:

Organ: eye
Tissue type: retinoblastoma

Organ: ovary
Tissue type: adenocarcinoma cell line

Organ: brain
Tissue type: hippocampus

Organ: colon
Tissue type: adenocarcinoma cell line

Human Sequences producing significant alignments: (bits) Value

gi¦9124275¦gb¦BE253854.1¦BE253854 601112818F1 NIH_MGC_16 Ho... 454 e-125
gi¦10156435¦gb¦BE742443.1¦BE742443 601575210F1 NIH_MGC_9 Ho... 428 e-117
gi¦13967002¦gb¦BG699072.1¦BG699072 602678713F1 NIH_MGC_95 H... 422 e-115
gi¦13401922¦gb¦BG469647.1¦BG469647 602534103F1 NIH_MGC_15 H... 412 e-112
gi¦12604238¦gb¦BG110732.1¦BG110732 602279029F1 NIH_MGC_86 H... 410 e-112
gi¦12609069¦gb¦BG115563.1¦BG115563 602317253F1 NIH_MGC_88 H... 404 e-110
gi¦12761697¦gb¦BG251881.1¦BG251881 602364502F1 NIH_MGC_90 H... 402 e-109
gi¦9186637¦gb¦BE302889.1¦BE302889 ba70g10.y1 NIH_MGC_20 Hom... 398 e-108
gi¦14809963¦gb¦BI255993.1¦BI255993 602976353F1 NIH_MGC_12 H... 394 e-107
gi¦10160188¦gb¦BE746196.1¦BE746196 601578644F1 NIH_MGC_9 Ho... 391 e-106
gi¦12678524¦gb¦BG171821.1¦BG171821 602322603F1 NIH_MGC_89 H... 385 e-104
gi¦8144363¦gb¦AW954680.1¦AW954680 EST366750 MAGE resequence... 371 e-100
gi¦12687397¦gb¦BG180694.1¦BG180694 602329481F1 NIH_MGC_91 H... 365 5e-98
gi¦13336094¦gb¦BG429588.1¦BG429588 602501268F1 NIH_MGC_75 H... 363 2e-97
gi¦13999085¦gb¦BG719898.1¦BG719898 602691430F1 NIH_MGC_97 H... 349 3e-93
gi¦11953928¦gb¦BF680033.1¦BF680033 602154752F1 NIH_MGC_83 H... 349 3e-93
gi¦13972135¦gb¦BG701616.1¦BG701616 602682503F1 NIH_MGC_95 H... 337 1e-89
gi¦10348906¦gb¦BE890514.1¦BE890514 601431585F1 NIH_MGC_72 H... 337 1e-89
gi¦13969001¦gb¦BG700048.1¦BG700048 602681055F1 NIH_MGC_95 H... 335 4e-89
gi¦14053553¦gb¦BG742900.1¦BG742900 602632481F1 NCI_CGAP_Skn... 329 3e-87

>gi|12850643|dbj|BAB28800.1| putative [Mus musculus]

EST Search:

Tissue type: T cells from T cell leukemia

Tissue type: T cells from T cell leukemia

Tissue type: placenta

Organ: brain
Tissue type: neuroblastoma

Organ: brain
Tissue type: neuroblastoma cells

Human Sequences producing significant alignments: (bits) Value

gi|12903888|emb|AL558907.1|AL558907 AL558907 LTI_NFL008_TC2... 613 e-173
gi|12900345|emb|AL557084.1|AL557084 AL557084 LTI_FL012_TC1 ... 613 e-173
gi|12897788|emb|AL555756.1|AL555756 AL555756 LTI_NFL006_PL2... 613 e-173
gi|13515355|gb|BG519629.1|BG519629 602578744F1 NIH_MGC_19 H... 611 e-172
gi|12952470|emb|AL583473.1|AL583473 AL583473 LTI_NFL004_NBC... 609 e-172
gi|12783279|emb|AL519786.1|AL519786 AL519786 LTI_NFL004_NBC... 607 e-171
gi|13515189|gb|BG519532.1|BG519532 602578613F1 NIH_MGC_19 H... 593 e-167
gi|12903886|emb|AL558906.1|AL558906 AL558906 LTI_NFL008_TC2... 593 e-167
gi|12900344|emb|AL557083.1|AL557083 AL557083 LTI_FL012_TC1 ... 593 e-167
gi|12790972|emb|AL527479.1|AL527479 AL527479 LTI_NFL003_NBC... 583 e-164
gi|14177068|gb|BG829481.1|BG829481 602763779F1 NIH_MGC_42 H... 571 e-160
gi|13583928|gb|BG576275.1|BG576275 602595778F1 NIH_MGC_87 H... 565 e-158
gi|10157401|gb|BE743409.1|BE743409 601573650F1 NIH_MGC_9 Ho... 565 e-158
gi|10161376|gb|BE747384.1|BE747384 601580434F1 NIH_MGC_9 Ho... 561 e-157
gi|14177225|gb|BG829638.1|BG829638 602763994F1 NIH_MGC_42 H... 557 e-156
gi|13980226|gb|BG705661.1|BG705661 602668874F1 NIH_MGC_96 H... 543 e-152
gi|12786487|emb|AL522994.1|AL522994 AL522994 LTI_NFL003_NBC... 541 e-151
gi|9806674|gb|BE562954.1|BE562954 601336395F1 NIH_MGC_44 Ho... 539 e-151
gi|12340198|gb|BF972983.1|BF972983 602241285F1 NIH_MGC_46 H... 537 e-150
gi|14060190|gb|BG749537.1|BG749537 602707687F1 NIH_MGC_43 H... 535 e-150

>gi|12851759|dbj|BAB29156.1| putative [Mus musculus]

EST Search:

Organ: colon
Tissue type: adenocarcinoma cell line

Organ: pancreas
Tissue type: adenocarcinoma

Organ: lung
Tissue type: small cell carcinoma
Cell line: MGC3

Organ: ovary
Tissue type: fibrotheoma

Human Sequences producing significant alignments: (bits) Value

gi|13135151|gb|BG328713.1|BG328713 602427988F1 NIH_MGC_15 H... 369 1e-99
gi|10149412|gb|BE735420.1|BE735420 601304204F1 NIH_MGC_39 H... 365 2e-98
gi|9141043|gb|BE267452.1|BE267452 601189745F2 NIH_MGC_7 Hom... 359 1e-96
gi|10984835|gb|BF115433.1|BF115433 7n81h06.x1 NCI_CGAP_Ov18... 355 2e-95
gi|10700778|gb|BF000503.1|BF000503 7h32a01.x1 NCI_CGAP_Co16... 345 2e-92
gi|6197433|gb|AW149537.1|AW149537 xf39b12.x1 NCI_CGAP_Brn50... 341 3e-91
gi|14080921|gb|BG770268.1|BG770268 602744858F1 NIH_MGC_49 H... 339 1e-90
gi|13411959|gb|BG479680.1|BG479680 602527142F1 NIH_MGC_21 H... 339 1e-90
gi|10940810|gb|BF111120.1|BF111120 7n43g10.x1 NCI_CGAP_Lu24... 337 5e-90
gi|9510747|gb|BE464972.1|BE464972 hv76a11.x1 NCI_CGAP_Lu24 ... 335 2e-89
gi|13134589|gb|BG328151.1|BG328151 602427216F1 NIH_MGC_15 H... 331 3e-88
gi|6710858|gb|AW301181.1|AW301181 xs57d11.x1 NCI_CGAP_Kid11... 331 3e-88
gi|11450749|gb|BF438232.1|BF438232 7q68g12.x1 NCI_CGAP_Lu24... 327 5e-87
gi|6709918|gb|AW300318.1|AW300318 xs59g06.x1 NCI_CGAP_Kid11... 327 5e-87
gi|3056175|gb|AA916783.1|AA916783 on10d05.s1 NCI_CGAP_Lu5 H... 325 2e-86
gi|9126816|gb|BE256444.1|BE256444 601108430F1 NIH_MGC_16 Ho... 323 8e-86
gi|4985638|gb|AI697738.1|AI697738 we16g07.x1 NCI_CGAP_Lu24 ... 321 3e-85
gi|3675611|gb|AI147929.1|AI147929 qb38g05.x1 Soares_pregnan... 319 1e-84
gi|13705885|gb|BG184198.1|BG184198 RST3119 Athersys RAGE Li... 313 8e-83
gi|9333920|gb|BE388555.1|BE388555 601281843F1 NIH_MGC_44 Ho... 313 8e-83

>gi|12861668|dbj|BAB32258.1| putative [Mus musculus]

EST Search:

Tissue type: corresponding non cancerous liver tissue
Develop. stage: Adult

Organ: kidney

Organ: pancreas
Tissue type: epithelioid carcinoma cell line

Organ: testis

Organ: brain
Tissue type: hippocampus

Human Sequences producing significant alignments: (bits) Value

gi|9875702|dbj|AV654688.1|AV654688 AV654688 GLC Homo sapien... 168 2e-39
gi|7702359|gb|AW770318.1|AW770318 hl78e09.x1 NCI_CGAP_Kid13... 123 1e-25
gi|14178068|gb|BG830481.1|BG830481 602767043F1 NIH_MGC_42 H... 121 5e-25
gi|13999085|gb|BG719898.1|BG719898 602691430F1 NIH_MGC_97 H... 121 5e-25
gi|13967002|gb|BG699072.1|BG699072 602678713F1 NIH_MGC_95 H... 121 5e-25
gi|12609069|gb|BG115563.1|BG115563 602317253F1 NIH_MGC_88 H... 121 5e-25
gi|12604238|gb|BG110732.1|BG110732 602279029F1 NIH_MGC_86 H... 121 5e-25
gi|9186637|gb|BE302889.1|BE302889 ba70g10.y1 NIH_MGC_20 Hom... 121 5e-25
gi|8144363|gb|AW954680.1|AW954680 EST366750 MAGE resequence... 121 5e-25
gi|1298897|gb|W22050.1|W22050 61A4 Human retina cDNA Tsp509... 121 5e-25

gi|10348906|gb|BE890514.1|BE890514 601431585F1 NIH_MGC_72 H... 115 3e-23
gi|13336094|gb|BG429588.1|BG429588 602501268F1 NIH_MGC_75 H... 113 1e-22
gi|13527202|gb|BG535657.1|BG535657 602563366F1 NIH_MGC_77 H... 111 5e-22
gi|13523981|gb|BG532442.1|BG532442 602561968F1 NIH_MGC_61 H... 111 5e-22
gi|1960040|gb|AA307691.1|AA307691 EST178577 Colon carcinoma... 111 5e-22
gi|9186545|gb|BE302797.1|BE302797 ba69a06.y1 NIH_MGC_20 Hom... 109 2e-21
gi|13972135|gb|BG701616.1|BG701616 602682503F1 NIH_MGC_95 H... 107 8e-21
gi|13969001|gb|BG700048.1|BG700048 602681055F1 NIH_MGC_95 H... 107 8e-21
gi|9770617|gb|BE541972.1|BE541972 601064273F1 NIH_MGC_10 Ho... 107 8e-21
gi|13336068|gb|BG429562.1|BG429562 602501238F1 NIH_MGC_75 H... 105 3e-20

>gi|14318640|gb|AAH09118.1|AAH09118 Unknown (protein for MGC:6971) [Mus musculus]

EST Search:

Organ: lung
Tissue type: carcinoid

Tissue type: Adrenal gland

Organ: liver
Tissue type: adenocarcinoma, cell line

Organ: lymph node
Tissue type: follicular lymphoma

Human Sequences producing significant alignments: (bits) Value

gi|10940429|gb|BF110739.1|BF110739 7n56b09.x1 NCI_CGAP_Lu24... 367 5e-99
gi|10721718|dbj|AV704400.1|AV704400 AV704400 ADB Homo sapie... 341 3e-91
gi|12613045|gb|BG119539.1|BG119539 602347238F1 NIH_MGC_90 H... 305 2e-80
gi|1472212|gb|AA011185.1|AA011185 ze22d01.s1 Soares_fetal_h... 293 6e-77
gi|3838022|gb|AI242625.1|AI242625 qu37c10.x1 NCI_CGAP_Lym5 ... 212 2e-52
gi|14166353|gb|BG818766.1|BG818766 602779096F2 NCI_CGAP_Brn... 180 6e-43
gi|13708617|gb|BG186930.1|BG186930 RST5907 Athersys RAGE Li... 153 1e-34
gi|4331367|gb|AI469277.1|AI469277 tm07g05.x1 NCI_CGAP_Co14 ... 153 1e-34
gi|3677291|gb|AI148822.1|AI148822 qc65e11.x1 Soares_placent... 153 1e-34
gi|3145479|gb|AA969966.1|AA969966 op60e04.s1 Soares_NFL_T_G... 153 1e-34
gi|13707564|gb|BG185877.1|BG185877 RST4830 Athersys RAGE Li... 151 6e-34
gi|10897098|gb|BF091388.1|BF091388 CM0-TN0034-150900-551-e0... 145 3e-32
gi|5744726|gb|AI952416.1|AI952416 wx73e03.x1 NCI_CGAP_Ov38 ... 145 3e-32
gi|8166900|gb|AW975682.1|AW975682 EST387791 MAGE resequence... 127 8e-27
gi|3040766|gb|AA905643.1|AA905643 oj97e05.s1 Soares_NFL_T_G... 127 8e-27
gi|14051179|gb|BG740526.1|BG740526 602633034F1 NCI_CGAP_Skn... 115 3e-23
gi|12610022|gb|BG116516.1|BG116516 602317614F1 NIH_MGC_88 H... 113 1e-22
gi|2767868|gb|AA736634.1|AA736634 nw53d05.s1 NCI_CGAP_Ew1 H... 113 1e-22
gi|2752111|gb|AA730907.1|AA730907 nw50c08.s1 NCI_CGAP_Ew1 H... 96 3e-17
gi|8015591|gb|AW877247.1|AW877247 PM3-PT0039-010300-001-b06... 80 2e-12

>gi|13097495|gb|AAH03479.1|AAH03479 Unknown (protein for MGC:6908) [Mus musculus]

EST Search:

Organ: skin
Tissue type: melanotic melanoma, high MDR (cell line)

Organ: placenta

Organ: ovary
Tissue type: adenocarcinoma cell line

Organ: lung
Tissue type: small cell carcinoma

Human Sequences producing significant alignments: (bits) Value

gi|14073190|gb|BG762537.1|BG762537 602733994F1 NIH_MGC_49 H... 339 1e-90
gi|844959|gb|R71442.1|R71442 yi51f01.r1 Soares placenta Nb2... 321 3e-85
gi|10156033|gb|BE742041.1|BE742041 601594721F1 NIH_MGC_9 Ho... 313 8e-83
gi|10219393|gb|BE798195.1|BE798195 601582662F1 NIH_MGC_7 Ho... 297 4e-78
gi|10216541|gb|BE795343.1|BE795343 601586662F1 NIH_MGC_7 Ho... 297 4e-78
gi|10150854|gb|BE736951.1|BE736951 601306912F1 NIH_MGC_39 H... 297 4e-78
gi|9331772|gb|BE386407.1|BE386407 601273578F1 NIH_MGC_20 Ho... 297 4e-78
gi|1146469|gb|N28234.1|N28234 EST51e15 WATM1 Homo sapiens c... 283 7e-74
gi|9334357|gb|BE388992.1|BE388992 601284814F1 NIH_MGC_44 Ho... 281 3e-73
gi|9148949|gb|BE274012.1|BE274012 601104628F1 NIH_MGC_14 Ho... 270 1e-69
gi|6926374|gb|AW407317.1|AW407317 UI-HF-BL0-adj-e-12-0-UI.r... 270 1e-69
gi|1383218|gb|W73084.1|W73084 zd54a11.r1 Soares_fetal_heart... 268 4e-69
gi|9335068|gb|BE389703.1|BE389703 601281945F1 NIH_MGC_44 Ho... 244 6e-62
gi|5674161|gb|AI935291.1|AI935291 wp16e06.x1 NCI_CGAP_Lu19 ... 244 6e-62
gi|12678574|gb|BG171871.1|BG171871 602322675F1 NIH_MGC_89 H... 238 4e-60
gi|5920966|gb|AW055263.1|AW055263 wz16b09.x1 NCI_CGAP_Ut4 H... 236 1e-59
gi|1166345|gb|N42314.1|N42314 yy06e04.r1 Soares melanocyte ... 220 8e-55
gi|1319356|gb|W37623.1|W37623 zc12d10.r1 Soares_parathyroid... 212 2e-52
gi|10265680|gb|BE833302.1|BE833302 QV3-OT0065-280600-250-c0... 206 1e-50
gi|13409767|gb|BG477488.1|BG477488 602521540F1 NIH_MGC_20 H... 202 2e-49

>gi|13278172|gb|AAH03930.1|AAH03930 RIKEN cDNA 1110029G07 gene [Mus musculus]

EST Search:

Organ: skin
Tissue type: melanotic melanoma

Organ: pancreas
Tissue type: adenocarcinoma

Organ: brain
Tissue type: hippocampus

Organ: ovary
Tissue type: adenocarcinoma cell line

Human Sequences producing significant alignments: (bits) Value

gi|10355896|gb|BE893982.1|BE893982 601437772F1 NIH_MGC_72 H... 529 e-148

gi|9759837|gb|BE531278.1|BE531278 601278395F1 NIH_MGC_39 Ho... 523 e-146
gi|13979738|gb|BG705419.1|BG705419 602685545F1 NIH_MGC_95 H... 519 e-145
gi|10157906|gb|BE743914.1|BE743914 601577970F1 NIH_MGC_9 Ho... 498 e-138
gi|9897009|gb|BE615410.1|BE615410 601280872F1 NIH_MGC_39 Ho... 468 e-129
gi|9896295|gb|BE614698.1|BE614698 601281684F1 NIH_MGC_39 Ho... 466 e-128
gi|13545873|gb|BG547208.1|BG547208 602574620F1 NIH_MGC_77 H... 436 e-120
gi|10320048|gb|BE871272.1|BE871272 601448967F1 NIH_MGC_65 H... 428 e-117
gi|10364365|gb|BE898169.1|BE898169 601431135F1 NIH_MGC_72 H... 412 e-112
gi|13671951|gb|BG620580.1|BG620580 602619745F1 NIH_MGC_79 H... 406 e-111
gi|13576308|gb|BG568655.1|BG568655 602587668F1 NIH_MGC_76 H... 391 e-106
gi|12340258|gb|BF973043.1|BF973043 602241361F1 NIH_MGC_46 H... 341 4e-91
gi|10084502|gb|BE697355.1|BE697355 QV1-CT0417-080800-299-a0... 333 9e-89
gi|9898221|gb|BE616622.1|BE616622 601278895F1 NIH_MGC_39 Ho... 329 1e-87
gi|2069938|gb|AA410814.1|AA410814 zt36a05.r1 Soares ovary t... 297 5e-78
gi|2538826|gb|AA626439.1|AA626439 ab49g08.r1 Stratagene lun... 276 2e-71
gi|1049638|gb|H75695.1|H75695 yu07a04.r1 Soares fetal liver... 270 1e-69
gi|12397382|gb|BF991057.1|BF991057 CM1-GN0160-271000-502-a1... 266 2e-68
gi|992140|gb|H52299.1|H52299 yq81f07.r1 Soares fetal liver ... 264 7e-68
gi|1963274|gb|AA310946.1|AA310946 EST181721 Jurkat T-cells ... 262 3e-67

>gi|12857745|dbj|BAB31099.1| putative [Mus musculus]

EST Search:

Organ: brain
Tissue type: neuroblastoma cells

Tissue type: mammary gland

Tissue type: placenta

Tissue type: ovary, tumor tissue

Human Sequences producing significant alignments: (bits) Value

gi|12783826|emb|AL520333.1|AL520333 AL520333 LTI_NFL004_NBC... 835 0.0
gi|10936759|dbj|AU121524.1|AU121524 AU121524 MAMMA1 Homo sa... 831 0.0
gi|11000513|dbj|AU138992.1|AU138992 AU138992 PLACE1 Homo sa... 686 0.0
gi|10994408|dbj|AU133869.1|AU133869 AU133869 OVARC1 Homo sa... 654 0.0
gi|12893255|emb|AL553429.1|AL553429 AL553429 LTI_NFL006_PL2... 630 e-178
gi|13289457|gb|BG396009.1|BG396009 602458738F1 NIH_MGC_16 H... 628 e-177
gi|13999988|gb|BG720801.1|BG720801 602692025F1 NIH_MGC_97 H... 622 e-175
gi|13049086|gb|BG291280.1|BG291280 602388439F1 NIH_MGC_93 H... 609 e-171
gi|10936667|dbj|AU121432.1|AU121432 AU121432 MAMMA1 Homo sa... 567 e-159
gi|14063903|gb|BG753250.1|BG753250 602731650F1 NIH_MGC_43 H... 519 e-144
gi|10995473|dbj|AU134934.1|AU134934 AU134934 PLACE1 Homo sa... 511 e-142
gi|8278290|gb|BE018271.1|BE018271 bb77h08.y1 NIH_MGC_12 Hom... 498 e-138
gi|13994779|gb|BG715592.1|BG715592 602675925F1 NIH_MGC_96 H... 496 e-137
gi|9347181|gb|BE410731.1|BE410731 601301615F1 NIH_MGC_21 Ho... 492 e-136
gi|11285372|gb|BF338952.1|BF338952 602036022F1 NCI_CGAP_Brn... 428 e-117
gi|9873394|dbj|AV652380.1|AV652380 AV652380 GLC Homo sapien... 414 e-113
gi|1966540|gb|AA314211.1|AA314211 EST186056 Colon carcinoma... 408 e-111

gi|6922170|gb|AW403277.1|AW403277 UI-HF-BK0-abb-g-11-0-UI.r... 379 e-102
gi|10293319|dbj|AV691456.1|AV691456 AV691456 GKC Homo sapie... 371 e-100

gi|6896706|gb|AW392047.1|AW392047 QV4-ST0234-181199-037-c05... 363 2e-97

>gi|14789662|gb|AAH10758.1|AAH10758 Similar to carbonyl reductase 2 [Mus musculus]

EST Search:

Human Sequences producing significant alignments: (bits) Value

gi|14620169|gb|BI160168.1|BI160168 602864026F1 NIH_MGC_42 H... 88 6e-15
gi|14320386|gb|BG925863.1|BG925863 HNC21-1-B11.R HNC (Human... 88 6e-15
gi|14178945|gb|BG831358.1|BG831358 602766220F1 NIH_MGC_42 H... 88 6e-15
gi|14177680|gb|BG830093.1|BG830093 602764845F1 NIH_MGC_42 H... 88 6e-15
gi|14058983|gb|BG748330.1|BG748330 602706579F1 NIH_MGC_43 H... 88 6e-15
gi|14058856|gb|BG748203.1|BG748203 602705827F1 NIH_MGC_43 H... 88 6e-15
gi|13982131|gb|BG706614.1|BG706614 602674104F1 NIH_MGC_96 H... 88 6e-15
gi|13413874|gb|BG481595.1|BG481595 602528316F1 NIH_MGC_21 H... 88 6e-15
gi|13404430|gb|BG472244.1|BG472244 602513756F1 NIH_MGC_16 H... 88 6e-15
gi|13340715|gb|BG434209.1|BG434209 602506154F1 NIH_MGC_79 H... 88 6e-15
gi|13137575|gb|BG331137.1|BG331137 602431839F1 NIH_MGC_18 H... 88 6e-15
gi|13032709|gb|BG283133.1|BG283133 602406785F1 NIH_MGC_91 H... 88 6e-15
gi|12683322|gb|BG176619.1|BG176619 602313206F1 NIH_MGC_85 H... 88 6e-15
gi|12615652|gb|BG122143.1|BG122143 602349585F1 NIH_MGC_90 H... 88 6e-15
gi|12412330|gb|BG025585.1|BG025585 602274505F1 NIH_MGC_85 H... 88 6e-15
gi|12343809|gb|BF976594.1|BF976594 602244271F1 NIH_MGC_48 H... 88 6e-15
gi|12342418|gb|BF975203.1|BF975203 602244705F1 NIH_MGC_48 H... 88 6e-15
gi|11970704|gb|BF685296.1|BF685296 602141648F1 NIH_MGC_46 H... 88 6e-15
gi|11949082|gb|BF675187.1|BF675187 602138110F1 NIH_MGC_83 H... 88 6e-15
gi|11641972|gb|BF568592.1|BF568592 602184218F1 NIH_MGC_42 H... 88 6e-15
gi|11617689|gb|BF530338.1|BF530338 602071618F1 NCI_CGAP_Brn... 88 6e-15
gi|11263622|gb|BF315274.1|BF315274 601902672F1 NIH_MGC_19 H... 88 6e-15
gi|11258150|gb|BF310575.1|BF310575 601895295F2 NIH_MGC_19 H... 88 6e-15
gi|11252161|gb|BF305282.1|BF305282 601892747F1 NIH_MGC_17 H... 88 6e-15

gi|11251336|gb|BF304588.1|BF304588 601887980F1 NIH_MGC_17 H... 88 6e-15
gi|11151599|gb|BF237681.1|BF237681 601841865F1 NIH_MGC_46 H... 88 6e-15
gi|11098442|gb|BF204856.1|BF204856 601867158F1 NIH_MGC_17 H... 88 6e-15
gi|11098117|gb|BF204531.1|BF204531 601868138F1 NIH_MGC_17 H... 88 6e-15
gi|10726004|dbj|AV708739.1|AV708739 AV708739 ADC Homo sapie... 88 6e-15
gi|10404479|gb|BE909167.1|BE909167 601501782F1 NIH_MGC_70 H... 88 6e-15
gi|10390490|gb|BE901372.1|BE901372 601674675F1 NIH_MGC_21 H... 88 6e-15
gi|10346623|gb|BE889373.1|BE889373 601513264F1 NIH_MGC_71 H... 88 6e-15
gi|10297085|dbj|AV695222.1|AV695222 AV695222 GKC Homo sapie... 88 6e-15
gi|10296576|dbj|AV694713.1|AV694713 AV694713 GKC Homo sapie... 88 6e-15
gi|10296182|dbj|AV694319.1|AV694319 AV694319 GKC Homo sapie... 88 6e-15
gi|10293455|dbj|AV691592.1|AV691592 AV691592 GKC Homo sapie... 88 6e-15
gi|10216172|gb|BE794974.1|BE794974 601589746F1 NIH_MGC_7 Ho... 88 6e-15
gi|9882981|dbj|AV661967.1|AV661967 AV661967 GLC Homo sapien... 88 6e-15
gi|9882826|dbj|AV661812.1|AV661812 AV661812 GLC Homo sapien... 88 6e-15
gi|9875231|dbj|AV654217.1|AV654217 AV654217 GLC Homo sapien... 88 6e-15
gi|9874551|dbj|AV653537.1|AV653537 AV653537 GLC Homo sapien... 88 6e-15
gi|9874547|dbj|AV653533.1|AV653533 AV653533 GLC Homo sapien... 88 6e-15
gi|9156256|gb|BE281240.1|BE281240 601155341F1 NIH_MGC_21 Ho... 88 6e-15
gi|9137978|gb|BE264422.1|BE264422 601191730F1 NIH_MGC_7 Hom... 88 6e-15
gi|9137251|gb|BE263706.1|BE263706 601192146F1 NIH_MGC_7 Hom... 88 6e-15
gi|9133208|gb|BE313377.1|BE313377 601147921F1 NIH_MGC_19 Ho... 88 6e-15
gi|8750451|gb|BE207053.1|BE207053 ba09d08.y1 NIH_MGC_7 Homo... 88 6e-15
gi|8147585|gb|AW957902.1|AW957902 EST369972 MAGE resequence... 88 6e-15
gi|8147508|gb|AW957825.1|AW957825 EST369895 MAGE resequence... 88 6e-15
gi|6588561|gb|AW245568.1|AW245568 2822726.5prime NIH_MGC_7 ... 88 6e-15
gi|2537901|gb|AA625514.1|AA625514 af72e06.r1 Soares_NhHMPu_... 88 6e-15
gi|2159374|gb|AA446709.1|AA446709 zw84d08.r1 Soares_total_f... 88 6e-15
gi|2112928|gb|AA429728.1|AA429728 zv60c08.r1 Soares_testis_... 88 6e-15
gi|2111979|gb|AA430753.1|AA430753 zw52g09.r1 Soares_total_f... 88 6e-15
gi|1272012|gb|W00611.1|W00611 yy71a11.r1 Soares_multiple_sc... 88 6e-15
gi|1271974|gb|W00555.1|W00555 yy70g11.r1 Soares_multiple_sc... 88 6e-15
gi|1087367|gb|H91789.1|H91789 yv04c07.r1 Soares fetal liver... 88 6e-15
gi|1063794|gb|H84670.1|H84670 ys66c06.r1 Soares retina N2b4... 88 6e-15
gi|1044285|gb|H72469.1|H72469 ys07a02.r1 Soares fetal liver... 88 6e-15
gi|1023609|gb|H64869.1|H64869 yr68e02.r1 Soares fetal liver... 88 6e-15
gi|663547|gb|T60510.1|T60510 yb86c11.r1 Stratagene liver (#... 88 6e-15
gi|13976241|gb|BG703674.1|BG703674 602686647F1 NIH_MGC_95 H... 84 1e-13
gi|14568476|gb|BI117575.1|BI117575 602866754F1 NIH_MGC_7 Ho... 82 4e-13
gi|9155643|gb|BE280635.1|BE280635 601155778F1 NIH_MGC_21 Ho... 82 4e-13

gi¦1046607¦gb¦H73548.1¦H73548 ys10h05.r1 Soares fetal liver... 80 2e-12
gi¦11154540¦gb¦BF240616.1¦BF240616 601875744F1 NIH_MGC_55 H... 78 6e-12

Table 3: Bacterial SDRs derived from non-redundant NCBI Database

>gi|13701031|dbj|BAB42326.1| 3-oxoacyl- reductase [Staphylococcus aureus subsp. aureus N315]

>gi|3170581|gb|AAC18111.1| ketoreductase [Streptomyces roseofulvus]

>gi|2226002|emb|CAA74371.1| glucose-1-dehydrogenase [Staphylococcus xylosus]

>gi|4240408|gb|AAD13539.1| reductase homolog [Streptomyces cyanogenus]

>gi|14521852|ref|NP_127328.1| 3-OXOACYL-[ACYL-CARRIER-PROTEIN] REDUCTASE [Pyrococcus abyssi]

>gi|9789233|gb|AAF98275.1|AF197933_5 beta-ketoacyl-ACP reductase [Streptococcus pneumoniae]

>gi|9967599|emb|CAC05675.1| putative keto reductase [Streptomyces antibioticus]

>gi|12513057|gb|AAG54602.1|AE005204_12 putative oxidoreductase [Escherichia coli O157:H7 EDL933]

>gi|12513383|gb|AAG54850.1|AE005230_10 putative oxidoreductase [Escherichia coli O157:H7 EDL933]

>gi|12720847|gb|AAK02663.1| YdfG [Pasteurella multocida]

>gi|12744823|gb|AAK06787.1|AF324838_6 putative ketoreductase SimA6 [Streptomyces antibioticus]

>gi|13622804|gb|AAK34493.1| putative beta-ketoacyl-ACP reductase [Streptococcus pyogenes M1 GAS]

>gi|14280346|gb|AAK57528.1| polyketide ketoreductase PgaD [Streptomyces sp. PGA64]

>gi|14346021|gb|AAK60002.1| ketoreductase-like protein [Streptomyces aureofaciens]

>gi|14346023|gb|AAK60004.1| oxygenase-like protein [Streptomyces aureofaciens]

>gi¦14486276¦gb¦AAK61717.1¦ ketoreductase-like protein [Streptomyces aureofaciens]

>gi¦294354¦gb¦AAA16128.1¦ The first start codon in the ORF is found at position 2466 [Pseudomonas sp.]

>gi¦1502421¦gb¦AAC44307.1¦ 3-ketoacyl-acyl carrier protein reductase

>gi¦4160474¦gb¦AAD05259.1¦ 3-ketoacyl-CoA reductase PhaB [Bacillus megaterium]

>gi¦4416467¦gb¦AAD20367.1¦ dehydrogenase dhgA [Mycobacterium avium]

>gi¦4886772¦gb¦AAD32035.1¦AF093787_3 CylG [Streptococcus agalactiae]

>gi¦14520705¦ref¦NP_126180.1¦ OXIDOREDUCTASE [Pyrococcus abyssi]

>gi¦5669916¦gb¦AAD46515.1¦AF145724_4 oxidoreductase homolog [Streptomyces albus]

>gi¦6018300¦gb¦AAF01806.1¦AF187532_2 C-7 ketoreductase [Streptomyces nogalater]

>gi¦8896110¦gb¦AAF81238.1¦ putative beta-ketoacyl reductase [Streptomyces griseus subsp. griseus]

>gi¦11354347¦pir¦¦F82128 3-oxoacyl-(acyl-carrier-protein) reductase VC2021 [imported] - Vibrio cholerae (group O1 strain N16961)

>gi¦9944997¦gb¦AAG03070.1¦AF293355_6 putative bifunctional cyclase/reductase [Streptomyces collinus]

>gi¦9944998¦gb¦AAG03071.1¦AF293355_7 putative reductase [Streptomyces collinus]

>gi¦10174123¦dbj¦BAB05225.1¦ oxidoreductase [Bacillus halodurans]

>gi¦11036625¦gb¦AAG01883.1¦ ribitol dehydrogenase [Escherichia coli]

>gi¦12382035¦dbj¦BAB20935.2¦ ORF [Staphylococcus aureus]

>gi¦12514413¦gb¦AAG55660.1¦AE005304_5 putative fatty acyl chain reductase [Escherichia coli O157:H7 EDL933]

>gi¦12514637¦gb¦AAG55839.1¦AE005319_8 3-oxoacyl-[acyl-carrier-protein]

>gi|12515117|gb|AAG56223.1|AE005351_2 putative oxidoreductase [Escherichia coli O157:H7 EDL933]

>gi|12515526|gb|AAG56544.1|AE005380_3 putative oxidoreductase [Escherichia coli O157:H7 EDL933]

>gi|12517239|gb|AAG57883.1|AE005505_1 putative oxidoreductase [Escherichia coli O157:H7 EDL933]

>gi|12656392|gb|AAK00851.1|AF298896_1 hypothetical protein [Burkholderia pseudomallei]

>gi|12721234|gb|AAK03000.1| unknown [Pasteurella multocida]

>gi|12722349|gb|AAK04000.1| FabG [Pasteurella multocida]

>gi|12744826|gb|AAK06790.1|AF324838_9 putative reductase SimA9 [Streptomyces antibioticus]

>gi|13507282|gb|AAK28547.1| putative oxidoreductase [Yersinia pseudotuberculosis]

>gi|13621828|gb|AAK33602.1| putative 5-keto-D-gluconate 5-reductase [Streptococcus pyogenes M1 GAS]

>gi|13702422|dbj|BAB43563.1| ORFID:SA2260~hypothetical protein, similar to glucose 1-dehydrogenase [Staphylococcus aureus subsp. aureus N315]

>gi|2337820|emb|CAA74250.1| putative FabG protein [Bacillus subtilis]

>gi|11356556|pir||T44878 3-oxoacyl-[acyl-carrier protein] reductase homolog [imported] - Mycobacterium leprae

>gi|11890400|gb|AAG41118.1|AF080431_1 putative blue fluorescent protein [Vibrio vulnificus]

>gi|12514398|gb|AAG55648.1|AE005303_4 putative oxidoreductase [Escherichia coli O157:H7 EDL933]

>gi|12516801|gb|AAG57544.1|AE005472_11 putative oxidoreductase [Escherichia coli O157:H7 EDL933]

>gi|12518153|gb|AAG58600.1|AE005571_17 putative beta-ketoacyl-ACP reductase [Escherichia coli O157:H7 EDL933]

>gi|12519258|gb|AAG59448.1|AE005657_8 putative oxidoreductase [Escherichia coli O157:H7 EDL933]

>gi|13621671|gb|AAK33459.1| putative dehydrogenease / oxidoreductase [Streptococcus pyogenes M1 GAS]

>gi|13622089|gb|AAK33840.1| putative oxidoreductase [Streptococcus pyogenes M1 GAS]

>gi|13700042|dbj|BAB41341.1| acetoinreductase [Staphylococcus aureus subsp. aureus N315]

>gi|13702428|dbj|BAB43569.1| ORFID:SA2266~hypothetical protein, similar to oxidoreductase [Staphylococcus aureus subsp. aureus N315]

>gi|13883461|gb|AAK47965.1| 3-oxoacyl-(acyl-carrier-protein) reductase [Mycobacterium tuberculosis CDC1551]
Formularende

>gi|13622804|gb|AAK34493.1| putative beta-ketoacyl-ACP reductase [Streptococcus pyogenes M1 GAS]
Formularende

>gi|12054781|emb|CAC20627.1| hypothetical protein [Listeria monocytogenes]

>gi|1742522|dbj|BAA15229.1| 3-oxoacyl-[acyl-carrier protein] reductase (EC 1.1.1.100) (3-ketoacyl- acyl carrier protein reductase). [Escherichia coli]

>gi|11353996|pir||F81902 probable oxidoreductase NMA1336 [imported] - Neisseria meningitidis (group A strain Z2491)

>gi|6715317|gb|AAF26372.1|AF204735_4 putative NADP-dependent oxidoreductase [Streptomyces coelicolor A3(2)]

>gi|7471791|pir||C75365 daunorubicin C-13 ketoreductase - Deinococcus radiodurans (strain R1)

>gi|146280|gb|AAC13413.1| glucitol-6-phosphate dehydrogenase (gutD) [Escherichia coli]

>gi|5688848|dbj|BAA82699.1| Orf2 [Streptomyces coelicolor]

>gi|2842819|gb|AAC38850.1| pteridine reductase [Trypanosoma cruzi]

>gi|13701301|dbj|BAB42595.1| ORFID:SA1333~hypothetical protein, similar to oxidoreductase [Staphylococcus aureus subsp. aureus N315]

>gi|11356654|pir||T44745 probable oxidoreductase [imported] - Mycobacterium leprae

>gi|6562733|emb|CAB62872.1| conserved hypothetical protein, MAL4P2.31 [Plasmodium falciparum]

>gi|11355853|pir||C82155 probable C-factor VC1815 [imported] - Vibrio cholerae (group O1 strain N16961)

>gi|14587405|dbj|BAB61742.1| cyclohexanol dehydrogenase [Acinetobacter sp. NCIMB9871]

>gi|14600158|gb|AAK71281.1|AF387640_27 keto acyl carrier protein reductase [*Coxiella burnetii*]

>gi|14245893|dbj|BAB56288.1| acetoin(diacetyl)reductase [Staphylococcus aureus subsp. aureus Mu50]

>gi|14247001|dbj|BAB57393.1| 3-oxoacyl-(acyl-carrier protein) reductase [Staphylococcus aureus subsp. aureus Mu50]

>gi|14247273|dbj|BAB57664.1| hypothetical protein [Staphylococcus aureus subsp. aureus Mu50]

>gi|14248102|dbj|BAB58490.1| hypothetical protein [Staphylococcus aureus subsp. aureus Mu50]

>gi|14248246|dbj|BAB58634.1| hypothetical protein [Staphylococcus aureus subsp. aureus Mu50]

>gi|14248252|dbj|BAB58640.1| hypothetical protein [Staphylococcus aureus subsp. aureus Mu50]

>gi|14280348|gb|AAK57530.1| oxygenase-reductase PgaM [Streptomyces sp. PGA64]

>gi|14289341|gb|AAK58906.1|AF279141_4 cis-diol dehydrogenase [Rhodococcus sp. 19070]

>gi|14324288|dbj|BAB59216.1| glucose 1-dehydrogenase [Thermoplasma volcanium]

>gi|14325607|dbj|BAB60510.1| 3-oxoacyl-acyl carrier protein reductase [Thermoplasma volcanium]

>gi|14325671|dbj|BAB60574.1| glucose 1-dehydrogenase [Thermoplasma volcanium]

>gi|14349112|emb|CAC41336.1| acetoacetyl-CoA reductase [Azotobacter sp. FA8]

>gi|14423345|gb|AAK62355.1|AF380367_5 DbtB [Burkholderia sp. DBT1]

>gi|14518347|ref|NP_116830.1| MS142, putative gluconate dehydrogenase [Microscilla sp. PRE1]

>gi¦14523094¦gb¦AAK64694.1¦ putative [Sinorhizobium meliloti]

>gi¦14523350¦gb¦AAK64928.1¦ IdnO1 gluconate 5-dehydrogenase [Sinorhizobium meliloti]

>gi¦14523471¦gb¦AAK65040.1¦ putative [Sinorhizobium meliloti]

>gi¦14523623¦gb¦AAK65178.1¦ probable [Sinorhizobium meliloti]

>gi¦38683¦emb¦CAA37101.1¦ nodG protein (AA 1-254) [Azospirillum brasilense]

>gi¦487893¦gb¦AAA19620.1¦ ORF5

>gi¦510725¦gb¦AAB36565.1¦ ketoreductase [Streptomyces venezuelae]

>gi¦12824504¦gb¦AAE49410.1¦ Sequence 2 from patent US 6110704

>gi¦1828502¦gb¦AAB42956.1¦ Sequence 5 from patent US 5573915

>gi¦3010372¦gb¦AAC10978.1¦I74231 Sequence 13 from patent US 5686590

>gi¦9928758¦emb¦CAC05159.1¦ SEQ ID NO 46F [Mycobacterium tuberculosis]

>gi¦13443714¦emb¦CAC34889.1¦ ORF16; 3,4-Reduktase [Saccharopolyspora spinosa]

>gi¦12542824¦emb¦CAC25795.1¦ RXA02474 [Corynebacterium glutamicum]

>gi¦12542826¦emb¦CAC25796.1¦ RXA02453 [Corynebacterium glutamicum]

>gi¦12542872¦emb¦CAC25819.1¦ RXA00825 [Corynebacterium glutamicum]

>gi¦12542900¦emb¦CAC25833.1¦ RXA00251 [Corynebacterium glutamicum]

>gi¦12542902¦emb¦CAC25834.1¦ RXN02654 [Corynebacterium glutamicum]

>gi¦12544154¦emb¦CAC26450.1¦ RXA01764 [Corynebacterium glutamicum]

>gi¦12544216¦emb¦CAC26481.1¦ RXA00681 [Corynebacterium glutamicum]

>gi¦12544300¦emb¦CAC26523.1¦ RXN01090 [Corynebacterium glutamicum]

>gi¦10050763¦gb¦AAE27670.1¦ Sequence 2 from patent US 5955319

>gi¦10280064¦emb¦CAC09972.1¦ Glucose-Degydrogenase aus Bacillus megaterium

>gi¦6741907¦emb¦CAB69606.1¦ unnamed protein product [unidentified]

>gi¦6741907¦emb¦CAB69606.1¦ unnamed protein product [unidentified]

>gi¦6740927¦emb¦CAB69495.1¦ CONIFERYLALKOHOL-DEHYDROGENASE [unidentified]

>gi¦1247706¦emb¦CAA01852.1¦ CoA reductase [Allochromatium vinosum]

>gi¦345143¦emb¦CAA00174.1¦ glucose dehydrogenase [Bacillus megaterium]

>gi¦532243¦gb¦AAA65204.1¦ daunorubicin-doxorubicin polyketide synthase

>gi¦13702128¦dbj¦BAB43420.1¦ ORFID:SA2119~hypothetical protein, similar to dehydrogenase [Staphylococcus aureus subsp. aureus N315]

>gi¦13622711¦gb¦AAK34408.1¦ putative oxidoreductase [Streptococcus pyogenes M1 GAS]

>gi¦12514413¦gb¦AAG55660.1¦AE005304_5 putative fatty acyl chain reductase [Escherichia coli O157:H7 EDL933]

>gi¦15026474¦gb¦AAK81319.1¦AE007836_1 Possible S-layer protein [Clostridium acetobutylicum]

>gi¦15026554¦gb¦AAK81391.1¦AE007844_1 3-oxoacyl-acyl carrier protein reductase [Clostridium acetobutylicum]

>gi¦15026670¦gb¦AAK81497.1¦AE007854_4 3-ketoacyl-acyl carrier protein reductase [Clostridium acetobutylicum]

>gi¦15004706¦ref¦NP_149166.1¦ Oxidoreductase [Clostridium acetobutylicum]

>gi¦15004755¦ref¦NP_149215.1¦ Oxidoreductase [Clostridium acetobutylicum]

Table 4: FabG SDR Proteins derived from non redundant NCBI Database

>gi|14782791|ref|XP_042583.1|FabG (beta-ketoacyl-[acyl-carrier-protein] reductase, E coli) like [Homo sapiens]

>gi|13701031|dbj|BAB42326.1|3-oxoacyl- reductase [Staphylococcus aureus subsp. aureus N315]

>gi|13622804|gb|AAK34493.1|putative beta-ketoacyl-ACP reductase [Streptococcus pyogenes M1 GAS]

>gi|14247001|dbj|BAB57393.1|3-oxoacyl-(acyl-carrier protein) reductase [Staphylococcus aureus subsp. aureus Mu50]

>gi|14041700|emb|CAC38444.1|dJ1033B10.9.1 (FabG (beta-ketoacyl-[acyl-carrier-protein] reductase, E coli) like, isoform 1) [Homo sapiens]

>gi|14041699|emb|CAC38443.1| dJ1033B10.9.2 (FabG (beta-ketoacyl-[acyl-carrier-protein] reductase, E coli) like, isoform 2) [Homo sapiens]

>gi|12514637|gb|AAG55839.1|AE005319_8 3-oxoacyl-[acyl-carrier-protein] reductase [Escherichia coli O157:H7 EDL933]

>gi|13360935|dbj|BAB34894.1|3-oxoacyl-[acyl-carrier-protein] reductase [Escherichia coli O157:H7]

>gi|12722349|gb|AAK04000.1|FabG [Pasteurella multocida]

>gi|12824504|gb|AAE49410.1| Sequence 2 from patent US 6110704

>gi|10580854|gb|AAG19676.1|3-oxoacyl-[acyl-carrier-protein] reductase; FabG [Halobacterium sp. NRC-1]

>gi|10175111|dbj|BAB06210.1|3-oxoacyl-(acyl-carrier protein) reductase [Bacillus halodurans]

>gi|8978670|dbj|BAA98506.1|oxoacyl (carrier protein) reductase [Chlamydophila pneumoniae J138]

>gi|4376571|gb|AAD18445.1|Oxoacyl (Carrier Protein) Reductase [Chlamydophila pneumoniae CWL029]

>gi|1787335|gb|AAC74177.1|3-oxoacyl-[acyl-carrier-protein] reductase [Escherichia coli K12]

>gi|3328647|gb|AAC67830.1|Oxoacyl (Carrier Protein) Reductase [Chlamydia trachomatis]

>gi|10639611|emb|CAC11583.1|3-oxoacyl-[acyl-carrier-protein] reductase related protein [Thermoplasma acidophilum]

>gi|10639394|emb|CAC11396.1|3-ketoacyl-acyl carrier protein reductase related protein [Thermoplasma acidophilum]

>gi|10039021|dbj|BAB13055.1|3-oxoacyl-[acyl-carrier protein] reductase [Buchnera sp. APS]

>gi|9949065|gb|AAG06355.1|AE004722_11 3-oxoacyl-[acyl-carrier-protein [Pseudomonas aeruginosa]

>gi|9789233|gb|AAF98275.1|AF197933_5 beta-ketoacyl-ACP reductase [Streptococcus pneumoniae]

>gi|5459072|emb|CAB50558.1|3-OXOACYL-[ACYL-CARRIER-PROTEIN] REDUCTASE [Pyrococcus abyssi]

>gi|2738155|gb|AAB94395.1|3-oxoacyl-acyl carrier protein reductase [Pseudomonas aeruginosa]

>gi|1651536|dbj|BAA35901.1|3-oxoacyl-[acyl-carrier-protein] reductase (EC 1.1.1.100). [Escherichia coli]

>gi|3861291|emb|CAA15190.1|3-OXOACYL REDUCTASE (fabG) [Rickettsia prowazekii]

>gi|1561753|gb|AAC69638.1|3-ketoacyl reductase [Mycobacterium smegmatis]

>gi|2183267|gb|AAC46203.1|ketoacyl-reductase [Mycobacterium avium]

>gi|1502421|gb|AAC44307.1|3-ketoacyl-acyl carrier protein reductase [Bacillus subtilis]

>gi|1173841|gb|AAC43589.1|3-ketoacyl-ACP reductase [Vibrio harveyi]

>gi|3282804|gb|AAC38650.1|3-oxoacyl-acyl carrier protein reductase [Salmonella typhimurium]

>gi|2253068|emb|CAB10712.1|hypothetical protein Rv2129c [Mycobacterium tuberculosis]

>gi|1573112|gb|AAC21824.1|3-ketoacyl-acyl carrier protein reductase (fabG) [Haemophilus influenzae Rd]

>gi|2337820|emb|CAA74250.1|putative FabG protein [Bacillus subtilis]

>gi|2633963|emb|CAB13464.1|3-ketoacyl-acyl carrier protein reductase [Bacillus subtilis]

>gi|1651214|dbj|BAA13560.1|beta-ketoacyl-ACP reductase [Actinobacillus actinomycetemcomitans]

>gi|145881|gb|AAA23739.1|biotin carboxylase [Escherichia coli]

>gi|2313678|gb|AAD07627.1|3-ketoacyl-acyl carrier protein reductase (fabG) [Helicobacter pylori 26695]

>gi|4155047|gb|AAD06084.1|ACETYL-COENZYME A CARBOXYLASE SUBUNIT A [Helicobacter pylori J99]

>gi|6045047|dbj|BAA85256.1|3-oxoacyl-[acyl carrier protein] reductase homolog [Moritella marina]

Table 5: SDRs in Fungi derived from non redundant NCB Database

>gi|5689604|emb|CAB51900.1| 1,3,6,8-tetrahydroxynaphthalene reductase [Aspergillus fumigatus]

>gi|13570027|gb|AAG29497.2|AF290182_1 tetrahydroxynaphthalene reductase [Magnaporthe grisea]

>gi|1592833|gb|AAB42156.1| ketoreductase [Aspergillus parasiticus]

>gi|431103|gb|AAA19514.1| polyhydroxynaphthalene reductase [Magnaporthe grisea]

>gi|3425989|dbj|BAA32378.1| Brn1 [Curvularia intermedia]

>gi|450261|gb|AAA53572.1| verA [Emericella nidulans]

>gi|12718334|emb|CAC28569.1| conserved hypothetical protein [Neurospora crassa]

>gi|11359360|pir||T51084 3-oxoacyl-[acyl-carrier-protein]-reductase (oar-1) [imported] - Neurospora crassa

>gi|4499846|emb|CAB39316.1| oxidoreductase [Claviceps purpurea]

>gi|1902911|dbj|BAA18962.1| reductase [Colletotrichum lagenarium]

Claims

1. A method for identifying or verifying members of the short chain dehydrogenase (SDR) family comprising the steps

(a) providing a target sequence of molecules to be classified,

(b) comparing said target sequence with core SDR motifs selected from

(i) MV1 being derived from the motif MT1:TGxxxGxG by replacement of 0 to 2 amino acids,

(ii) MT2:NN(0-2:x)AG,

(iii) MT3:N, located at a position 90-110 relative to MT1,

(iv) MV4 being derived from the motif MT4:S(11-52:x)YxxxK by replacement of 0-2 amino acids and

(v) MT5:PG,

(c) determining positive SDR candidates containing

(i) at least the core SDR motifs MV1 and MV4 and

(ii) at least 7 of the 14 amino acids contained in the motifs MT1, MT2, MT3, MT4 and MT5 and

(d) classifiying positive SDR candidates as belonging to the SDR family.

2. The method according to claim 1 further comprising a step

(e) ranking of the positive SDR candidates obtained according to the number of amino acids matching with motifs MT1, MT2, MT3, MT4 and MT5.

3. The method according to claim 1 or 2, wherein in step (b) the target sequence is compared with core SDR motifs selected from

(i) MT1:TGxxxGxG,

(ii) MT2:NN(0-2:x)AG,

(iii) MT3:N, located at position 90-110 relative to MT1,

(iv) MT4:S(11-52:x)YxxxK and

(v) MT5:PG, and

in step (c) positive SDR candidates are determined containing

(i) at least the core SDR motifs MT1 and MT4 and

(ii) at least 7 of the 14 amino acids contained in the motifs MT1, MT2, MT3, MT4 and MT5.

4. The method according to any of claims 1-3, wherein in step (c) positive SDR candidates are determined containing

(i) at least the core SDR motifs MV1, MV4 and one of MT2, MT3 and MT5 and

(ii) at least 7 of the 14 amino acids contained in the motifs MT1, MT2, MT3, MT4 and MT5.

5. The method according to any of claims 1-4, wherein in step (c) positive SDR candidates are determined containing

(i) the core SDR motifs MV1, MV4, MT2, and MT3 or MV1, MV4, MT2 and MT5 or MV1, MV4, MT3 and MT5.

6. The method according to any of claims 1-5, wherein positive SDR candidates are determined containing the core SDR motifs MV1, MV4, MT2, MT3 and MT5.

7. The method according to claim 1, wherein in step (c) positive candidates are determined containing at least 9, preferably at least 11 of the 14 amino acids contained in the motifs MT1, MT2, MT3, MT4 and MT5.

8. The method according to any of the preceding claims, wherein MT2 is defined as NNAG.

9. The method according to any of the preceding claims, wherein MV4 is derived from the motif MT'4:S(11-52:x)YxASK by replacement of 0-2 amino acids.

10. The method according to claim 9, wherein in step (c) positive candidates are determined containing at least 9, preferably at least 11, particular preferably at least 13 of the 16 amino acids contained in the core motifs used.

11. The method according to any of the preceding claims, wherein MT2 and/or MT5 are extended for identifying or verifying FabG_SDRs, wherein MT_y2:VxVNNAG, wherein V can be replaced and MT_y5:PGFI, wherein F and/or I are used as search motif.

12. The method according to any of the preceding claims further comprising one or more of the following further steps:
(i) three-dimensional structure comparison and
(ii) biological function analysis.

13. Member of the short-chain dehydrogenase (SDR) family identified with the method according to any of claims 1-12.

14. SDR according to claim 13, wherein it is selected from the SDRs shown in Tables 1-5.

15. A method for providing modulators for members of the short chain dehydrogenase (SDR) family comprising the steps
(a) providing one or more target sequences of members of the short chain dehydrogenase family based on an algorithm using core SDR motifs for searching members of the SDR family and
(b) providing modulators, which enhance or inhibit the activity of the members of the short chain dehydrogenase family.

16. The method according to claim 15, wherein in step (a) the method according to any of claims 1-12 is applied.

17. The method according to claim 15 or 16, wherein in step (b) a protein sequence alignment with known SDR sequences is performed for pre-selecting possible modulators.

18. A method for evaluation of lead-candidates for possible modulators of a member of the SDR family comprising the steps
(a) providing one or more target sequences of members of the short chain dehydrogenase family based on an algorithm using core SDR motifs for searching members of the SDR family,

(b) ranking the target sequences according to the number of amino acids matching with the core SDR motifs used and

(c) deriving lead-candidates from metabolites of evolutionary related SDR enzymes.

19. The method according to claim 18, wherein in step (a) the method according to any of claims 1-12 is applied.

20. A method for providing a pharmaceutical agent comprising the steps

(a) providing one or more target sequences of members of the short chain dehydrogenase family based on an algorithm using core SDR motifs for searching members of the SDR family,

(b) providing modulators, which enhance or inhibit the activity of the members of the short chain dehydrogenase family and

(c) formulating said modulators as pharmaceutical agent.

21. The method according to claim 20, wherein in step (a) the method according to claims 1-12 is applied.

22. The method according to claim 20 or 21, wherein in step (b) the method according to any of claims 15-17 is applied.

23. The method according to any of claims 20-22, wherein a modulator is provided, which enhances the activity of the members of the short chain dehydrogenase family.

24. The method according to any of claims 20-22, wherein a modulator is provided, which inhibits the activity of the members of the short chain dehydrogenase family.

25. The method according to any of claims 20-24, wherein the validation of a modulator or a function of a SDR enzyme found with an algorithm using core SDR motifs is performed with biochemical methods.

26. The method according to any of claims 20-29, wherein expressed sequence tags and gene sequence comprison are used to provide a function of the member of the short chain dehydrogenase family, which has been identified or verified with an algorithm using core SDR motifs.

27. The method according to any of claims 20-26, wherein a modulator or a function of an SDR enyzme found with an algorithm using core SDR motifs is validated high throughput function screening for function identification, UHTS for lead compounds, molecular homolgy modelling, substrate docking simulations, tissue expression, cDNA arrays or analysis of disease in animal or in vitro model systems.

28. The method according to any of claims 20-27, wherein a human SDR enzyme is provided and the pharmaceutical agent is applied for therapeutical or diagnostical purposes.

29. The method according to claim 28, wherein the human SDR enzyme is selected from the human SDRs shown in Table 1 or 2.

30. The method according to any of claims 20-28, wherein an SDR from a pathogen or/and a fungi is provided to obtain a high specific pharmaceutical agent.

31. The method according to claim 30, wherein the SDR is selected from the SDRs shown in Table 3, 4 or 5.

32. The method according to claims 20-31, wherein an SDR enzyme with high homology is provided, which constitutes an essential enzyme.

33. The method according to any of of claims 20-31, wherein a SDR enzyme with low homology or high divergence between different species is provided, which allows for a species specific modulation.

34. Pharmaceutical agent obtainable by a method according to any of claims 20-33.

35. Pharmaceutical agent according to claim 34 for the prophylaxis, treatment or/and diagnosis of diseases.

36. Pharmaceutical agent according to any of claims 34 or 35, which is a fungicide or antibiotic.

37. A method for detection of clinically relevant polymorphisms or single nucleotide polymorphisms comprising the steps

(a) providing one or more target sequences or members of the short chain dehydrogenase family based on an algorithm using core SDR motifs for searching members of the SDR family,

(b) ranking the members of the short chain dehydrogenase family according to the number of amino acids matching with the core SDR motifs applied, and

(c) comparing evolutionary patterns within the SDR enzymes.

38. The method according to claim 37, wherein disease mechanisms are characterised.

39. The method according to claim 37 or 38, wherein metabolisms of xenobiotics are characterised.

40. The method according to any of claims 37-39, wherein structure-function relationships are identified and/or substrates of SDR members with unknown function are identified.

41. The method according to claim 20-33, wherein a pharmaceutical agent for affecting immune regulation is provided by developing a modulator for 17ß HSD type 3, 17ß HSD type 7, 17ß HSD type 8, 17ß HSD type 10, 11ß HSD-1, CR1, UDP glucose epimerase, SDR_SRL, AF067174, AF151840, AF151844, AF0078850, Fvt-1, HEP-27, DKFZ_ORF, WWOX_ORF, or CR3.

42. The method according to claims 20-33, wherein a pharmaceutical agent for affecting autoimmunity is provided by developing a modulator for 17ß HSD-3, 17ß HSD-8, 11ß HSD-1, AF057034, U89717, CR1, AF0078850, HEP-27, or CR-3.

43. The method according to claim 20-33, wherein a pharmaceutical agent for wound healing or partial recovery is provided by developing a modulator for 17ß HSD-3, 17ß HSD-8, 11ß HSD-1, U89717, CR1, AF0078850, HEP-27, or CR-3.

44. The method according to claim 20-33, wherein a pharmaceutical agent for treatment of leukemia is provided by developing modulators for 17-ß HSD-10 or Fvt-1.

45. The method according to claim 20-33, wherein a pharmaceutical agent for apoptosis regulation is provided by developing a modulator for 17ß HSD-10, U89717, SDR_SRL; or for providing a pharmaceutical agent for affecting immune response by providing a modulator for AF016509, or providing a pharmaceutical agent for the treatement of cancer by providing modulators for AF016509, or providing a pharmaceutial agent for affecting cell growth by providing a modulator for U89717, or providing a pharmaceutical agent for the treatment of lung carcinoma by providing a modulator for SDR_SRL, or providing a pharmaceutical agent for the regulation of inflammation or vasculitis by providing a modulator for DKFZ_ORF.

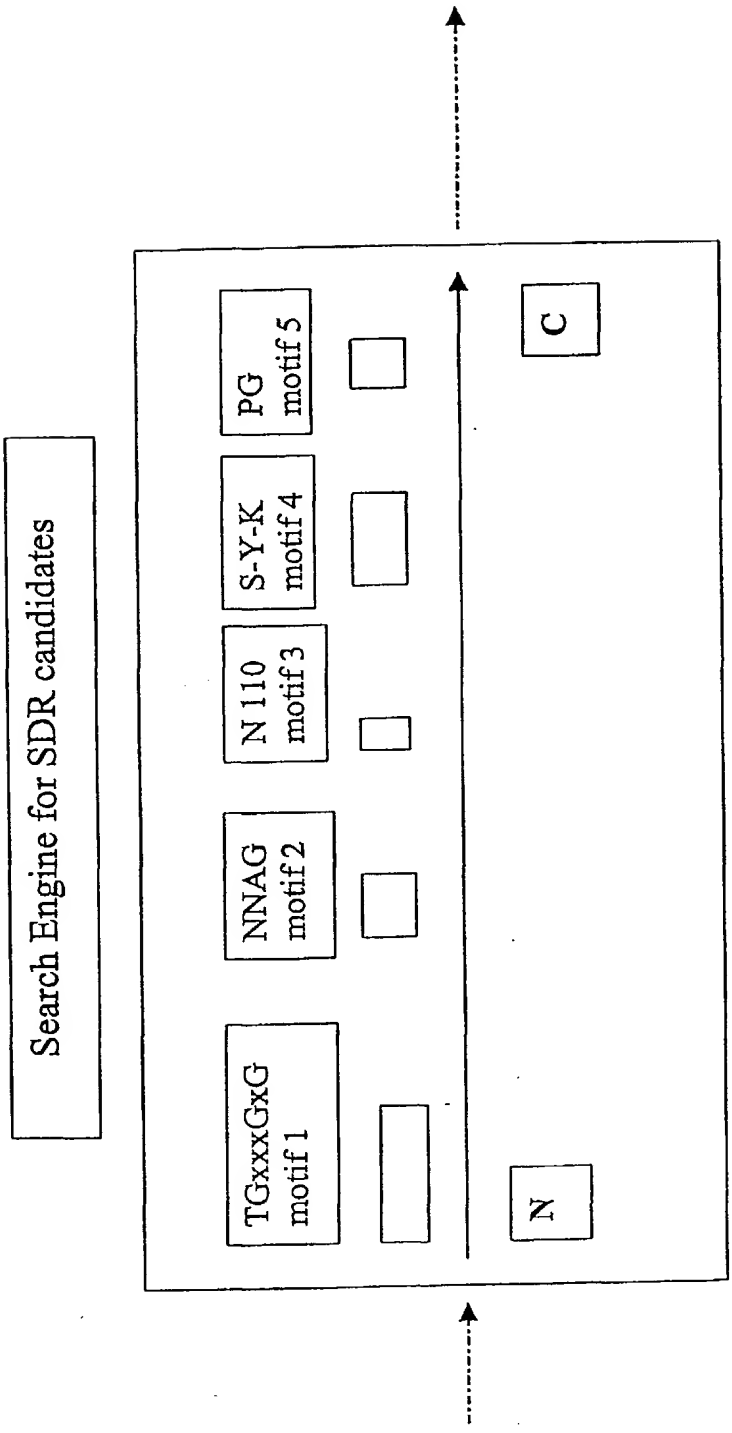
Search Engine for SDR candidates
TGxxxGxG motif 1
NNAG motif 2
N 110 motif 3
S-Y-K motif 4
PG motif 5
N
C

Fig. 1

Flowchart for data processing

Fig. 2a

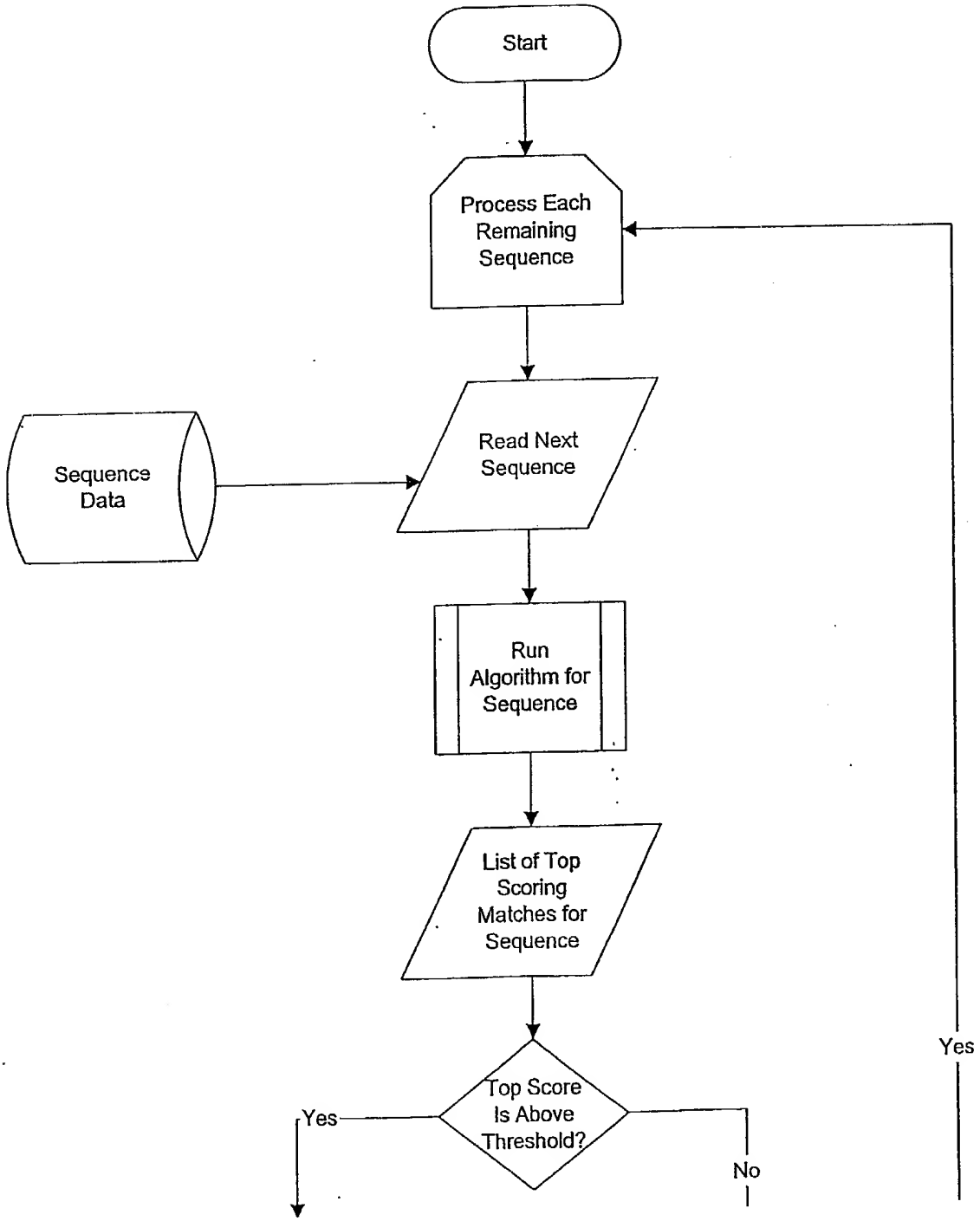

Fig. 2a continued

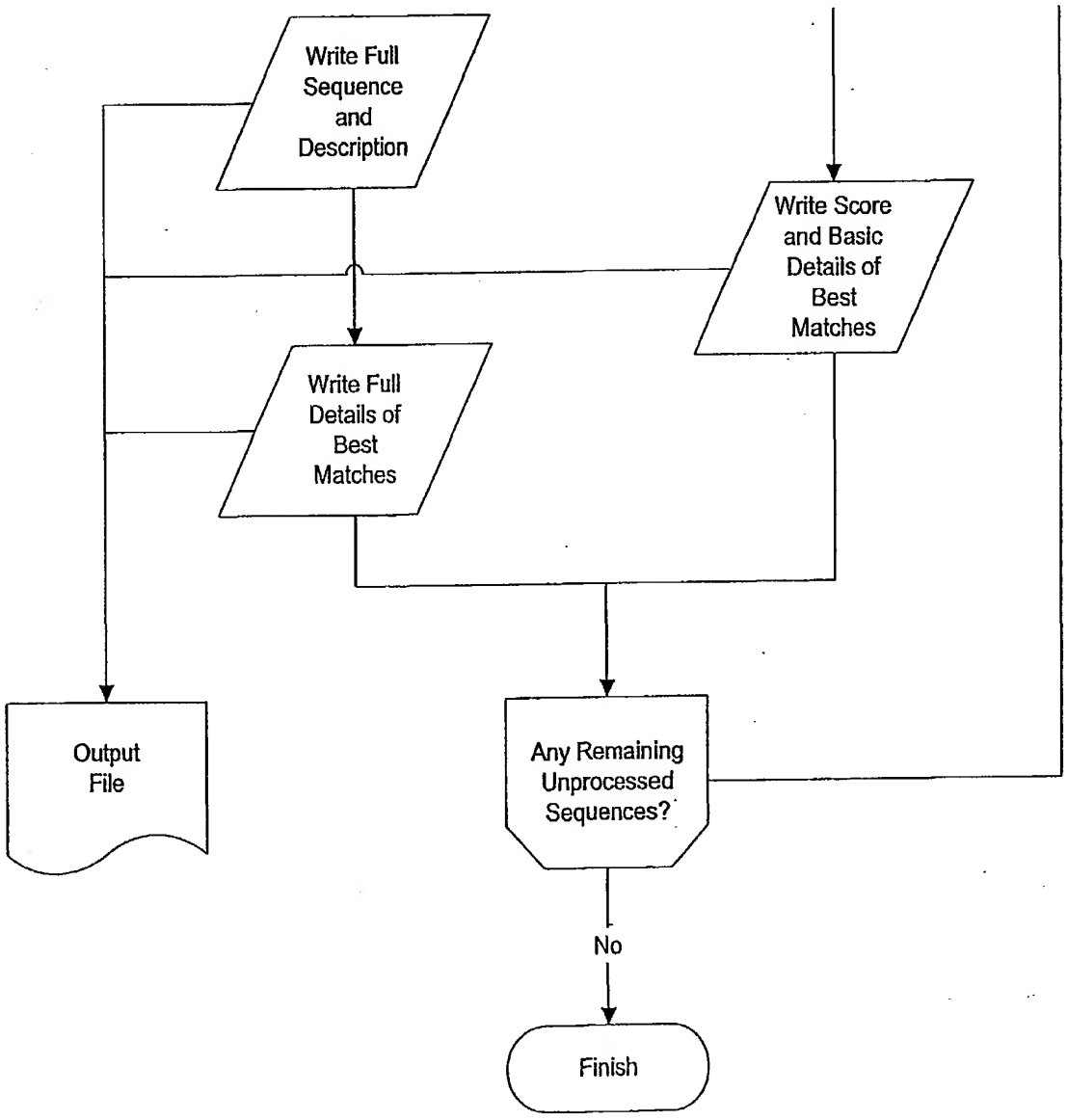

Fig. 2b

Flowchart for the algorithm

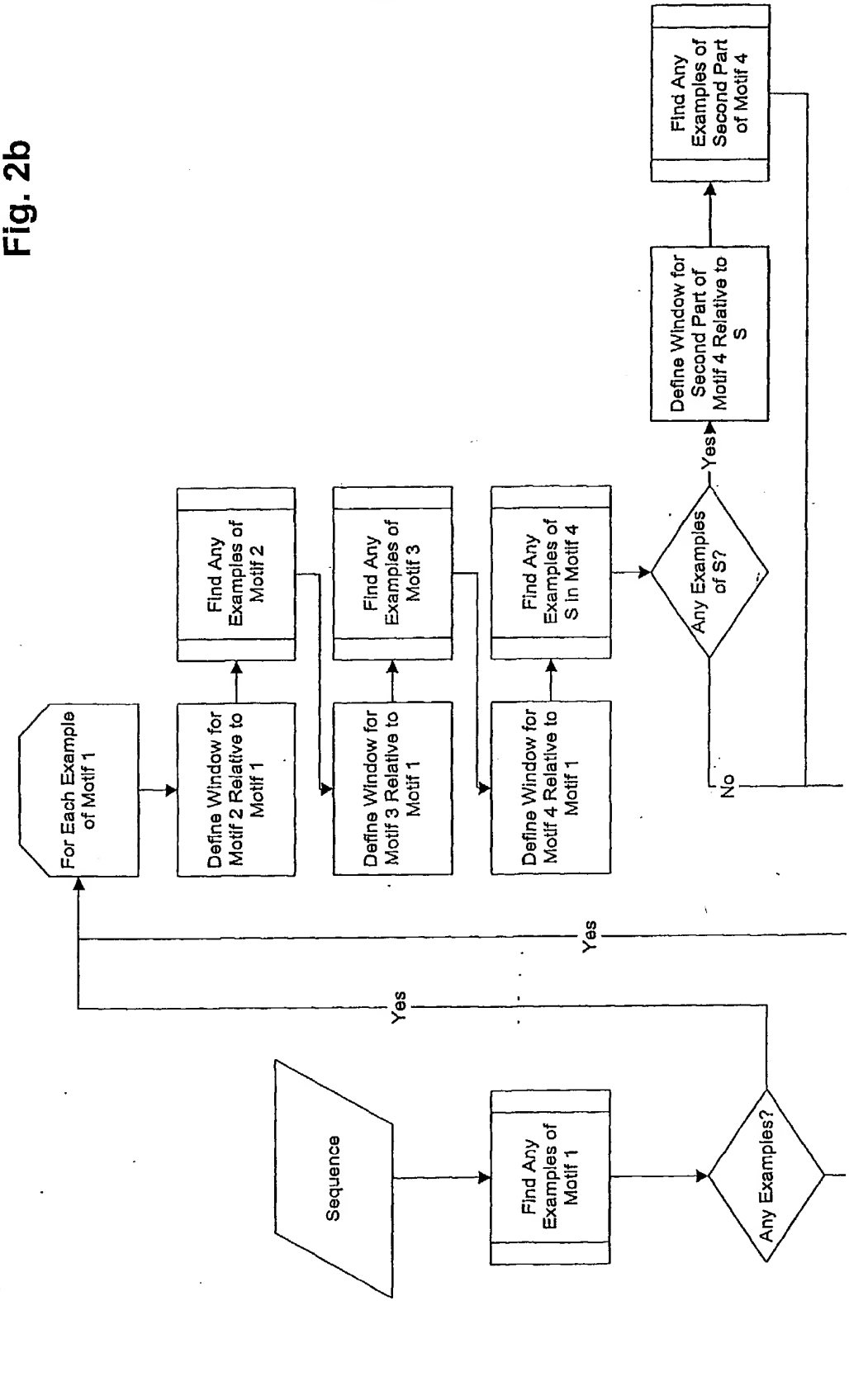

Fig. 2b continued

Flowchart for the algorithm

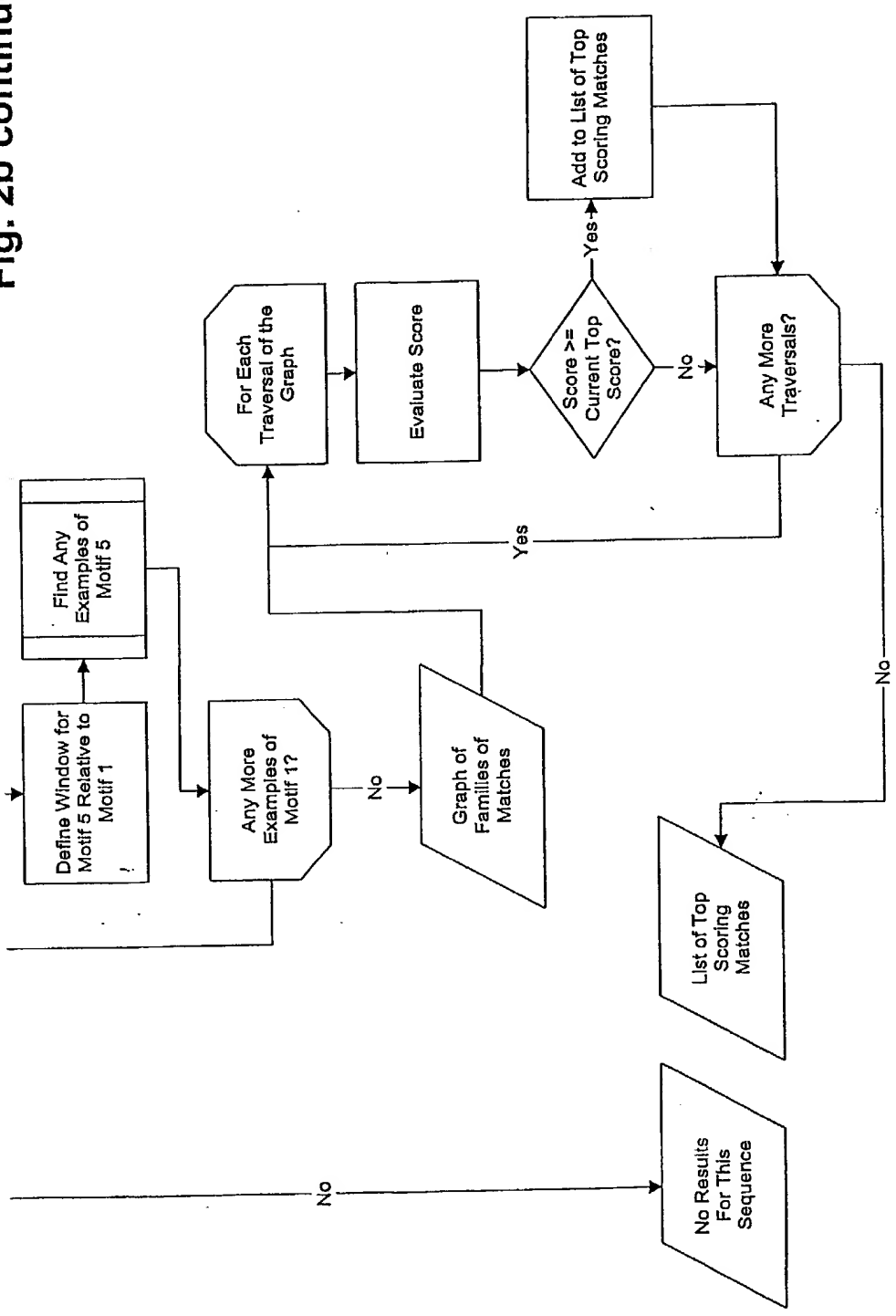

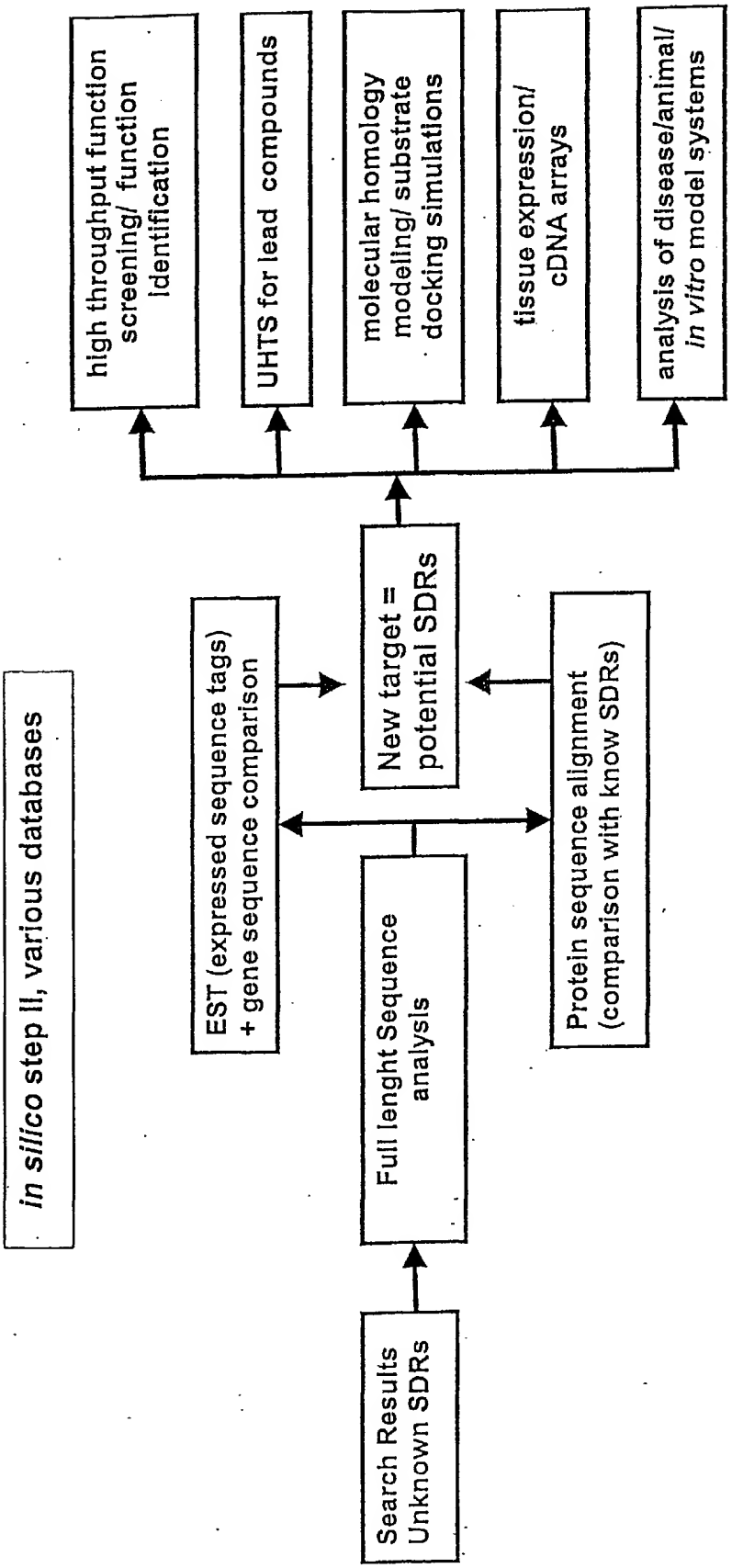
high throughput function screening/ function identification
UHTS for lead compounds
molecular homology modeling/ substrate docking simulations
tissue expression/ cDNA arrays
analysis of disease/animal/ in vitro model systems
New target = potential SDRs
EST (expressed sequence tags) + gene sequence comparison
Protein sequence alignment (comparison with know SDRs)
Full lenght Sequence analysis
Search Results Unknown SDRs
in silico step II, various databases

Fig. 3

Fig. 4a-top left

M

CGI-93	M S T F F S D T A W I C L A V P T V L	10
DKFZ-ORF	M E R W P W P S G G A W L L V A A R A	10
CR-1		
CR-3		
SRL		
Hep-27		
SDH-RDH		
RODH4		
RDH		
9cis-RDH		
3beta-HSD-		
3beta-HSD-		
RDH_ORF		
CGI-86		
BDH		
17beta-HSD		
11beta-HSD		
CR-AG		
11cis-RDH		
17beta-HSD		

8/30

Fig. 4a-top middle

```
KLIDYGLSGYQEESAEVKAMDFITSTAILPLLFGCLGVFGLF------RLLQWVR--GKAY
       MVSPATRKSLPKVKAMDFITSTAILPLLFGCLGVFGLF------RLLQWVR--GKAY
                                                            MSS
                                                            MSS
                                                  MASSGMT--RRDP
                          MLSAVARGYQGWFHPCARLSVR------MSSTGID--RKGV
                                     MWLYLAVFVGLY------YLLHWYR--ERQV
                                     MWLYLAVFVGLY------YLLHWYR--ERQV
                                     MWLYLAAFVGLY------YLLHWYR--ERQV
                                     MWLPLLLGALLW------AVLWLLR--DRQS

                                     MLFWVLGLLILC------GFLWTRK--GKLK
                     MNWELLLWLLVLCALLLLLVQLLRFLRADG---DLTLLWAEWQGRRP
                GLRPPPPGRFSRLPGKTLSACDRENGARRPLLLGS---TSFIPIGRRTYASA
CGTVFCKYKKSSGQLWSWMVCLAGLCAVCLLILSPFWGLILFS---VSCFLMYTYLSGQE
LLQLLRSDLRLGRPLLAALALLAALDWLCQRLLPPPAALAVLA---AAGWIALSRLARPQ
                                                            M
                                                            MNF
                                                            SQL
```

Fig. 4a-top right

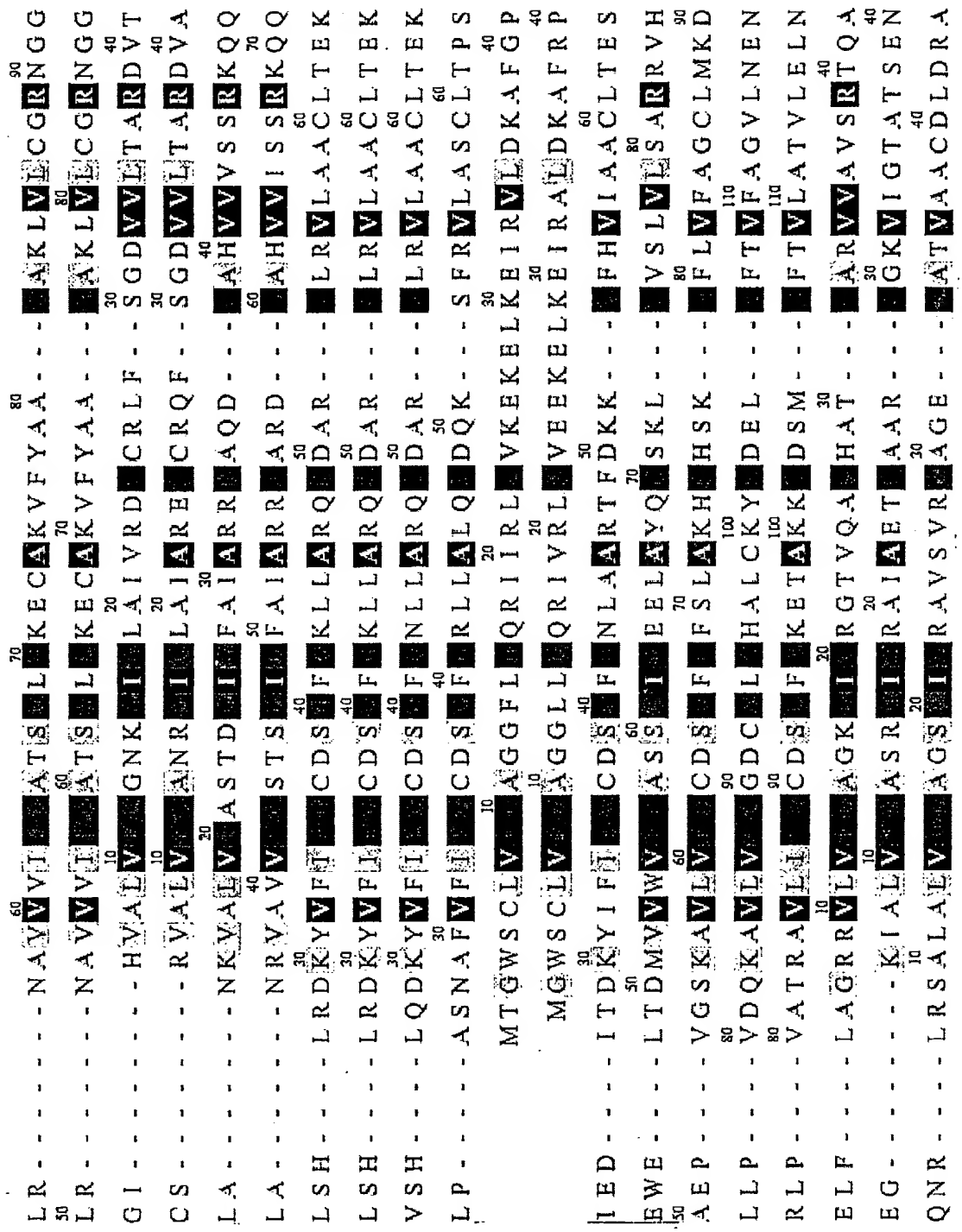

Fig. 4a-bottom left

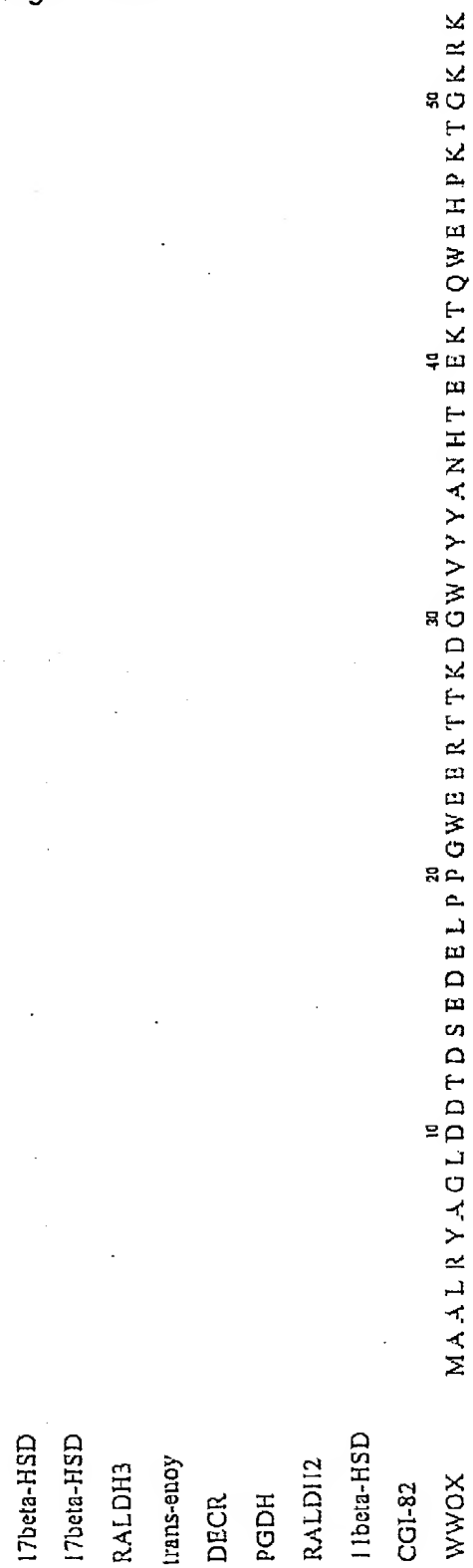

Fig. 4a-bottom middle

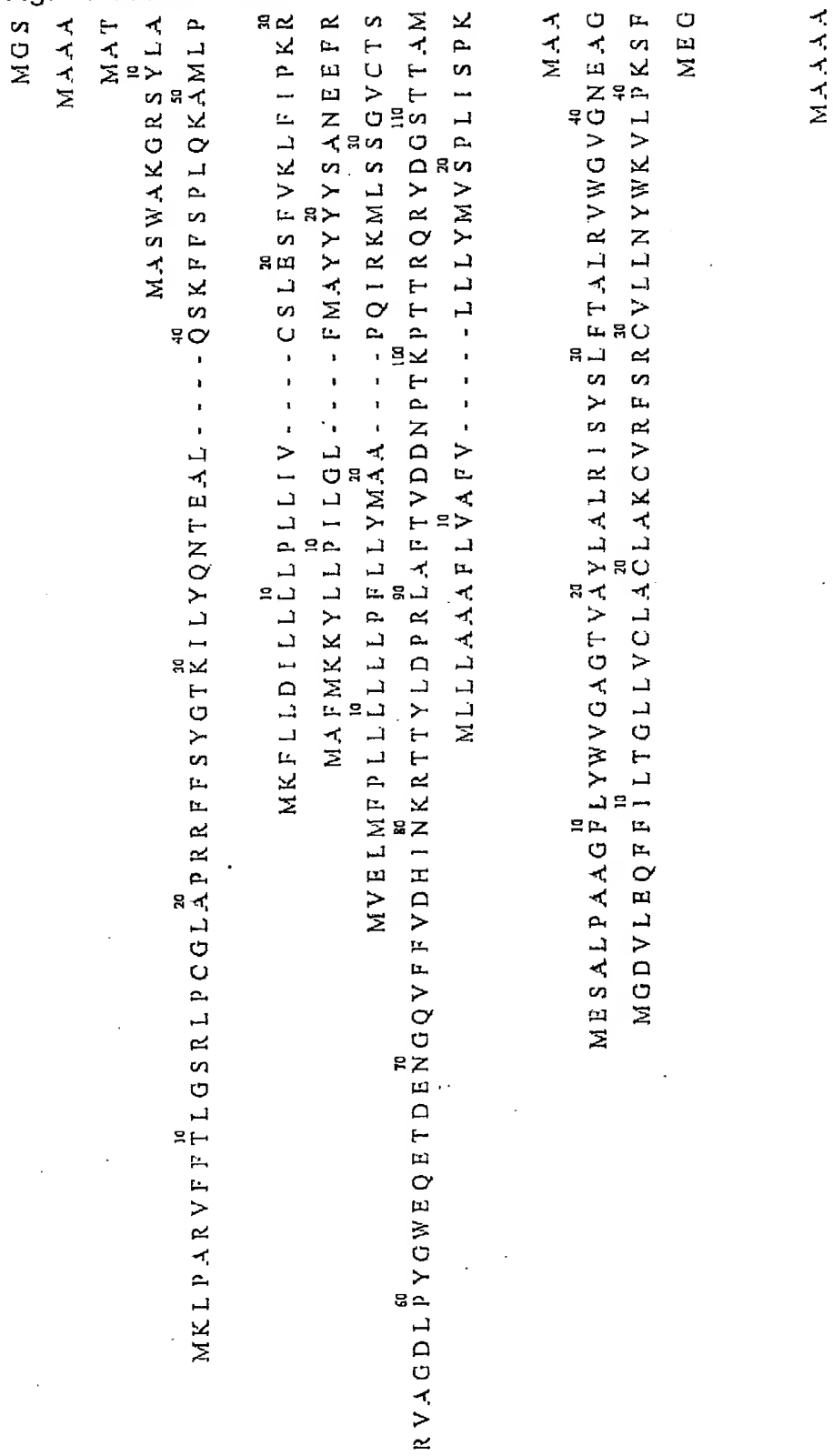

Fig. 4a-bottom right

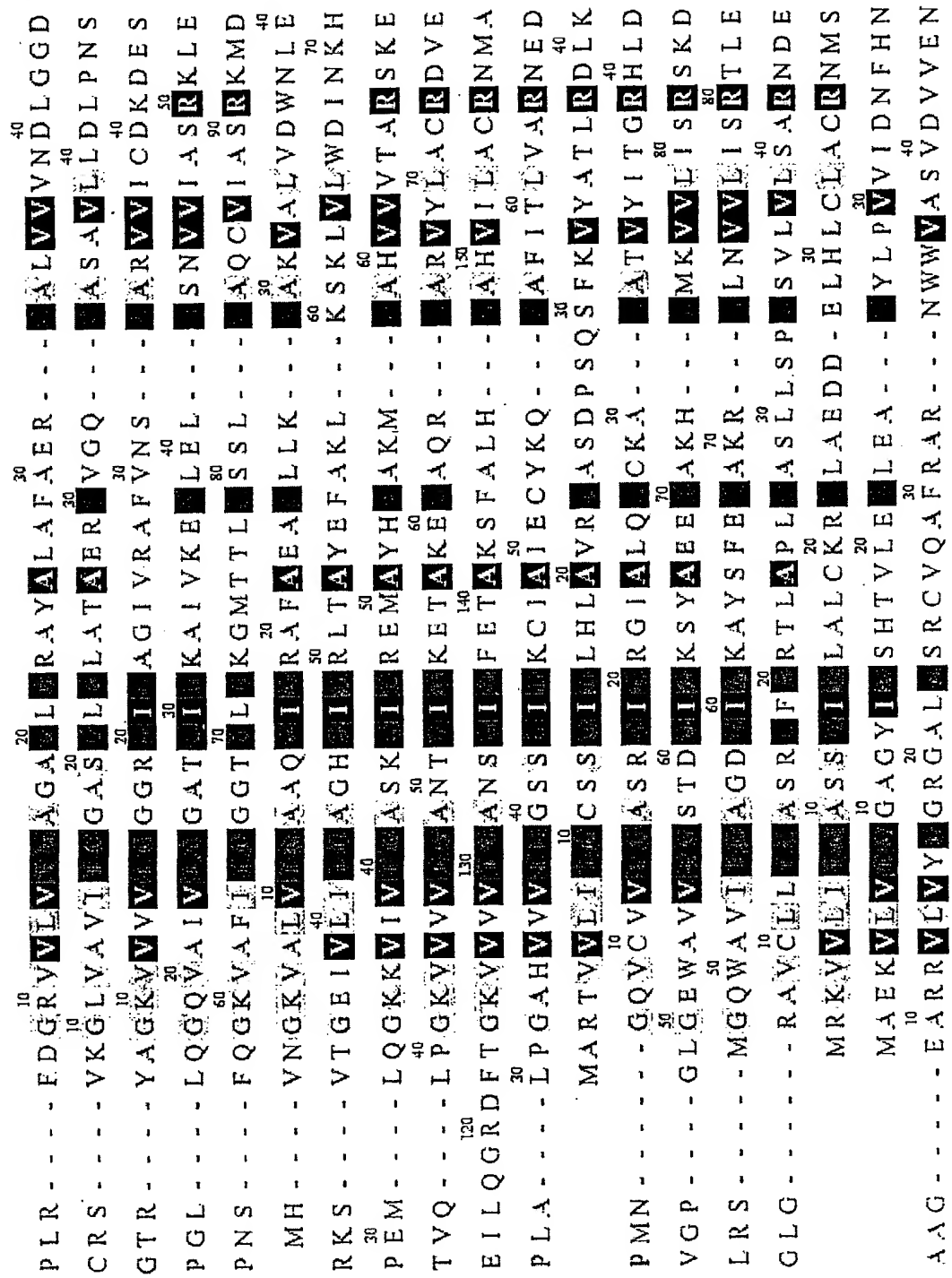

Fig. 4b-top left

Fig. 4b-top middle

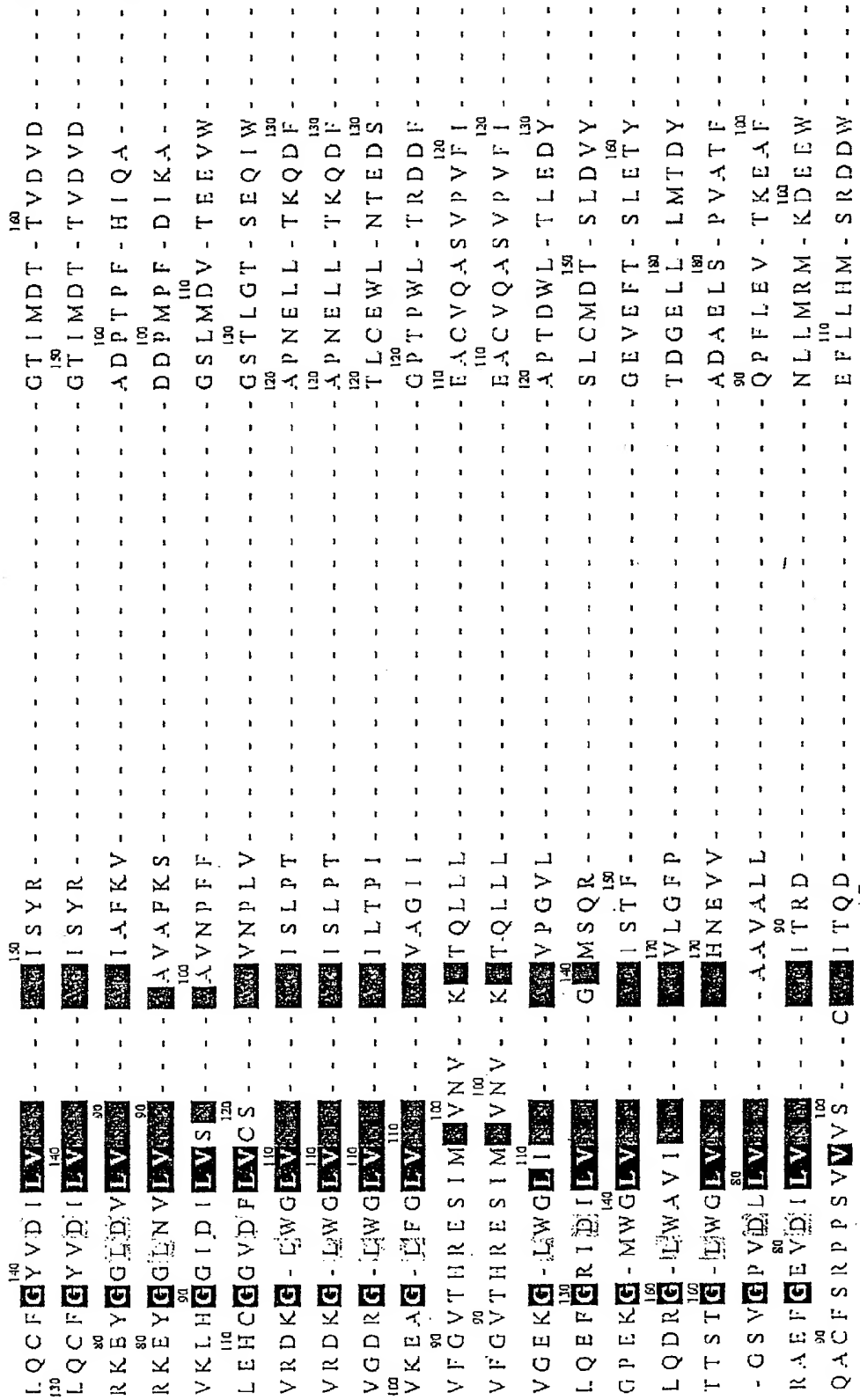

Fig. 4b-top right

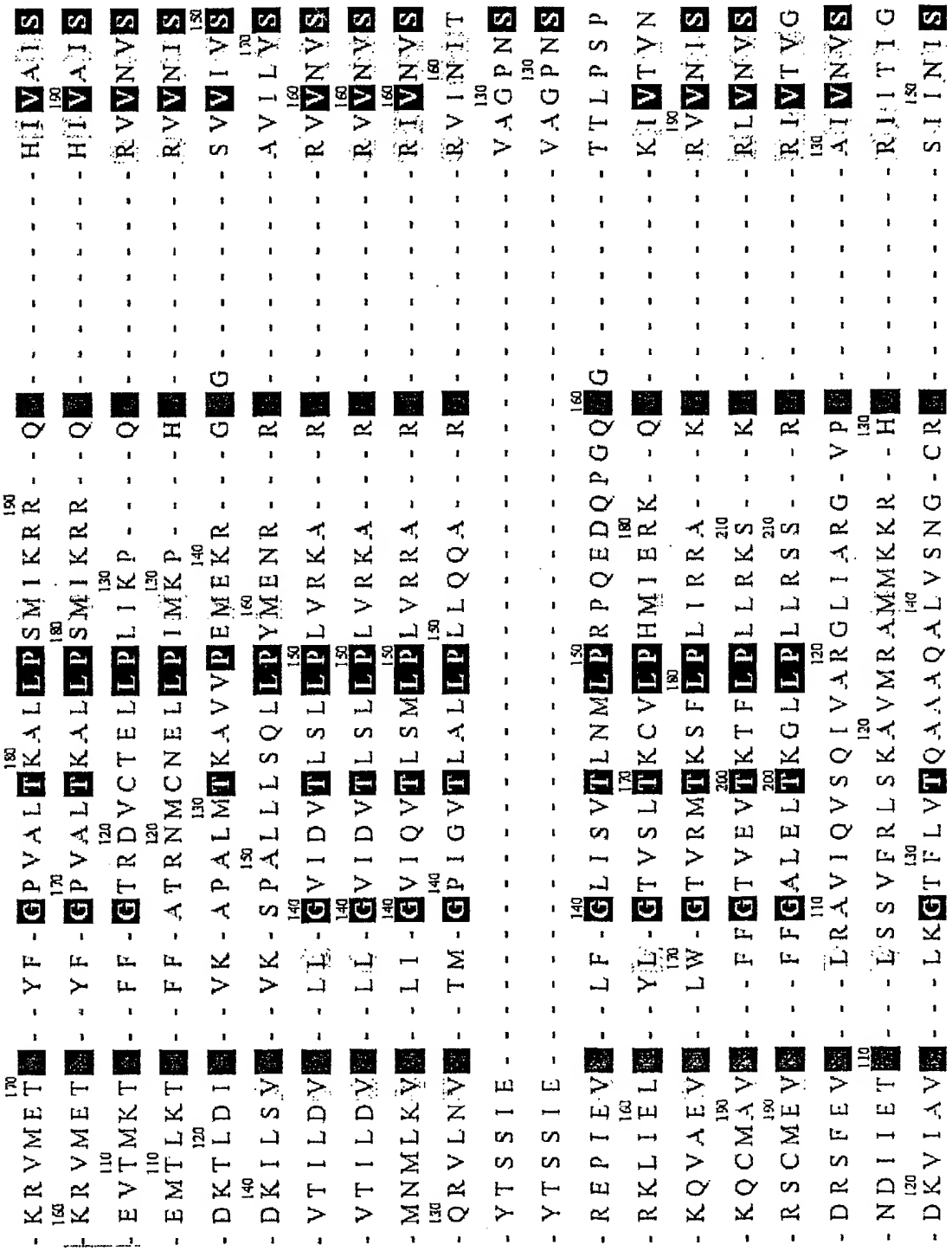

Fig. 4b-bottom left

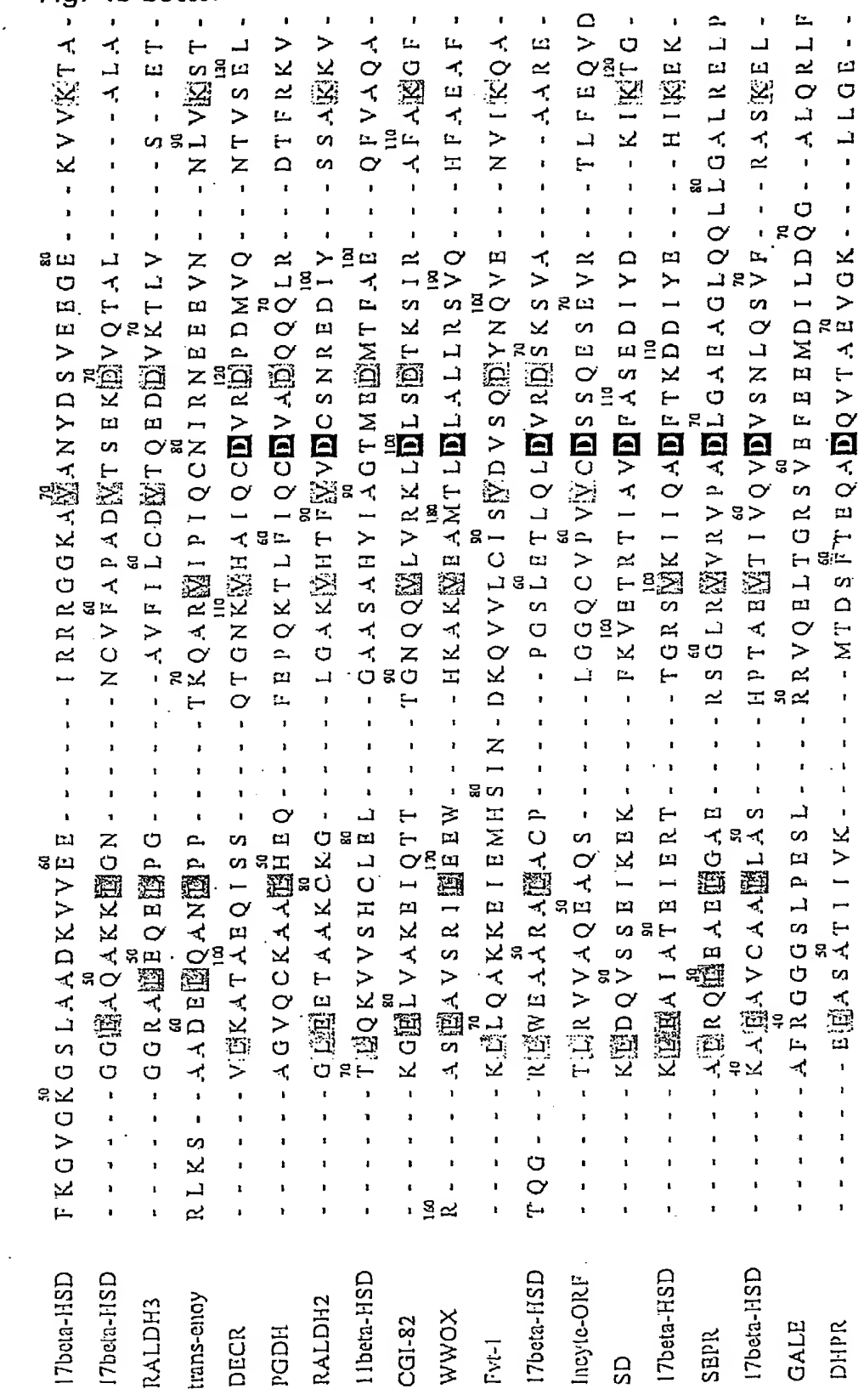

Fig. 4b-bottom middle

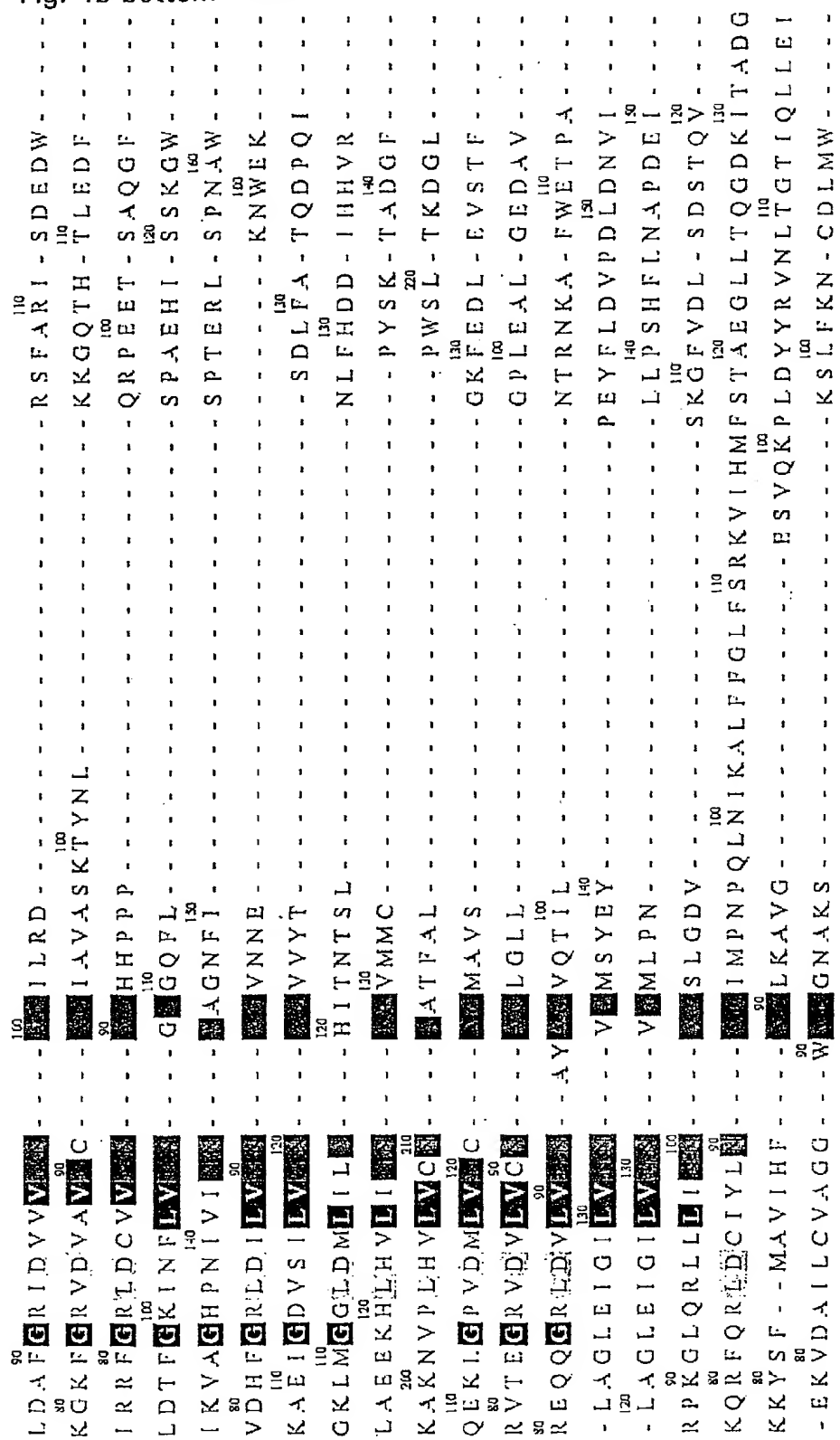

Fig. 4b-bottom right

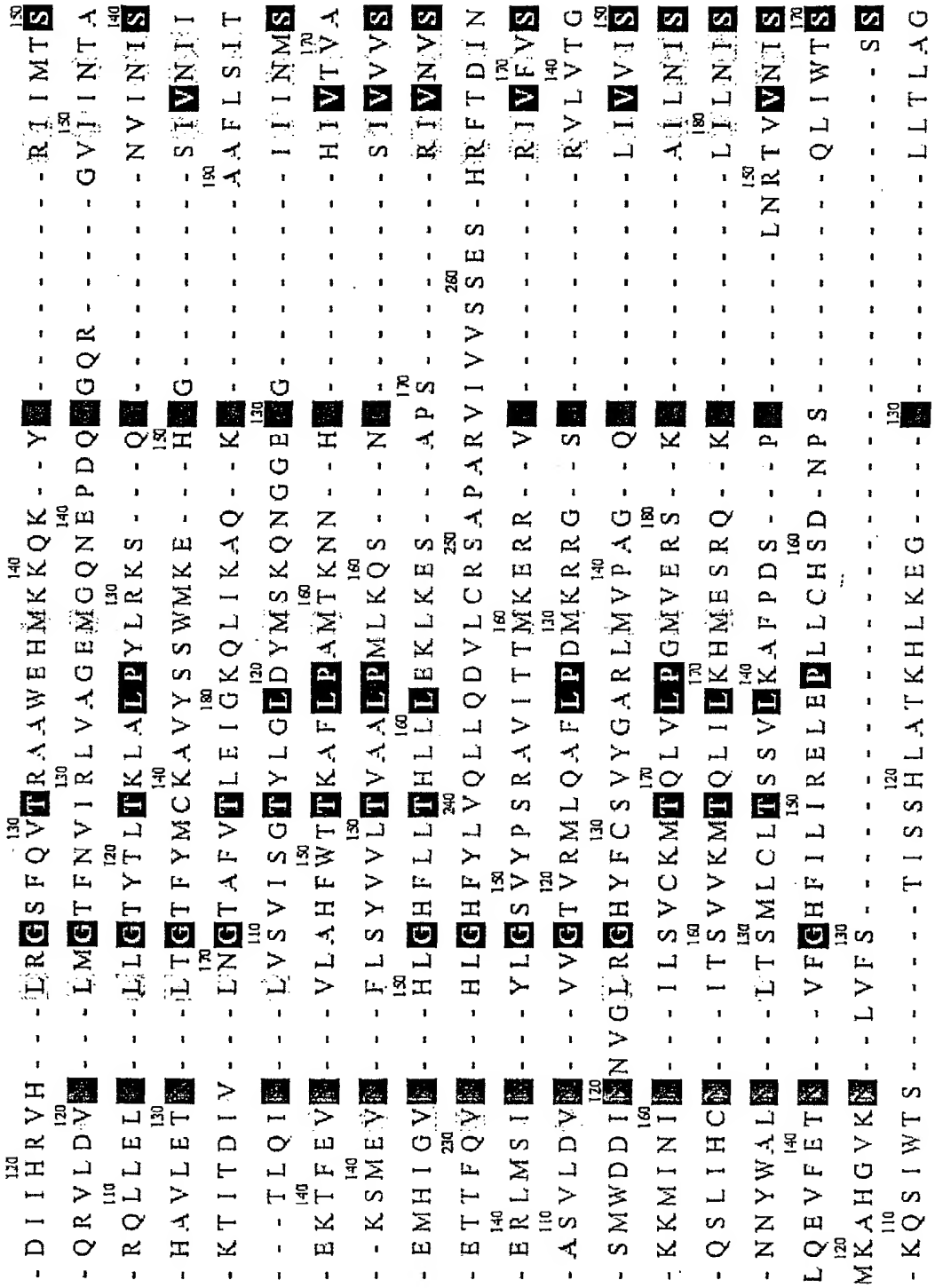

Fig. 4c-top left

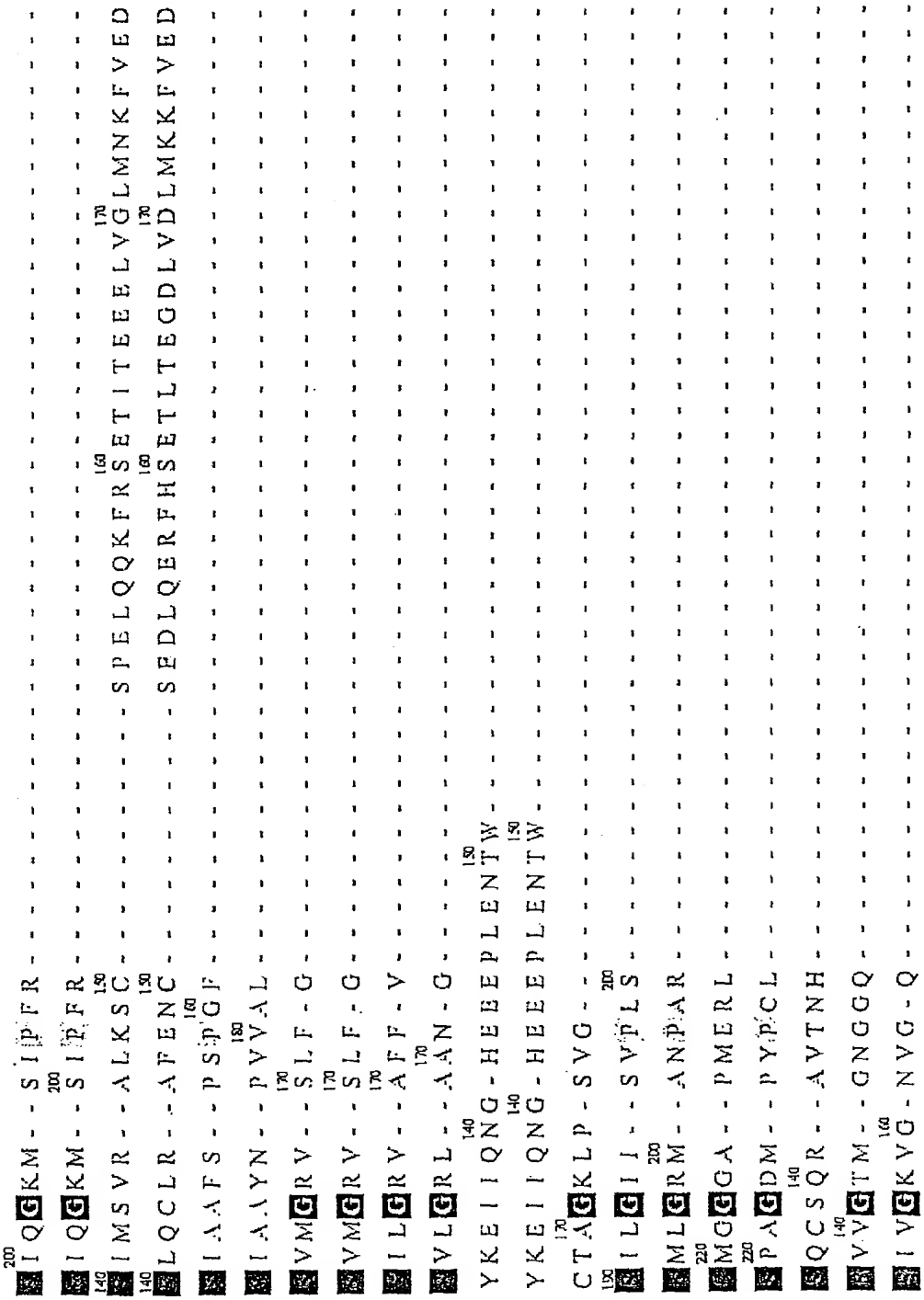

Fig. 4c-top middle

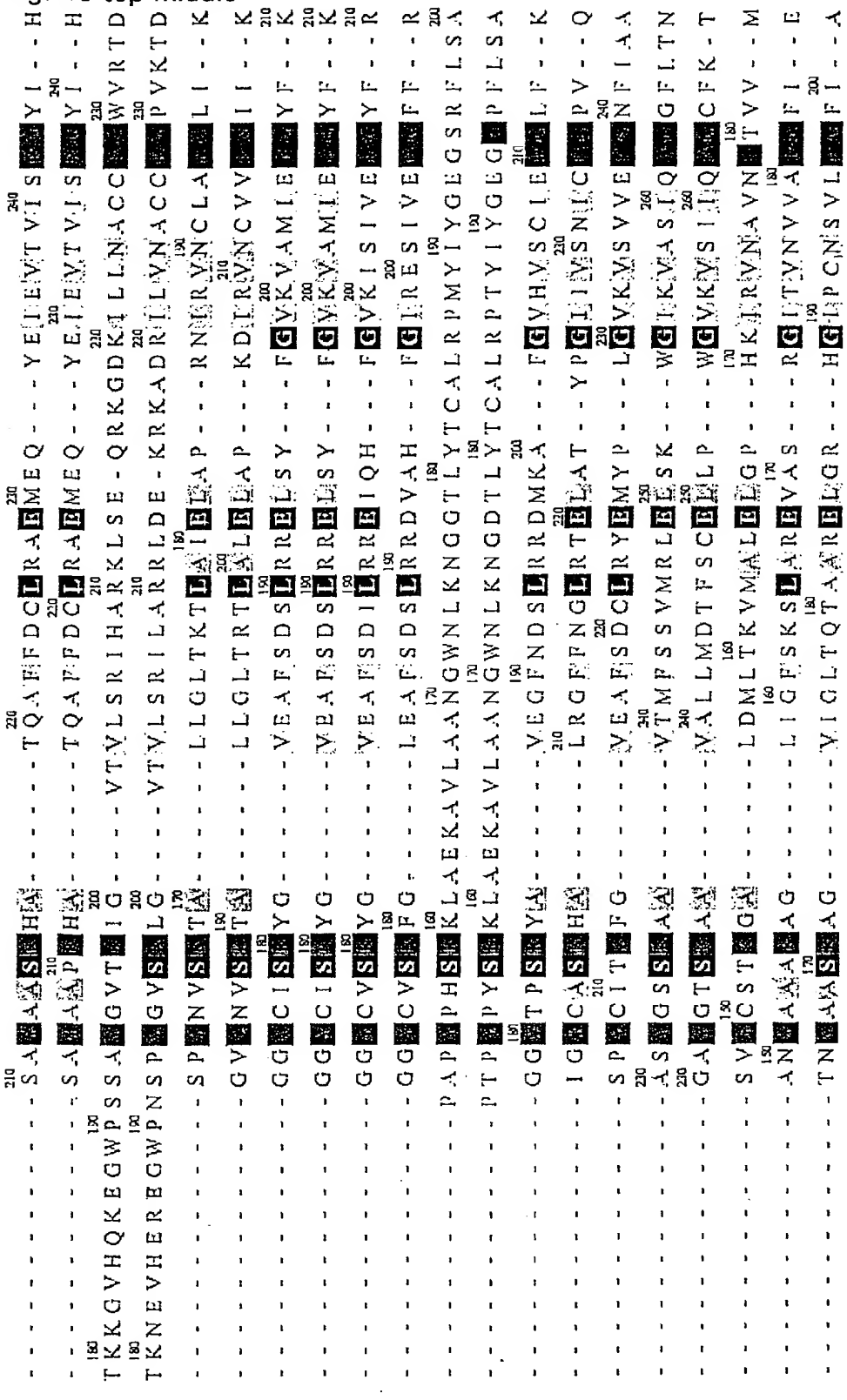

Fig. 4c-top right

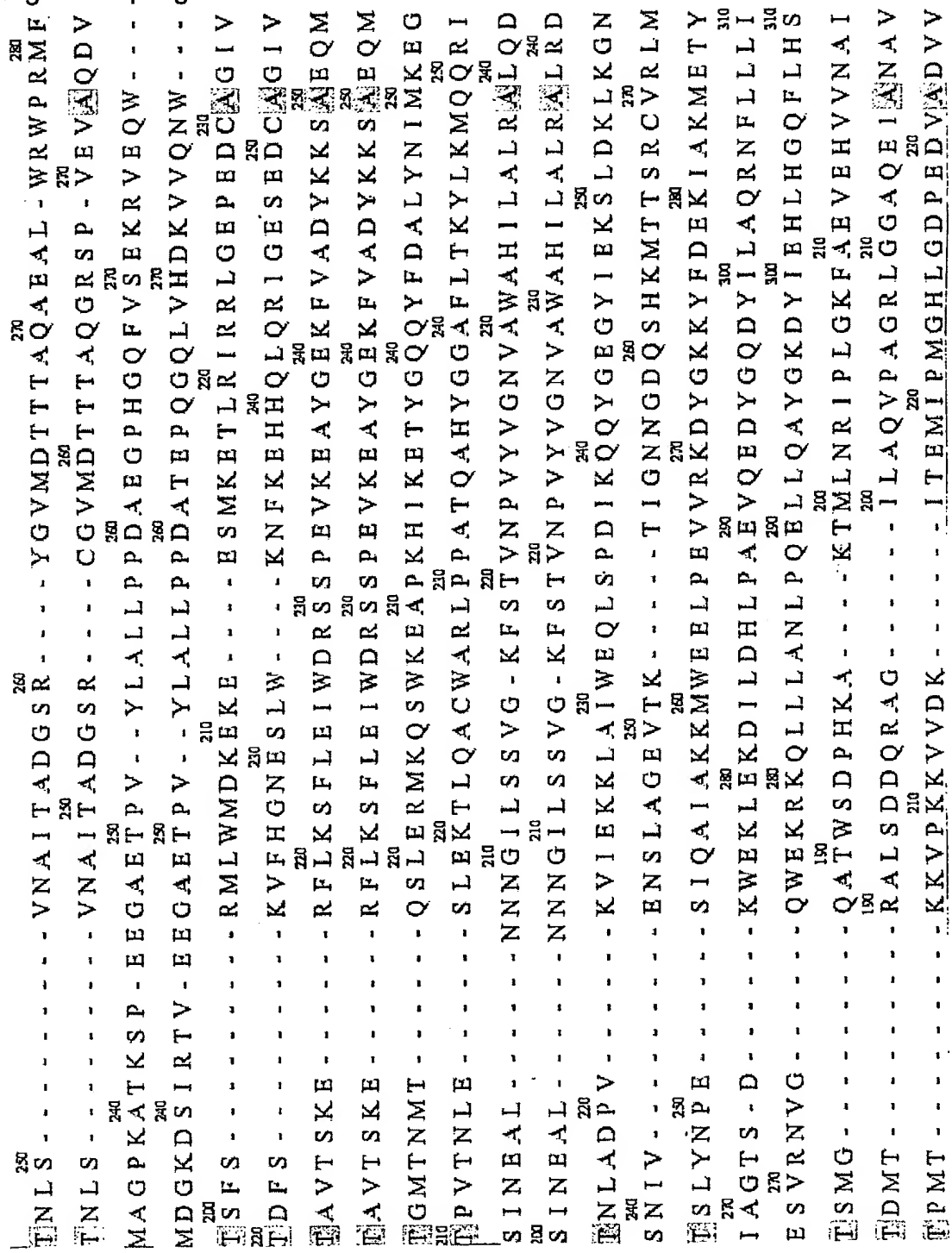

Fig. 4c-bottom left

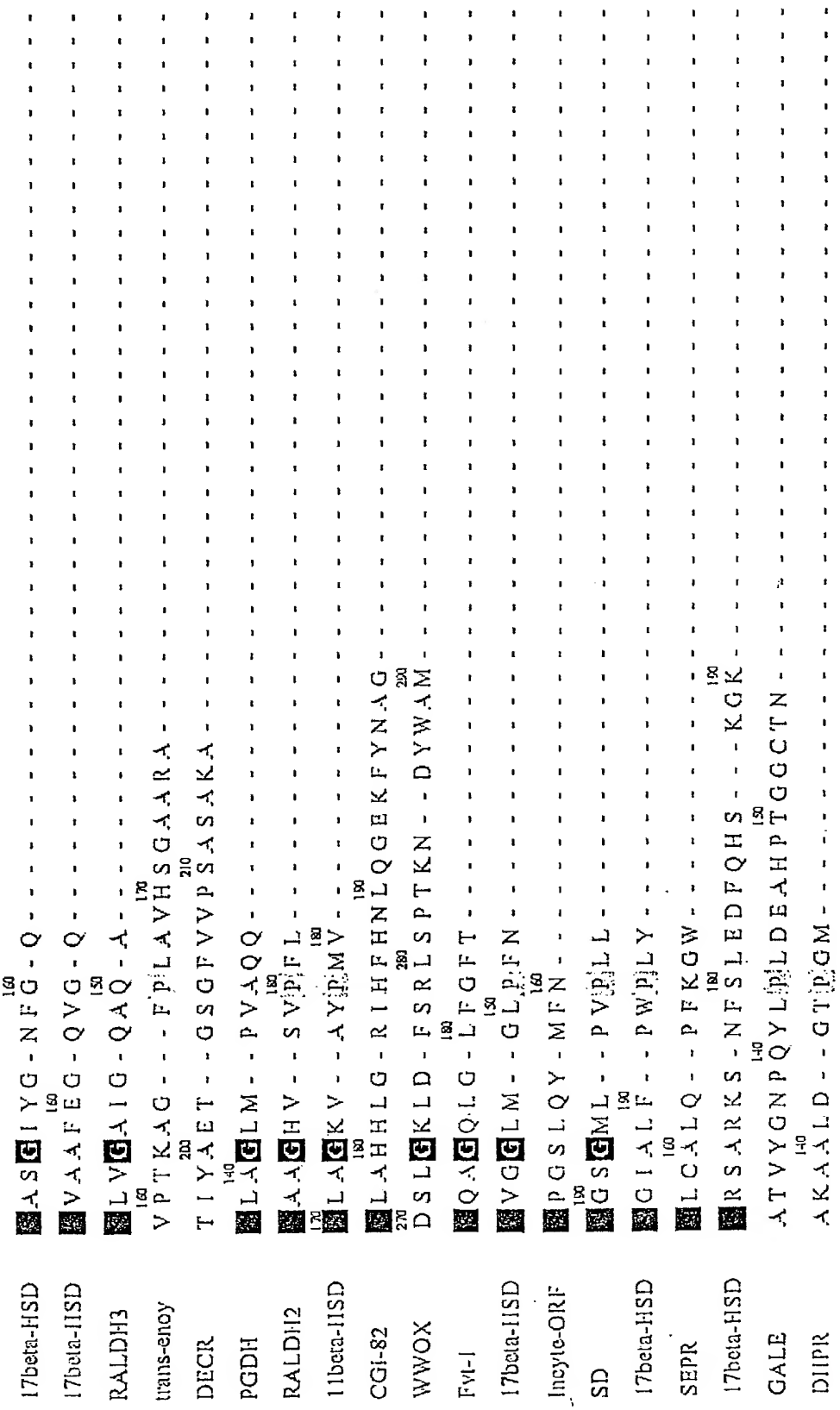

Fig. 4c-bottom middle

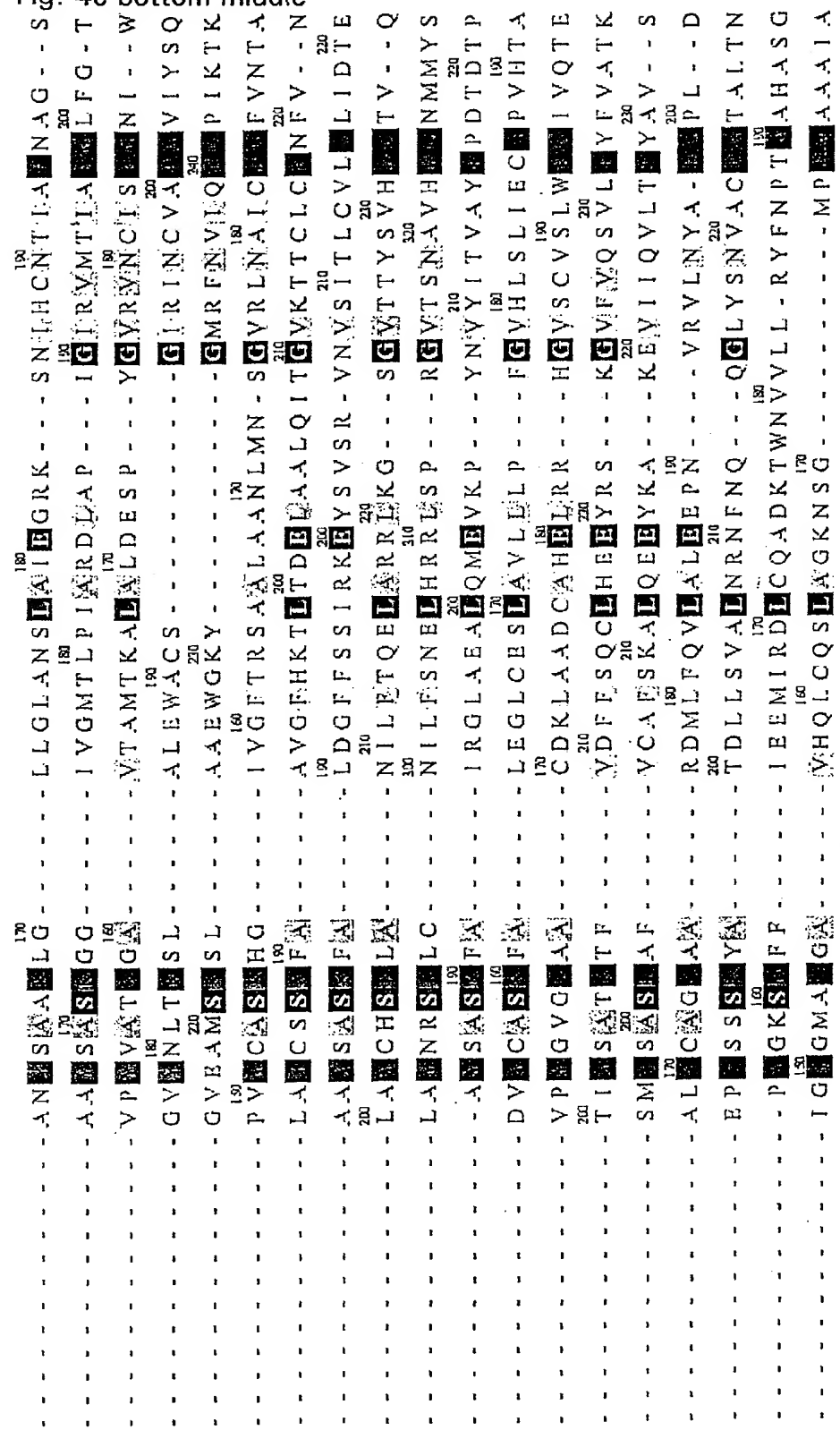

Fig. 4c-bottom right

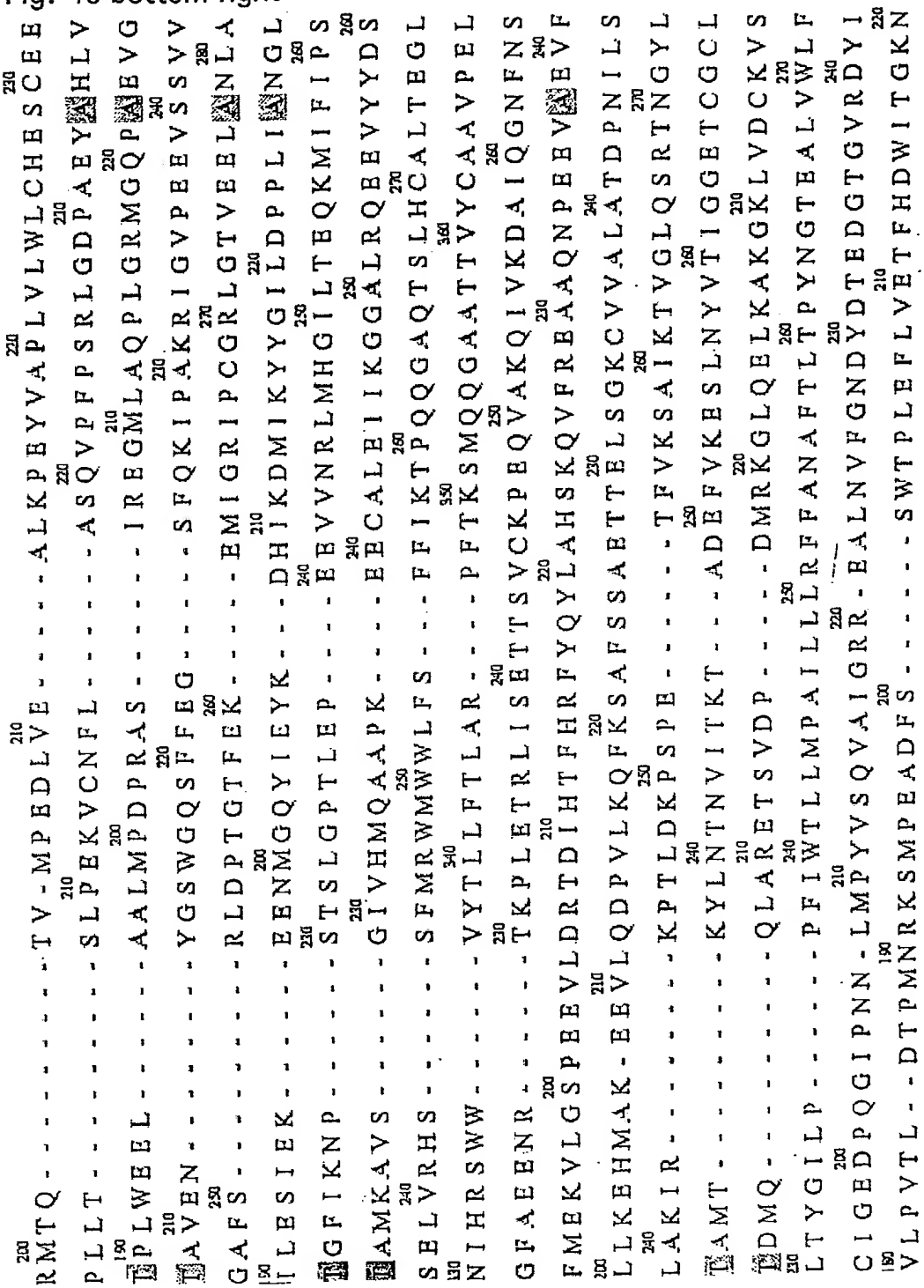

Fig. 4d-top left

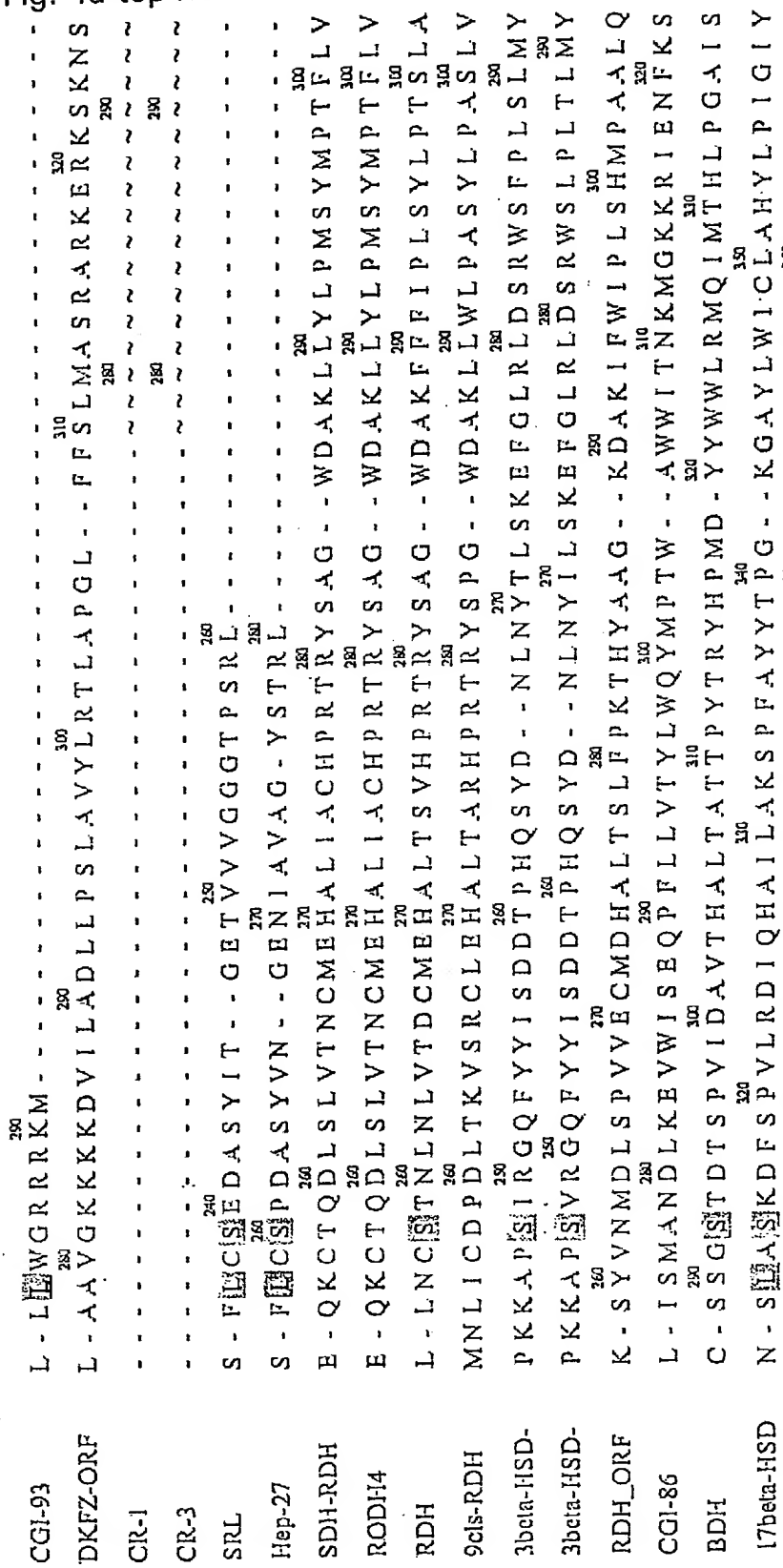

Fig. 4d-top middle

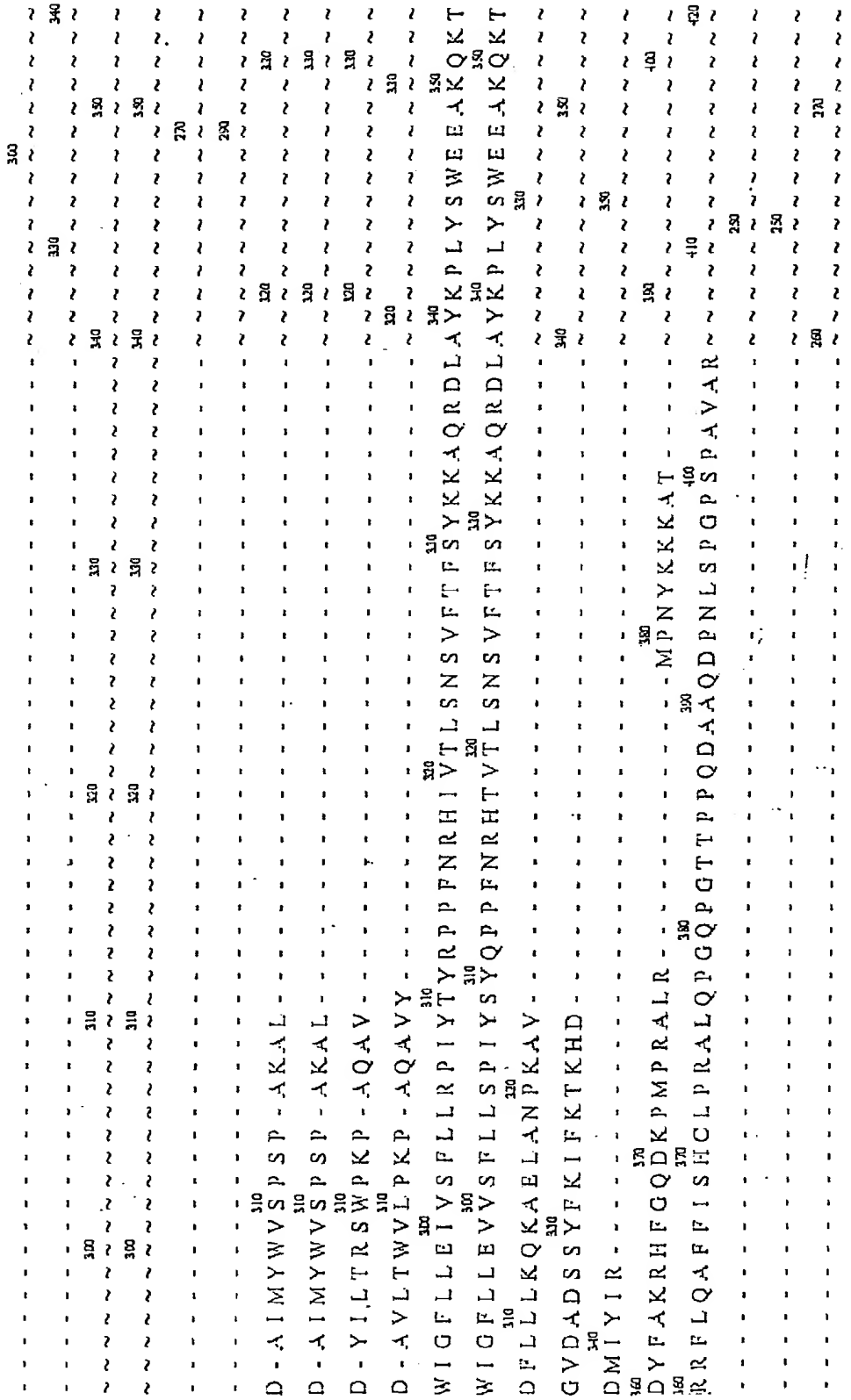

Fig. 4d-top right

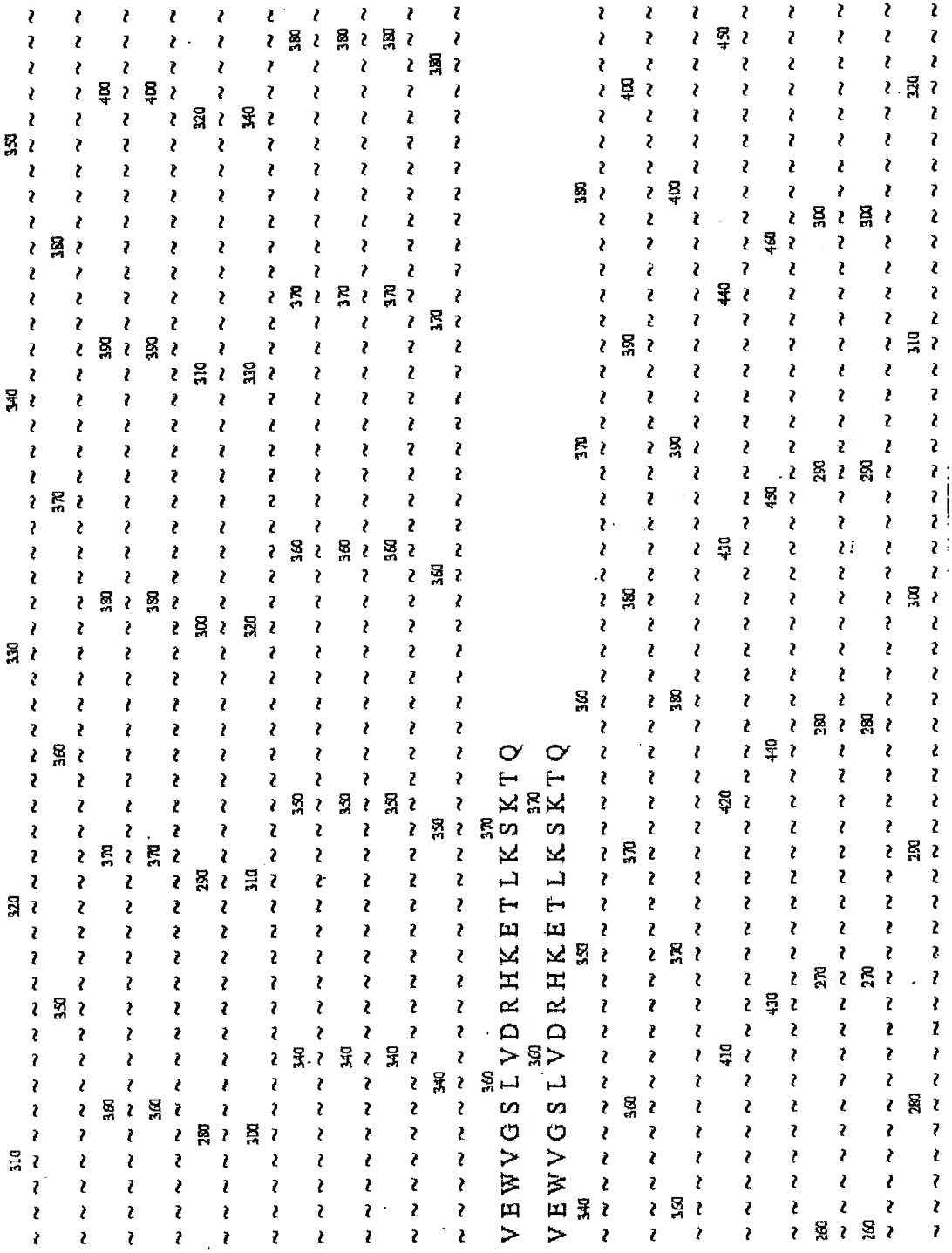

Fig. 4d-bottom left

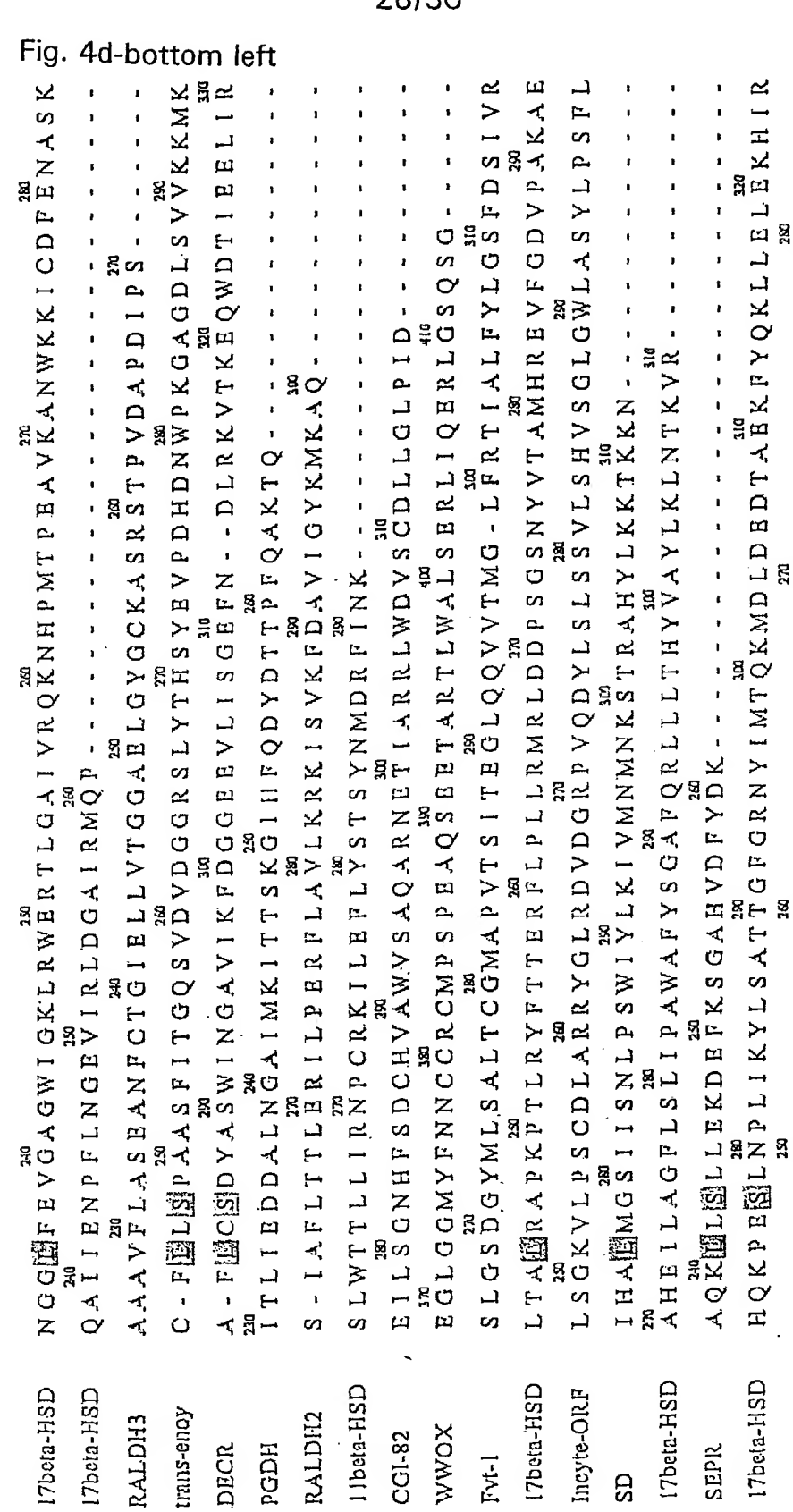

Fig. 4d-bottom middle

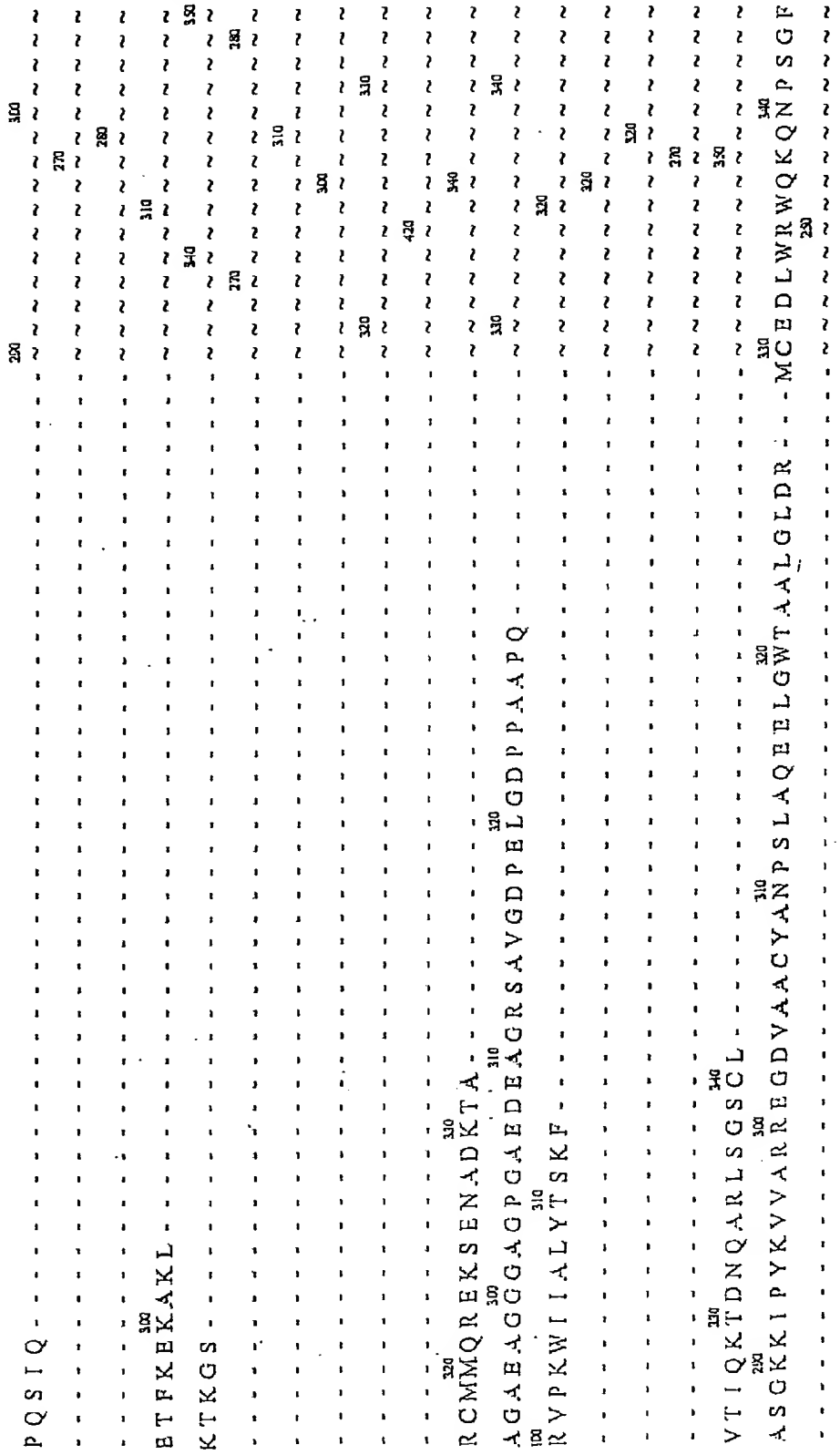

Fig. 4d-bottom right